NOVEL STABILIZATION METHODS FOR SULFATE AND NON-SULFATE SOILS

by

CHAKKRIT SIRIVITMAITRIE

Presented to the Faculty of the Graduate School of

The University of Texas at Arlington in Partial Fulfillment

of the Requirements

for the Degree of

DOCTOR OF PHILOSOPHY

THE UNIVERSITY OF TEXAS AT ARLINGTON

December 2008

ACKNOWLEDGEMENTS

The author would like to express his sincere appreciation to his advising professor, Dr Anand J Puppala, for his excellent guidance and encouragement through out this research study. His intelligence and immeasurable effort always inspire him. The effort has lead to the successful of this dissertation.

The author would also like to convey his gratitude to Dr. Laureano R. Hoyos, Dr Ali Ablomaali, Dr Mohammad Najafi and Dr Chein-Pai Han for accepting to be on examination committee.

Appreciations are broadened to all the members of Department of Public Work staffs for their unconditional help in various aspects throughout this research project.

The author would like to extend his sincere appreciations to his colleagues, Deepti Vasudev, Deepti Devulapalli, Gautham Pillappa, Thammanoon Manosuthikij for their sincere supports, encouragement and contribution in laboratory and field studies of this research work. The value of their friendship will not be forgotten.

December 3, 2008

ABSTRACT

NOVEL STABILIZATION METHODS FOR SULFATE AND NON-SULFATE SOILS

Chakkrit Sirivitmaitrie, PhD.

The University of Texas at Arlington, 2008

Supervising Professor: Anand Puppala

Expansive soils are commonly found in arid and semi-arid climate zones. These soils typically exhibit moderate to high plasticity, moderate to high strength, and high swell and shrinkage characteristic. They also undergo large amounts of swelling and shrink related volume changes when these soils are subjected to moisture fluctuations from seasonal changes. These volumetric movements weaken the subgrade soils, which in turn lead to structural distresses on pavements. Another type of expansive soil is chemically treated expansive soil with high amounts of sulfates, which undergo heaving due to the formation of Ettringite mineral.

This dissertation project was conducted to develop stabilization methods for both natural and chemical treated sulfate rich expansive soil types. Both soils are prevalent in Arlington, Texas and these soil types were hence locally collected and used in the present research. The performance of stabilization methods considered in this research were evaluated in both laboratory and field conditions in order to select ideal stabilization method(s) for modifying expansive soils to minimize heave and shrinkage induced distresses. Four types of chemical treatment methods including Type V Cement, Ground Granulated Blast Furnace Slag (GGBFS), Class F Fly Ash with Type V Cement and Lime with Polypropylene fibrillated fibers

were considered for sulfate soil stabilization studies and a combined lime-cement treatment was considered for stabilization studies for non-sulfate expansive soils.

Laboratory testing programs were also conducted to assess properties relating to volume change behavior, strength and resilient properties. The experimental programs included other basic soil property tests, chemical and mineralogy tests to assess strength improvements in the treated soils. Based on the laboratory studies, stabilizers and their dosages were selected and used for field treatments to support pavement infrastructure.

Field monitoring studies were also conducted through instrumentation studies, elevation surveys, Dynamic Cone Penetrometer (DCP) tests and visual field inspection studies to monitor the performance of pavements built over the stabilized expansive subgrades. Site investigation with an array of sensors and appropriate data acquisition in pavement instrumentation and elevation surveys provides valuable data that were utilized to assess the performance of pavement layers in real field conditions. Based on the field studies, type V cement and type V cement and fly ash treatment methods are considered effective whereas combined lime-cement treatment provided better enhancements to soil properties.

Life cycle cost analyses (LCCA) were also performed on all treatment methods considered for both sulfate and non-sulfate soils. Design recommendations and summarized specifications for the construction of stabilizer treated subgrades for both sulfate rich and non-sulfate soils are presented.

TABLE OF CONTENTS

LIST OF ILLUSTRATIONS

LIST OF TABLES

CHAPTER 1

INTRODUCTION

1.1 Introduction

Expansive soils are commonly found in arid and semi-arid climate zone, which including Australia, Canada, China, India, Israel, Iran, Italy, South Africa, United Kingdom and the United States. These soils typically exhibit moderate to high plasticity, low to moderate strength, and high swell and shrinkage characteristic (Holts and Gibbs, 1956; Sherwood, 1962 Lytton, 1981).

Subgrade soils in North Texas, especially in Southeast Arlington and Dallas - Forth Worth region, are known to be problematic expansive soils as they demonstrate low strength, high swell and shrinkage characteristics (Kota et al., 1996; Chen, 1988). Expansive soils generally undergo large volumetric changes due to moisture fluctuations from seasonal variations. Consequently, these volumetric movements result in cracking in subgrade soils, which in turn result in more swelling problems when the soil absorbs water (Nelson and Miller, 1992). Both low strength characteristic and volumetric movements weaken the subgrade soils that they may lead to structural distress on road pavements. These damages are estimated to cost several billons of dollars annually (Nelson and Miller, 1992). Therefore, it is essential to remedy the expansion behavior of the soils, prior to the construction.

A number of control methods are extensively used in the field to stabilize expansive soils. These methods include treatment with calcium-based stabilizers, non-calcium based stabilizers, asphalt-stabilization, and by geo-synthetic reinforcement (Kota et al., 1996). Soil stabilization is known as an alteration of soil properties to meet particular engineering requirements and among these stabilization methods, calcium- based stabilizers such as lime,

cement and fly ash are most commonly used. The calcium-based stabilizers are commonly used to control the expansion behavior of the soils, as it could reduce the plasticity index (PI), enhance soil strength, and it is cost effective. The reductions in plasticity index have been proven to extend the design life of structures built over the expansive soils (Kota et al., 1996).

This research project was conducted at the City of Arlington, Texas. Soils in Arlington are known to be highly expansive. The expansive soils consist of both sulfate- rich soils and non-sulfate soils. Currently, the ‘‘sulfate-rich soils’’ and ‘‘non-sulfate soils’’ are the expansive soils with soluble sulfates more than 2,000 ppm and less than 2,000 ppm, respectively (Kota et al. 1996; Mitchell and Dermatas 1990; Puppala et al. 2005).

For sulfate-rich soils, calcium-based stabilizers including lime and cement, have been traditionally used to stabilize expansive soils. These stabilizing agents increase strength, decrease plasticity index, swell and shrinkage strain potentials of expansive soils (Hausmann, 1990). However, several studies have shown that the use of calcium- based stabilizers for sulfate-rich soils may lead to a new distress problem instead of mitigating it (Mitchell, 1986; Hunter, 1988; Mitchell and Dermatas, 1992; Petry, 1994; Kota et al., 1996; Puppala et al., 1999; Rollings et al., 1999).

Sulfate-induced heave is primarily attributed to the presence of sulfates in sulfate-rich soils. It usually occurs when lime or cement treatments are used for stabilizing these soils (Hunter, 1988; Mitchell and Dermatas, 1990; Petry and Little, 1992). Reaction of calcium components of stabilizers with free alumina and soluble sulfates in soils at a basic environment (pH between 11 and 13) leads to the formation of ettringite mineral (Hunter, 1988). Ettringite is a weak sulfate mineral. The ettringite will undergo significant heaving when hydrated. Then, this mineral will continue to form as long as there are sufficient amounts of reactants present in the soil (Puppala et al., 2005). These problems are further supplemented by seasonal temperature disparity typical to North Texas. Therefore, the traditional calcium-based stabilizers do not provide satisfactory solution since they lead to sulfate induced heaving (Hunter, 1988).

Based on laboratory studies by Wattanasanticharoen (2000) and literature reviews, the four of the following stabilization methods were selected for stabilizing sulfate-rich soils:

- Sulfate Resistant Type V Cement
- Class F Fly ash with Type V Cement
- Ground Granulated Blast Furnace Slag
- Lime with Polypropylene Fibers

These studies also provided a recommendation for optimum dosage levels to achieve better results in the stabilizations of sulfate-rich soils. Some of these stabilizers were used on other expansive soils by earlier investigators towards the stabilization of expansive soils (Usman and Bowders 1990; Puppala and Musanda, 2000; and Viyanant, 2000).

For non-sulfate soils, there are many factors that affect the expansion behavior of non-sulfate soil. The primary factors are including soils mineralogy, moisture fluctuation and the amount and type of the clay size particle in the soils. The secondary factors include the state of the soils in terms of dry density and moisture content, and the magnitude of the surcharge pressure from structures built over the soils (Day, 2001).

For non-sulfate soils, lime and cement stabilization methods have been used as traditional treatment methods to modify problematic soils. Lime has the ability to improve workability and reduce volumetric changes of soils. Cement has the ability to improve strength and also lower the volume changes of soils. Lime modification is more effective on a treatment of high-plasticity clays. On the other hand, cement stabilization is more effective on granular and moderately effective on cohesive soils (Chavva et al. 2005).

At present, it has long been seen that the majority of works done for stabilization of problematic soils involve either using lime modification or using cement stabilization. Lime stabilizer is mostly preferred since it can reduce volume change related soil movements and also due to cost consideration. Recent research showed the potential of combined cementitious stabilizers that are proven effective on plastic clays. The concept of using combined lime and

cement stabilization has been explored, but not extensively reported in the literature, primarily due to high initial cost and lack of long-term field monitoring (Prusinski and Battacharja. 1999).

Researchers at The University of Texas at Arlington have been attempting to investigate the effectiveness of combined lime and cement treatment method for enhancing properties of local clay subgrades with low sulfate levels. Based on the available literature, recommendations for optimum additive dosage levels, construction methods, specifications for the utilization of combined lime and cement treatments to improve the subgrade soils are already prepared.

The City of Arlington is currently sponsoring two research studies at The University of Texas at Arlington (UTA) to evaluate novel stabilization methods for effectively stabilizing both sulfate-rich and non-sulfate soils in Arlington, Texas.

Although the stabilizers mentioned above for sulfate soils have demonstrated good performance in the laboratory, field monitoring of the subgrades stabilized with the selected chemicals and documentation of the pavement performance are considered important to further understand and validate the effectiveness of stabilizers. The field monitoring is also essential since the soil in natural field conditions undergo true moisture and temperature fluctuations which may affect the stabilization mechanisms. Hence, performance assessment in field conditions is needed for an accurate evaluation of the effectiveness of the stabilizers in sulfate soil conditions. The same is also valid for combined lime and cement treatments for non-sulfate soils, which need to be validated in both laboratory and field conditions. Effectiveness of each stabilizer for both soil types was addressed in controlling pavement distress such as rutting and pavement cracking caused by elevational differences due to swell and shrink related soil movements.

Mohan (2002) and Pillappa (2005) designed and developed appropriate field instrumentation to evaluate treated sulfate rich subgrade soils. Strain gauges and pressure cells were installed and monitored to measure compressibility and load carrying potentials of

stabilized subgrades. In addition to pavement instrumentation, elevation surveys and Dynamic Cone Penetrometer (DCP) tests were conducted. Elevation surveys were performed in order to evaluate the heave and related movements of other types of soil including erosions of stabilizer treated soils. DCP tests were performed to analyze the in-situ strength and moduli properties of treated subgrade soils. Chemical tests and mineralogical tests were also conducted to identify the presence of ettringite mineral, which is the sulfate heave source mineral in treated soils.

1.2 Research Objectives

Each year, the local cities in north Texas have spending considerable amounts of funds for annual maintenances and repairs of distressed pavements including those deteriorated by sulfate-rich soils and non-sulfate soils. Therefore, it is necessary to explore new and alternate stabilization methods with the aim of constructing stronger and stable subgrades with negligible heave distress problems in the future. In order to achieve this goal, this dissertation research is attempted with the following specific objectives:

1. To identify the factors which directly influence the expansion behavior of both sulfate-rich and non-sulfate expansive soils
2. To study and investigate new stabilization methods for providing effective stabilization of the present expansive soils located in north Texas
3. To evaluate the effectiveness of stabilization by addressing heave movements, surficial deformations, and pavement cracking problems
4. To develop a design guidelines on the selection of stabilization for a better pavement design in different subsoil conditions

The outcome of this dissertation research is to provide recommendations and construction guidelines for implementing novel stabilization methods for the construction of new pavement infrastructure, which in turn will result in much better performance of the pavement with minimum rehabilitation and maintenance activities.

1.3 Organization of the Dissertation

This thesis report is composed of seven chapters: introduction (chapter 1), theoretical background and literature review (chapter 2), experimental program (chapter 3), analysis of laboratory results (chapter 4), field section and studies (chapter 5), analysis of field results (chapter 6), Life Cycle Cost Analysis (LCCA) (chapter 6), summaries, conclusions and recommendations (chapter 7).

Chapter 1 provides the introduction, research objectives and thesis organization. The introduction to expansive soils, problems associated with expansive soils and the suggested remediation techniques are presented in this chapter.

Chapter 2 provides literature review includes a comprehensive and detailed description on background of the expansive soils, problems associates with expansive soils, characteristics of stabilizers used in this research and case reviews on pavement distress. It also includes summarization of the importance of instrumentations, different instrumentation methodologies based on the application areas and case reviews involving instrumentation and their findings.

Chapter 3 provides the experimental program designated to determine the basic soil properties, soils mineralogy, and strength enhancement. This chapter also provides a detailed description on sample preparation and the procedures for the tests.

Chapter 4 provides a comprehensive results and analysis of laboratory tests including basic soils property tests, chemical and mineralogical characteristics, and strength assessment tests conducted in this research. Results on both sulfate and non-sulfate soils will be covered here.

Chapter 5 includes field test sections and performance monitoring studies. The detailed descriptions of construction operations, instrumentation design, installation of sensors, data collection procedures, elevation surveys and field DCP tests are also discussed.

Chapter 6 provides the results and analyses of field studies. This chapter presents a complete description of field studies and the results and performance assessments of stabilized

road sections. The field results include instrumentation results, elevation survey results and DCP test results.

Chapter 7 focuses on conducting investigations on vertical movement of rigid pavements for each stabilization method by utilizing finite element models in which the soil properties including resilient modulus, Poisson's ratio are taken into account in the analysis.

Chapter 8 provides the summaries, conclusions and recommendations of the research study results. Some recommendations of stabilizers based on the study results are also included.

CHAPTER 2

LITERATURE REVIEW

2.1 Introduction

Background information and literature review presented in this chapter was collected from conventional library and electronic resources as well as from journals, and research reports. The introduction to expansive soils is first mentioned in this chapter. Then, this section is followed by a detailed description of problems associated with both sulfate-rich soils and non-sulfate soils and their remediation strategies. The comprehensive descriptions of problems associated with the application of calcium-based stabilizers for the treatment of sulfate-rich soils are described. Moreover, the natural process of ettringite formation in soils and possible heave mechanisms, which cause distress to structures are also explained. The later part of the chapter explains the details of pavement instrumentation and their advantages, sensors commonly used in monitoring geotechnical earth structures, followed by a few case studies on current sensor applications in pavement systems.

2.2 Sulfate-rich Soils

Sulfate-rich soils are typically found in arid and semiarid regions whereas natural and non-sulfate expansive soils are located in the southwestern and western United States. When these soils are stabilized with calcium-based stabilizers such as lime and cement, sulfate minerals appeared in these soils react with calcium component of the stabilizer and free reactive alumina of soils to form highly expansive crystalline minerals, namely ettringite and thaumasite (Sherwood, 1962; Mehta and Wong, 1928; Mitchell, 1986; Hunter, 1988). Thaumasite forms after ettringite undergoes certain crystalline changes. These sulfate minerals expand considerably when subjected to hydration process. The mineral also expand due to

continuous crystal growth. Both hydration reactions and crystal growth will result in a significant amount of heaving in the sulfate-rich soils.

Infrastructures including buildings, embankments, runways and highways built over lime and cement treated sulfate-bearing soils have been affected by this heave distress. This distress is termed as sulfate-induced heave distress (Mitchell, 1986; Mitchell and Dermatas, 1992; Dermatas 1995; Hawkins, 1988). Sulfate induced heave distresses are known to cause serious problems throughout the state of Texas (Hunter, 1988). Figure 2.1 present the sulfate concentration in Texas.

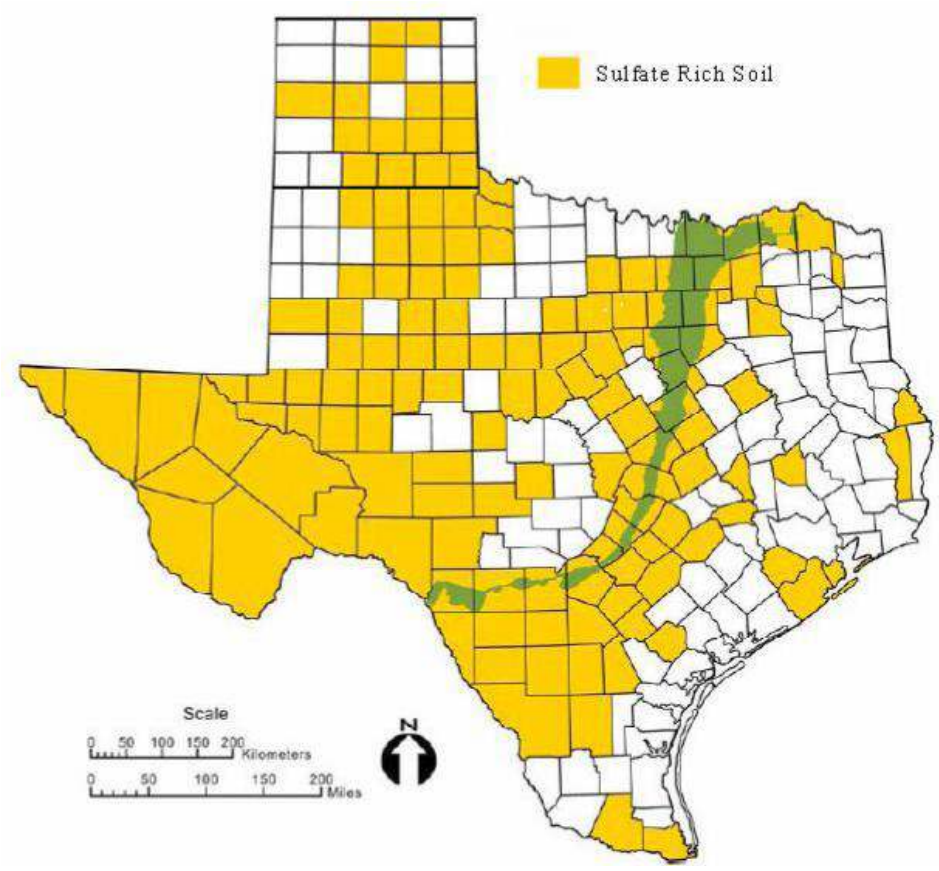

Figure 2.1 Map Showing Sulfate Concentrations in Texas (Harris et al., 2004).

In addition, the increase in the use of industrial wastes for soil stabilization and solidification further signify the importance of understanding the heave mechanisms of chemically treated sulfate soils (Dermatas, 1995). Waste materials such as phosphogypsum and other sulfate wastes are used as base and subbase material to support pavements. The leachate of these wastes further can increase sulfate levels in the soils. Moreover, the presence of sulfates can be from the construction water used in the project. Such sulfate could potentially lead to heaving when calcium-based stabilizers are used to stabilize the soils.

Petry (1994) and Kota et al (1996) reported that repairs and maintenances of heave distressed problems on pavements are estimated to cost several millions of dollars annually In late 80s, City of Las Vegas, Nevada spent nearly 2.7 million dollars to repair and maintain the pavements damaged by sulfate-induced have distress (Hunter, 1988). Also, the United States of Army Corps of Engineers rebuilt an auxiliary runway of Laughlin Air Force base near Spofford, Texas at a cost of more than 1.5 million dollars. These costs explain the severity nature of this type of heave problem (Perrin, 1992).

2.3 Mechanism of Sulfate Heave in Soils

Sulfates are introduced into the soils in many different forms such as acid rain, construction water, underground water flow, or moisture percolation due to evapo-transpiration process (Dermatas, 1995). The sulfates are present in natural soils in various forms such as gypsum or calcium sulfate, sodium sulfate, and magnesium sulfate (Puppala et al. 2003). The most common sulfate mineral present in soils is gypsum ($CaSO_4.2H_2O$) because of its relatively low solubility (2.6 gm/L) level when compared to both sodium sulfate Na_2SO_4 (408 gm/L) and magnesium sulfate or $MgSO_4$ (260 gm/L) (Puppala et al. 2003).

Several studies show that when sulfate-rich soils are stabilized with calcium-based stabilizers such as lime or cement, sulfate in the soils will react with calcium component of the stabilizers in order to form a combination series of calcium-alumina-sulfate hydrate compounds (Mitchell and Dermatas, 1992). These compounds lead to the formation of ettringite minerals

(Ca_6 [Al $(OH)_6]_2$*$(SO_4)_3$*26H $_2$O) which has the potential to expand two or three times of their original sizes when subject to hydration. The chemical structure of ettringite crystals are hexagonal prisms and are often in elongated form with different shapes. Figures 2.2 illustrate the structure of ettringite crystals. Others form of ettringite are needle-like (Figure 2.3), lath-like (Figure 2.4) or rod-like, (Figure 2.5) depending on the time and pH conditions during the formation period.

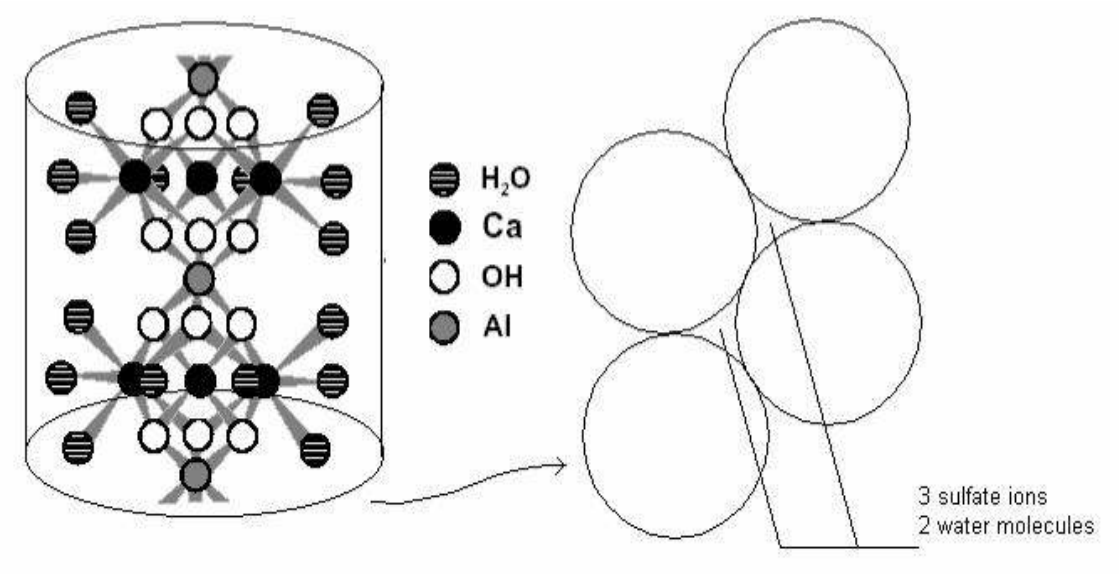

Figure 2.2 Structure of Ettringite Column (Day, 1992 and Intharasombat, 2003).

Figure 2.3 Needle-like Ettringite, from SEM analysis (Talero, 2002).

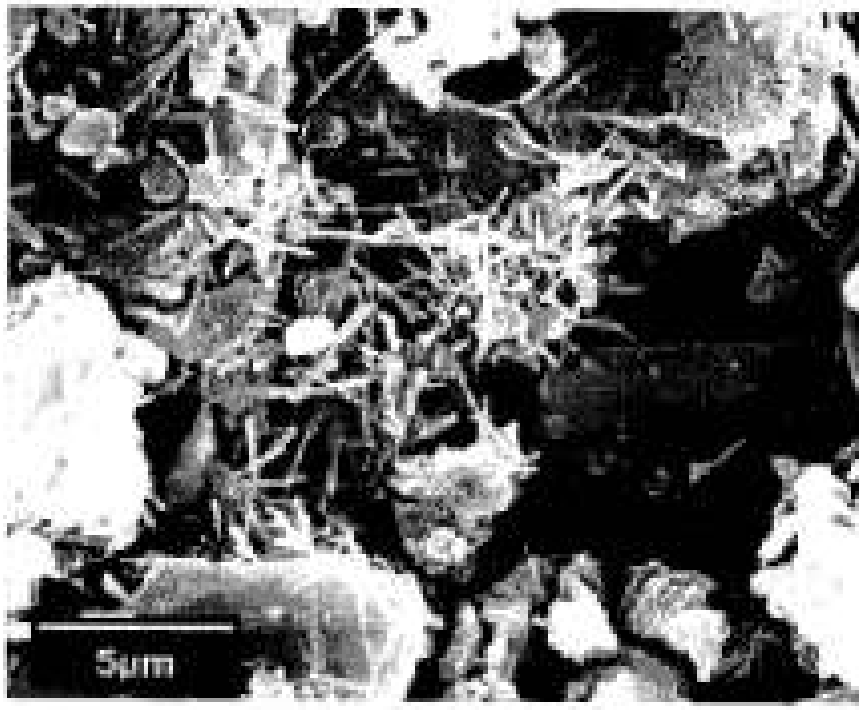

Figure 2.4 Lath-like Ettringite (Wang, 2002).

Figure 2.5 Rod-like Ettringite (Mitchell and Dermatas, 1992).

When the temperature is less than 15°C and soluble carbonate content is present, ettringite is transformed by a series of intermediate reactions to thaumasite mineral, $[Ca_3Si(OH)_6]_2(SO_4)(CO_3)_2*26H_2O$). This transformation in mineral structure occurs by isostructure subsolution of silica for alumina and carbonate for sulfate (Kollman and Strubel, 1981). Thaumasite crystal is very expansive when exposed to water hydration and its expansion potential is much higher than that of ettringite.

In order for ettringite to form, free alumina content from the original clay mineral interstices should be first released during the early period of the hydration process. This usually occurs at the pH greater than 10.5, which equals to the pH of lime stabilization. In cement stabilization, alumina is liberated from pozzalonic compounds formed in cement stabilizations. At this stage, the presence of soluble sulfate, and calcium ions from chemical stabilizers should be present to form ettringite mineral. Finally, the most important factor is the presence of water. Water facilitates the chemical reactions to take place for final formation of this mineral.

Factors that affect the amount of heaving are quantity of ettringite formed, the crystal morphology and size, restraint of the system, and ion accessibility. All factors depend on different environmental conditions including pH, presence of soluble sulfates and carbonates and water.

2.4 Non-Sulfate Expansive Soils

According to the American Geological Institute Glossary of Geology, expansive soils are "soils that are capable of absorbing large quantities of water, thus increasing greatly in volume" (Chen, 1988). Expansive soils are typically found in arid and semiarid regions. The expansive soils are located particularly in the southwestern and western states in the United States. Chen (1988) reported that Colorado, Texas, Wyoming, and California are more susceptible to damage from expansive soils rather than other states. Soils in these areas contain large surface deposit of clay and climates characterized by alternating periods of rainfall and drought. Figure 2.6 presents the locations of the expansive soils in the United States.

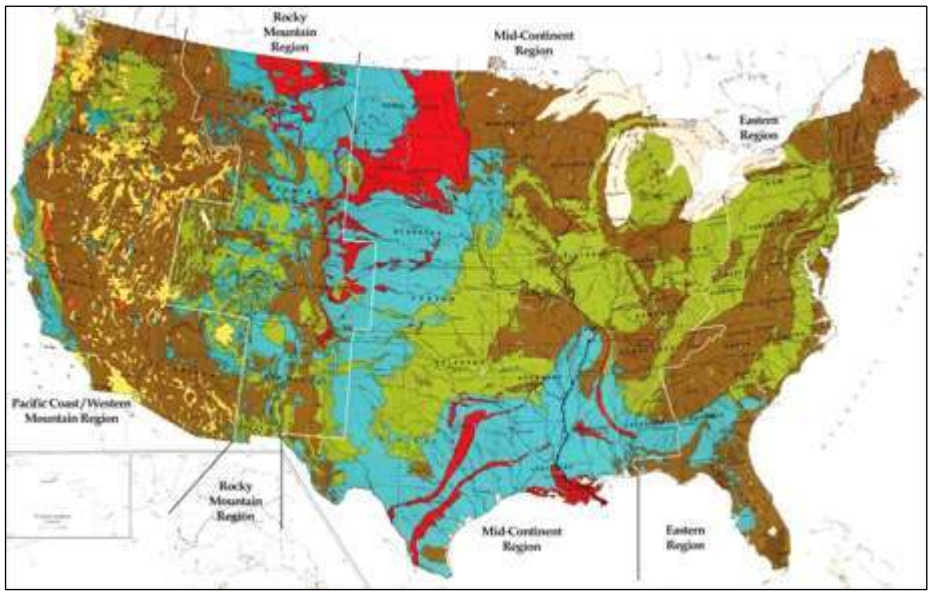

Map Legend

Unit contains abundant clay having high swelling potential

Part of unit (generally less than 50%) consists of clay having high swelling potential

Unit contains abundant clay having slight to moderate swelling potential

Part of unit (generally less than 50%) consists of clay having slight to moderate swelling potential

Unit contains little or no swelling clay

Data insufficient to indicate clay content of unit and/or swelling potential of clay (Shown in westernmost states only)

Figure 2.6 The Locations of The Expansive Soils in The United States.

In unconfined environment, dry soils absorb water and increase in volume in an amount proportional to the amount of water absorbed. Many factors including moisture fluctuation and the amount and type of the clay mineral contained in the soil will influence the expansion behavior of the soil. Other factors affecting the expansion behavior include the state of the soil

in terms of dry density and moisture content and the magnitude of the confining pressure (Day, 2001). All these factors are discussed below in detail.

2.4.1 Moisture Fluctuation

The main factor for expansive soils is moisture fluctuation. In the United States, the expansion of soils that causing extensive damage to infrastructures is mainly in the desert area (Day, 2001). Because the lack of rain in dry season, the clay layers that are close to the ground surface are shrunk due to moisture loss. Hence, the clay layers often turned into a desiccated or powdery state. Then, in wet season the clay layers absorbs water and swells. The shrink and swell behavior of the soils causes extensive damage to the structure built over them.

Other parts of the country may also have expansive soils problems, but the soils do not pose any significant damage to the infrastructures because there is enough precipitation throughout the year to keep moisture in the soils constant. Therefore, the expansive soils in these areas tend to remain relatively dormant and they neither swell nor shrink.

2.4.2 Amount of clay particles

Clay particles usually absorb and hold water to their particle faces and expand. As a result, soils that contain more clay particles tend to exhibit higher swell potential (Day, 2001).

2.4.3 Clay Mineralogy

The type of minerals contained in the soils significantly affects the expansion of the soils. Montmorillonite mineral is a much smaller and more active than Kaolinite. This clay mineral has the highest moisture susceptibility and greatest expandability of all the clay minerals. Therefore, soils that contain montmorillonite mineral exhibit high swell potential (Day, 2001). Figure 2.7 shows plots of montmorillonite, just below the U line.

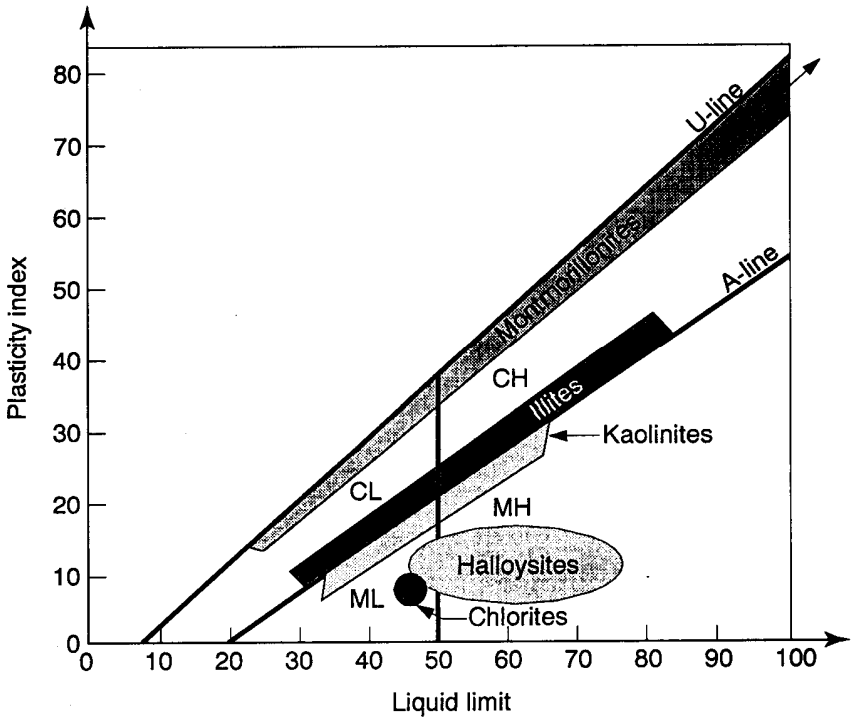

Figure 2.7 Plasticity Characteristics of Common Clay Minerals (Day, 2001).

Montmorillonite mineral was found in 1847. It was named after locality, Montmorillon, France. This mineral also presents in many locations world wide and known by other names for example, bentonite was found in 1890 and named by an American geologist for the one time Fort Benton (on the Fort Benton Formation geological stratum) in the eastern Wyoming Rock Creek area (http://en.wikipedia.org).

Montmorillonite is typically found in the form of microscopic crystals. It has a 2:1 structure, 2 tetrahedral sheets sandwiching a central octahedral sheet. The particles are plate-shaped with an average diameter of approximately 1 micrometer. When water gets in these particles, they tend to absorb water into their molecular layers causing swelling, and expansion of the interlayer spacing due to the mineral variety. (http://www.answers.com). Figure 2.8 and Figure 2.9 show a structure of montmorillonite and the SEM image of montmorillonite, respectively.

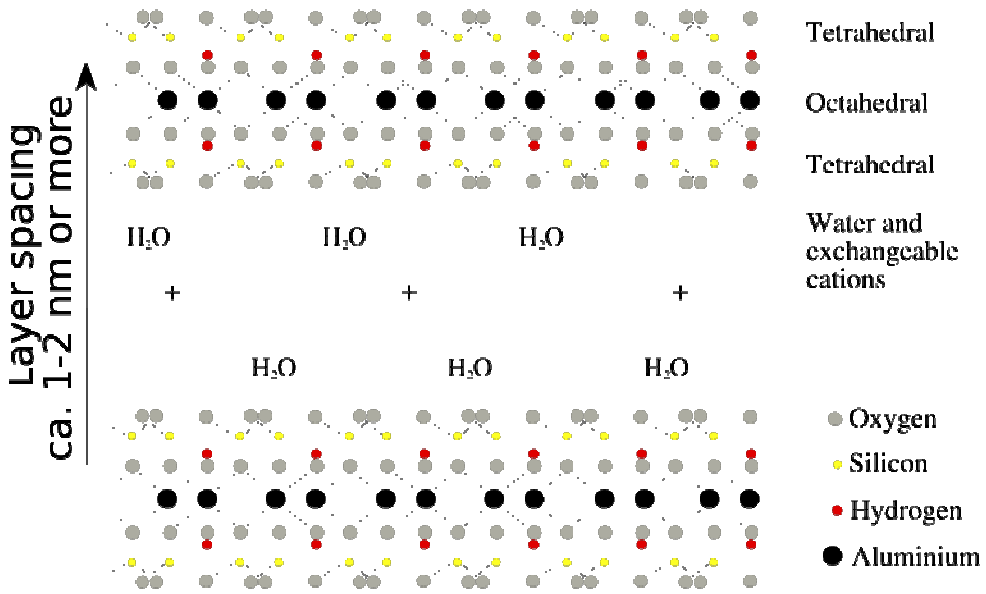

Figure 2.8 Structure of Montmorillonite (Image:Montmorillonit.svg).

Figure 2.9 Anthigenic Smectite (Montmorillonite) Overgrown on Pore Spaces and Authigenicly-Overgrown Quartz Grains in Sandstone, SEM Image of a Core Sample: Scale 67 micron (OMNI Laboratories, Inc).

Montmorillonite is a member of the Montmorillonite/Smectite Group. Chemically, montmorillonite is hydrated sodium calcium aluminium magnesium silicate hydroxide. Potassium, iron, and other cations are common substitutes, the exact ratio of cations varies with sources. It often occurs intermixed with chlorite, muscovite, illite, cookeite and kaolinite (http://www.answers.com). The general formula of montmorillonite is as following:

$$(Na,Ca)(Al,Mg)_6(Si_4O_{10})_3(OH)_6 - nH_2O$$

where n represents the variable amount of water that members of this group could contain (http://en.wikipedia.org). The chemical and physical properties of montmorillonite are shown in Table 2.1 and 2.2, respectively.

Table 2.1 Chemical Properties of montmorillonite (http://mineral.galleries.com)

Properties	Description
Chemistry	$(Na,Ca)(Al,Mg)_6(Si_4O_{10})_3(OH)_6 - nH$: Hydrated Sodium Calcium Aluminum Magnesium Silicate Hydroxide
Class	Silicates
Subclass	Phyllosilicates
Group	The Montmorillonite/Smectite Group

Table 2.2 Physical Characteristics of montmorillonite (http://mineral.galleries.com/)

Properties	Description
Color	White, gray of pink with tints of yellow or green
Transparency	Crystals are translucent and masses are opaque
Crystal System	Monoclinic
Crystal Habits	Usually found in compact or lamellar masses. Also seen as inclusions in quartz as fibers and
Hardness	1-2
Specific Gravity	2.3-3
Streak	White
Expansion Behavior	Crystals expand to many times their original volume when added to water
Associated Minerals	Garnets, biotite and quartz
Occurrences	France, Italy, USA and many other localities world wide
Field Indicators	Softness, color, soapy feel, luster and expandability when added to water

Montmorillonite is common in clays, shales, soils, Mesozoic and Cenozoic sediments, and non-micaceous recent marine sediments. It usually occurs in areas of poor drainage. The water content of montmorillonite is variable. With the addition of water, montmorillonite swells

like other clays. The amount of expansion depends significantly to the type of exchangeable cation contained in the soils for example, the presence of sodium as the predominant exchangeable cation in the soils can cause the clay to swell to several times its original volume (http://mineral.galleries.com).

2.4.4 Density and water content

The dry density and water content of the soils are the very important factors in the amount of expansion of the soils. The expansive potential increases as the dry density increases and the water content decreases. The most expansive condition is when near-surface clays become desiccated, the soil has a very high dry density and very low moisture content, in dry season (Day, 2001).

2.4.5 Surcharge pressure

The surcharge pressure is an important factor of expansive soils because the amount of swell decreases as the confining pressure is increased. In general, the lightly loaded structure such as concrete pavement, slab on grade foundations and concrete flatwork are often impacted by expansive soils (Day, 2001).

Several stabilizing agents are widely used to control the expansion of soils. Properties of soils can be altered by the addition of stabilizing agents. These stabilizing agents include calcium-based stabilizers, non-calcium-based stabilizers, bitumen, geo-synthetic reinforcements and compaction of the subgrade. The main interest is typically in reducing water susceptibility, lowering plasticity and increasing strength of the soils. The main functions of the stabilizing agent are: bonding the soil particles together, protecting the soils from water penetration or a combination of bonding and protecting the soils. Among those stabilizing agents, calcium-based stabilizers, such as lime and cement are the most commonly used stabilizers. These stabilizers stabilize the soils by bonding the soil particles together so that the volumetric change of the soils is lessened. The chemical reactions between the stabilizers and the soil particles also decrease plasticity index (PI) and increase strength of the soils (Sherwood, 1993).

2.5 Mechanism of Soils Expansion

Due to moisture fluctuation, these soils undergo volumetric changes upon wetting and drying that causing extensive damages, such as sulfate heave and settlement to the infrastructures built over them (Puppala et al., 1999).

Water is introduced to the soils in several ways including rainfall infiltration, construction water, underground water and moisture percolation due to evapo-transpiration process. The orientation of H_2O molecules on the clay surface is mainly due to the electronic forces between clay particles and water molecules. Clay particles appear in the nature as a flat shape. These particles are electrically charged and the high potential charges are concentrated on the surface of the clay particles that causing attraction of bipolar H_2O molecules. As a distance from the clay surface increases, water molecules are distinguished in layer due to the electronic forces. The mechanism of soil expansion is shown in Figure 2.10 (Stavredakis, 2003).

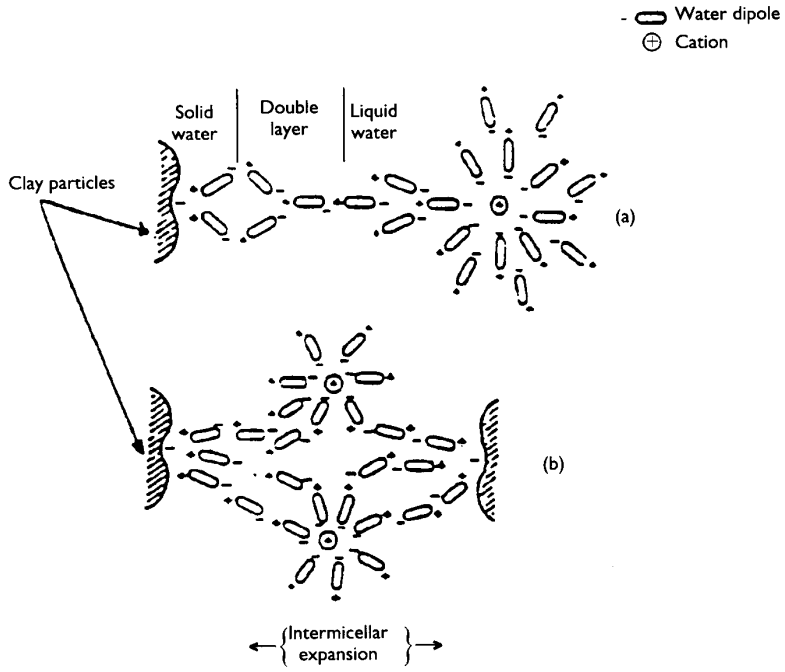

Figure 2.10 The Mechanism of Soil Expansion a) water molecules are distinguished in layers related to the attraction forces, b) clay particles are held by solid water (Stavredakis, 2003).

In Figure 2.10, solid water holds very firmly in a thin layer of clay surface. The electronic force in double layer is less attractive and there is a viscous thick liquid layer responsible for the plasticity of clay. Within this layer, the grains of clay slip on each other without elastic rebound, rupture and volume change (Stavredakis, 2003).

The natural clay soils are formed by the electronic charge between clay particles and water molecule. The pressure of the overburden load from the structure built on the soils causes this soft, loose, low shear strength clay to form a denser soil as the clay particles come closer. This process only happens when the low viscosity water is squeezed out from the grain spaces under the high pressure at the points of contact. In the double layer, the process requires higher pressures and longer periods of time. Clay particles absorb water and they are held to each other at the end of the process (Stavredakis, 2003)

In the dry and undisturbed environment, the expansive soils are loose, brittle and have high shear strength. These kinds of soils have high swell potential and high expansion behavior. Soil expansion occurs when the soils are submerged in water. This is because these soils are partially elastic materials. Therefore, when these soils are submerged in water, there is no surface tension and no capillary compression on the soil particles. The elastic rebound is a result of the compressive forces. Moreover, restoration of the moisture-absorbing capacity of the soils is restored during desiccation (Stavredakis, 2003)

2.6 Remediation Methods for Expansive Soils

Several control methods are extensively used in the field to improve the plasticity properties of expansive soils. These methods include treatment with calcium-based stabilizers, non-calcium-based stabilizers, asphalt-stabilization, and by geo-synthetic reinforcement (Kota et al., 1996). All mentioned methods will be discussed below.

2.6.1 Stabilizing Agents available

Properties of soils can be altered by the addition of stabilizing agents. Plasticity, compressibility and permeability can all be altered by the addition of stabilizing agents. In this

research, the main interest is to find a means of increasing soil strength and reducing the expansion behavior of the soils.

Many stabilizing agents have been proposed as primary soil stabilizing agents although ordinary Portland cement, lime and bitumen have been extensively used. By their nature, these stabilizing agents have to be used in significant amounts, which are typically more than 2% (Sherwood, 1993). Sherwood (1993) recommended that the stabilizing agents should ideally have the following properties:

a) Be able to stabilize a wide range of soils
b) Have a permanent stabilizing effect
c) Be readily available at relatively low cost in large quantities
d) Present no serious storage or transport problem
e) Be relatively non-toxic and non-corrosive

From the recommendation given above, only lime, cement and bitumen are considered satisfying the requirement. Further discussion on lime, cement, fly ash, ground granulated blast furnace slag, and bitumen and their applications are presented below. Additionally, other additives used for sulfate soil stabilization are also discussed here. These include combinations of type V cement with fly ash and lime and poly propylene fibers.

2.6.1.1 Ordinary Portland Cement

Portland cement is defined in ASTM C595-77 as “a product consisting mostly of calcium silicate”. Portland cement is attained by heating to partial fusion a pre-determined and homogenous mixture of materials containing mostly lime (CaO) and silica (SiO_2) with a small proportion of alumina (AL_2O_3) and iron oxide (Fe_2O_3). The lime (CaO) is obtained from calcareous materials, typically chalk or limestone. SiO_2, AL_2O_3 and Fe_2O_3 are obtained from argillaceous materials, such as clay or shale (Sherwood, 1993).

Cement has been extensively used as a stabilizing agent for soils for many years. The adding of cement to the soils is termed as “cement-stabilized” soils (Hausmann, 1990). Cement

can be used to stabilize virtually every kind of soils include granular materials, silts and clays. In 1935, the first cement stabilized road in the United States was constructed in Jacksonville in North Carolina (Das, 1998). Cement stabilization involve mixing pulverized soil with fixed quantity of Portland cement and water. Then, the mixture is compacted to a specified density and protected against moisture loss during curing period. The curing of the mixture for a specified time enhances the soil properties.

Cement stabilization improves strength and also lower the volume changes of soils by immediately reducing the plasticity of the soils. The reduction of soils plasticity is a result of calcium ions released during the initial hydration reactions (Bugge et al., 1961). In general, cement stabilization is more effective on granular and moderately effective on cohesive soils (Chavva et al. 2005). It is more economical to use cement to stabilize granular soils due to the ease of pulverization and mixing. In the soils that have plasticity index more than 30, cement becomes more difficult to mix with the soils. In this case, lime can be added as to improve workability prior to cement stabilization (Hick, 2002). Addition of cement to the clay soils reduces liquid limit, plasticity and swell potential of the soils.

The hydration reactions of Portland cements caused by the production of different compounds and gels which increase the soils strength though complex pozzolanic reaction (Chen, 1988; Nelson and Miller, 1992). This reaction bonds soil particles together and also prevent them from swelling and softening from moisture absorption and from detrimental freezing and thawing (Bugge et al., 1961).

The ability to attract and hold water is known as plasticity in clay soils. Cement stabilization results in the immediate reduction in the plasticity of the soils due to the initial cement hydration (Bugge et al., 1961). The hydration of cement results in a release of calcium ions. These calcium ions and the clay particles, which have a charge deficiency, are capable of cation exchange by means of replacement. The replacement consists of an exposed hydroxyl of the clay particle being replaced by another type of cation (Mitchell, 1993). Due to the electrical

charge that the clay particles hold, they are attracted to one another. The attraction between these clay particles initiates the structure to flocculate. Flocculation of particles helps increase the overall strength and stability of the cement stabilized clay structure. Hydration is a primary process that supplies the compounds required for the secondary reaction.

The secondary process results in the cementation at contact points of flocculated clay particles. In the primary process, the number of complex reactions takes place and material needed for cementation of the structure is formed. The following transformed compounds are the byproducts for the interaction between Portland cement and water (Kezdi, 1979). As shown in equation 2.1, tricalcium silicate with addition of water forms tobermorite gel (silicate hydrates) and calcium hydroxide. At the next stage, as shown in equation 2.2, bicalcium silicate with addition of water will form tobermorite (silicate hydrates) gel and calcium hydroxide.

$$2(3\mathbf{Ca.SiO_2}) + 6\mathbf{H_2O} \rightarrow 3\mathbf{CaO.2SiO_2.3H_2O} + 3\mathbf{Ca(OH)_2} \quad (2.1)$$

(Tricalcium Silicate with addition of water will form tobermorite gel and calcium hydroxide)

$$2(2\mathbf{Ca.SiO_2}) + 46\mathbf{H_2O} \rightarrow 3\mathbf{CaO.2SiO_2.3H_2O} + \mathbf{Ca(OH)_2} \quad (2.2)$$

(Bicalcium silicate with the addition of water will form tobermorite and calcium hydroxide)

$$4\mathbf{CaO.Al_2O_3Fe_2O_3} + 10\mathbf{H_2O} + 2\mathbf{Ca(OH)_2} \rightarrow 6\mathbf{CaO.Al_2O_3.Fe_2O_3}12\mathbf{H_2O} \quad (2.3)$$

(Tetracalciumaluminoferrite with the addition of water and calcium hydrocide will form calcium aluminoferrite hydrate)

$$3\mathbf{Ca.Al_2O_3} + 12\mathbf{H_2O} + \mathbf{Ca(OH)_2} \rightarrow 3\mathbf{CaO.Al_2O_3.Ca(OH)_2.}12\mathbf{H_2O} \quad (2.4)$$

(Tricalcium aluminate with the addition of water and calcium hydroxide will form tetracalcium aluminate hydrate)

$$3\mathbf{Ca.Al_2O_3} + 10\mathbf{H_2O} + \mathbf{CaSO_4.2H_2O} \rightarrow 3\mathbf{CaO.Al_2O_3.Ca(SO)_4}12\mathbf{H_2O} \quad (2.5)$$

(Tricalcium aluminate with the addition of water and gypsum will form calcium monosulfoaluminate).

Compounds formed from equation 2.1 and 2.2 produce tobermorite gel, which contributes to the strength increase by. Calcium hydroxide increases the ability of the clay to flocculate by means of cation exchange during cement hydration. The reactions shown in equation 2.3, 2.4 and 2.5 produces the silicates and aluminates required for the cementation of clay particles. Through these reactions, the clay particles are transformed into a stabilized matrix structure which consists of clay sheets attracted by forces created by various transformed compounds (Kezdi, 1979). These compounds initiate the process of cementation of clay sheets through flocculation process. The new arrangement of cement particles results in increased strength and reduced volumetric changes in the structure. The overall benefits of cement-stabilized soils are increased strength and stiffness, reduced volumetric changes, and increased durability (Kezdi, 1979).

Several types of cements are available in the market. In order to meet different physical and chemical requirements for various applications, eight types of cement are manufactured. These are Type I to Type V and Type IA, IIA and IIIA are Portland cements (Kezdi, 1979). Type I cement is used for general purposes such as RC structures. Type II is used for structures built on soils with moderate amounts of sulfate content. Type III cement is one which develops high strength at an early stage usually in a week. Type IV is used for massive structures such as dams as it moderates the heat generated by hydration process. Type V cement is often suitable to stabilize high sulfate soils as it resists chemical attack due to sulfates. Table 2.3 presents the chemical compositions of Type V Cement used in the present research.

Table 2.3 Chemical Composition of Type V Cement used in this Research

Chemical Composition	Percent (%)
Calcium Oxide (CaO)	53.10
Silicon Dioxide (SiO_2)	29.33
Aluminum Oxide (AL_2O_3)	n/a

Table 2.3 - *Continued*

Sulfur Trioxide (SO_3)	3.30
Magnesium Oxide (MgO)	1.44
Loss of Ignition	0.93
Total Alkalies as (Na_2O_{eq})	0.59
Insoluble Residue (IR)	13.72
% Class F Ash	20.75
Sulfate Expansion (C-1012)	n/a

2.6.1.2 Lime

Lime or hydrated lime is a term typically used to describe calcium oxide (CaO). Hydrated lime is a term used for calcium hydroxide $Ca(OH)_2$. The relations between these three types of lime can be represented by the following equations:

1) $CaCO_3$ + heat = CaO + CO_2

2) CaO + H_2O = $Ca(OH)_2$ + heat

3) $Ca(OH)_2$ + $CaCO_3$ + H_2O

Hydrated lime comes in the form of a fine and dry powder. Quicklime is available either in granular form or as a powder. Quicklime reacts violently with 32% of its own weight to water in order to produce substantial amount of heat (approx 17 x 10^9 Joules per kg of quicklime) (Sherwood P.T., 1993). Hydrated lime and quicklime are typically added to soils in the solid form but they may also be mixed with water and added to the soil as slurry.

Lime has been successfully used to stabilize high-plasticity clay soils. Lime stabilization enhances important soils properties, such as improving their strength and resistance to fracture, fatigue and permanent deformation; improving resilient properties; reducing swelling; and improving a resistance to damages from moisture. Lime also has the ability to improve workability and reduce volumetric changes of soils (Little et al., 1987).

Lime can be used to either modify or stabilize clay soils. Lime modification provides substantial improvement to the performance of high-plasticity clay soils. The modification is a

result of calcium cation exchange between lime and clay soils in high pH environment. The modification takes place as the hydrated lime reacts with the surface of clay mineral. Results of this reaction are plasticity reduction, reduction in moisture holding capacity as well as reduction in swell and stability improvement (Little, 1987).

Lime stabilization, on the other hand, provides a substantial improvement to a long-term strength. The strength gained is a result of long-term pozzalonic reaction. The pozzalonic reaction takes place as the calcium from lime reacts with aluminates and silicates soluble from the surface of clay mineral. Lime stabilization usually offers a ten-fold stiffness increase over the untreated soils.

A protocol for lime mixture design is developed based on the following steps (Little,1987):

1) Select soils that are mineralogically reactive with lime

2) Establish optimum lime content base on a pH test and a compressive strength test

3) Evaluate resistance to moisture-induced damage through a capillary suction test in which the surface dielectric value of the cured, lime-treated sample is measured

The addition of lime to problematic soils reduces swell potential, liquid limit, plasticity index and maximizes dry density of the soils whereas increase the optimum moisture content and strength (Croft, 1967). The optimum amount of lime required for modification is typically between 1% and 3% lime by dry weight. Further addition of lime does not enhance plasticity of soils but it will only enhance strength (Croft, 1967). In comparison, the optimum amount of lime required for soil stabilization is usually between 2% and 8% measured in the dry weight of soils (Basma and Tuncer, 1991).

Resilient properties of soils stabilized by lime are very sensitive to the level of compaction, molding moisture content and curing time. Lime stabilization substantially

increases shear and tensile strength of the soils, hence enhances stiffness of subgrade layer in pavement structure.

2.6.1.3 Class F Fly ash with Type V Cement

One of the byproducts of coal combustion in electrical generating units is coal ash (Ferguson, 1993). Coal ash is comprised of three main components including fly ash (flue gas stream), boiler slag (coats boiler tubes) and bottom ash (sand size material + boiler slag). The components of coal ash have different percentages of compositions and particle sizes. Based on the types of coal, burners and boiler, 65 % to 85 % of the organic material is fly ash. The finest particle is the fly ash that is collected from the suspension of combustion chamber in the exhaust gases in which most of the fly ash is Class F type of fly ash. Bottom ash is a relatively coarser and denser material than fly ash and it is collected by gravity of the lower level (Nicholson and Kashyap, 1993).

Fly ash is defined as the mineral matter extracted from the flue gases of a furnace fired with coal. Fly ash is composed of hollow spheres of silicon, aluminum and iron oxides, and unoxidized carbon (Nicholson and Kashyap, 1993). Fly ash can be classified as class F and Class C types as per ASTM C 618 method. Class F fly ash is made from the burning of bituminous or anthracite coals while Class C fly ash is produced from the burning of sub-bituminous or lignite materials. The composition of fly ash varies considerably depending on the nature of the burned coal and the characteristics of power plant operational (Nicholson and Kashyap, 1993). Fly ash is a known pozzalonic material, which is defined as siliceous or siliceous and aluminous. Therefore, its engineering behavior can be improved by the addition of cement or lime. The chemical compositions of Class F and Class C Fly ash are shown in Table 2.4.

Table 2.4 Chemical Composition of Fly ash

Properties	Fly ash Classes	
	Class F	Class C
Silicon dioxide (SiO_2) plus aluminium oxide (AL_2O_3) plus iron oxide (Fe_2O_3), min, %	70.0	50.0
Sulfur trioxide (SO_3), max, %	5.0	5.0
Moisture Content, max, %	3.0	3.0

The most significant difference between Class F fly ash and Class C fly ash is the amount of calcium, silica, alumina and iron contained in the ash. Class F Fly ash contains calcium in the range of 1 to 12%. Calcium presented in Class F Fly ash is mostly in the form of calcium hydroxide, calcium sulfate, and glassy components in combination with silica and alumina. Moreover, others differences between Class F fly ash and Class C fly ash are: content of sulfates are generally higher in Class C fly ash when compared to Class F fly ash; percentage of free calcium in Class C fly ash is higher when compared to Class F fly ash.

The addition of cement to fly ash provides a considerable increase in soil strength and stiffness properties to the soils (McManus and Nataraj, 1993). The stabilization of the soils by fly ash consists of short-term and long-term reactions (Diamond and Kinter, 1965; Usmen and Bowders, 1990; Glenn and Handy, 1963; Davidson et al., 1958). The short-term reaction involves flocculation and agglomeration of clay particles. The flocculation and agglomeration of clay particles take place due to ionic exchange at the surface of soil particles. The long-term reactions involve the increase of the strength properties in the treated soil, which depend on the

rate of chemical breakdown and hydration reactions of silicates and aluminates. These reactions may take a few weeks up to many years.

A hydration of free lime (CaO) and the pozzalons (AlO3, SiO2, Fe2O3) with water is required to form cementitious material. These hydration reactions occur by alkali or alkali earth hydroxides to form cementitious products in the presence of moisture at room temperatures. The hydrated calcium silicate gel or calcium aluminate gel (cementitious material) binds the inert materials together. The availability of pozzalons is very important in order to form cementation reaction. This is because pozzalons is the source of silica and alumina. (Nicholson and Kashyap, 1993).

The calcium oxide (CaO) in Class C fly ash can react with the siliceous and aluminous materials (pozzolans) presented in the fly ash itself. On the other hand, the pozzolanic reactions from Class F Fly ash require the addition of lime since a lime content in Class F Fly ash is relatively low. Fly ash may be used as an admixture to eliminate the pozzalonic deficiency of soil with the supply of steady source of pozzolans. (Usmen and Bowders, 1990).

Factors that affect the reaction rate of the fly ash are soil types, surface area of the soil particles, temperature, moisture content, chemical composition of fly ash admixture, and the amount of stabilizer used in the mixture (Usmen and Bowders, 1990). The pozzalonic reactions in lime stabilization rely on the siliceous and aluminous materials in the soils. The reactions in the stabilization of lime to the soils are:

$$\mathbf{Ca(OH)_2 => Ca^{++} + 2[OH]^-} \qquad (2.6)$$

$$\mathbf{Ca^{++} + 2[OH]^- + SiO_2 => CSH} \qquad (2.7)$$

(silica) (gel)

$$\mathbf{Ca^{++} + 2[OH]^- + Al_2O_3 => CAH} \qquad (2.8)$$

(alumina) (gel)

Equation 2.6 shows the primary cementitious products as a result of hydration of tricalcium aluminate in the Fly ash. The quick setting of these compounds is due to rapid hydration rate of tricalcium aluminates which in turn delays the compaction process and results in lower strength enhancement to the stabilized soils (Usmen and Bowders, 1990).

Wattanasanticharoen (2000) reported that the utilization of cement along with Fly ash provides a better treatment for the soils in Southeast Arlington. The addition of Cement and Fly ash to the soils also enhances plasticity properties to the soils (Nicholson and Kashyap, 1993). Furthermore, the researches at The University of Texas at Arlington also show that the stabilization of Fly ash reduces both swell and shrinkage strains of soils by decreasing the plasticity index of the soils (Puppala et al., 2000).

In this research project, Class F Fly ash was selected as one of the stabilizers to stabilize high sulfate soils in Southeast Arlington. Class F Fly ash is preferable over Class C Fly ash because Class F Fly ash contain lower amount of calcium which in turn reducing the formation of ettringite based heaving (Nicholson and Kashyap, 1993). The chemical composition of Class F Fly ash is shown in Table 2.5.

Table 2.5 Chemical Characteristic of Class F Fly ash (Wattanasanticharoen, 2000)

Chemical Analysis	Results
Silicon Dioxide (SiO_2), %	56.7
Aluminum Oxide (AL_2O_3), %	29.5
Iron Oxide (Fe_2O_3), %	4.9
Sum of SiO_2, AL_2O_3, Fe_2O_3, %	91.1
Calcium Oxide (CaO), %	1.1
Magnesium Oxide (MgO), %	0.8
Sulfur Trioxide (SO_3), %	0.1
Moisture Content, %	0.2
Loss on Ignition, %	2.2

Table 2.5 - *Continued*

Amount Retained on No. 325 Sieve, %	29.8
Specific Gravity	2.28

2.6.1.4 Ground Granulated Blast Furnace Slag (GGBFS)

Ground Granulated Blast Furnace Slag (GGBFS) has been used as a stabilizing agent in many countries include the United States, the United Kingdom, Germany, Holland and other Asian countries. The chemical composition of GGBFS is similar to that of Portland cement. Blast furnace slag is a by-product of iron production. Slag is composed of siliceous components of iron ore and limestone flux Coal ash that is used for melting iron (Sherwood, 1995). Various kinds of slag are produced during the manufacture of metals from their ores but the only product that is suitable to be used as a cementitious material is GGBFS (Ozyildirim et al., 1990). When slag is ground to the fine particles of Portland cement, the granules are called GGBFS. The alkalies are released by the hydration of cement when GGBFS is mixed with cement. GGBFS has been successfully applied as a raw material of cement block, pavement block, and slag cement.

The addition of cement along with GGBFS increases the strength of the stabilized soil. Because the cost of GGBFS is lesser than the cost of cement, the cost efficiency of soils stabilization can be achieved by designing appropriate cement and GGBFS proportions. Ozyildirim et al (1990) achieved a successful replacement of Portland cement in soil stabilization with slag, which resulted in a significant decrease in the cost of the soil stabilization.

Ozyildirim et al (1990) reported that the permeability of the soil stabilized with GGBFS can be reduced significantly. The reduction of permeability of the stabilized soils depends on the amount of the slag added. The permeability is reduced by a reduction of pore size associated with the production of dense calcium silicate hydrates in hydration process which takes place

during the stabilization. The decrease in permeability in turn would provide high chemical resistance in aggressive environments and increase the sulfate resistance to the soils.

The slag stabilization enhances soils properties, such as increasing the resistance to sulfate of the soils, increasing shear strength and decreasing the plasticity index, swelling potential and shrinkage strains (Ozyildirim et al., 1990). The amount of slag in the Portland cement clinker may vary from very low to as high as 85%. The properties of these cementitious materials are essentially similar to those of Portland cement (Sherwood, 1995).

Wang et al. (1998) conducted a research program in England to study the behavior of the GGBFS stabilization on sulfate-rich soils. The study showed that the addition of 20% GGBFS by dry weight of soils results in the considerable strength improvements along with a reduction in plasticity properties and swell and shrinkage behavior of the soils, after three days of curing by addition of 20% of GGBFS stabilizer (Wang et al, 1998). Therefore, GGBFS was selected as one of the four stabilizers used in the present research. The chemical composition of the GGBFS used in this research is presented in Table 2.6.

Table 2.6 Composition of Blast Furnace Slag (Wattanasanticharoen, 2000)

Chemical Constituents (Oxides)	Range of Composition, (Percent by Mass)
SiO_2	32-40
Al_2O_3	7-17
CaO	29-42
MgO	8-19
S	0.7-2.2
Fe_2O_3	0.1-1.5
MnO	0.2-1.0

2.6.1.5 Lime Mixed with Polypropylene Fibers

Lime is the most widely used stabilizing agents for expansive soils (Gedney and Weber, 1978). In the United States, lime has been successfully used in various applications to improve the foundation of infrastructures, including highways, railroads and runways (Winterkorn & Pamukcu, 1991). During the past two decades, lime stabilization has significantly increased in the United States Scandinavia and Southeast Asia (Bergado et al., 1991; Broms, 1984; Holm et al., 1983). In 1987, 750,000 tons of limes were used in the soil stabilization projects all across the United States. Approximately 80% of the lime used was hydrated lime and the remaining 20% of the lime was quicklime (Gillott, 1987).

Hydrated lime is available in the form of a fine and dry powder while quicklime is available either in granular form or as a powder form. Both hydrated lime and quicklime are used in slurry form. The addition of lime to expansive soils increases the plasticity properties of the soils, including a reduction in swell and shrinkage strains, an increase in shear strength and a reduction in the compressibility and permeability properties (Broms and Boman, 1979; Littlle, 1987; Puppala et al., 1998).

When a certain amount of lime is added to the soils, the dehydration reaction will take place. Calcium hydroxide is a product of the dehydration reaction. In the presence of water, the dissociation of calcium hydroxide increases the electrolytic concentration and the pH of the soil. The calcium hydroxide dissociation is explained in the equation 2.4 (Schoute, 1999):

$$\mathbf{Ca(OH)}_2 \Rightarrow \mathbf{Ca}^{2+} + 2\mathbf{[OH]}^- \qquad (2.4)$$

The released calcium ions will participate in the cation exchange reactions in soils and the following important processes occur in soils are due to the mentioned reactions (Rogers et al., 1997):

- Reduction in susceptibility to water addition due to reduced thickness of electric double layer.

- Flocculation of the clay particles with weak bonds between the particles, which is caused by an increase in mutual attraction due to decrease in electric double layer (Diamond & Kinter, 1965).
- Internal angle of friction between the particles increases due to flocculation.
- Textural change from plastic clay to a granular, friable material.

Although lime has been extensively used in the United States, the addition of lime to sulfate-rich soils results in sulfate induced heave distress problems (Kota et al., 1996). Several infrastructure projects in Texas, Oklahoma, Kansas, Nevada and Colorado suffer from sulfate induced heave distress problems due to the formation of ettringite mineral when treated with lime (Puppala et al., 2000). Therefore, several research studies have been conducted to understand the heaving mechanism in chemically stabilized sulfate-rich soils and to develop appropriate stabilization methods to control sulfate induced heave problems (Viyanant, 2000). Moreover, lime stabilization has also caused some leaching problems and it is not suitable for granular soils and other soils that require significant strength enhancements.

In order to overcome the problems associated with lime, polypropylene fibers are used to reinforce soils since they are cost effective and also reduce the intake of natural raw materials when compared to chemical stabilizing agents. Fibers can be manufactured with desirable properties from recyclable materials to the specified dimensions. At present, fibers are used to enhance the soils properties including strength enhancements, reduction of shrinkage properties and reduction of chemical and biological degradation (Puppala and Musenda, 2000). Fibers are used in concrete and mortar to reduce shrinkage related cracks (Puppala and Musenda, 2000). Similar advantages of fibers are expected to improve the soil properties when used along with lime stabilization to control the volume change behavior.

Properties of the fibrillated polypropylene fibers are presented in Table 2.7 (Boral Material Technologies)

Table 2.7 Fiber Properties used in this Research

Physical Properties	Magnitude
Material	100% virgin polypropylene
Tensile Strength	97 ksi
Young's Modulus	580ksi
Melting Point	330 °F
Ignition Point	1100 °F
Specific Gravity	0.91
Bulk Density	56 lbs/ cubic ft.
Dosage	1.5 lb/ cubic yard
Form	Fibrillated Polypropylene
Fiber Count	8-12 million/ lb
Chemical Resistance	Excellent
Alkali Resistance	Excellent
Acid and Salt Resistance	High
Fiber Length	0.75"
Absorption	NIL

2.6.1.6 Bitumen

Bitumen occurs in natural asphalt either in the form of a solid or a viscous liquid. It can be derived from petroleum. This stabilizing agent consists mostly of hydrocarbons, thus it has strong adhesive properties (Day, 2000). In natural condition, bitumen is too viscous to be used for stabilization and it has to be rendered fluidizer either as "cutback" bitumen or a "bitumen emulsion" (Day, 2000). Cutback bitumen is a solution of bitumen in kerosene and diesel fuel. Emulsions are suspensions of bitumen particles in water. When emulsion is broken, the bitumen is deposited on the soils.

In comparison with lime and cement, bitumen does not react chemically with the soils. Bitumen acts as a binding agent which simply sticks the particles together and prevents ingress of water. Bitumen is suitable for the area that has hot dry climates where water has frequently to be added to ensure that adequate compaction is achieved.

2.6.1.7 Evaluation and Comparison of Stabilization Methods

The selection of a suitable stabilization method for the soils requires a thorough consideration of soil types, climatic conditions and drainage conditions. Hicks (2002) suggested the following guide to select suitable method of stabilization:

Soil type: a prime assessment for the method of stabilization for particular soils can be conducted though particle size distribution and Atterberg limits. The selection of stabilization methods is based on the amount of soils passing #200 sieve and the plasticity index of the soil. Figure 2.11 provides the initial guidance for selecting stabilizer type. Table 2.8 shows the comparison of the Process, effects and applicable soil type of the stabilizing agents

Climatic conditions: climatic condition is also a very important factor affecting the selection of the suitable stabilization method for the soils. This is because strength of soils can be greatly affected by moisture. For example, in wetter areas where the moisture content of the pavement materials is high, it is important to ensure that the wet strength of the stabilized material satisfies the designed target strength. In these conditions, cementitious binders are usually preferred. Though, asphalt and asphalt/cement blends would also work. Lime is suitable for cohesive soils, particularly when lime is used to dry out the soils. Lime can also work with silty soils if a pozzolan is added to promote the cementing reaction. Using emulsions in cold dry climates requires using cement or lime to facilitate moisture removal from the emulsion during the stabilization process and to promote the strength.

In order to enhance the strength and reduce free swell and shrinkage strain potentials of soft, expansive and sulfate-rich soils, Puppala et al. (2003) studied the use of four types of stabilizers including sulfate-resistant cement (Type V), lime mixed with polypropylene fibers,

ground granulated blast furnace slag (GGBFS) and Class F fly ash. This study showed that sulfate-resistant cement provided the most effective improvements to the soil properties. The improvements were due to ion exchange, flocculation, cementation and pozzalonic reactions. Combined lime and polypropylene fibers stabilization method provided the next best effective treatment. They enhanced UCS and reduced PI, swell and shrinkage strains. GGBFS provided the third best performance. It reduced the swell, shrinkage and plasticity characteristics while increasing the UCS values. Nevertheless, the soils stabilized by GGBFS exhibited less improvement in strength, and swell and shrinkage behaviors compared to the cement and lime plus fiber treatment methods. Class F fly ash provided low-to-moderate strength improvements that could be attributed to the low amounts of calcium present in this type of fly ash. On the other hand, fly ash stabilization was more cost-effective than the others methods.

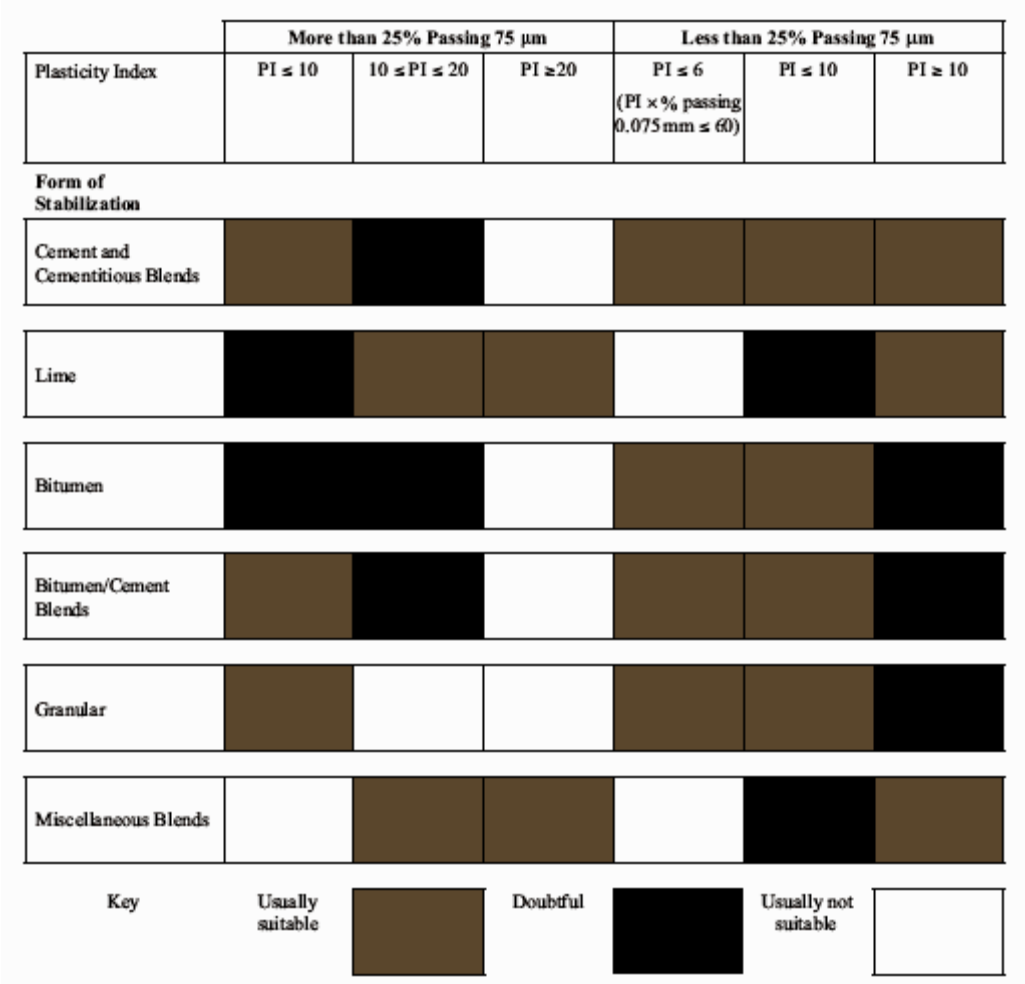

Figure 2.11 Guides to Select Stabilization Method* (Hick, 2002).

Table 2.8 Comparison of Stabilizing Process, Impact on Soil types (Hicks, 2002)

Stabilizing Agent	Process	Effects	Applicable Soil Types
Cement	• Cementitious inter-particle bonds are developed.	• Low additive content (<2%): decrease susceptibility to moisture changes, resulting in modified or bound materials. • High additive content: increases modulus and tensile strength significantly resulting in bound materials	• No limited apart from deleterious components (organics, sulfates, etc., which retard cement reactions). • Suitable for granular soils but insufficient in predominantly one sided materials and heavy clays.
Lime	• Cementitious inter-particle • Bonds are developed but rate of development is slow compared to cement. • Reactions are temperature	• Improve handling properties of cohesive materials. • Low additive content (<2%): reduce decreases susceptibility to moisture changes, and improves strength, resulting in modified or bound materials.	• Suitable for cohesive soils. • Requires clay components in the soil that will react with lime (i.e., contain natural pozzolan). Organic materials will retard reactions.

Table 2.8 - *Continued*

	dependent and require natural pozzolan to be present. Otherwise, a blended binder that includes pozzolan can be used.	• High additive content: increases modulus and tensile strength, resulting in bound materials.	
Blended slow-setting binders (for example: fly ash/lime, slag/lime/fly ash blends)	• Lime and pozzolan modifies particle size distribution and develops cementitious bonds.	• Generally similar to cement but rate of gain of strength similar to lime. Also improves workability. Generally reduces shrinkage cracking problems.	• Same as for cement stabilization. Can be used where soils are not reactive to lime.

43

Al-Rawas et al. (2005) evaluated the effectiveness of lime, cement, and combinations of lime and cement stabilization on swell potential of expansive soils. The liquid limit of all treated samples except for samples treated with 5% lime plus cement showed an initial increase at the addition of 3% stabilizer, followed by a gradual decrease. In contrast, the samples treated with combinations of lime and cement exhibited an initial reduction at 3% lime + 3% cement and 5% lime + 3% cement followed by a general increase with further additions. All stabilizers caused a reduction in both swell pressure and swell potential. With the addition of 6% lime, both the swell potential and swell pressure were reduced to zero.

2.6.1.8 Injection of Aqueous Solution

The utilization of an aqueous solution of potassium and ammonium ions to treat expansive clay soils was introduced by Pengelly and Addison (2001). In general, the type of clay mineral associated with heave is Montmorillonite. All clay particles or minerals are composed of sheets of silica and alumina. This stabilization technique relies on reactions between the solution ions and the clay soil.

Ions such as calcium, magnesium or sodium are attracted to the surface of the clay particle in an attempt to balance the net negative charge of the clay particle. Swell potential of clay is directly related to cation hydration energy (its attraction to water molecules) and the hydrated radius of the interlayer cations. The repulsive forces from the hydration cause swelling. Pengelly and Addison (2001) recommended four commonly occurring cations with high hydration energies and low hydrated radii as follow: potassium, ammonium, rubidium and cesium.

Pengelly and Addison (2001) used potassium and ammonium as cations and mixed them in a solution of water to modify clays underneath an existing building structure. The addition of potassium and ammonium to the clays significantly reduced swelling at lower moisture contents. In addition, swell caused by the addition of an aqueous solution containing potassium and ammonium was consistently lower than that caused by water alone.

Mowafy et al. (1985b) also reported that the presence of sodium chloride in the pore fluid causes a decrease in swell potential. The injection of salt solutions could be a possible remediation method to overcome swelling problem if the soil permeability is sufficiently high.

Although chemical stabilization has been successful used to enhance plasticity of expansive soils, there are situations where chemical stabilization cannot be used. For example, chemical stabilization cannot be used when the temperature is below 40 °F and in some cases there are not enough time for curing period to be achieved (Hopkins et al., 2005). Hence other treatment methods for stabilizing expansive soils

2.6.2 Moisture Control

The M-E Design Guide recommended the following options to be used for conventional and deep-strength HMA pavements:

• Full-width paving to eliminate the lane/shoulder cold joint, which is a major source of water in the pavement structure.

• Provision of a granular layer between the subgrade and base course to reduce erosion, allow bottom seepage and minimize frost susceptibility that could increase pavement roughness.

2.6.2.1 Horizontal moisture barriers

Horizontal moisture barriers have the main function to prevent the access of rainfall infiltration to the subgrade layer of pavement structure. The advantages of waterproofing the pavement structure are: reducing moisture variance, reducing swell potential of subgrade soils, and hence maintaining pavement smoothness. Browning (1999) reported that horizontal moisture barriers maintain a good riding quality to the pavement compared to unprotected pavement.

2.6.2.2 Vertical Moisture Barriers

Vertical moisture barriers have been extensively and successfully used across the United States. The function of the vertical moisture barriers is to prevent the expansion of subgrade soils from rainfall infiltration (Jayatilaka et al., 1993). The vertical moisture barrier is

used to prevent the lateral migration of moisture to subgrade soils beneath the pavement and also used to prevent them from expansion and shrinkage during wet and dry periods (Picornell and Lytton, 1986).

Evans and McManus (1999) have reported that the effectiveness of the barrier is proportional to the barrier depth. Field trials have also shown that the deeper barrier (8 ft) outperformed the shallow barrier (6 ft) in maintaining a more moisture consistence in the soils; hence further reduced the vertical movements. However, the deeper barrier is more expensive than the shallow barrier. Therefore, the use of vertical moisture barriers has been limited to be used for major highways only.

Evans and McManus (1999) reviewed current construction methods for the vertical moisture barrier in the United States and developed a new economical barrier construction technique for low-volume roads. The technique comprised of a spray seal surface over the low-quality base and subgrade. Although the construction of moisture barriers in the United States over the last 20 years has led to the cheaper barrier, this barrier is still too expensive for low-volume road applications. The cost of this new barrier is about $3.10 per foot and this technique also has several disadvantages. The rounded gravel backfill commonly used in Texas (TxDOT Special Specification No. 5431) is not ideal materials since this kind of backfill provide a moisture path to the bottom of the barrier that promotes deep-seated swelling. Figure 2.12, Figure 2.13 and Figure 2.14 show equipments and constructions of vertical moisture barriers.

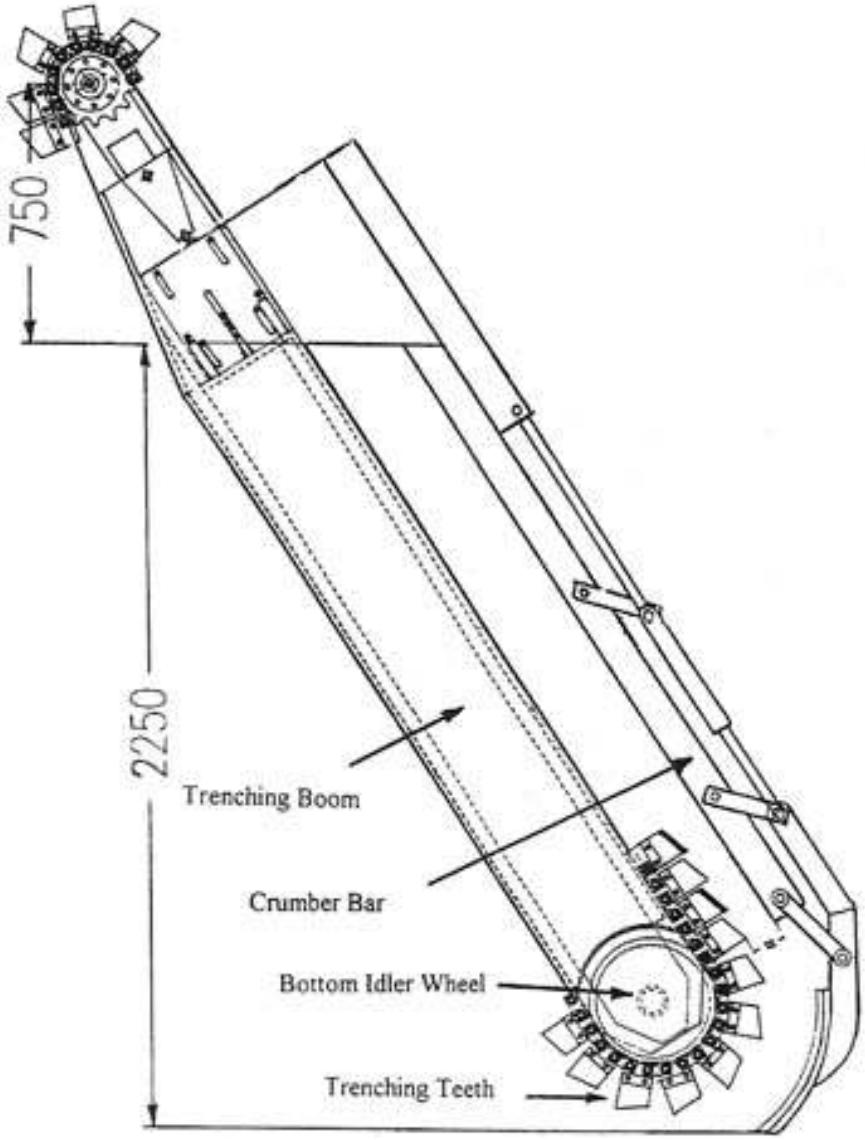

Figure 2.12 Slim-line Trenching Boom and Crumber Bar Design (Evans and McManus, 1999).

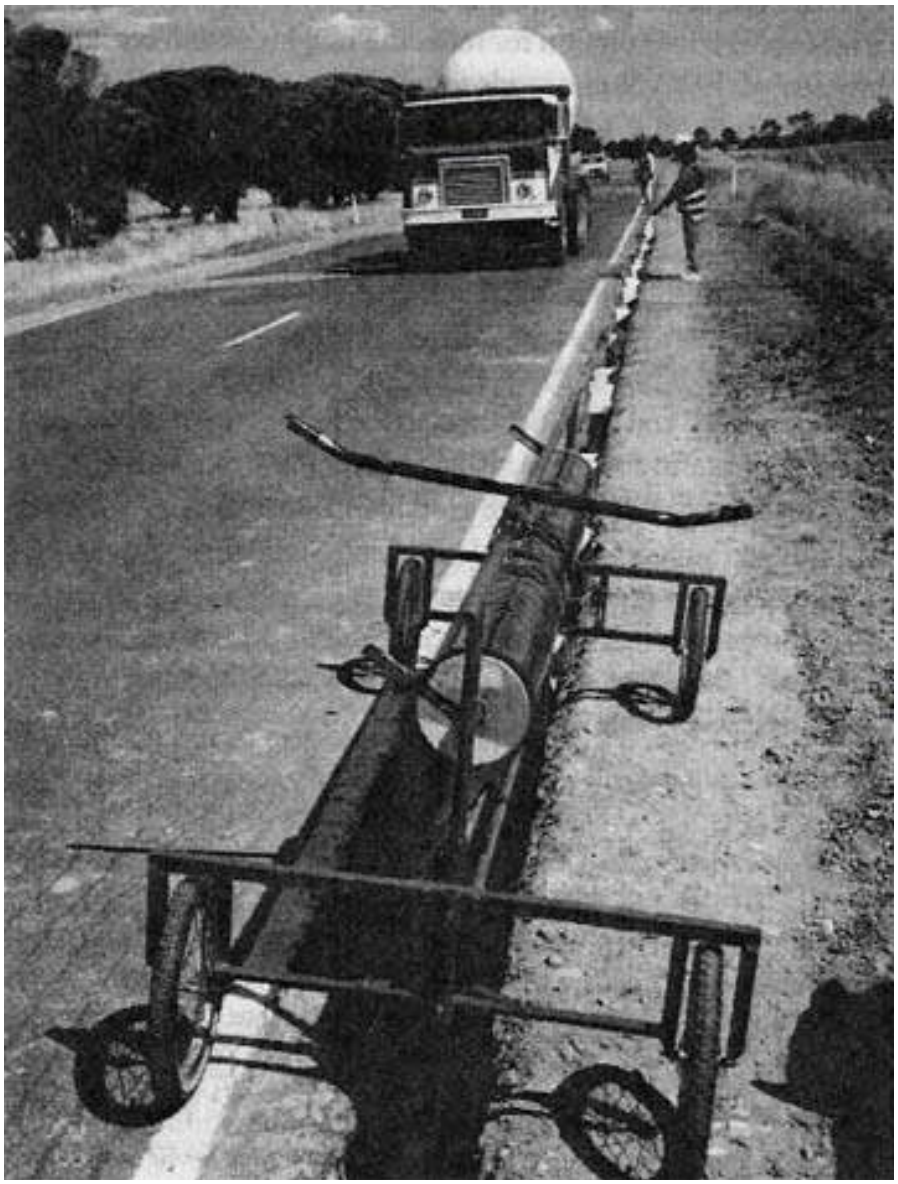

2.13 Membrane Dispenser and Membrane Held by Polystyrene Wedges (Evans and McManus, 1999).

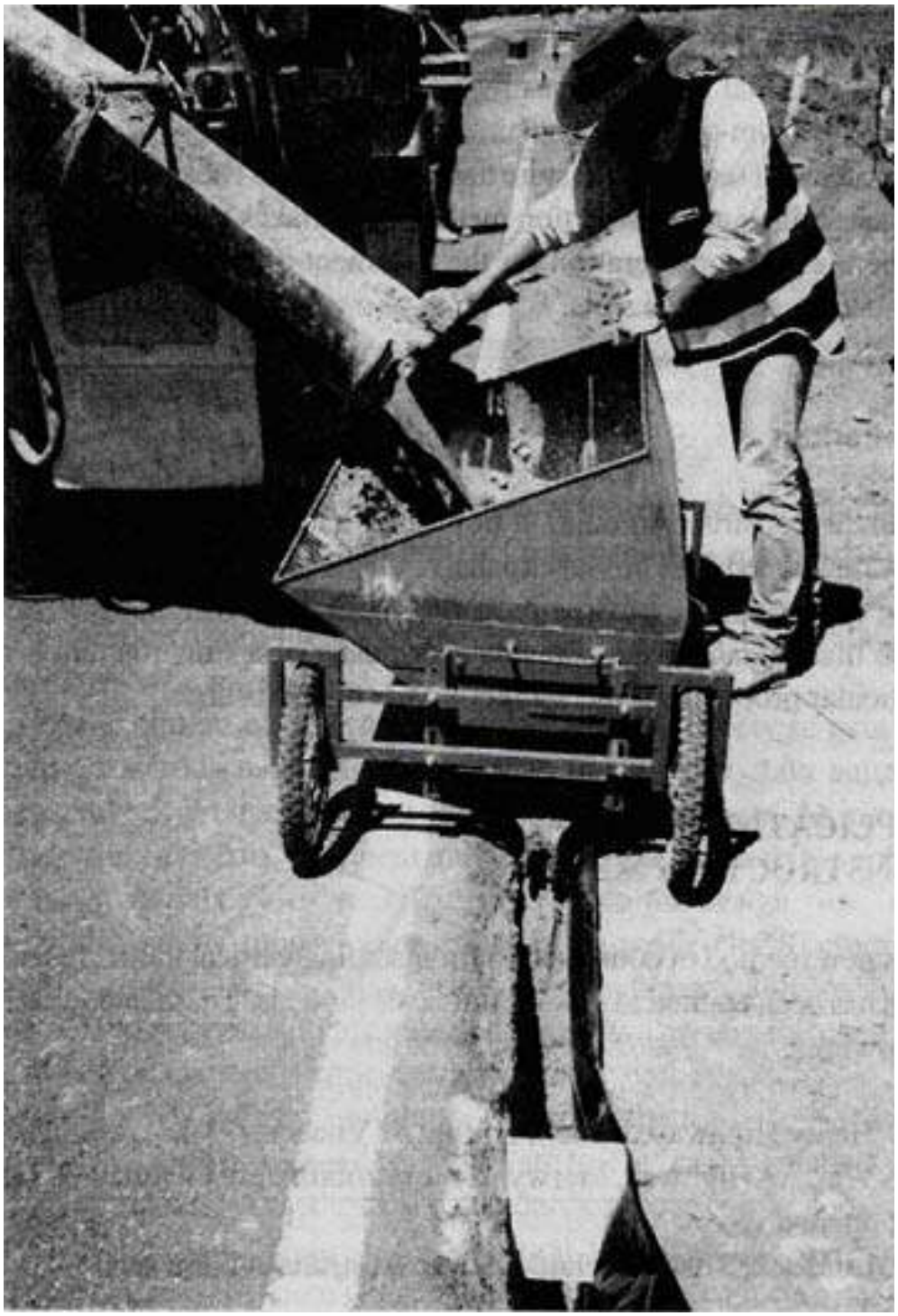

Figure 2.14 Membrane, Polystyrene Wedges, and Placement of Flowable Fill (Evans and McManus, 1999).

.

2.6.2.3 Drainage Improvement

According to M-E Design Guide, the application of subsurface drainage is recommended inpavement construction as to:

- Lower the ground water level
- Intercept the lateral flow of subsurface water beneath the pavement structure
- Remove the moisture in pavement structure

The application of surface drainage is necessary in pavement construction. For example, placing a permeable layer over swelling soils can limit and prevent drainage from it. Moisture buildup in this layer maintains the soils in a stable and saturated condition. The lack of adequate surface drainage causes problems with both collapsible and expansive soils (Rolling and Burke, 1999).

2.6.3 Use of Geosynthetics

Subgrade bearing capacity is one of the major factors for a better performance pavement. The addition of a geosynthetic layer to a pavement structure can increase the bearing capacity of the soils by forcing the soil surface that responsible for the potential bearing capacity to develop the alternate and higher shear strength surfaces. The geosynthetic reinforced layer can absorb the additional shear stresses which would otherwise be applied to the problematic subgrade soils. For example, in case of rutting, geosynthetic reinforcement is distorted and tensioned. The curved geosynthetic exerts an upward force caused by its stiffness to support the wheel load. Hence, the lateral restraint and/or membrane tension forces can also contribute to load carrying capacity of the subgrade soils (Hufenus et al., 2006). However, the addition of geosynthetic layer to flexible pavements is difficult due to number of uncertainties arise when geosynthetic is applied under distress. There are no simple rules to make a guideline for a geosynthetic reinforced flexible pavement. The absence of an acceptable design technique explains why this topic is still being researched despite geosynthetics were used in pavement design and construction over many years ago.

In general, there are eight types of geosynthetics (Figure 2.15): geotextiles, geogrids, geonets, geomembranes, geosynthetic clay liners, geopipe, geofoam, and geocomposties (Koerner, 2005). Geotextiles and geogrids are the most widely used geosynthetics in the pavement construction industry.

Geotextiles are composed of synthetic fibers rather than natural fibers. These synthetic fibers can be classified as woven, non-woven, or knitted textile fabric. Geogrids are plastics formed into a very open and grid-like configuration. Geofoams are lightweight foam blocks that can be stacked and to provide lightweight fill in numerous applications. Geocomposites consist of a combination of geotextiles, geogrids, and/or other geosynthetics in a factory-fabricated unit.

Geogrids have higher tensile strengths than geotextiles. Geogrids should be used on weak subgrades with CBR values less than three (Tutumluer et al., 2005). According to the SpectraPave2™ analysis results, the use of geogrids can effectively reduce the aggregate thickness requirements when compared to the unreinforced section results. Geogrids with higher tensile strength and high aperture stability moduli were found to give overall higher geosynthetic stiffness and hence work better than geotextiles (Giroud and Han, 2004a, b). Stiff biaxial geogrids were first used for the reinforcement of pavement in 1982 at Canvey Island, near to London, England to control reflective cracking. The use of geogrids and geotextiles is becoming more common nowadays (Austin and Gilchrist, 1996).

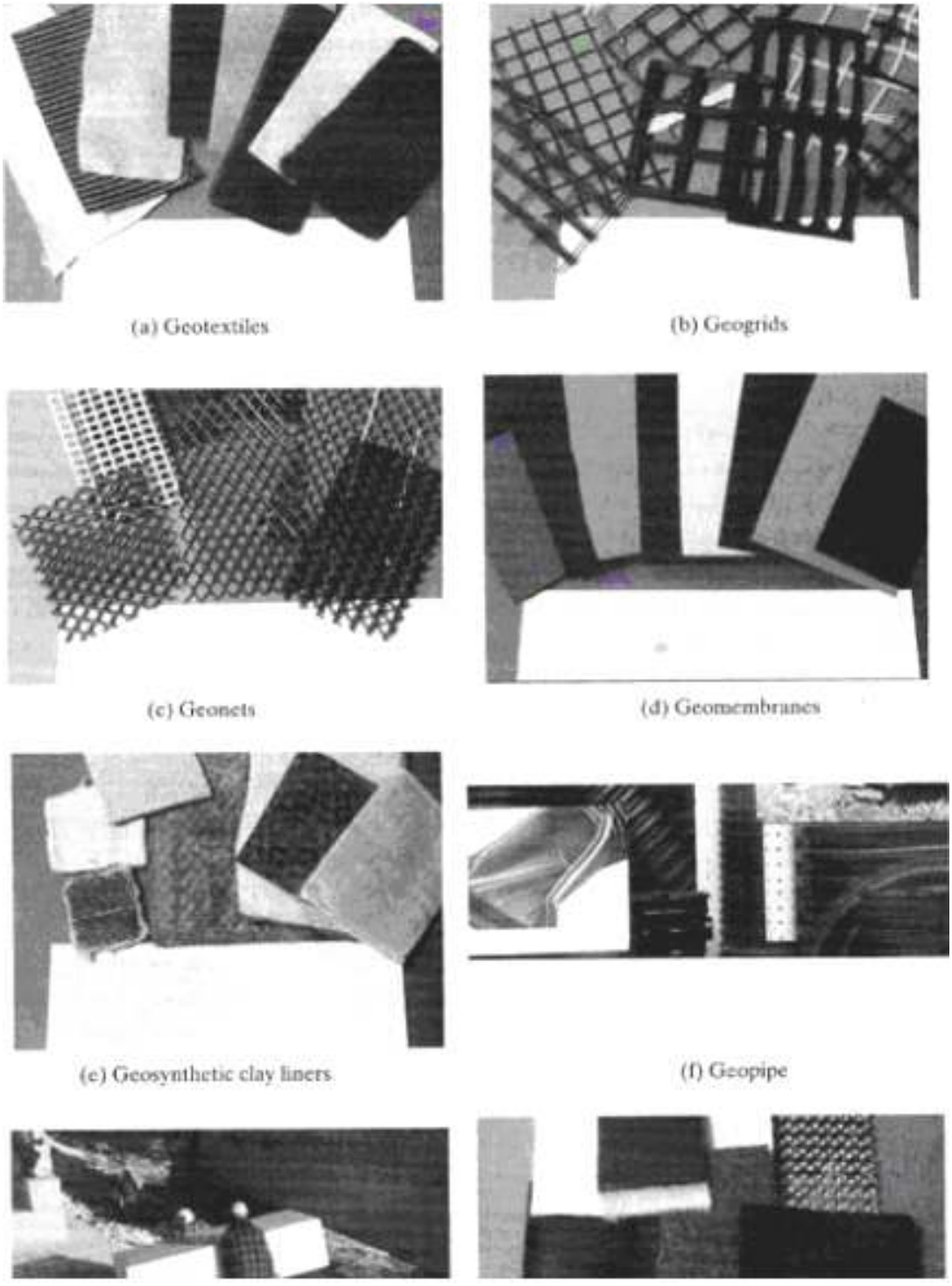

Figure 2.15 Eight Types of Geosynthetics (Koerner, 2005).

Expansive soils can be stabilized by reducing volume changes behavior of the soils. This can be done by controlling the soil water content and also by reducing the swell and shrink potential of the soil. The commonly used methods to control water access to subsoils include placement of vertical moisture barriers either by grout columns or cutoff walls or geomembranes. Vertical moisture barriers placed adjacent to pavements down to the maximum depth of moisture changes can be effective in maintaining uniform soil moisture within the barrier. Steinberg (1992) presented a case study in San Antonio. In this case study, geomembranes were used for subgrade encapsulation. Although the final outcome of this research was mixed, it offered a potential method to maintain moisture variations within the barrier.

The main objective of chemical stabilization is to reduce the heaving nature of expansive soils by chemically altering the plasticity property and reduce their volume change behavior. Selections of the chemical treatment methods are currently influenced by the amount of soluble sulfates present in the subsoils and as a result, other alternate methods including sulfate resistant cement, combined lime-fiber and GGBF treatments are currently being explored (Puppala et al., 2003). All these methods and their results were reviewed and considered as the final strategy guidelines for potential stabilization of expansive high PI clayey soils.

In order to minimize the damages caused by sulfates and calcium-based stabilizers, Kota et al. (1996) provided the following suggestions:

- Low calcium stabilizers, such as cement and fly ash
- Non-calcium stabilizers
- Asphalt stabilization of the sulfate bearing soils
- Geotextile or Geogrid soil reinforcement
- Stabilization of the top with non-sulfate select fill
- Pretreatment with barium compounds

- Compacting to lower densities

The first four methods are already described. The last three methods including use of select backfill, barium treatment, and compacting lower densities provided improvements in sulfate soils. However, they also have some limitations such as lower strength, requires environmental permits as in the case of barium treatment. As a result, newer treatment methods are always seeked by the researchers. A few of them that are under research evaluation are already described in earlier sections.

2.7 Pavement Instrumentation

The growing demands of a better performance pavement have been a challenge to pavement engineers. During the past three decades, attempts were made to enhance the performance of pavements by analysis and design, which involve a measure of stresses and strains at critical locations inside a pavement system, and then compare them to calculated strain levels at critical locations in the pavement system for determining failure strains. This may be conducted through pavement instrumentation. Pavement instrumentation is the device used to monitor the behavior of road pavements. These devices are used to identify the critical sections in the pavement, select and calibrate sensors, and identify the possible errors in the pavement structure.

The primary requirement of any pavement instrumentation project is that it should be part of a lucid pavement research program to obtain maximum benefits (Nassar, 2001). A few published reports show the variability associated with pavement instrumentation. The process itself is complex, with a lot of variability associated with the installation, sensor-pavement interactions, data acquisition, and interpretations.

Without proper understanding of the functions of sensors, the assessment of pavement performance through the use of instrumentation may lead to unreliable results (Nassar, 2001). The benefits from pavement instrumentation projects are undoubtedly significant and there is a lot of information can be achieved. Once proper planning is accomplished, collected data can

be used to validate existing or novel design approaches. These design approaches are accomplished by evaluating field measurements such as stresses, strains and deflections in the field. This part of the literature reviews and discussion of the instrumentation facilities are available at present.

Currently, pavement instrumentation is experiencing a technological uprising to withstand the infrastructure demands by understanding the material performance in the field, as well as pavement system response to loading and environment. This uprising is towards the developing sensors to measure pavement response parameters. Parameters that are needed to be considered in the field include strains, stresses, deflections, moisture, and temperature. Measuring these parameters in the field allows for providing accurate performance and designing better pavements (Nassar, 2001).

Soil properties required in the analysis and design in geotechnical engineering have been conventionally determined based on laboratory and in-situ test results (Nassar, 2001). The laboratory tests conducted in controlled environments provide the physical strength and compressibility characteristics of the soils. Soils demonstrate large variations in its behavior in real field conditions due to its heterogeneous nature when compared to other civil engineering materials. The variation in its nature can be attributed to geological history of soil formation, location of formation, temperature and environmental characteristics (Nassar, 2001). Laboratory test results can only provide an approximate behavior. These results need further assessments in real field conditions for the more accurate analysis and design. Therefore, field instrumentations are needed as more accurate and reliable techniques to measure physical and engineering properties of soil in the field conditions.

2.7.1 Instrumentation Devices Used in Geotechnical Engineering

Instrumentation that has been used in geotechnical applications includes foundations, retaining walls, slope stability, and excavations. Parameters like volumetric and gravimetric moisture contents, pore water pressure, overburden pressure, displacement and strain are very important to be monitored as they directly influence the behavior of soil and structural response.

Therefore, the utilization of pavement instrumentation is essential to understanding material performance in the field as well as pavement system response to loading and environment. The following sections summarize the various instrumentation devices used in geotechnical engineering based on parameters they measure.

2.7.1.1 Strain Measurement Devices (Turner and Hill, 1999)

Attempts were made to enhance pavement analysis and design by measuring the strains at critical locations inside pavement structures. The results will be compared to the calculated strain levels at critical locations in the pavement system for determining failure strains. Measurement or calculation of traffic-induced pavement strains at specific locations is important to predict the failure mechanisms and understand material performance in the field. Formerly, mechanical strain measurement devices were used to correlate displacement of the arm of the gauge to the strain. This method is laborious as the strain readings have to be recorded manually. The only advantage of these mechanical gauges over electronic gauges is that they do not need electricity for the operation. However, the electronic gauges are preferred because they are easy to install and relatively simple to acquire data. At present, electrical and electronic strain gauges are widely used due to the ease of installation and data acquisition.

Electrical gauges operated by relating the resistance values to calibrated strain readings. The most widely used strain-measuring device is the electrical strain gauge. This strain gauge is available in quarter-bridge, half-bridge and full-bridge configurations. The bridge corresponds to a normal wheat stone bridge. Full-bridge configurations are mostly preferred as they are equipped with bridge balancing mechanism, which is very important to produce

consistent and repeatable readings under the same conditions. Readings from these gauges can be obtained by using readout boxes and data acquisition systems.

2.7.1.2 Displacement Measurement Devices (Dally et al., 1993)

There are two kinds of displacement measurement devices: linear displacement measuring devices and angular displacement measuring devices. Although their working principle is similar to that of strain measurement devices, all these devices require an anchor support. The displacement measurements are relative to anchor support. Some of the commonly used displacement measurement devices are described below:

- Potentiometers: These gauges contain a moving frame. Movements of this moving frame cause a drop in electrical potential. The strain measurement can be calculated by measuring the drops.
- LVDT or Linear Voltage Differential Transformer: These gauges work on the principle of variable inductance. Displacements of the rod cause a linear change in the inductance of the transformers. These displacements are related to variations in inductance values.
- Optical Displacement Measurements: These devices utilize fiber optics, digital videos, and high-speed photography camera along with specialized computer programs to analyze and interpret signals to obtain displacement readings. These devices are relatively more expensive than other displacement devices because they do not require any physical contact to the soil during monitoring.
- Extensometers: These devices provide relative displacements with respect to the anchor embedded. They are widely used as they are relatively cheap and they can be easily connected to data loggers to digitize and automate the data collection process (Ding et al., 2000).
- Tilt meters, Inclinometers and Electro Levels: These devices are used to measure the rotational deformation. However, due to their high cost and installation difficulties, they are not widely used.

2.7.1.3 Force and Pressure Measurement Devices (Dally et al., 1993)

These devices are composed of an elastic member, which measures the force or pressure exerted to produce strain data. These strains are transformed to their corresponding pressure values by strain converting units. The critical factors that affect the performance of these gauges are their shapes and actual contact areas of the gauge and the soils. Some of the commonly used force and pressure measurement devices are described below:

- Load Cells: Several types of load cells are currently available in the market. However, the main principle of all these devices are the same in which strain of the elastic member inside is measured and transformed to the force applied.
- Pressure Gauges: The main function of the pressure cells is to measure the subgrade pressure of pavements (Sargand et al., 1997; Metcalf, 1998). Although the measurement of strain is very important in terms of determining certain major failure modes of pavements, the importance of stress/pressure measurement cannot be ignored. The main function of pressure cells is to monitor the change in the stress-state of the overlying layers and to measure the increase in vertical pressure due to dynamic traffic loading. The main difference between the load cells and pressure gauges are that the load cells measures the total load on the surface, whereas the pressure gauges measure the average pressure to develop the tangential strain throughout the surface area of the gauge.
- Piezometers: Monitoring ground water levels and periodic analysis of pore pressure distributions in soils are very important in geotechnical engineering projects. In case of retaining walls and slopes assessment, pore pressure measurements are important as the stability of the structures depends on drainage conditions. Therefore, the main application of piezometers is to monitor ground water levels and to measure pore pressure.

2.7.1.4 Other Instruments

Temperature Gauges: These gauges are typically used to monitor the temperature of the soils. These gauges are generally used if the influence of temperature on soil properties is anticipated. Moreover, they are also used to include data corrections in the acquired data.

2.7.1.5 Instruments for Data Acquisition

Data acquisition systems are used along with electrical gauges to record continuous or periodic responses or variations from the installed gauges. Based on the format in which data is recorded, these systems are subdivided into analog and digital systems. Readout that is similar to voltmeters box is a commonly used analog device. Readings are obtained by converting the potential difference readings and manual recording of data from these gauges. The advantage in this module is that these readings can be installed in the site and the data can be obtained at regular intervals. Digital acquisitions are usually used and they are usually carried out with the help of data loggers. The data loggers have an internal storage unit and acquisition cards that are connected to computers and transfers data immediately to the computer. These are used in research projects to entail discrete data which the time interval between two readings is considerably high. The advantages of these modules when compared to data loggers are that they are comparatively cheaper in cost and they do not require continuous on site power supply.

2.7.2 Case Examples

As instruments are continuously getting upgraded, it is very important for design and practicing engineers to be aware of these technological advances. Instrumentation is done either to monitor structural disintegration, to assess the quality assurance of the construction or to develop, verify and modify analytical models. This section presents case reviews of the different sensors used and the typical responses obtained from these instrumentation projects.

2.7.2.1 Field Instrumentation from PENNDOT (Stoffels et al., 2006)

The Pennsylvania Department of Transportation (PENNDOT) is sponsoring the Superpave in-situ stress/ strain investigation (SISSI). SISSI is a state-of-art instrumentation project that includes eight Superpave sections across Pennsylvania in four projects. They are newly constructed pavements and the rest of the four are overlays over existing pavements. The objective of this project was to have full scale investigation of pavement performance with field instrumentation. It includes monitoring of construction process, materials characterization, detailed load response information, traffic and environmental data. Figure 2.16 shows the layout of gauges at one of the SISSI sites.

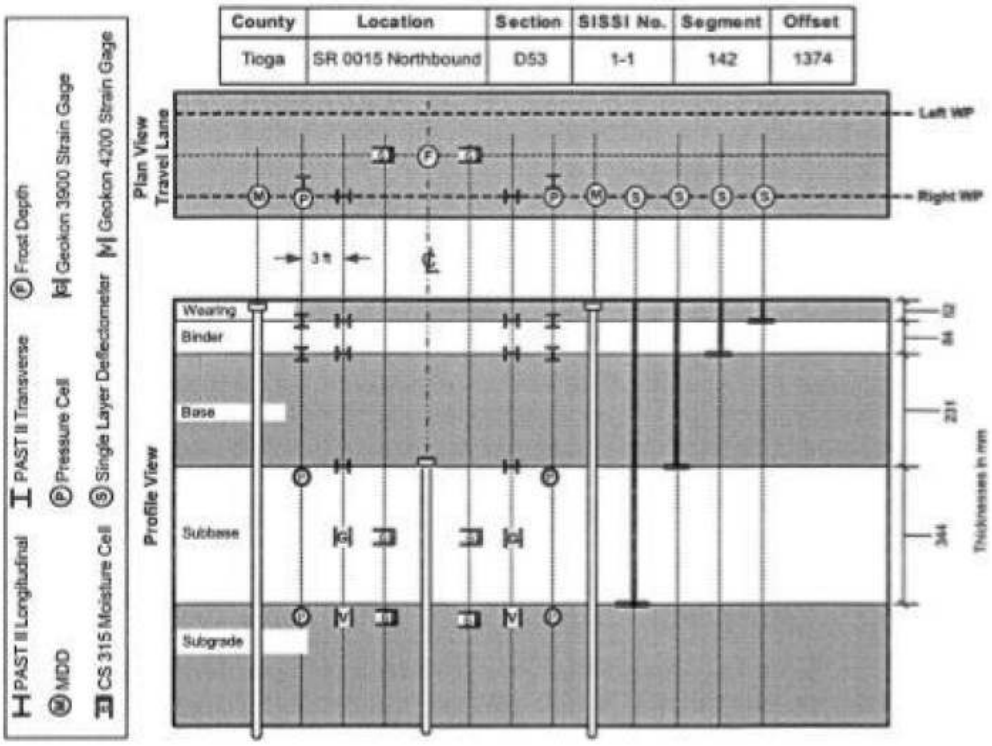

Figure 2.16 Layout of Gauges at SISSI site (Stoffels et al., 2006).

The instrumentation program included Dynatest PAST II Strain Gauge, CTL Multidepth Deflectometer, Geonor Pressure Cell and Geokon 3900 Strain Gauge. The main aim of this instrumentation program was to capture the dynamic data at various seasons of the year. The magnitude of strains and pressure experienced by the pavement under truck loading at different seasons were recorded. There was significant difference seen in response of pavement at different seasons, helping to understand how deflections and pressures vary with loading and seasonal variation in a pavement structure.

2.7.2.2 FHWA Pavement Testing, Virginia (Mitchell, 1993)

In summer 2002, 12 full-scale lanes of pavements with various modified asphalts were constructed at the Federal Highway Administration (FHWA) pavement testing facility in Virginia. The objective of this study was to use FHWA's two accelerated loading facility machines to validate and refine changes being proposed in Superpave binder specification. Each machine is capable of applying an average of 35,000 wheel passes per week from half-axle load ranging from 33 to 84 kN (7500 lbs to 19000 lbs). During the construction, 12 lanes were instrumented with strain gauges and survey plates. Multiple-depth deflectometers (MDDs) were installed in selected lanes. Pavement responses for both strain gauges and MDDs were measured after the construction and during loading in pavement rutting and fatigue tests. The thickness of Hot Mix Asphalt (HMA) and Composite Application Block (CAB) layers was 26-in and was constructed on silty clay soil. Lanes 1 through 7 were constructed with a 4-in. thick HMA and lanes 8 through 12 were constructed with 6-in. thick HMA layer.

Each pavement lane has four test sites for full-scale testing on two failure modes; rutting (at sites 1 and 2) and fatigue cracking (at sites 3 and 4). All 12 test lanes were instrumented during construction with strain gauges and survey plates. Thermocouples were installed in each site shortly before loading. MDDs were installed in selected lanes. Figure 2.17 presents the instrumentation locations for the test sites. The strain gauges were of H-bar type, the embedded asphalt strain gauges. A total of 60 strain gauges were installed in 12 pavement

lanes. Five strain gauges were embedded at the bottom of HMA layer in each lane. These gauges were placed both longitudinally and transversely. Two sets of MDDs were installed prior to loading in each site 1 of lanes 4 and 11 respectively.

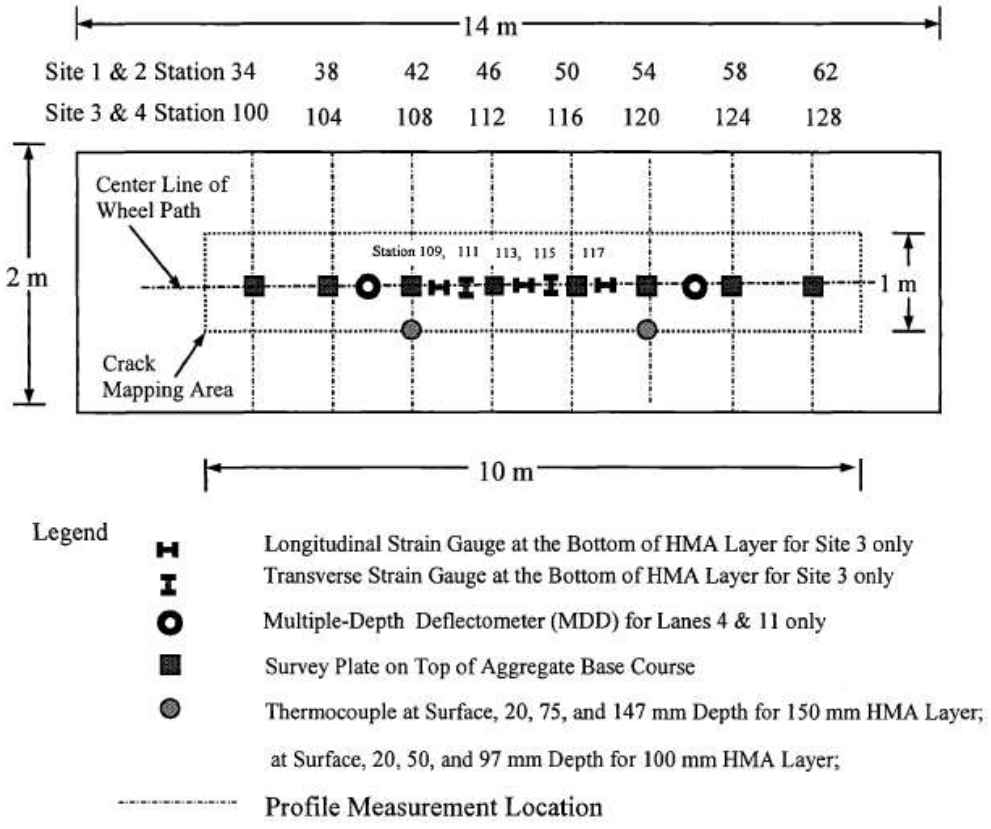

Figure 2.17 Instrumentation Locations for Test Site.

Permanent deformations were recorded during rutting tests with MDDs for lanes 4 and 11. Strain responses were measured under loading at various conditions. The results showed that the predicted strains were consistently lower than measured strains.

2.7.2.3 Bedford Project Case (Al-Qadi, 1999)

The main focus of this project was to study the effectiveness of the use of geosynthetic in flexible pavements and how it can be factored in the design procedure. Nine instrumented secondary road test sections were constructed as part of the realignment of Routes 757 and

616 located in Bedford County, Virginia. Each test section was 15 m long. Three test sections were constructed using a geogrid, three with a geotextile, and the other three were non-stabilized. The constructed base course thicknesses were 100, 150, and 200 mm. The HMA thickness averaged 8.9mm. The pavement test sections were instrumented with earth pressure cells, soil strain gauges, soil moisture sensors, and thermocouples. The geotextiles and geogrids were also instrumented with strain gauges. The majority of the instruments were placed in the right wheel path of the inside lane of the test sections. All instrumentation, cabling, and data acquisition facilities were located underground. The data acquisition system was triggered by truck traffic passing over piezoelectric sensors, and was operated remotely. Once the system was triggered, the instrumentation was continuously sampled at a frequency of 200 Hz for a period of either 12 or 10 seconds, depending on the triggering location (Al-Qadi, 1999). The corresponding data were transferred to Virginia Tech via a modem for processing.

All instruments were placed during construction of each corresponding layer. Instruments located in the subgrade were Kulite earth pressure cells, Carlson earth pressure cells, soil strain gauges, thermocouples, and gypsum blocks. Pressure cells, gypsum blocks, and thermocouples were installed below the compacted surface of the base course and backfill each sensor to avoid instrument damage from large angular aggregate.

2.7.2.4 Pavement Responses in Denver Airport (Rufino and Roesler, 2006)

In 1992, the Federal Aviation Administration (FAA) initiated a major research in an effort to study the in-situ response and performance of Portland cement concrete pavements. FAA, in cooperation with the U.S. Army Corps of Engineers and Waterways Experiment Station (CEWES), instrumented several pavement slabs in the take-off area of Runway 34R at the Denver International Airport (DIA). During the construction of the Denver International Airport, the FAA and the U.S. Army Corps of Engineers instrumented 16 slabs in the take off area of runway 34R-16L (Lee et al., 1997). The instrumented section is located 121.9 m (400 ft.) from the runway threshold and is 22.9 m (75 ft.) wide and 24.4 m (80 ft.) long. There are 460 static

and dynamic sensors to monitor pavement responses (Lee et al., 1997). As an aircraft passes over the instrumented section, infrared sensors trigger the dynamic sensors and data acquisition system, which then captures the pavement responses due to combined aircraft loading and environmental conditions. Dynamic responses include strains, vertical displacements, and aircraft information (position, speed, and acceleration). The information related to each aircraft pass is stored in a database as a unique event.

Position sensors cast in the concrete slabs during construction are used to identify the aircraft lateral location. The methodology developed to identify aircraft location within the instrumented pavement section is described in (Rufino et al., 2006). F-Single and paired H-bat strain gauges and linear variable differential transtruders (LVDTs) were used to collect strains and deflections respectively during each aircraft pass. Figure 2.18 shows 8 of the 16 instrumented slabs associated with the location of H-bar strain gauges and LVDT sensors. The focus of the test was to determine the effect of aircraft loading on pavement design and service life, as well as monitor deterioration of pavement due to environmental loading. Both multi depth deflectometer (MDD) and strain gauges were used to characterize the interface condition and determine the most significant factors affecting this interface condition. Measured slab responses from actual aircraft passes were also used in comparisons with theoretical results for the two extreme interface conditions.

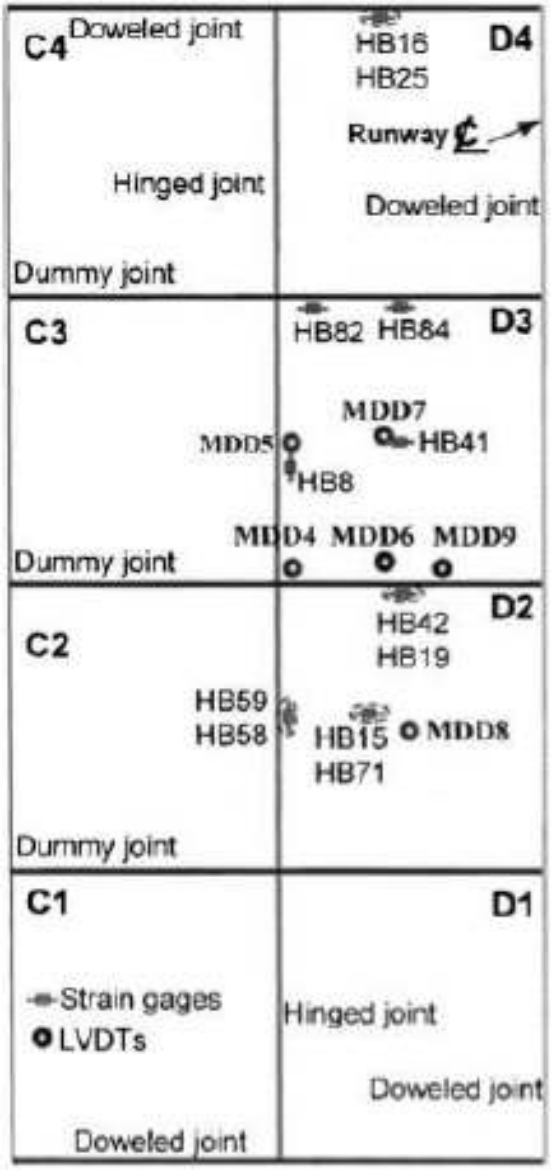

Figure 2.18 Location of H-bar Strain Gauges and LVDT Sensors.

2.7.2.5 Instrumentation in Open Car Park

An expansion joint in an open car park of 295.4 ft. in length and 235 ft. in width was instrumented and monitored over a period of one year. The joints were instrumented with four vibrating-wire displacement transducers and with integrated temperature sensors which were

connected to data loggers. Transducer measurements were recorded on an hourly basis. Figure 2.19 shows the placement of vibrating wire displacement transducer.

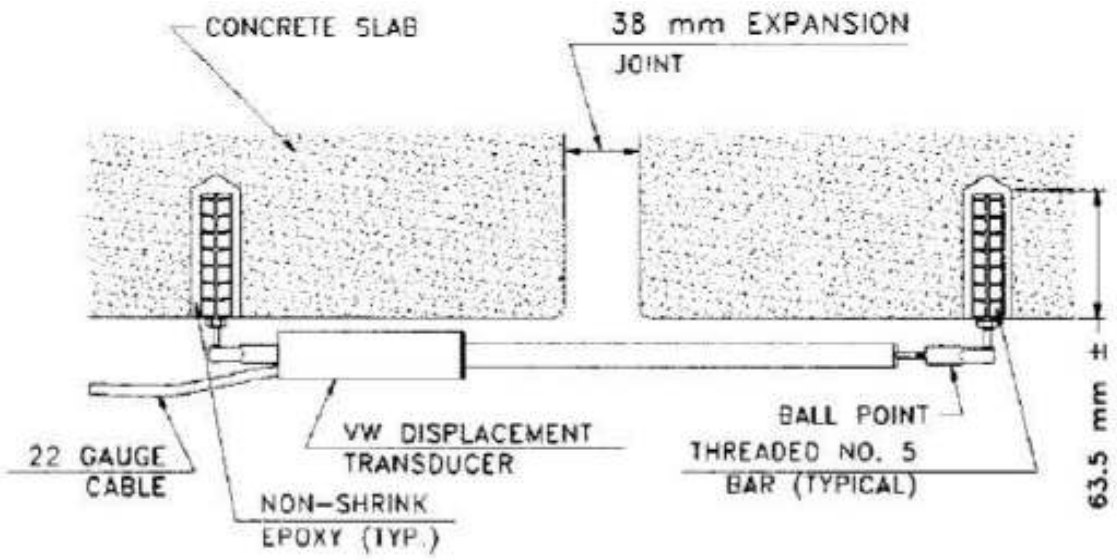

Figure 2.19 Placement of Vibrating Wire Displacement Transducer.

From the instrumentation data, it was found that the use of concrete walls with relatively large mass and rigidity, cast monolithically with floor slabs would impose additional restraint on thermal movements of the slabs and result in ineffective presence of thermal joints due to reduced thermal co-efficient.

2.7.2.6 Minnesota Road (MnRoad)

A pavement research facility was constructed in the state of Minnesota: Minnesota Road (MnRoad) which consists of approximately 40-160m of pavement test sections. Twenty-three of these test sections were loaded with freeway traffic, and the remaining sections were loaded with calibrated trucks. Freeway traffic loading began in June 1994. 4,572 electronic sensors were embedded in the roadway and 1,151 of them were used to measure pavement response to dynamic axle loading. The specific brands and models of each type of sensor were selected based on recommendations made by Minnesota Department of Transportation

(MnDOT's), which was derived from research contracts for evaluation of pavement sensors, and by consultation with government agencies and worldwide instrumentation experts. The main purpose of this instrumentation was to verify and improve existing pavement design models and learn more about the factors that affect pavement response and performance. Learning the affecting factors can help developing new pavement models that can allow building and maintaining more economical roadways.

2.8 Summary

This chapter has presented problems associated with both sulfate rich and non-sulfate expansive soils and stabilization techniques that have been used to better stabilize these soils. The chapter has also described the available chemical and physical stabilization methods for the problematic soils. Then the chapter has summarized the various geotechnical instrumentations for measuring strains, pressures, displacements, moisture, inclinations and temperatures. Several case histories which described the importance of instrumentation were also reviewed.

CHAPTER 3

EXPERIMENTAL PROGRAMS

3.1 Introduction

The main objective of this research project is to study, analyze and select appropriate method for a stabilization of expansive subgrade soils in both sulfate-rich and non-sulfate environments. Two laboratory testing programs are hence designed to assess the properties relating to volume change behavior of expansive soil samples taken from the City of Arlington, Texas. The experimental programs include basic soil property tests, chemical and mineralogy tests, and strength improvement assessments on the soils from Arlington. Figure 3.1 and Figure 3.2 shows the laboratory studies programs in this research project for sulfate-rich soils and non-sulfate soils, respectively. A summary of the laboratory procedures and equipments used for this research project are presented in this chapter.

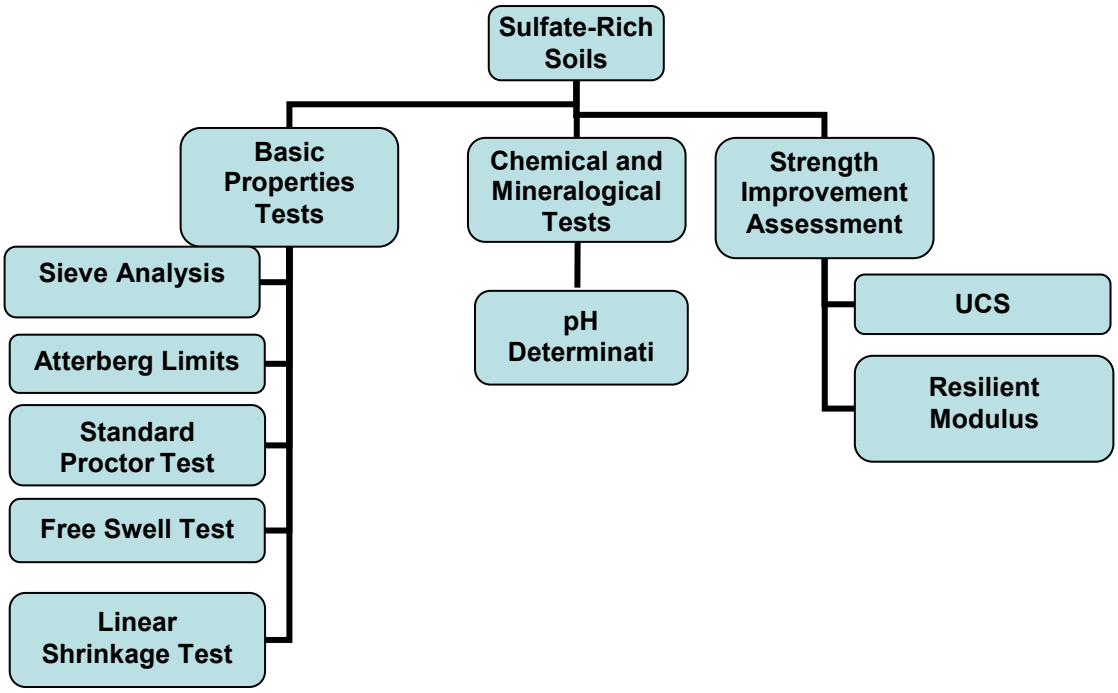

Figure 3.1 Laboratory Studies for Sulfate-rich Soils.

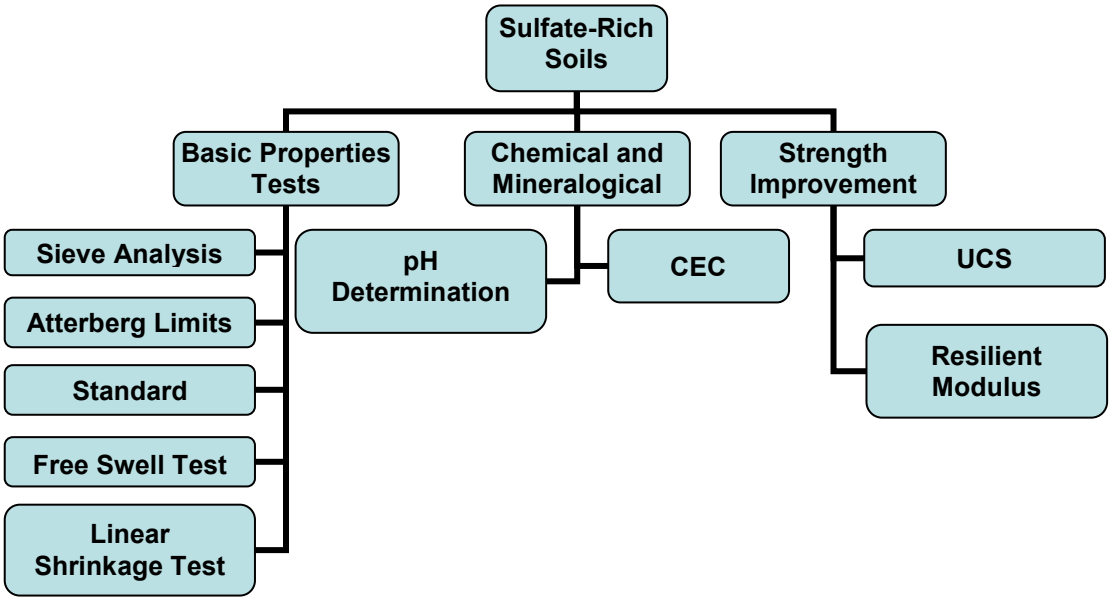

Figure 3.2 Laboratory Studies for Non-sulfate Soils.

3.2 Basic Properties Tests

The tests were conducted in order to measure the basic soil properties, which are usually conducted for most of geotechnical investigations. The tests include specific gravity test, Atterberg limits, standard Proctor compaction tests, one-dimensional free swell test, and linear shrinkage strain test. The tests descriptions and procedures are presented below.

3.2.1 Atterberg Limit Tests

Atterberg limit tests reveal the plasticity properties of the soil. The properties include liquid limit (LL), plastic limit (PL) and plasticity index (PI). The plasticity properties of the soils are important factors to correlate the shrink-swell potential of the soils from dry, semisolid, plastic and finally to liquid states. The water content at the boundaries of these states is known as shrinkage limit (SL), plastic limit (PL) and liquid limit (LL), respectively. The liquid limit is measured as the water content at which the soil flows. The plastic limit is measured as the water content at which the soil starts crumbling when rolled into a 1/8-inch diameter thread. The numerical difference between LL and PL values is known as plasticity index (PI). The Atterberg limit tests were conducted as per Tex-104-E for Liquid Limit and Tex-105-E for plastic limit tests.

3.2.2 Standard Proctor Compaction Test

Standard Proctor compaction test is the test used to determine the optimum moisture content and dry unit weight of the soil. It is necessary to conduct standard Proctor compaction tests in order to establish compaction curves. Specimens were prepared as per ASTM D-4218 (Ramakrishna, 2002). The optimum moisture content of the soil is the water content at which the soils are compacted to a maximum dry unit weight condition. In general, the specimens that exhibit a high compaction unit weight are best in supporting infrastructures because void spaces are minimal and settlement is less. The compaction tests were conducted as per Tex-114-E on all types of soils to determine moisture content and dry unit weight relationships.

3.2.3 One-Dimensional Free Swell Test

The free swell test measures swell potential of the expansive soils in one dimension. Prior to the test, loose soil specimen was mixed with water at the optimum moisture content determined from a standard Proctor compaction test. Then, the specimen was compacted in the confinement rings measuring 2.5 inches in diameter and 1 inch in thickness. Free swell tests were conducted as per ASTM standard procedures. Porous stones were placed at both top and bottom of the soil specimens to allow the access of water. These specimens were then placed in a container and filled with water. The amount of heave was measured by a micrometer dial gauge against the elapsed time and the actual time. Maximum swell values were observed over a period of three days (Chavva, 2002). The final displacements and the original heights were used to calculate the free swell values in the vertical directions.

3.2.4 Linear Shrinkage Strain Test

Linear shrinkage strain test was conducted as per TxDOT standard specified by Tex-107-E (Chavva, 2002). Soil paste mixed at moisture content level of liquid limit state is placed in the linear shrinkage mould. The samples were air dried at room temperature for twelve hours and then oven dried for twenty-four hours. The length of dried samples was measured by using vernier calipers and the linear shrinkage was expressed as percentage of its original length.

3.3 Chemical and Mineralogical Tests

Two types of laboratory tests are required to monitor the formation of ettringite mineral. These tests include chemical tests and mineralogical tests. Chemical tests were conducted in order to determine the pH and soluble sulfate content in the soils. Mineralogical tests were conducted to determine the formation of Ettringite in stabilized soils which included X-Ray Diffraction (XRD) test and Scanning Electron Microscope (SEM) analysis.

3.3.1 Chemical Tests

Two types of chemical tests which included pH test and soluble sulfate determination test were conducted. The pH and sulfate content in the treated soil determine if the soil conditions are favorable for ettringite formation.

3.3.1.1 pH Determination of Stabilized soils

The pH test is preformed in order to identify the acidic and basic conditions of the soils. This test was conducted as per ASTM D-4972 specification. Prior to the test, a 1:1 ratio by weight of dried soil to distilled water was mixed in a flask. Then, the mixture was shaken and mixed again to ensure thorough mixing. The pH was monitored by inserting an electrometric indicator into the soil mixture. Then, the pH reading was taken. The test was conducted on both controlled and all the treated soil samples.

3.3.1.2 Soluble Sulfate Determination

This test is performed to assess the amount of soluble sulfates in the soil. The method is a modified procedure from the standard gravimetric method outlined in the seventeenth edition of Standard Methods for the Examination of Water and Wastewater by Clesceri (1989). As recommended by Petry and Little (1992), the water extraction ratio was 1:10. Therefore, the procedure started with 10 grams of dried soils was added with 100 ml of distilled water. Then, the soils needed to be extracted from the solution. This could be obtained by placing the solution in the centrifugal device at the speed of 14,000 rpm. Then, hydrochloric acid was added to the solution in order to keep the pH values within the range of 5 to 7. Then, the solution was heated up to the boiling point. Barium chloride ($BaCl_2$) was added to the boiling solution to bring out sulfate in the form of barite ($BaSO_4$). Then the solution was placed in an oven at 85^{o}C for twelve hours. This process allowed the digestion process to take place and continue in order to obtain barite by precipitation process. Then, the solution was put through the filter paper to obtain the soluble sulfate contents in the soil samples. The barite precipitated from this process was then weighted and calculated. According to Puppala et al (2003), a smaller pore size filter

of 0.1 μm and higher speed of centrifuging of 14,000 rpm with longer time was recommended in order to segregate the small particles from the solution. This modified method provided results that matched the ion chromatography measurements. Hence, the modified method was adopted in the present research. Figure 3.3 presents the soluble sulfate test procedure used in this research.

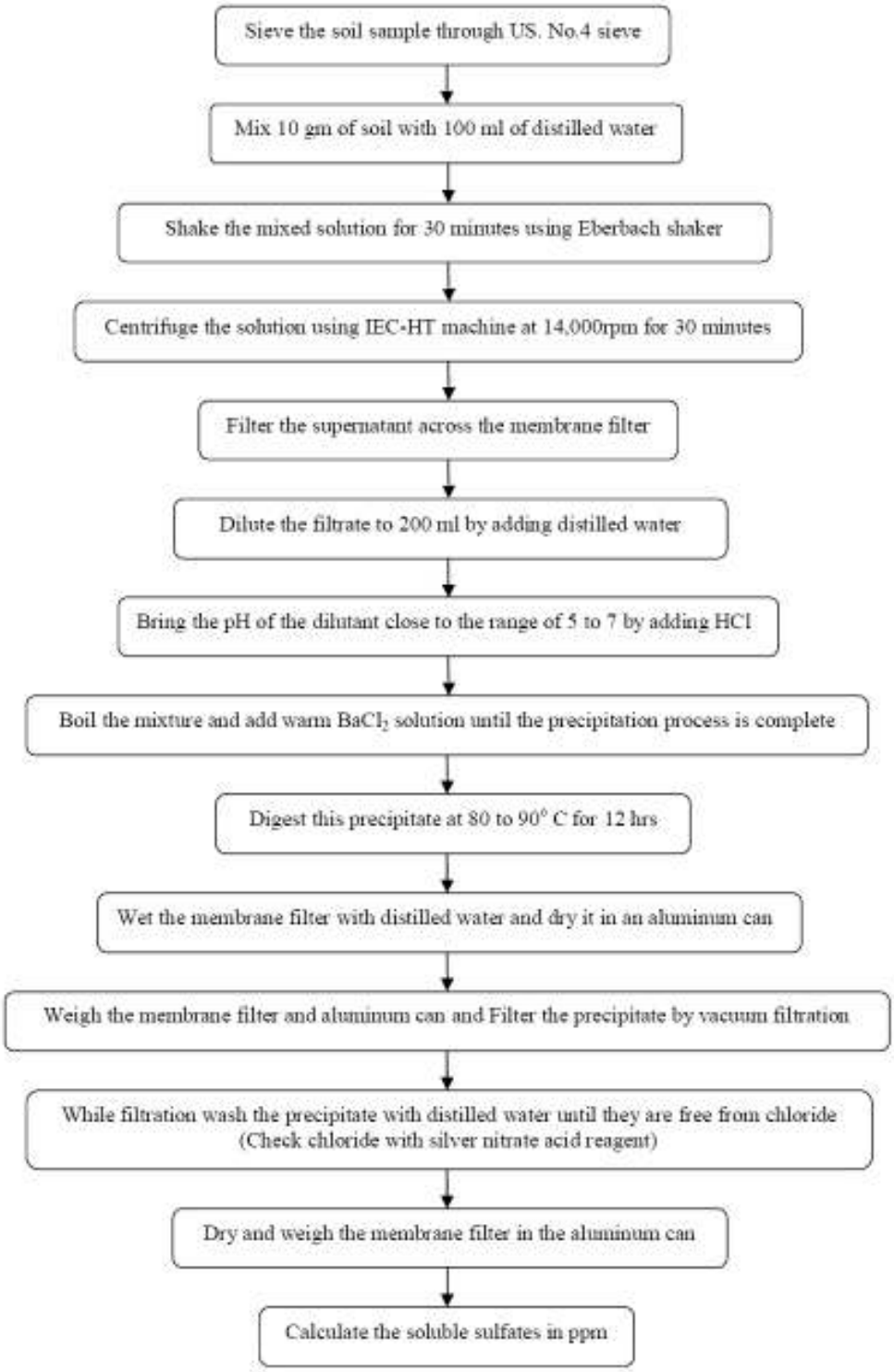

Figure 3.3 Soluble Sulfate Determinations (Puppala et al., 2000).

3.3.2 Mineralogical Tests

Mineralogical tests were conducted in this research to evaluate the presence of ettringite in soil samples while X-Ray diffraction (XRD) studies were conducted on all the soil samples.

3.3.2.1 X-Ray Diffraction Test

X-ray diffraction (XRD) test method is the most widely used non-destructive method for material characterization. Powder specimens were used to identify the mineral composition of the soil samples. This method mainly focused on the formation of ettringite minerals in the stabilized soils. Specimens were collected randomly from different locations of all the treated sections. Specimens were first obtained from the field, then oven dried and pulverized. The treated samples were pulverized into a fine powder and sieved using sieve No. 200. In order to read the basal spacing of the minerals present in the soil samples, these samples were put through to CuK_{α} radiation at a speed of 0.05 degrees per minute with a graphite monochrometer over a 2θ range of 1° to 80°. The data was recorded and analyzed to identify the cause of heaving in this research study. Figure 3.4 illustrates the X-Ray diffraction setup.

Figure 3.4 Illustration of X-Ray Diffraction Test Setup.

3.4 Strength Improvements Assessment

3.4.1 Unconfined Compressive Strength Test

The unconfined compressive strength (UCS) test is a special test (unconfined-undrained). Commonly, this test is used to determine shear strength of soils under unconfined conditions (Das, 1998). The UCS tests were conducted as per ASTM D-2166. Prior to the test, specimens were prepared and cured in the moisture controlled room for seven days. A specimen was placed on the compressive test platform. The sample was then loaded at a constant rate which was controlled by a loading device control. Vertical deformation and axial load were collected from a computer attached to a test setup. The maximum axial compressive load at which the sample failed was used to determine the unconfined compressive strength of the soil sample. The UCS setup is shown in Figure 3.5.

Figure 3.5 UCS Test Setup in the Laboratory.

3.4.2 Resilient Modulus Test

The resilient modulus (M_R) is defined as the ratio of the axial deviator stress to the recoverable axial strain (Puppala and Mohammad, 1996). Resilient modulus test was conducted to understand the effect of compaction moisture and confining pressure on M_R properties of control and stabilized soil. It was also conducted to analyze the effects of stabilizers on resilient properties of soil. The tests on materials were conducted with the confining and deviator stress levels following the procedure specified by AASHTO T307-99 for subgrade materials (Table 3.1). The test starts with applying a repeated deviatoric load on the specimen with fixed load duration of 0.1 second and 0.9 second period relaxation.

The test consists of a conditioning phase and 15 testing phases, with 1,000 cycles for conditioning and 100 cycles for each testing phase. The conditioning phase is conducted by

applying a thousand repetitions of a specified deviator stress in order to eliminate the effects of specimen disturbance caused by sampling, compaction and specimen preparation procedures. Once the conditioning phase has been done, test is conducted as specified by AASHTO T307-99 to cover the service range of stress that a subgrade material experienced due to traffic loading and over-burden conditions. Figure 3.6 shows the resilient modulus test setup in the laboratory.

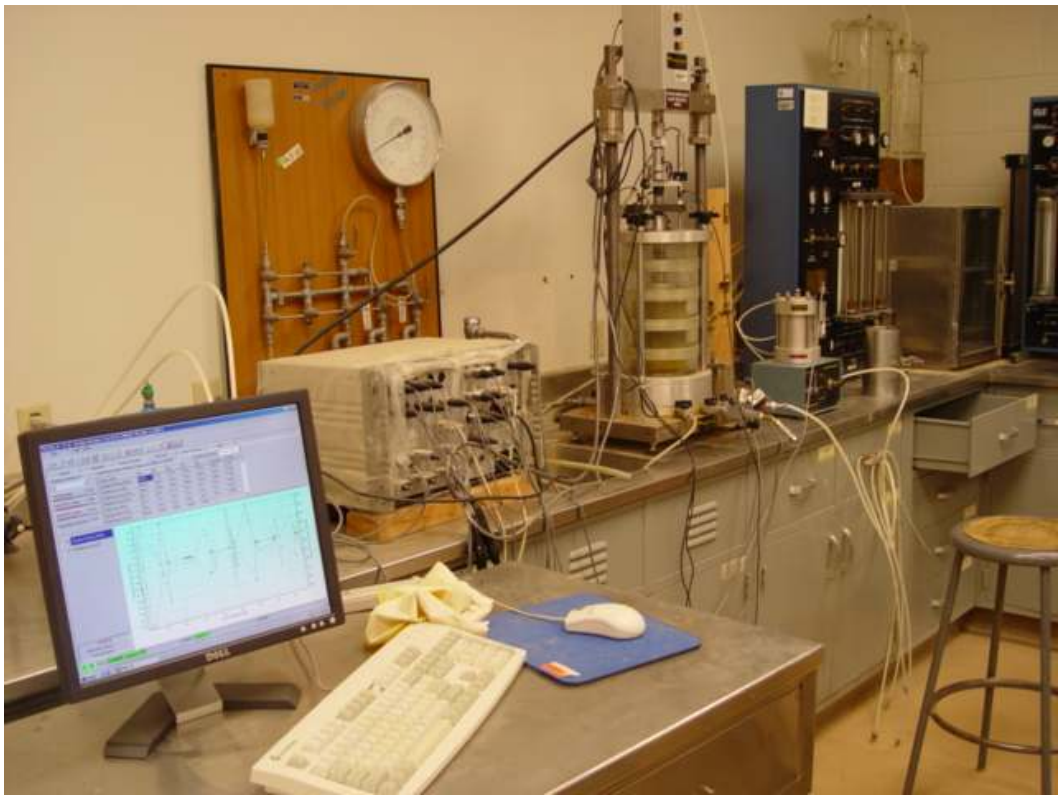

Figure 3.6 Resilient Modulus Test Setup in the Laboratory.

Table 3.1 The Confining Pressure and Deviatoric Stresses Applied (AASHTO 307-99)

Sequence #	Confining Pressure (kPa)	Maximum Stress (kPa)	No. of Load Cycles
0	41.4	27.6	1000
1	41.4	13.8	100
2	41.4	27.6	100
3	41.4	41.4	100
4	41.4	55.2	100
5	41.4	68.9	100
6	27.6	13.8	100
7	27.6	27.6	100
8	27.6	41.4	100
9	27.6	55.2	100
10	27.6	68.9	100
11	13.8	13.8	100
12	13.8	27.6	100
13	13.8	41.4	100
14	13.8	55.2	100
15	13.8	68.9	100

Figure 3.6 shows the resilient modulus test setup. The setup utilizes the cyclic triaxial test equipment which is designed to simulate the traffic wheel loading on the in situ soils by applying a sequence of repeated or cyclic loading on the sample specimens.

The stress levels, shown in Table 3.1, are used for testing the specimens as standardized by AASHTO testing guide. The stress levels are based upon the location which the specimen was taken within the pavement structure. The confining pressure shown in Table 3.1 represents overburden pressure of the specimen location in the subgrade. The axial deviatoric stress is composed of two main components, cyclic stress, which is the applied deviatoric stress, and a constant stress, typically represents a seating load on the soil specimen. It should be noted that the constant stress is typically equivalent to 10% of overall maximum axial stress. The tests were conducted on both sulfate-rich soils and non-sulfate soils, with and without treatments. Prior to the testing, specimens were prepared and compacted at the optimum moisture content.

3.4.3 Equipment Employed for the Resilient Modulus Testing

The resilient modulus test is conducted by using the UTM-5P dynamic triaxial system. The UTM-5P is a closed loop, servo control, materials testing machine. This machine is designed to facilitate triaxial testing. The UTM-5P system is composted of three major components including loading frame, controller and data acquisition system.

3.4.3.1 Loading Frame

The loading frame consists of a heavy flat base plate, supported on four leveling screws. Two threaded rods support the crosshead beam and provide height adjustment. The frame was designed to reduce deflection and vibrations that could influence the accuracy of measurements during the dynamic repeated load testing.

The loading forces are applied through the shaft of a pneumatic actuator which is mounted in the center of the crosshead. Sensitive and low friction displacement transducers were attached to the crosshead. These transducers were used to measure the permanent and small deflections of the specimen during the testing. The loading frame is as shown in the Figure 3.7 below.

Figure 3.7 Loading frame and triaxial cell setup.

3.4.3.2 The pneumatic loading system

The UTM pneumatic system is an air compressor controller unit which is used to control both load and pressures applied to the soil specimens. For bound materials, only the vertical force pneumatics is required, whereas unbound materials require both confining and axial deviatoric pressure pneumatics. The system requires filtered and clean air supply at a minimum pressure of 800 kPa. Figure 3.8 shows the Pneumatic system used in the laboratory.

Figure 3.8 Pneumatic System.

3.4.3.3 Triaxial Cell

The triaxial pressure cell unit can provide a maximum confining pressure of 1700 kPa. The cell chambers are made of Lucite-type material to provide maximum visibility during the testing. The cell is designed to serve pressurized liquid only. Therefore, the use of any compressible gas as a confining medium is not recommended.

3.4.3.4 Control and Data Acquisition System

The UTM Control and Data Acquisition System (CDAS) is a compact, self contained unit. This unit provides all critical control, timing and data acquisition functions for the testing frame and transducers. The CDAS consists of an Acquisition module (analog input/output) and a feedback control module (analog input/output). The acquisition module has eight normalized transducer input channels that are digitized by high speed 12 bit digital to analog (D/A)

converters for data analysis and presentation. The air pressure is controllable over the range 0 - 700 kPa. There are two output channels provided for applying confining pressures. The SOL1 is used as the trigger input to the feedback control module that creates and controls the waveform. The SOL2 output is used as a digital control signal from a computer to control the confining pressure in the triaxial test setup.

The feedback control module has three input channel controls. These channels are used for the actuator position, actuator force and auxiliary input (Aux). The module has a communication interface that provides a simultaneous PC connection which enabling increased speed of operation and flexibility. Figure 3.9 shows the control and data acquisition system.

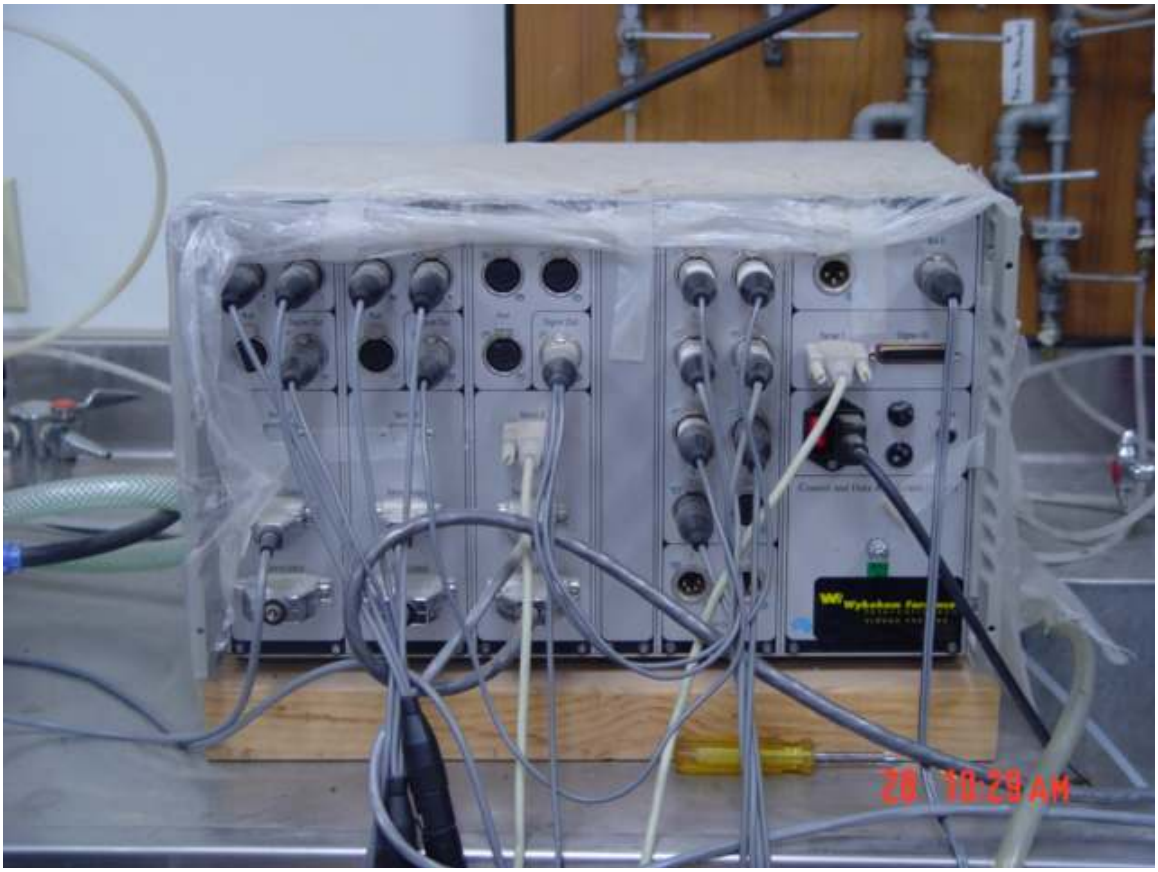

Figure 3.9 Controls and Data Acquisition System.

3.4.3.5 Linear Variable Displacement Transducers (LVDTs)

Based on the AASHTO T 307-99 testing procedure, high resolution LVDTs are required to measure the soil displacements. Two LVDTs are used to measure the vertical displacements. The LVDTs are placed on the top cover of the triaxial cell and fitted to the load shaft. The maximum scale stroke for these two LVDTs is +5 mm, with 0.001 mm accuracy. The output from each LVDT is monitored independently and compared to the output of the other LVDTs. Figure 3.10 shows the external transducer assembly employed in this project.

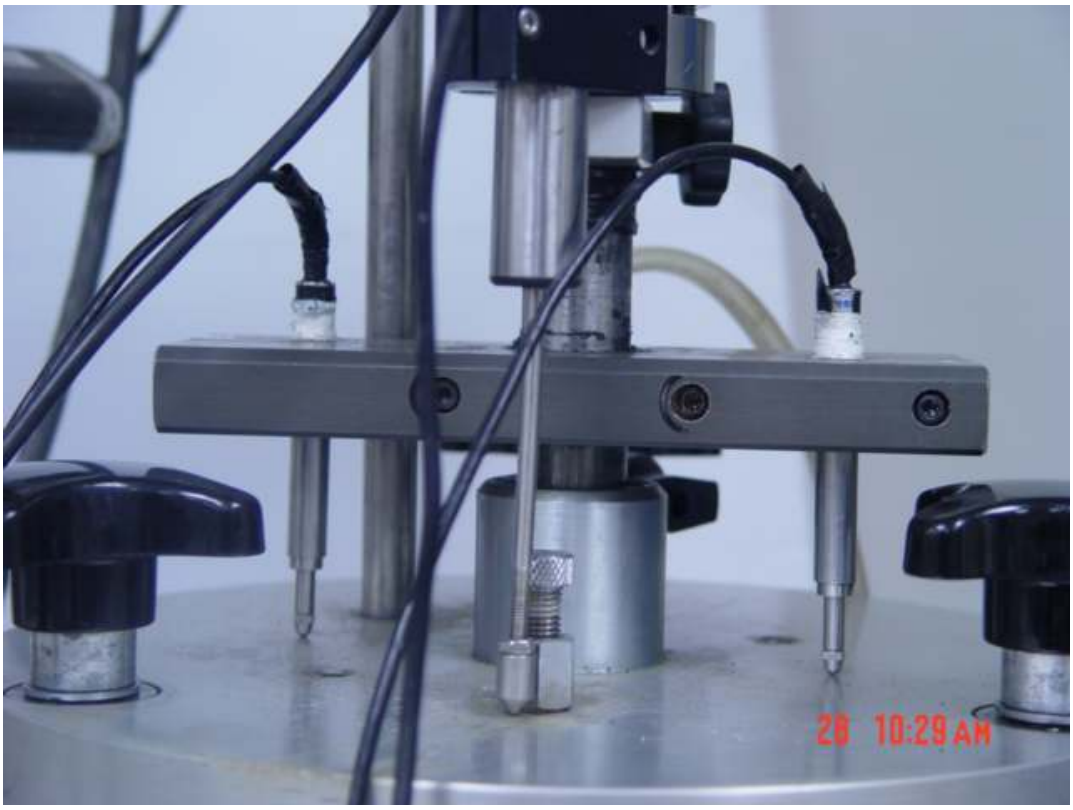

Figure 3.10 The External Transducer Assembly Employed in This Research Project.

3.4.3.6 Software

The UTM software is used for equipment control and data acquisition operations. This software contains several preprogrammed test procedures including unconfined compressive strength test, resilient modulus test, and unconsolidated undrained test, consolidated undrained test, consolidated drained test. In addition, this software also contains the user defined program which allows the operators to create their own testing methods and protocols.

3.5 Summary

This chapter provides a complete description of basic soil property test, chemical and mineralogical tests, and strength improvement assessment. The details of instrumentation design, installation of sensors, data collection procedures, elevation survey and DCP test details are also discussed.

In practice, field performance assessments are required to assess the performance of all the stabilization methods in a real field conditions over a period of time. Field monitoring is performed for twenty six months on a weekly basis. Field sections and study are presented in Chapter 5 and field results are discussed and analyzed in Chapter 6.

CHAPTER 4

ANALYSIS OF LABORATORY RESULTS

4.1 Introduction

The assessment of basic properties, chemical and mineralogical characteristics, and strength improvement of stabilized subgrades are very important to validate the effectiveness of stabilizers. Stabilizers that showed promising results in the laboratory will be used in the field. Moreover, the understanding of the soils properties is important in defining the functions of sensors and appropriate data acquisition in pavement instrumentation.

This chapter presents a comprehensive summary of the results acquired from laboratory including basic soil properties, chemical and mineralogical characteristic and strength properties of untreated and treated specimens. The laboratory results are presented in two sections. The first section presents the results of laboratory test for untreated and treated 'sulfate-rich' soils specimens collected from Harwood Road. Then, the second part covers the laboratory results of 'non-sulfate' soils specimens collected from three test sites before and after the stabilization. This chapter also presents the results of the two mineralogical studies conducted on stabilized soil samples collected from the field to detect the presence of ettringite mineral. These studies include X-ray diffraction and SEM studies.

4.2 Laboratory Results for Sulfate-rich Soils

Soil specimens were collected from the test site located at Harwood Road, Southeast Arlington. Prior to the stabilization, several laboratory tests were performed by Wattanasanticharoen (2000), Chavva (2002) and Ramakrishna (2002). The laboratory tests include sieve analysis, Atterberg limits, specific gravity, soluble sulfate and hydrometer tests. The results acquired from the tests are shown and discussed below.

4.2.1 Basic Soil Properties

4.2.1.1 Specimen Preparation

The compositional and environmental conditions such as moisture content, dry unit weight of soils and stabilizer dosages usually influences the plasticity index, swelling, shrinkage, and strength properties of soils. The variable conditions in specimen preparation are listed in Table 4.1. The soil was first oven dried and pulverized. Then the soil was mixed with selected chemical stabilizers at optimum moisture content and the corresponding dry unit weight. Specimen preparation for soil mixed with lime and fiber stabilizers were conducted as per ASTM D3551-90. For UCS and resilient modulus tests, the specimens were compacted in Standard Proctor molds and were carefully extracted. Then, the specimens were wrapped and cured in humidity rooms for forty eight hours prior to compacting. The specimens for other stabilizers i.e. cement, fly ash, and GGBFS were compacted immediately after mixing.

Table 4.1 List of Variable Conditions in Specimen Preparation

Description	Variables
Soil Type	Sulfate Rich Expansive Soil from Harwood Road
Stabilizers	Sulfate Resistant Type V Cement, Class F Fly ash with Type V Cement, GGBFS and Lime with Polypropylene Fibers
Stabilizer Dosage	One
Moisture Contents	Optimum, Dry of Optimum and Wet of Optimum
Temperature Conditions	Room Temperature
Curing Period	7 Days

4.2.1.2 Sieve Analysis

The grain-size distribution was acquired by sieve and hydrometer analysis. Figure 4.1 shows the grain-size distribution curve of natural (untreated) soil collected from Harwood Road. The grain-size distribution curve of this soil shows the percentage of fine and course grained particles contained in the soils.

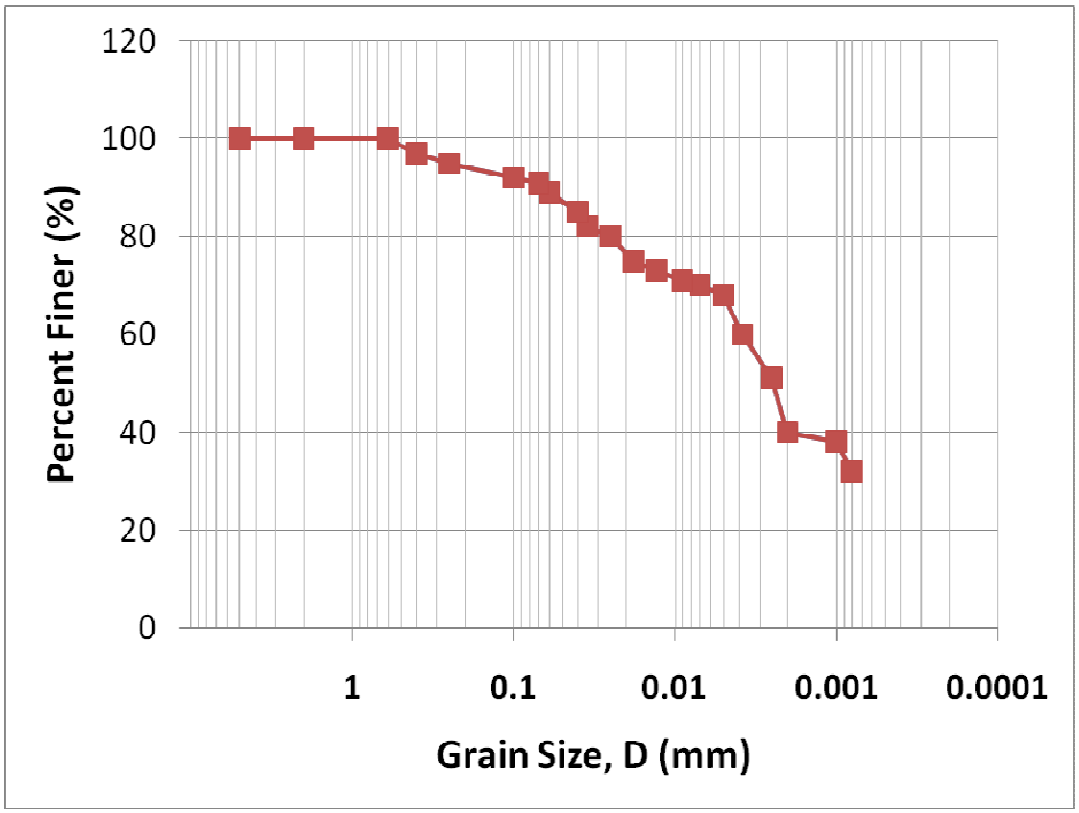

Figure 4.1 Grain-size distribution Curve of Untreated Soil Collected form Harwood Road

4.2.1.3 Atterberg Limits

Atterberg limit tests were conducted as per ASTM D-4318 method to determine the consistency of the soil (Chavva, 2002). According to sieve analysis and Atterberg limit values, the soil was classified as A-7-6 as per the AASHTO classification method and sandy fat clay with gravel, CH, as per the USCS classification method (Chavva, 2002). Table 4.2 summarizes the basic soil properties of natural Soils Collected from Harwood Road.

Table 4.2 Basic Soil Properties of Natural Soils Collected from Harwood Road (Chavva, 2002)

Soil Properties	Results
Color	Dark Brown
Passing #200 (%)	91.2
Specific Gravity	2.73
Liquid Limit (%)	55.5
Plasticity Index	22.2
Natural Moisture Content (%)	7.0
Soluble Sulfate Content (ppm)	4737
pH	8.13
AASHTO Classification	A-7-6
USCS Classification	CH

4.2.1.4 Standard Proctor Compaction Test

Standard proctor compaction tests were conducted in order to determine the optimum moisture content and dry unit weight of both control and treated soil. Specimens were prepared as per ASTM D-4218. Standard proctor test results are presented in Table 4.3 and Figure 4.2 respectively.

Table 4.3 Moisture Content and Dry Unit Weight of Raw and Treated Soil (Ramakrishna, 2002)

SL No.	Soil Type	Optimum Moisture Content (%)	Dry Unit Weight (pcf)
1	Control (Lime 8%)	18.65	105.50
2	Type V Cement (8%)	16.70	106.90

Table 4.3 - *Continued*

3	Class F Fly ash (15%) and Type V Cement (5%)	18.70	104.20
4	GGBFS	16.00	107.30
5	Lime (8%) and Polypropylene Fibers (0.15%)	18.00	96.00

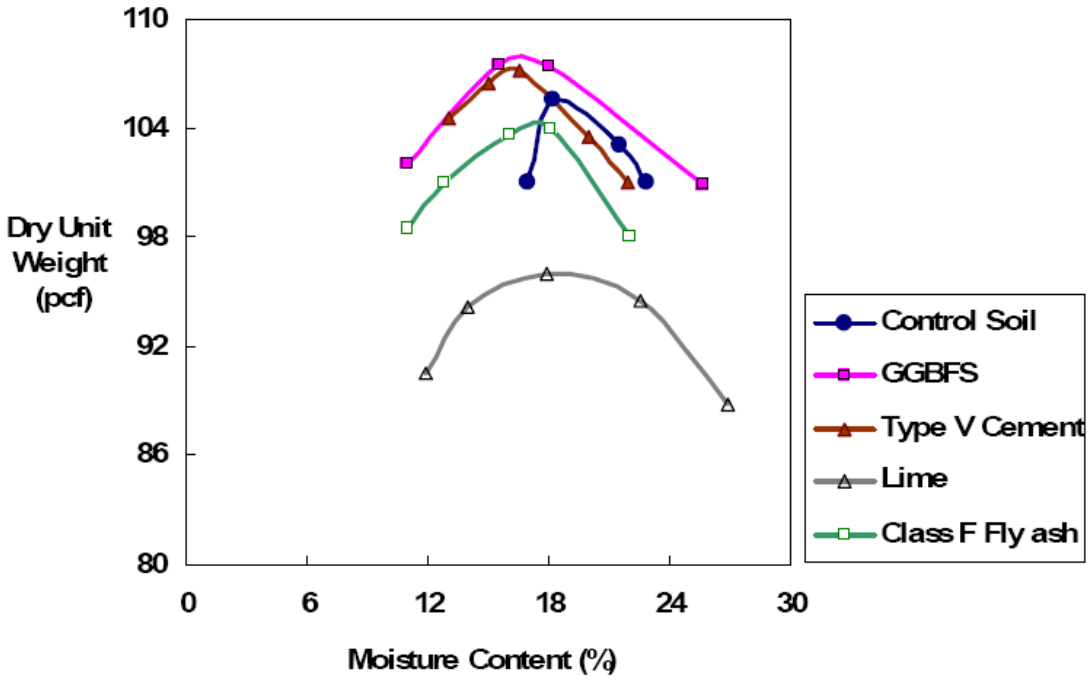

Figure 4.2 Standard Proctor Compaction Test Results (Ramakrishna, 2002).

4.2.1.5 One Dimensional Free Swell Test

Free swell test measures the amount of heave in a confined specimen. Both control and treated specimens measuring 2.5 inches in diameter and 1 inch in thickness were included as per ASTM standards. Porous stones were placed at the top and bottom of the specimen to facilitate water movement. These specimens were then placed in a container and filled with

water. The amount of heave was measured by a micrometer dial gauge against elapsed time and actual time. Maximum swell values were observed for over a period of three days. The final displacements and the original heights were used to calculate the free swell values in the vertical directions. Table 4.4 presents the free vertical swell of control and treated soil after three days.

Table 4.4 Free Vertical Swell Strain for Control and Treated Soils (Chavva, 2002)

Soil Type	Free Vertical Swell Strain at Optimum (%)
Control (Lime 8%)	7.5
Type V Cement (8%)	0.1
Class F Fly ash (15%) and Type V Cement (5%)	0.1
GGBFS (20%)	0.1
Lime (8%) and Polypropylene Fibers (0.15%)	0.64

The decrease in the free swell in all the stabilized soils was due to the decrease in plasticity property of the soils after chemical treatments. Among all stabilizers, lime and fiber treated specimen exhibited the highest swell potential. This was due to the addition of fibers induces the open fabric and decreases the unit weight of the treated specimen.

4.2.1.6 Linear Shrinkage Strain Test

Linear Shrinkage Strain Test was conducted as per Texas Department of Transportation (TxDOT) method specified by Tex-107-E. Soil paste mixed at moisture content level of liquid limit state is placed in the linear shrinkage mould. The specimens are air dried at room temperature for twelve hours and then oven dried for twenty-four hours. The length of dried specimens is measured by using vernier calipers and the linear shrinkage was expressed as percentage of its original length.

Table 4.5 presents the results for linear shrinkage strain test. It can be noticed from the results that the linear shrinkage values of control (lime treated) specimen is the highest. This was due to the reaction from sulfate contained in the soils, water and calcium based stabilizers as found in sulfate-induced heave. For the others stabilizers, the shrinkage strain values were significantly decreased. All four stabilization methods displayed similar low shrinkage strains which were due to the reduced plasticity property of the soils after treatment.

Table 4.5 Linear Shrinkage Strain for Control and Treated Soils (Chavva, 2002)

Soil Type	Linear Shrinkage Strain (%)
Control (Lime 8%)	6.2
Type V Cement (8%)	1.4
Class F Fly ash (15%) and Type V Cement (5%)	1.5
GGBFS (20%)	2.3
Lime (8%) and Polypropylene Fibers (0.15%)	1.4

4.2.2 Chemical and Mineralogical Studies on Treated Specimens

In order to study the causes of heave related movements observed in all treated and control sections, pH tests and soluble sulfate analysis were performed on the samples collected form all test sections included control section. These tests provide information that could be used to identify the ettringite formation and sulfate induced heaving. The following sections present these test results.

4.2.2.1 pH Test Results

pH tests were conducted on all the treated samples collected from the test site at two different time periods to understand acidic and basic conditions induced by soil stabilization process. The pH reading for all the specimens were conducted at room temperature with the pH meter. The tests were conducted at before the construction of concrete pavement and after the pavement have been in service for 26 months. These tests were conducted to determine the potential of ettringite formation, which is influenced by the pH of the treated subgrade soil. Table 4.6 presents the pH test results before and after the construction of stabilized pavement. It can be observed from the tests that the chemical compounds such as calcium, alumina, and sulfates in the chemically treated soils, are dissolved into a basic solution at pH greater than 10. The high pH condition in the treated soils leads to the formation of Ettringite (Hunter, 1988).

Table 4.6 pH Test Results of Stabilized Soils

Stabilized Soil	pH	
	Before Pavement Construction	After 26 months of pavement construction
Type V Cement	12.4	12.8
Cement and Fly ash	12.0	12.3
GGBFS	11.3	11.7
Lime and Fibers	13.5	13.4
Lime (Control)	13.6	13.6

From Table 4.7, it can be observed that the pH range for all the stabilized subgrade soils has remained practically same in the range of between 11.3 and 13.6. As the pH for all the stabilized soils are above 10, it can be concluded that all stabilizers are still present and no major leaching was recorded. It also leads to a concern that ettringite formation may still occur since alumina disassociation from clay minerals typically occurs at high pH conditions. Hence, these soils may experience heaving in the future.

4.2.2.2 Soluble Sulfate Test Results

In general, sulfate content which induces heaving to the soils varied from 3,000 ppm to as high as 10,000 ppm (Hunter, 1988; Mitchell and Dermatas, 1990). Puppala et al. (2005) showed that even at low sulfate levels (2,000 ppm), heaving will be possible if the void space is small and ettringite mineral growth is continuous. Soluble sulfate tests were conducted on both untreated and treated soils collected from the field. Table 4.7 summarizes the soluble sulfate content for the stabilized soils. It can be note that these levels are smaller in the treated soils. This could be of two reasons. First, the possible conversions of sulfates into insoluble sulfate mineral, such as ettringite, forms. Second reason attributes to the sampling variations of sulfates in the subgrade soils, which are found in pockets.

Table 4.7 Soluble Sulfate Contents for Stabilized Soil Sections

Stabilizers	Soluble Sulfate Content (ppm)
Untreated	4737.0
Type V Cement	730.9
Cement and Fly ash	396.1
GGBFS	362.2
Lime and Fibers	1014.0
Lime (Control)	1128.0

4.2.2.3 X-Ray Diffraction (XRD) Analyses

XRD Analyses were conducted by Vasudev (2007) on all the treated soil samples collected from Harwood Road. The intent of these studies is to identify the presence of the crystalline mineral, ettringite formation, which is known to cause sulfate induced heave. Figures 4.3 to 4.7 present XRD analyses data for the five treated sections. Tables 4.8 to 4.12 show the presence of ettringite as per their corresponding d-spacing values.

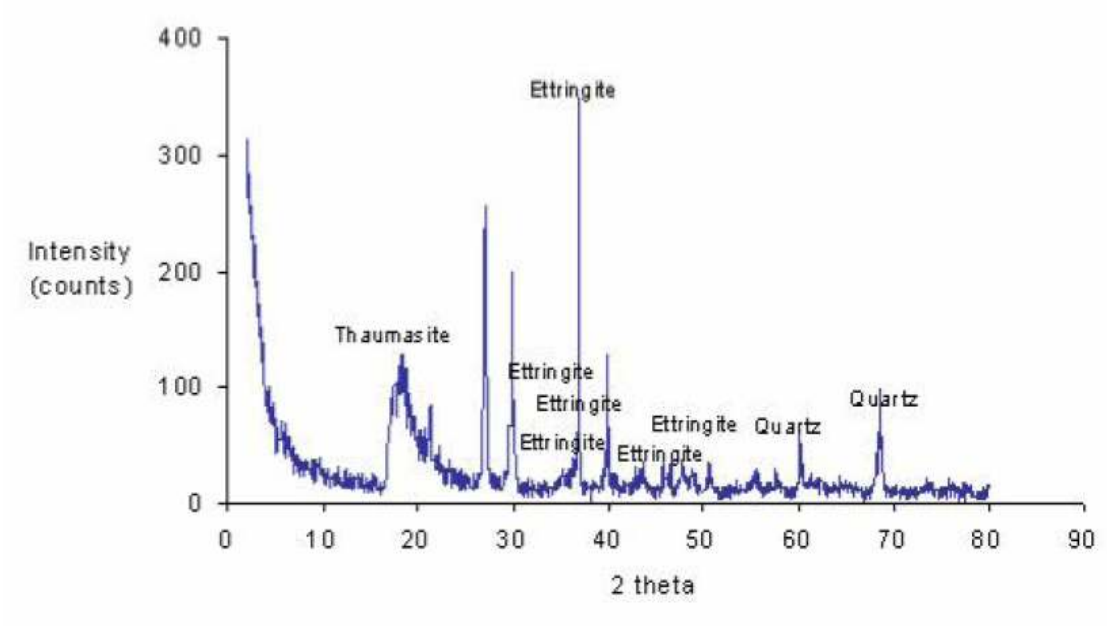

Figure 4.3 XRD Analysis for Type V Cement Treated Section.

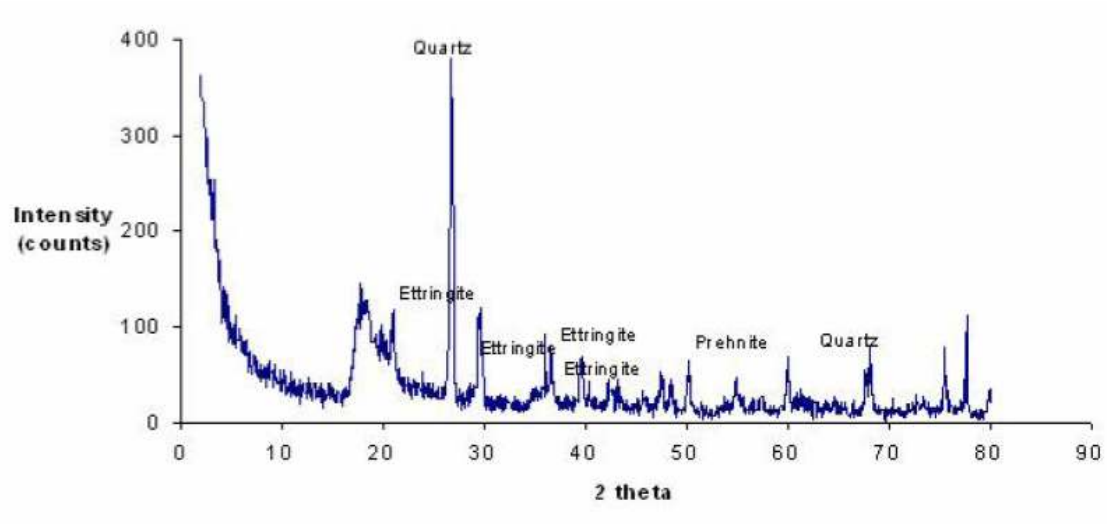

Figure 4.4 XRD Analysis for Cement and Fly ash Treated Section.

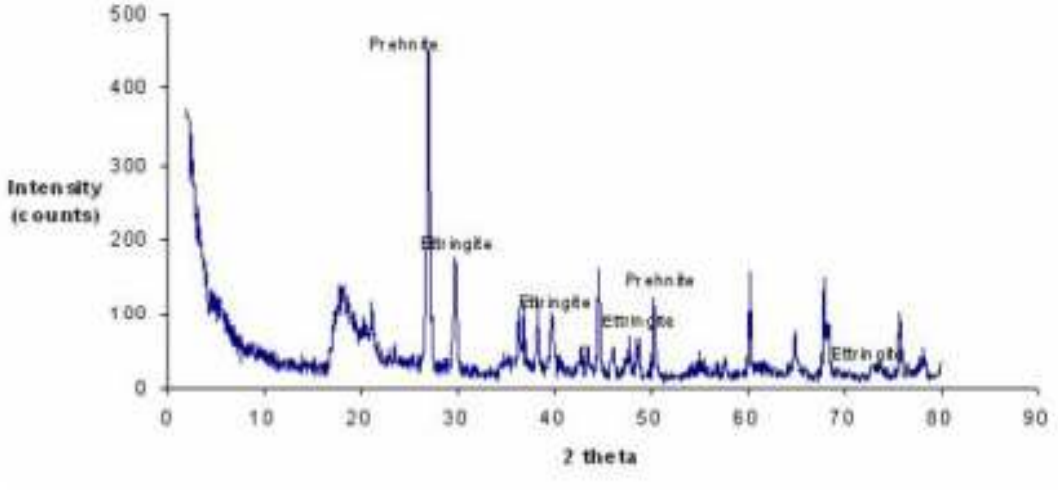

Figure 4.5 XRD Analysis for GGBFS Section.

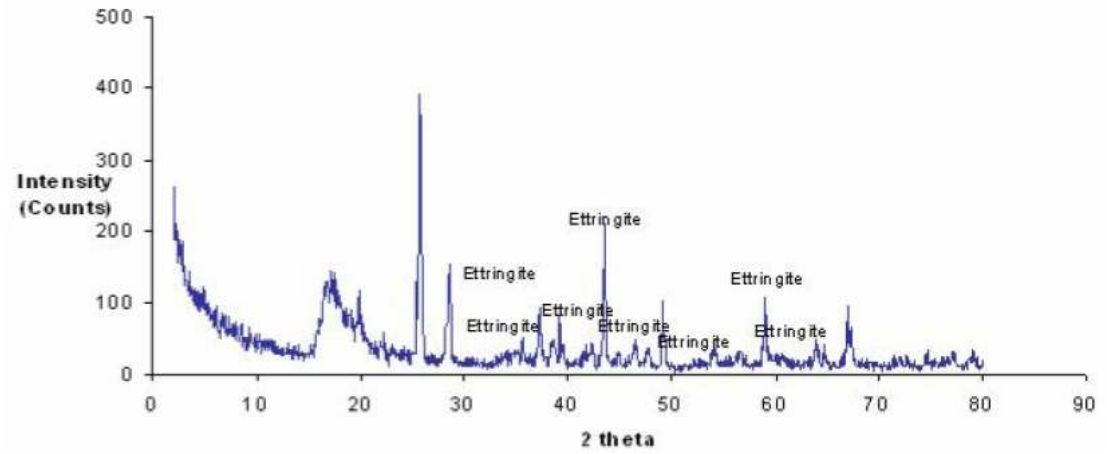

Figure 4.6 XRD Analysis for Lime-Fiber Section.

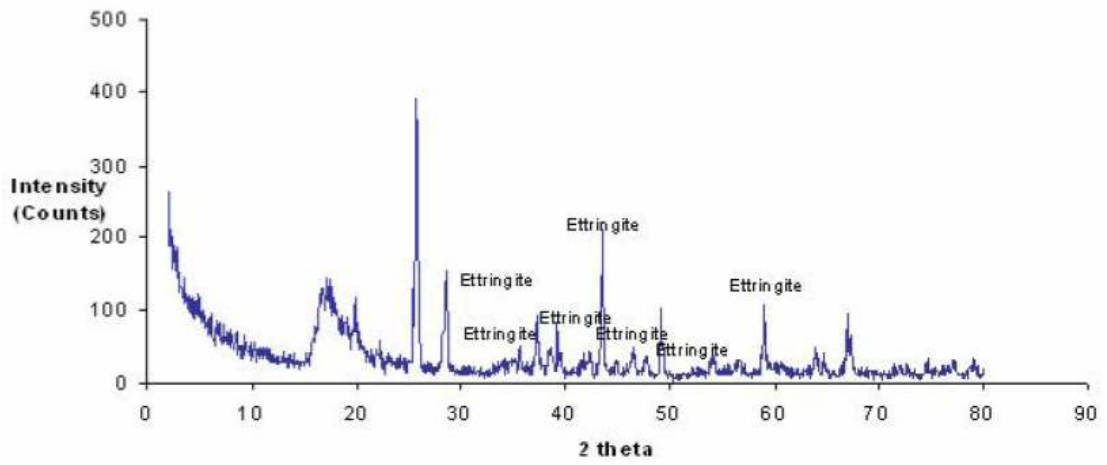

Figure 4.7 XRD Analysis for Lime (Control) Section.

Table 4.8 XRD Results for Type V Cement Treated Section

Intensity (%)	d-Spacing (A)	Quartz	Ettringite (1)	Ettringite (2)	Thaumasite	Prehnite
100	2.4326	×	O	×	×	×
72	3.2995	×	×	×	×	O
33.4	2.2595	×	×	×	×	×

Table 4.8 - *Continued*

16	1.5382	O	×	×	×	O
14.2	4.8862	×	×	×	O	×
9.6	1.9521	×	×	O	O	×
9.3	1.9792	×	×	O	×	×
9.3	1.3765	×	×	×	×	O
7.2	1.8013	O	×	O	×	×
6.3	2.074	×	O	O	×	×
5.4	1.6562	×	×	×	×	O

Note: (O) Indicates the probable presence of the mineral
(×) Indicate the absence of the mineral

Table 4.9 XRD Results for Cement and Fly ash Treated Section

Intensity (%)	d-Spacing (A)	Quartz	Ettringite (1)	Ettringite (2)	Thaumasite	Prehnite
100	1.6601	×	O	×	×	O
17	1.519	×	×	×	×	×
16.4	6.3736	O	×	×	×	×
15.2	2.8116	×	O	×	×	O
14	13.7296	×	×	×	×	×
13.1	2.1254	×	O	O	×	O
12.8	1.9678	×	×	×	×	×
12.5	4.0363	×	O	×	×	O
10.4	1.4648	×	×	×	×	O
8.9	2.5974	×	×	×	×	×
8.6	2.6728	O	×	×	×	×

Note: (O) Indicates the probable presence of the mineral
(×) Indicate the absence of the mineral

Table 4.10 XRD Results for GGBFS Treated Section

Intensity (%)	d-Spacing (A)	Quartz	Ettringite (1)	Ettringite (2)	Thaumasite	Prehnite
100	3.3053	×	×	×	×	×
25.2	1.8136	×	O	×	×	O
20.7	2.3474	×	O	×	×	×
17.1	2.4742	×	×	O	×	×
17.1	4.0363	×	×	×	×	×
12.6	4.1952	×	×	×	×	O
7.8	2.114	×	O	×	×	×

Note: (O) Indicates the probable presence of the mineral
(×) Indicate the absence of the mineral

Table 4.11 XRD Results for Lime- Polypropylene Fiber Section

Intensity (%)	d-Spacing (A)	Quartz	Ettringite (1)	Ettringite (2)	Thaumasite	Prehnite
100	1.3737	O	×	×	×	×
51.8	2.02947	×	O	×	O	×
29.4	2.345	×	O	O	×	×
14.6	4.8576	×	O	O	×	×
10.6	3.2379	×	O	O	×	×
9.6	2.9561	O	×	×	×	×
7.8	2.2436	×	O	O	×	×
7.1	5.216	×	×	×	O	×
6.4	2.2855	O	×	×	×	×

Note: (O) Indicates the probable presence of the mineral
(×) Indicate the absence of the mineral

Table 4.12 XRD Results for Lime (Control) Section

Intensity (%)	d-Spacing (A)	Quartz	Ettringite (1)	Ettringite (2)	Thaumasite	Prehnite
53.4	2.0741	×	O	×	×	O
24.8	1.5623	×	O	O	×	×
23.4	5.287	×	×	×	×	O
20.1	2.4063	×	O	×	×	×
12.9	5.5311	×	×	×	O	×
9.4	1.9475	×	O	O	×	×
9.1	1.4555	×	×	×	×	×
8.3	2.5155	×	O	O	×	×
8	2.1349	×	O	×	×	×
7.2	2.1653	×	O	O	O	×
6.3	1.9051	×	O	×	×	×
5.8	1.6952	×	O	×	×	×
5	56.457	×	O	×	×	×

Note: (O) Indicates the probable presence of the mineral
(×) Indicate the absence of the mineral

It can be mentioned from the above charts and tables that the ettringite mineral is present in all stabilized soil sections. The presence of other minerals including Quartz, Thaumasite and Prehnite minerals are also indicated in these tables. Thaumasite typically forms after ettringite undergoes transformations at cold temperatures, and it typically contains Calcium Carbonate Silicate Sulfate Hydrate. This mineral also contributes to sulfate induced heave distress. Prehnite consists of Calcium Aluminum Silicate Hydroxide and is a known stabilization compound. Its traces are found in all treated soils suggesting that stabilization reactions involving CSH did occur in the present treated soils.

From the results, the presence of ettringite is more evident as more traces match with d-spacing of pure ettringite of both lime-fiber section and lime (control) sections. Type V Cement with Fly ash and GGBFS sections showed a fewer ettringite traces, which was followed by Type V Cement section whereas lime and lime-fiber treated sections showed more traces of ettringite 1 mineral (more than five basal spacings matched with those of standard mineral). Higher heave related movements could be seen in elevation survey results in the case of lime-fiber and lime (control) sections. This indicates there is a correlation between the formation of ettringite in the treated sections and the corresponding heaving. Conversely, cement and GGBFS sections showed less heaving and a fewer number of traces that matched with ettringite mineral. This shows that sulfate heaving was minimal in these treated sections.

4.2.2.4 Scanning Electron Microscope (SEM) Analysis

To cross verify the presence of Ettringite in these treated section, SEM analysis studies were also performed by Vasudev (2007) on the stabilized soil samples collected from the field. Figures 4.8 to 4.12 present the SEM images for all the five stabilized soils. Though, images show some traces of ettringite and thaumasite minerals, they are not definitive and difficult to identify. Other possible reasons could be the loss of minerals due to drying of the samples during SEM studies.

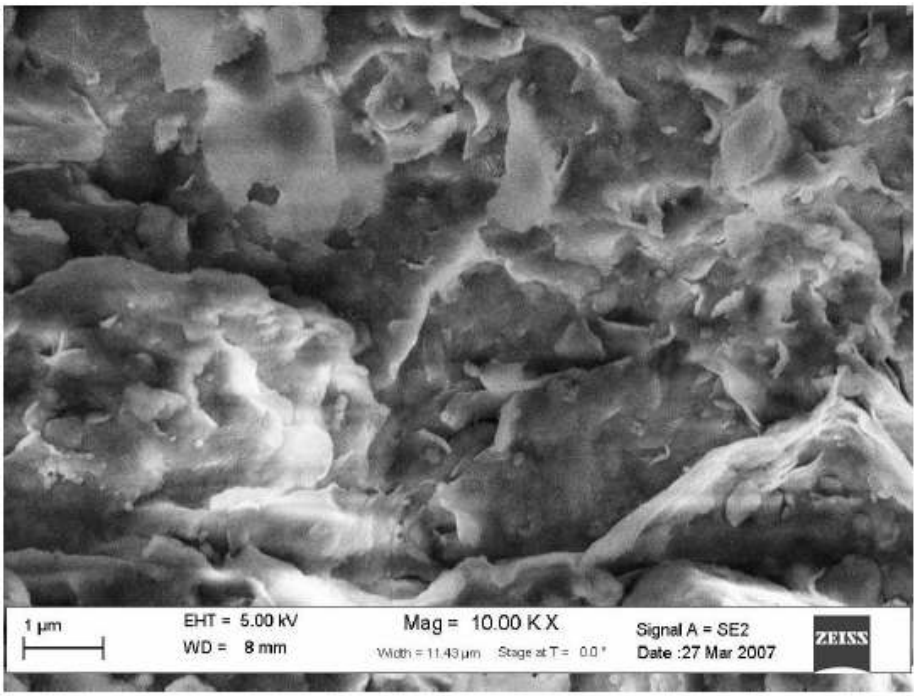

Figure 4.8 SEM Image for Type V Cement Treated Soil.

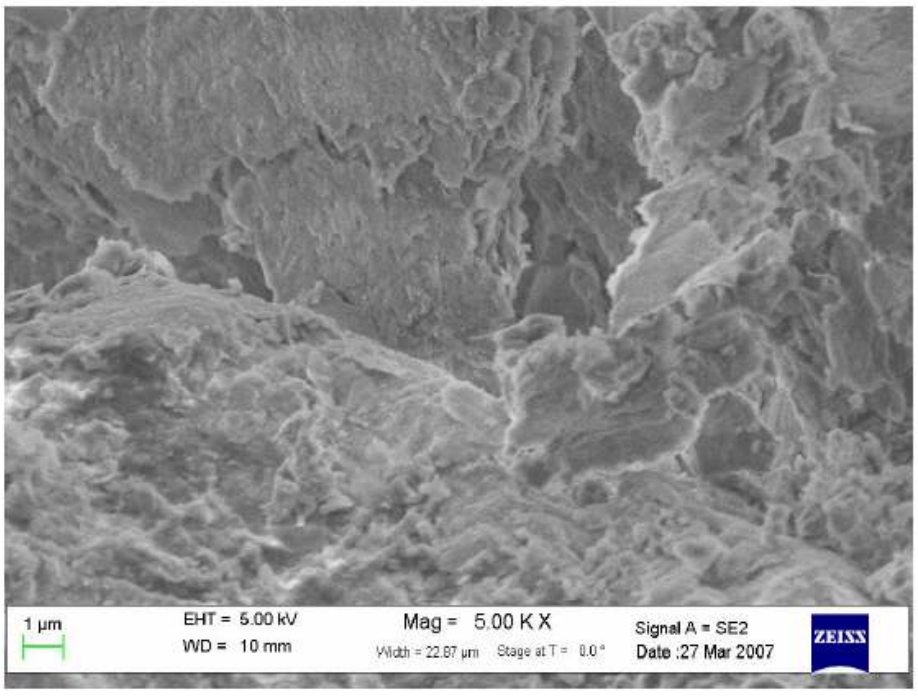

Figure 4.9 SEM Image for Cement with Fly ash Treated Soil.

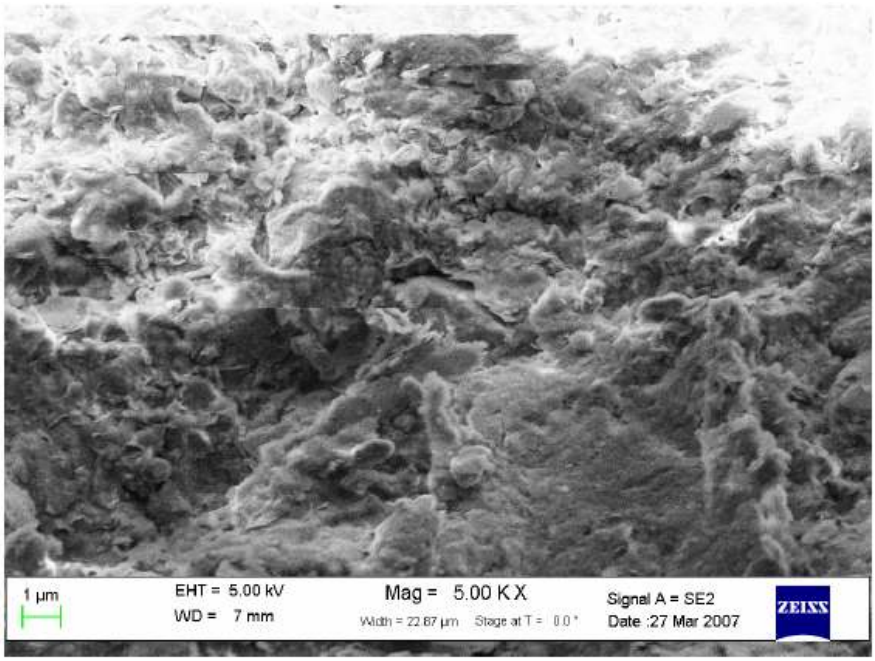

Figure 4.10 SEM Image for GGBFS Treated Soils.

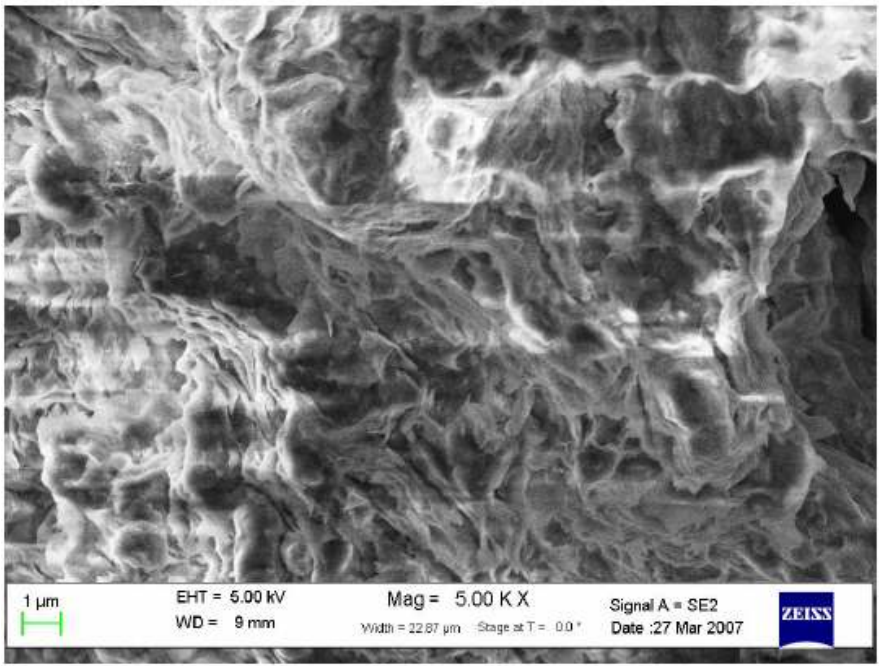

Figure 4.11 SEM Image for Lime with Fibers Treated Soils.

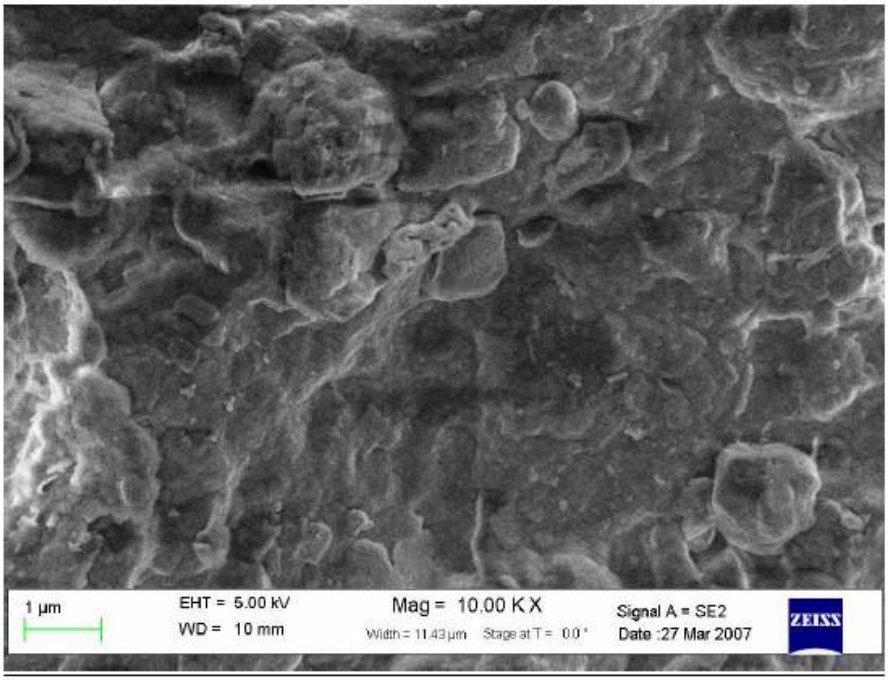

Figure 4.12 SEM Image for Lime (Control) Treated Soils.

4.2.2.5 Energy Dispersive X-Ray Microanalysis (EDAX) Results

In addition to the XRD and SEM analyses, The Energy Dispersive X-ray Analysis (EDAX) was conducted by (Vasudev, 2007) on all the specimens. This test was used to identify the chemical species present in the treated soils collected from the field. EDAX results are presented from Figure 4.13 through 4.17 for all the treated soils.

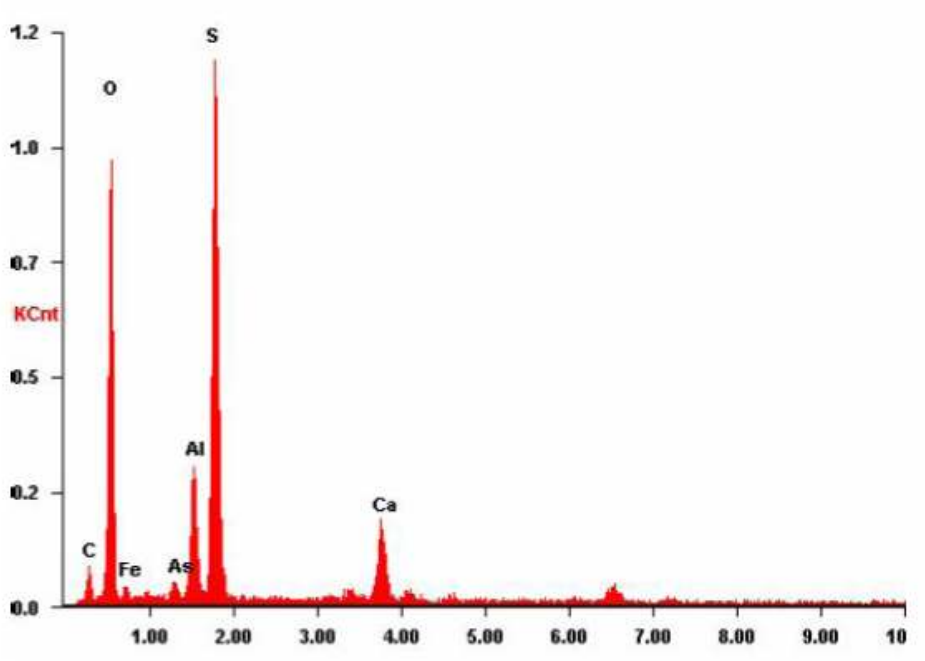

Figure 4.13 EDAX Results for Type V Cement Treated Soils.

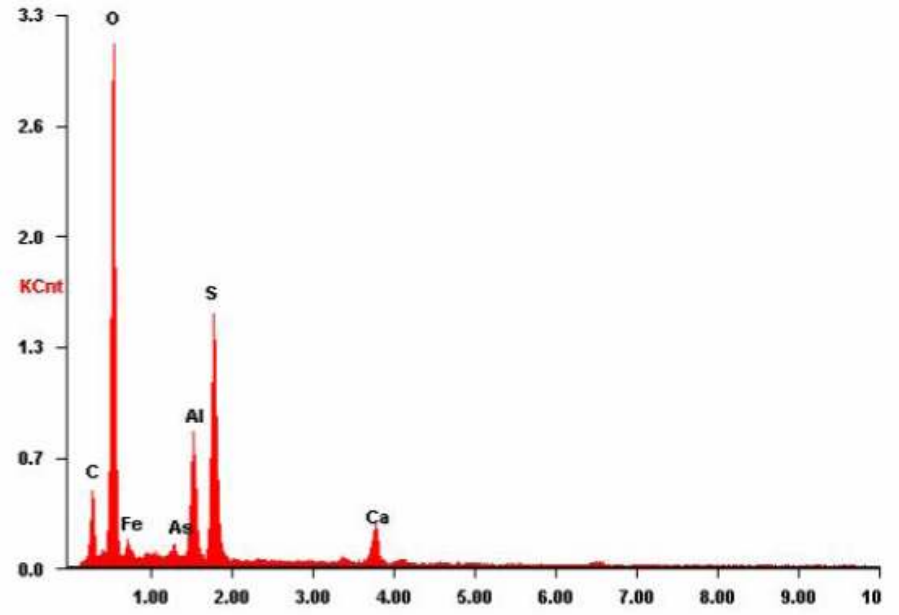

Figure 4.14 EDAX Results for Type V Cement and Fly ash Treated Soils.

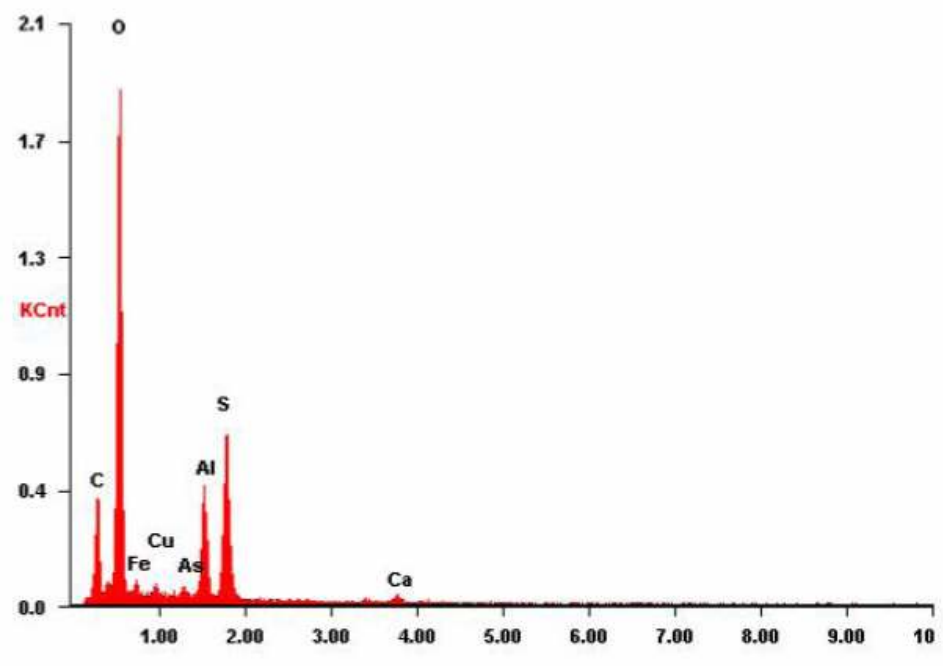

Figure 4.15 EDAX Results for GGBFS Treated Soils.

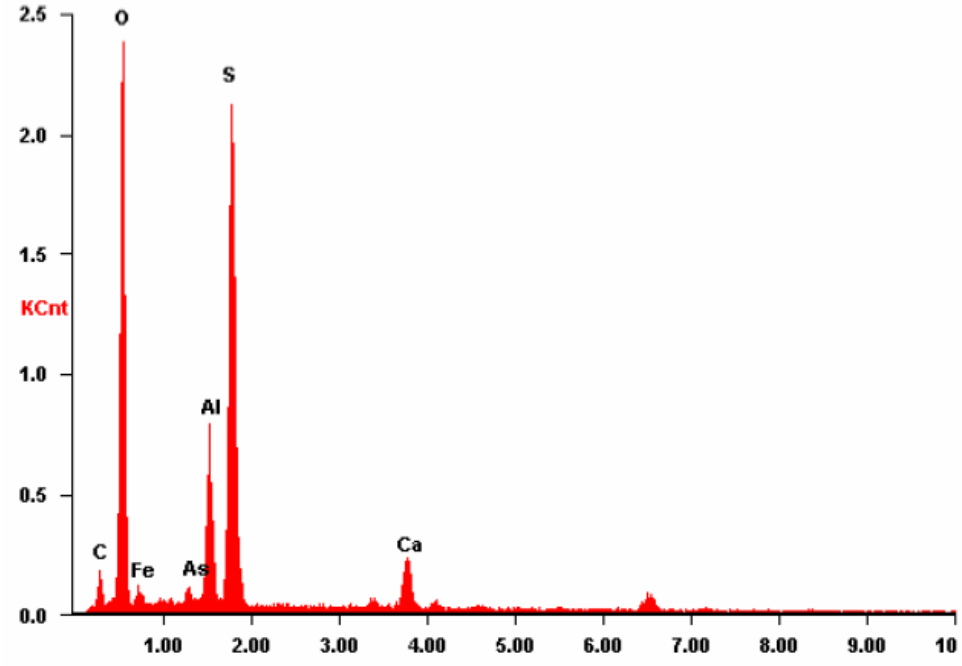

Figure 4.16 EDAX Results for Lime and Fibers Treated Soils.

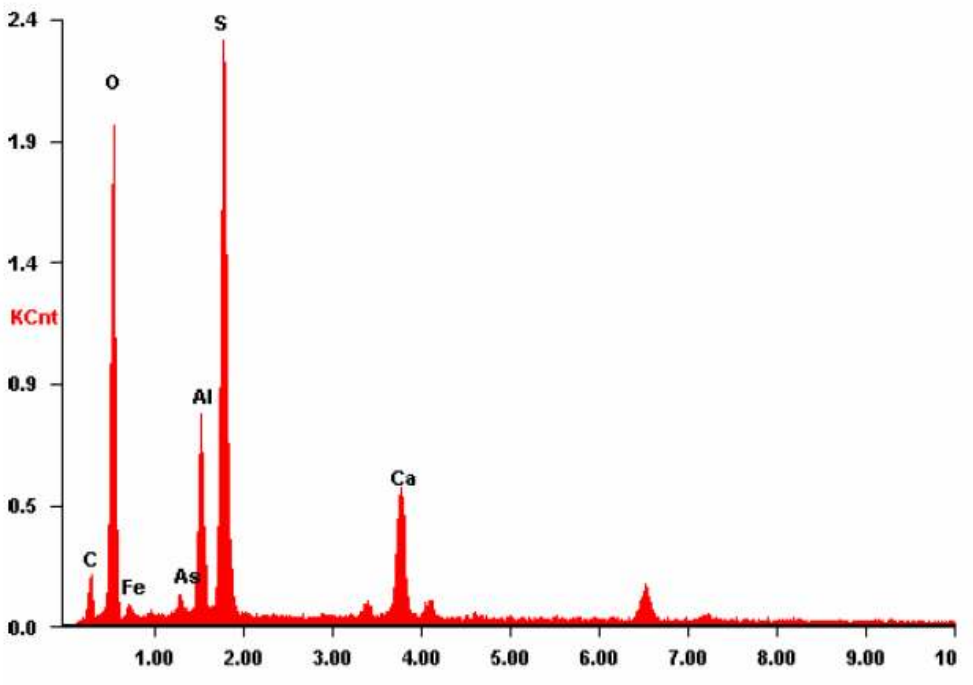

Figure 4.17 EDAX Results for Lime (Control) Treated Section.

EDAX analyses on treated soil samples show that all the ingredients, including suphur (S), aluminum (Al), and calcium (Ca), which contribute to ettringite formation are present in the treated soils. Higher peaks in a spectrum represent higher concentration of the elements in the soil specimen. Hence, it can be mentioned that ettringite formation is evident in treated soils.

4.2.3 Determination of Strength Properties of Harwood Road Soil

Strength assessment tests were performed by Chavva (2002), which are unconfined compressive strength (UCS) and resilient modulus (M_R) test results. The UCS tests were conducted on specimens at the optimum moisture condition after 7-day of curing. Resilient modulus tests were conducted to measure the moduli of soil specimens treated with variety of stabilizers.

4.2.3.1 Unconfined Compressive Strength Test

The UCS tests were conducted as per the ASTM D-2166 standards and specimens were prepared as mentioned in section 4.2.1.1. Once the specimen was prepared and cured,

they were placed in the triaxial test setup. The specimen is then loaded at a constant rate which was controlled by a loading device control. Deformation data and axial load was collected from a computer attached to a test setup. The maximum axial compressive load at which the specimen failed was used to determine the unconfined compressive strength of the soil specimen. Five specimens were tested for each stabilizer at the optimum moisture content and the average was calculated and shown in Table 4.13.

It can be seen from the UCS results that Type V cement, Class F Fly ash and GGBFS have yielded a noticeable strength enhancement to the treated specimens. The strength increase in the stabilized soil specimens were attributed to the cementitious reactions from the stabilization process.

Table 4.13 UCS Strength Values for Different Stabilizers (Chavva, 2002)

Soil Type	Unconfined Compressive Strength, psi (kPa)
Control (Lime 8%)	36.6 (252.17)
Type V Cement (8%)	225.8 (1555.76)
Class F Fly ash (15%) and Type V Cement (5%)	154 (1061.06)
GGBFS	108.8 (749.63)
Lime (8%) and Polypropylene Fibers (0.15%)	50.9 (350.70)

4.2.3.2 Resilient Modulus Test

The resilient modulus (M_R) is defined as the ratio of the axial deviator stress to the recoverable axial strain (Puppala and Mohammad, 1995). Resilient modulus test was conducted to study the effect of traffic load and overburden pressure, as represented by deviatoric stresses and confining pressures respectively, on M_R properties of control and stabilized soil. It was also conducted to analyze the effects of stabilizers on resilient properties of soil. The tests on

materials were conducted with the confining and deviator stress levels following the procedure specified by AASHTO T307-99 for subgrade materials. The test starts with applying a repeated deviatoric load on the specimen with fixed load duration of 0.1 second and a relaxation period of 0.9 seconds.

The test consisted of one conditioning phase and 15 testing phases, with 1,000 cycles of conditioning and 100 cycles for each testing phase under a variety of confining and deviatoric stresses. Specimens were conditioned by applying a thousand repetitions of a specified deviator stress in order to eliminate the effects of specimen disturbance caused by sampling, compaction and specimen preparation procedures. Once the specimen conditioning was done, test was conducted as specified by AASHTO T307-99 to cover the service range of stress that a subgrade material experienced due to traffic loading and over-burden conditions. Table 4.14 presents the average resilient modulus results for control and stabilized soils at a confining pressure of 13.80 kPa.

It can be seen from the above results that sulfate resistant cement yielded the highest enhancement in M_R and lime with polypropylene fibers yielded the lowest enhancement in M_R.

Table 4.14 Resilient Modulus (M_R) for Control and Treated Soils at Confining Pressure of 13.80 kPa (Ramakrishna, 2002)

Soil Type	Resilient Modulus, M_R (MPa)
Control (Lime 8%)	80.3
Type V Cement (8%)	762.7
Class F Fly ash (15%) and Type V Cement (5%)	389.8

Table 4.14- *Continued*

GGBFS (20%)	351.8
Lime (8%) and Polypropylene Fibers (0.15%)	80

4.3 Laboratory Results for Non-sulfate Soils

Soil specimens were collected from three test street sites in Arlington, Texas, including International Parkway, Southmoor and Southeast Parkway. Several laboratory tests were performed to determine basic and engineering properties of the soils. The laboratory tests include basic properties of soils, chemical and mineralogical characteristic and strength properties tests. The results acquired from the tests are shown and discussed below.

4.3.1 Determination of Basic Properties of Non-sulfate Soils

4.3.1.1 Specimen Preparation

As mentioned earlier in section 4.2.5, the compositional and environmental conditions such as moisture content, dry unit weight of soils and stabilizer dosages usually influences the plasticity index, swelling, shrinkage, and strength properties of soils. Soil specimens were collected immediately after the stabilization has been completed in the field. The soil was first oven dried and pulverized. This pulverized specimen was used for the determination of soils basic properties including soils classification, Atterberg Limits, shrink-swell potentials and soluble sulfate contents. The Standard Proctor compaction tests were then conducted to determine the optimum moisture content and the corresponding dry unit weight. For UCS and Resilient Modulus test., the specimens were compacted at optimum moisture content and dry unit weight in Standard Proctor molds and carefully extracted. Then the specimens were wrapped and cured in humidity rooms for 7 days prior to the testing.

4.3.1.2 Atterberg Limits

Atterberg limit tests were conducted as per ASTM D-4318 method to determine the consistency of the soil. According to results acquired from the Atterberg limit tests, the soil were

classified by the AASHTO classification method and the USCS classification method and shown in Table 4.15, the basic soil properties of natural soils collected from 3 test sites.

Table 4.15 Basic Soil Properties (Untreated)

Property	Soil Types		
	International Parkway	Southmoor	Southeast Parkway
Passing #40 (%)	100	100	100
Passing #200 (%)	>80%	>80%	>80%
Specific Gravity	2.7	2.7	2.7
Liquid Limit (LL, %)	58	60	51
Plastic Limit (PL, %)	21	21	23
Plasticity Index (PI, %)	37	39	28
AASHTO Classification	A-7-5	A-7-6	A-7-5
USCS Classification	CH	CH	CH

Tests on Atterberg limits for control or untreated soils from various bore holes from 3 locations yielded an average liquid limit (LL) of 56.3 with an average plasticity index (PI) of 34.67 for all three soils. In contrast, lime treated soils from same 3 locations yielded an average liquid limit of 44.33 with an average plasticity index of 11.67. Combined lime and cement treated soils yielded even better average liquid limit of 42.67 and an average plasticity index of 9.33. Individual results of each site are given in Table 4.16. The results are also plotted and shown in Figure 4.18, Figure 4.19 and Figure 4.20 for International Parkway, Southmoor Drive and Southeast Parkway, respectively.

Table 4.16 Atterberg Limits of Untreated and Treated Soils Specimens from 3 Sites

INTERNATIONAL PARKWAY			
Atterberg Limits	Untreated	Lime Treated	Lime-Cement treated
LL	58	43	39
PL	21	32	31
PI	37	11	8
SOUTHMOOR DRIVE			
Atterberg Limits	Untreated	Lime Treated	Cement and Lime treated
LL	60	39	41
PL	21	30	33
PI	39	9	8
SOUTHEAST PARKWAY			
Atterberg Limits	Untreated	Lime Treated	Cement and Lime treated
LL	51	51	48
PL	23	36	36
PI	28	15	12

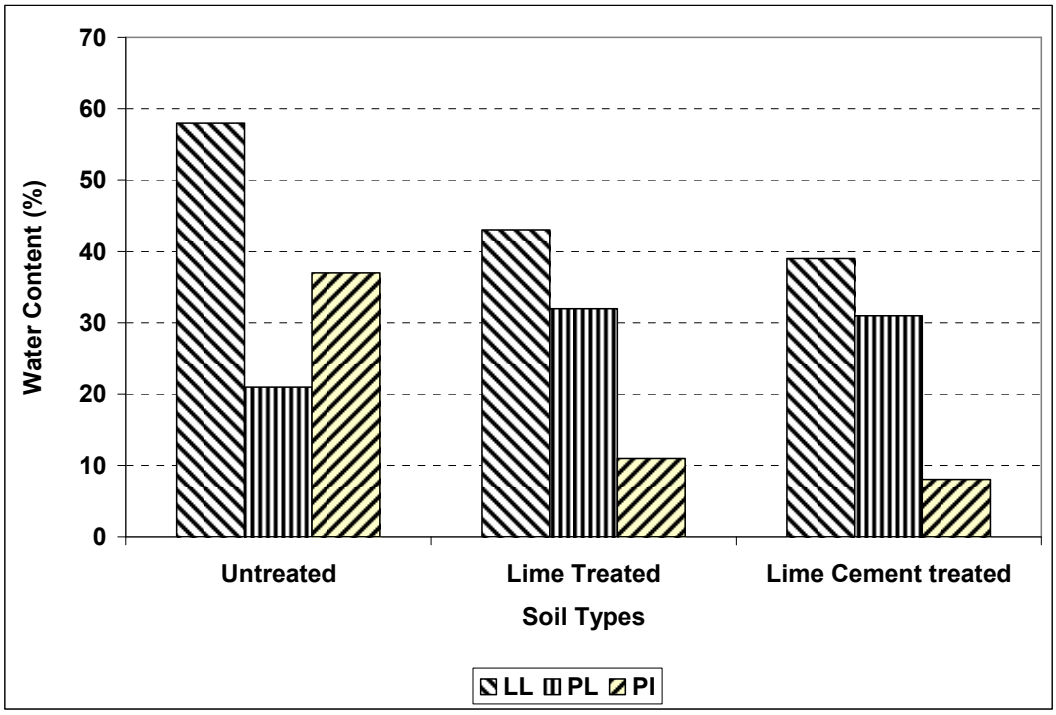

Figure 4.18 Atterberg Limits for Specimens Collected from International Parkway.

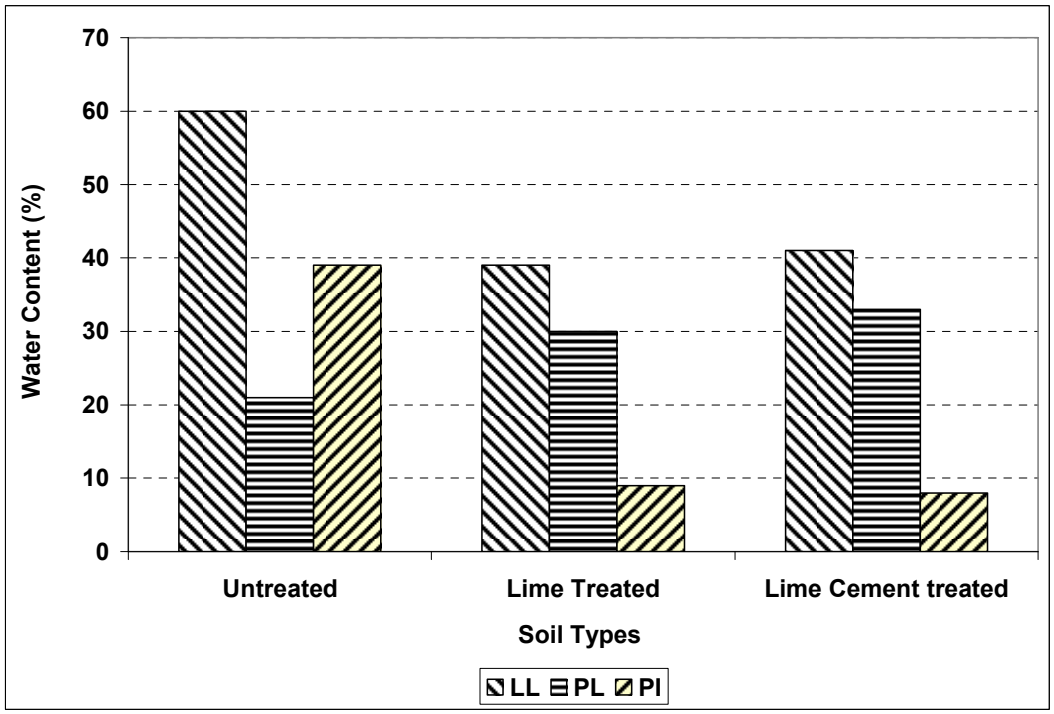

Figure 4.19 Atterberg Limits for Specimens Collected from Southmoor Drive.

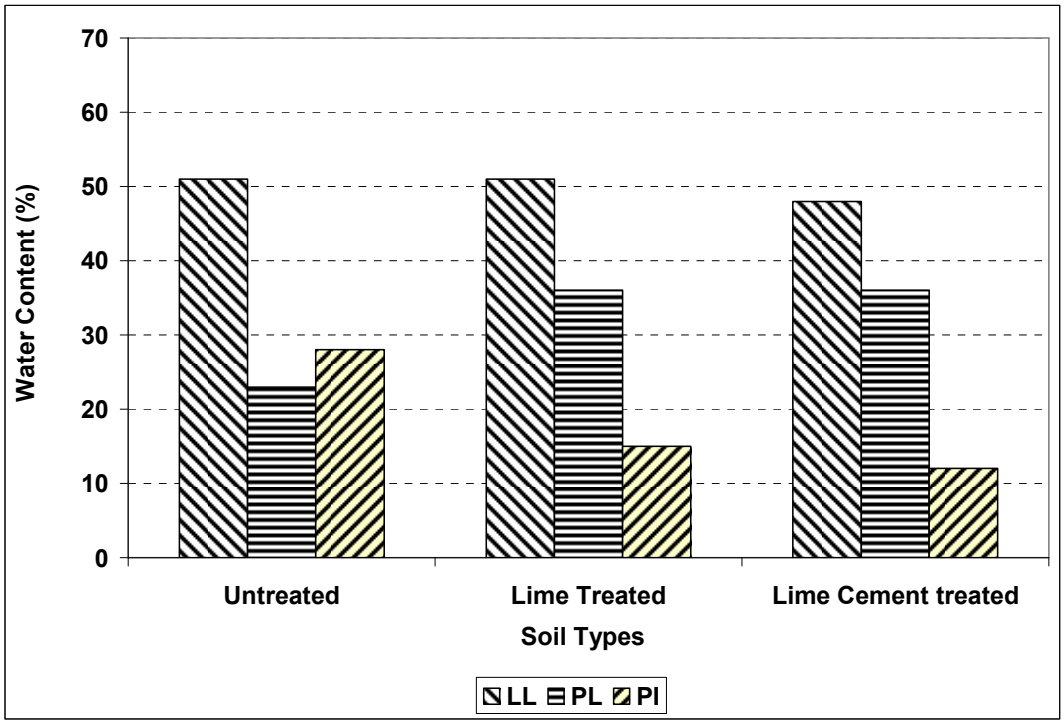

Figure 4.20 Atterberg Limits for Specimens Collected from Southeast Parkway.

There was a considerable decrease in Atterberg Limits of the chemical treated soils from each site, which is attributed to a decrease in the thickness of the diffused double layer as a result of cationic exchange reactions by the calcium ions from lime and cement binders. Overall, an increase in plastic limit and a decrease in plasticity index indicate a considerable enhancement in the workability characteristics of all three non-sulfate soils when treated with both lime and lime-cement treatments.

4.3.1.3 Standard Proctor Compaction Test

Standard proctor compaction tests were conducted in order to determine the optimum moisture content and dry unit weight of both control and treated soil. Specimens were prepared as per ASTM D-4218. Standard proctor test results are presented in Table 4.17 and Figure 4.20 respectively.

Optimum moisture contents varied from 23% to 32%, with higher optimum moisture contents being measured with lime - cement treatment. Optimum dry unit weights of treated soils were reduced considerably with the lime-cement treatment, following the trends observed for lime treated soils.

Table 4.17 Moisture Content and Dry Unit Weight of Raw and Treated Soil

Locations	Soil Types	Optimum Moisture Content (%)	γ_{dmax}, pcf (kN/m^3)
International Parkway	Control (untreated) soils	26.40	95.60 (15.02)
	Treated soils (6% lime and 6% cement)	32.60	87.70 (13.78)
Southmoor Drive	Control (untreated) soils	23.80	101.40 (15.93)
	Treated soils (6% lime and 6% cement)	29.70	89.00 (13.98)
Southeast Parkway	Control (untreated) soils	23.80	101.40 (15.93)
	Treated soils (6% lime and 6% cement)	28.00	93.00 (14.61)

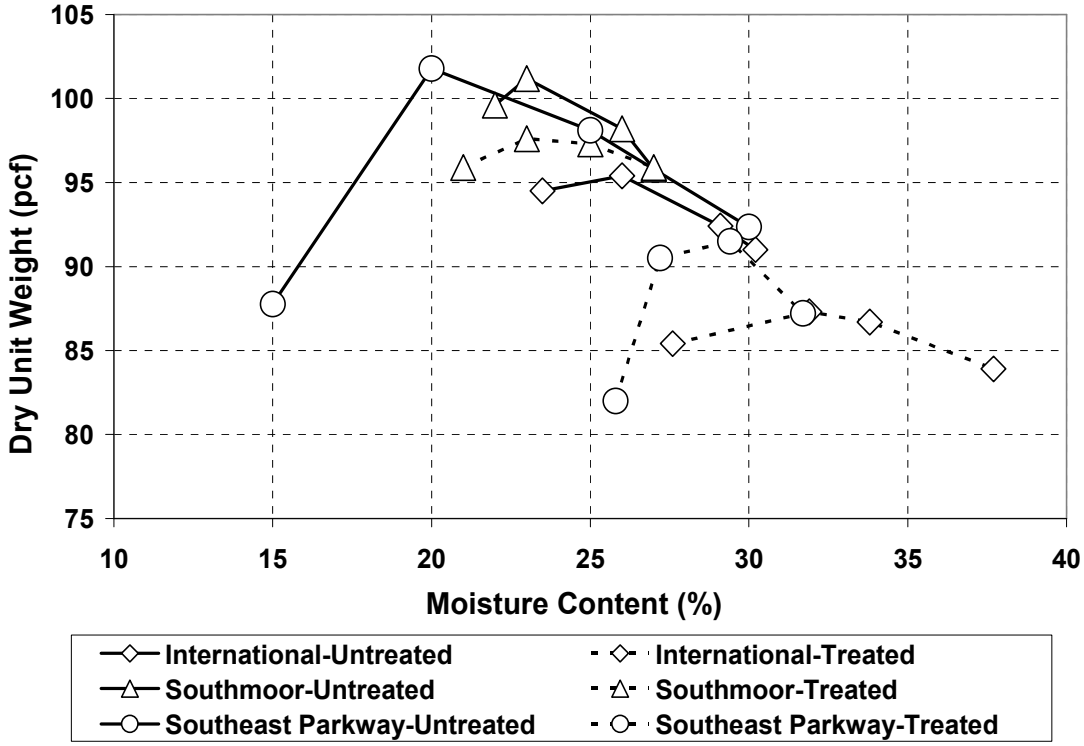

Figure 4.21 Standard Proctor Compaction Test Results for all Locations.

4.3.1.4 One Dimensional Free Swell Test

Free swell test measures the amount of heave in a confined specimen. Both control and treated specimens are measured 2.5 inches in diameter and 1 inch in thickness. The free swell tests were conducted as per ASTM standards. Table 4.18 presents the swell potential of control and treated soil. It can be seen from Table 4.18 that swell potential of the soils was significantly minimized after the treatments. The decrease in swell potential in all the treated soils was due to the decrease in plasticity properties of the soils as a result of chemical treatments.

Table 4.18 Free Vertical Swell Strains for Control and Treated Soils

Locations	Untreated Soil	Lime Treated Soil	Lime Cement Treated Soil
International Parkway	6.30%	2.27%	0.00%
Southmoor Drive	6.20%	2.90%	0.20%
Southeast Parkway	5.30%	2.10%	0.00%

4.3.1.5 Linear Shrinkage Strain Test

Linear Shrinkage Strain Test was conducted as per Texas Department of Transportation (TxDOT) method specified by Tex-107-E. Untreated soils showed an average linear shrinkage strain of 14.9% or higher, whereas treated soils showed minute or very small shrinkage strains due to the formation of hairline cracks. Shrinkage strain test on 7-days cured specimens showed no volume changes in the treated soils, which was attributed to plasticity decrease and reductions of moisture affinity of treated soil particles due to ionic exchange reactions. Table 4.19 present Linear Shrinkage Strain for Non-sulfate Soils

Table 4.19 Linear Shrinkage Strain for Non-sulfate Soils

Locations	Untreated	Lime Treated	Lime Cement treated
International Parkway	20.21 %	1.20 %	0.00 %
Southmoor Drive	14.91 %	1.40 %	0.00 %
Southeast Parkway	19.24 %	1.00 %	0.00 %

4.3.2 Chemical and Mineralogical Studies on Treated Specimens

Two types of laboratory tests are required to study the potential of ettringite formation. These tests include chemical tests and mineralogical tests. Chemical tests were conducted in order to determine the pH and soluble sulfate content in the soils. Mineralogical tests were

conducted to determine the potential of ettringite formation in stabilized soils which included X-Ray Diffraction (XRD) test and Scanning Electron Microscope (SEM) analysis.

4.3.2.1 Soluble Sulfate Test Results

Soluble sulfate tests were conducted on untreated soil specimens collected from 3 test sites in order to measure the amount of soluble sulfate contained in the soils. In general, sulfate content is presented as a percent of soluble sulfate to dry weight of soil. The content of sulfate which induces heaving varies from 2000 ppm to as high as 10,000 ppm. Hunter (1988) mentioned that the initial threshold sulfate level of 10,000 ppm in soils would lead to sulfate-induced heave distress problems when such soils are stabilized with calcium-based stabilizers such as lime and cement. Mitchell and Dermatas (1990) reported that the problematic threshold sulfate levels occur close to 3000 ppm. Table 4.20 summarizes the soluble sulfate content for the stabilized soils. Results achieved from the soluble sulfate tests indicate that the presences of sulfate in the soil specimens collected from all 3 test sites are not a major concern as sulfate levels are lower than 2,000 ppm. Therefore, these soils could be considered as non-sulfate soils.

Table 4.20 Soluble Sulfate Contents for Stabilized Soil Sections

Stabilizers	Soluble Sulfate Content (ppm)
International Parkway	1480.35
Southmoor Drive	1708.49
Southeast Parkway	1609.2

4.3.2.2 X-Ray Diffraction (XRD) Analysis

XRD Analyses were conducted on all the treated soil samples collected from three test sites. The objective of these studies is to identify the cementitious properties and examine the microstructure of the soils stabilized with combined lime and cement. Figures 4.22 to 4.24 present XRD analyses data for three test sites. Tables 4.21 to 4.23 show the presence of ettringite as per their corresponding d-spacing values.

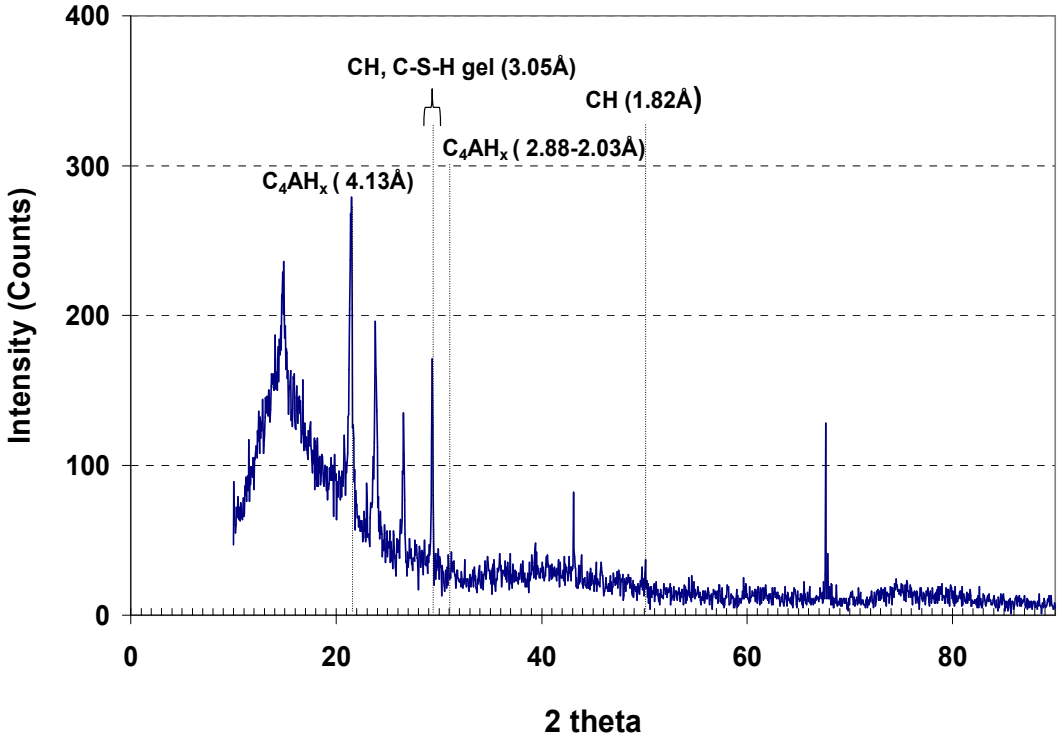

Figure 4.22 XRD Analysis for Combine Lime and Cement Treated Section at International Parkway

Table 4.21 XRD Results for Combined Lime and Cement Treated Section at International Parkway

Intensity (%)	d-Spacing (A)	C-S-H	C_4AH_x	CH
100	4.1338	×	O	×
56.5	3.7341	×	×	×
45.4	3.7707	×	×	×
44.5	5.9467	×	×	×
29.3	3.355	×	×	×
28.1	3.0402	O	×	O
8.1	2.2852	×	O	×
7.7	1.3803	×	×	×
5.8	1.8197	×	×	O

Note: (O) Indicates the probable presence of the mineral
(×) Indicate the absence of the mineral

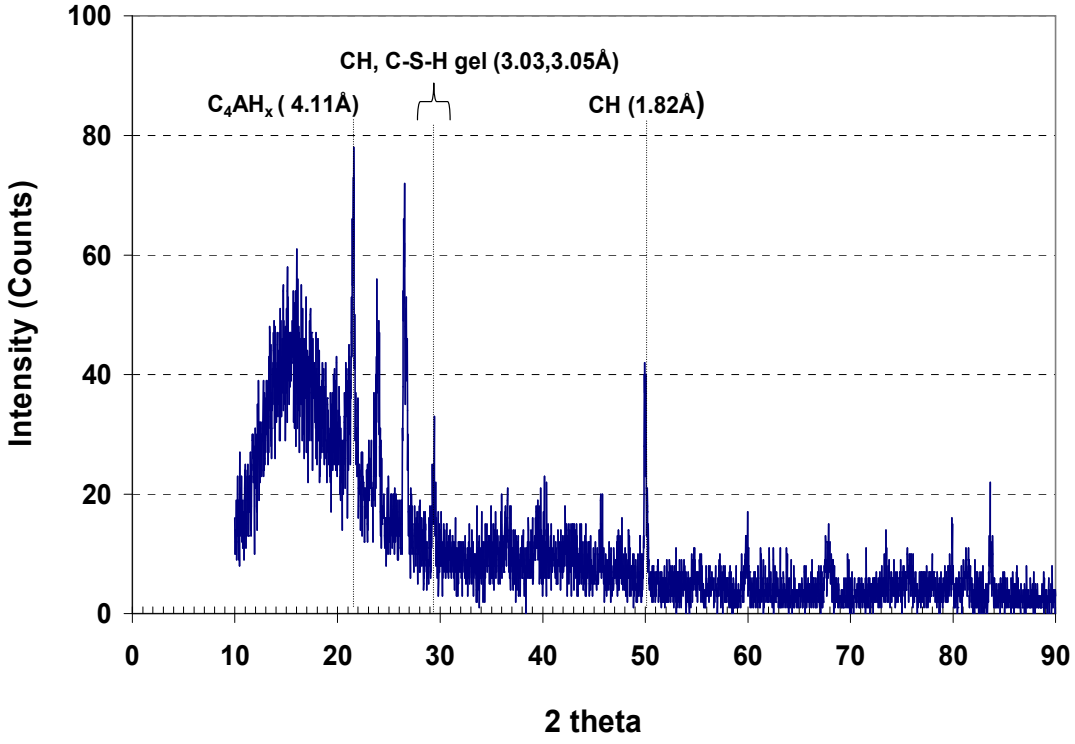

Figure 4.23 XRD Analysis for Combine Lime and Cement Treated Section at Southmoor Drive.

Table 4.22 XRD Results for Combined Lime and Cement Treated Section at Southmoor Drive

Intensity (%)	d-Spacing (A)	C-S-H	C_4AH_x	CH
100	3.3655	×	×	×
90.5	3.7288	×	×	×
88.4	4.1151	×	O	×
78.2	3.3363	×	×	×
76.2	3.7077	×	×	×
75.4	3.7029	×	×	×
74.2	3.6932	×	×	×
51.2	1.8248	×	O	×
39.3	3.0318	O	×	O
33.5	3.0514	O	×	O

Note: (O) Indicates the probable presence of the mineral (×) Indicate the absence of the mineral

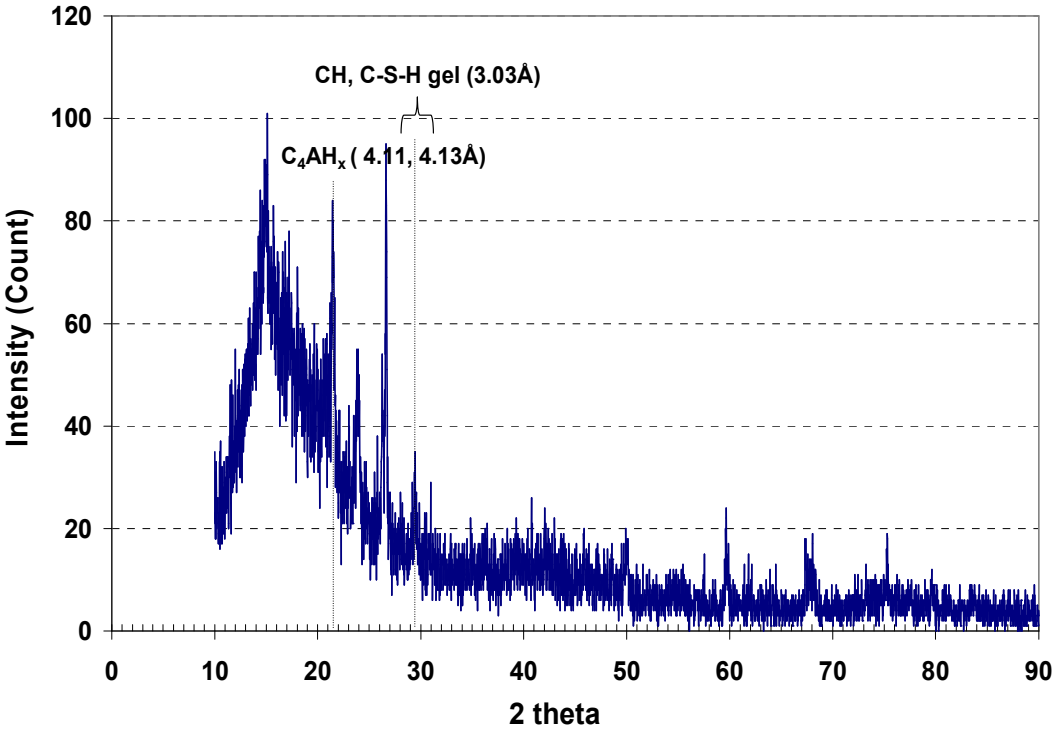

Figure 4.24 XRD Analysis for Combine Lime and Cement Treated Section at Southeast Parkway.

Table 4.23 XRD Results for Combined Lime and Cement Treated Section at Southeast Parkway

Intensity (%)	d-Spacing (A)	C-S-H	C_4AH_x	CH
100	5.9412	×	×	×
92.4	4.1832	×	×	×
85.8	3.3453	×	×	×
74.6	5.8650	×	×	×
71.9	4.1158	×	O	×
69.7	4.1336	×	O	×
52.6	3.7015	×	×	×

Table 4.23 - *Continued*

52.4	3.7353	×	×	×
52.3	3.3832	×	×	×
51.6	3.7168	×	×	×
30.4	1.3766	×	×	×
21.2	1.5486	×	×	×
20.5	3.0301	O	×	O

Note: (O) Indicates the probable presence of the mineral
(×) Indicate the absence of the mineral

From the XRD results on the stabilized soil specimens collected from three test sites presented above, it can be noted that soils stabilized with combined lime and cement are subjected to pozzolanic reaction where the strongest on XRD traces is for the development of C_4AH_{13} and C-S-H gel. The structure of the stabilized soils is common to all soils subjected to the addition of hydrated lime as an alkaline activator. The XRD results also show that there is no evident of ettringite formation as in the observation period of thirty months. This is due to the fact that soils from these locations contain low sulfate amount which is less than 2,000 ppm.

4.3.3 Determination of Strength and Stiffness Properties of Non-sulfate Soil

Laboratory tests were performed to assess strength and stiffness properties of the soils. These tests are unconfined compressive strength (UCS) and resilient modulus (M_R) tests. The UCS tests were conducted on untreated, lime treated and lime cement treated specimens at the optimum moisture condition after 7-day curing in order to study the effects of the stabilizers on strength enhancement of the soils. The resilient modulus tests were conducted to measure the moduli of untreated and treated soil specimens. The resilient modulus tests were also conducted to study the influence of lime-cement stabilization on the non-sulfate soils. The results from these tests are shown and discussed below.

4.3.3.1 Unconfined Compressive Strength Test

Quality control of the lime and cement stabilized specimens is often assessed in term of strength improvement that the stabilizers made to the soil specimens. Hence, the most popular

test used is Unconfined Compression Strength (UCS) test. UCS tests were carried out on both treated and untreated soil specimens in order to compare their strength variations with respect to lime and combined cement-lime treatments.

The UCS tests were conducted were as per the ASTM D-2166 standards and specimens were prepared as mentioned in section 4.3.1.1. Once the specimen was prepared and cured, they were placed in the triaxial setup. A total number of 27 specimens, 9 specimens (3 untreated, 3 lime treated and 3 lime cement treated specimens) from each test site, were tested at the optimum moisture content. The results were averaged and shown in Table 4.24.

Table 4.24 UCS Strength Values for Treated and Untreated Specimens from Three Test Sites

Soil Designation	Untreated psi (kPa)	Lime Treated psi (kPa)	Combined Lime and Cement Treated psi (kPa)
International	12.59 (86.76)	202.30 (1394.81)	250.90 (1729.89)
Southmoor	26.97 (185.98)	198.00 (1365.00)	256.93 (1834.03)
Southeast Parkway	47.35 (326.47)	331.87 (2288.19)	499.24 (3442.14)

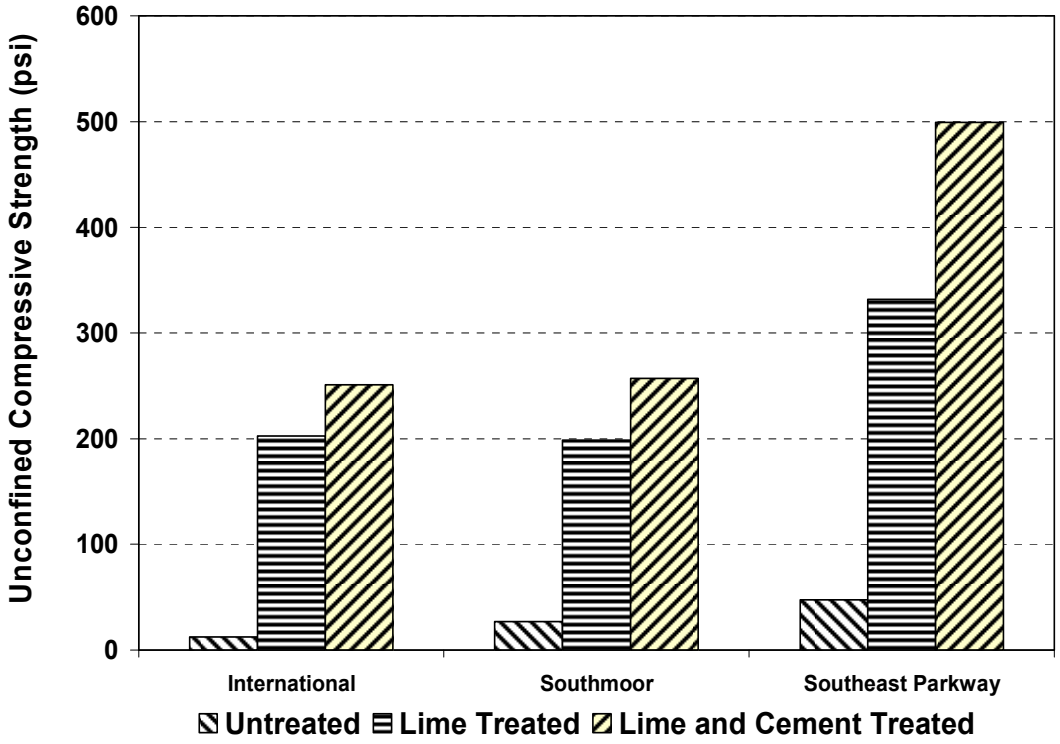

Figure 4.25 The Comparison of UCS Values for Treated and Untreated Specimens from 3 test sites.

For the untreated soil specimens, the average UCS of all three sites are 28.97 psi (199.60 kPa), whereas both lime and combined lime-cement treated soils exhibited higher UCS strengths in the range of 200 psi (1378.95 kPa) to 500 psi (3445 kPa), giving a tenfold increase in the UCS of untreated soil. This strength increase meet the UCS criterion often used (more than 200 psi of stabilized soil) in soil cement materials for low volume traffic conditions.

The compressive strength of untreated soil specimens is considerably enhanced (more than ten times) after both treatments. The combined lime and cement treatment has resulted in slightly higher compressive strength than the isolated lime treatment. Strength enhancements overall are attributed to pozzalonic compounds formed due to chemical reactions between stabilizers and soil in the presence of moisture.

4.3.3.2 Resilient Modulus Test

The resilient modulus tests were conducted as per AASHTO T 307-99 standard test procedure. These tests have been employed for the determination of resilient moduli of the soils specimens collected from three test sites. The combinations of various deviatoric and confining stresses applied in the test sequence were shown in Table 3.2 presented in Chapter 3. In each test sequence, the specimen was subjected to 3 different confining stresses with 5 levels of deviatoric stresses applied at each confinement. A haversine loading wave with a frequency of 10 Hz was used to simulate the traffic wheel loading. Each loading cycle subjects the specimen to 0.1 sec of deviatoric or repeated loading and 0.9 sec of relaxation. During the test, the average total vertical deformation was monitored and recorded using two linear variable displacement transducers (LVDTs) placed on top of the triaxial cell. The internal load transducer placed inside the triaxial chamber recorded the deviatoric stress applied to the soil specimen.

In an attempt to evaluate the repeatability and reliability of the resilient modulus test results, tests were conducted on a total number of 27 specimens, 9 specimens (3 untreated, 3 lime treated and 3 lime cement treated specimens) from each test site, were tested in this assessment. For each condition, two specimens were used. Results from these tests were averaged and are presented in the form of bar chart graph and clustered column to study the influences of both confining pressures and deviatoric stresses applied to the specimens during the tests. Table 4.25, Table 4.26 and Table 4.27 presents the average of resilient modulus (M_R) test results for untreated and treated specimens collected from International Parkway, Southmoor Drive and Southeast Parkway, respectively.

Table 4.25 The Average of Resilient Modulus (M_R) Test Results for Untreated and Treated Specimens Collected from International Parkway

Sequence Number	Confining Pressure (kPa)	Maximum Stress (kPa)	Untreated (MPa)	Lime Treated (MPa)	Combined Lime and Cement Treated (MPa)
0	41.40	27.60	46.04	202.67	243.27
1	41.40	13.80	27.75	93.28	184.86
2	41.40	27.60	41.86	196.15	242.56
3	41.40	41.40	68.27	252.16	300.22
4	41.40	55.20	96.82	291.77	329.59
5	41.40	68.90	131.81	333.05	351.02
6	27.60	13.80	26.78	104.60	174.18
7	27.60	27.60	41.87	167.35	244.87
8	27.60	41.40	67.73	253.62	295.74
9	27.60	55.20	94.15	296.17	332.69
10	27.60	68.90	130.69	331.20	340.85
11	13.80	13.80	26.02	96.47	162.39
12	13.80	27.60	40.99	161.17	241.29
13	13.80	41.40	67.26	221.79	287.03
14	13.80	55.20	95.45	257.22	335.10

Table 4.26 The Average of Resilient Modulus (M_R) Test Results for Untreated and Treated Specimens Collected from Southmoor Drive

Sequence Number	Confining Pressure (kPa)	Maximum Stress (kPa)	Untreated (MPa)	Lime Treated (MPa)	Combined Lime and Cement Treated (MPa)
0	41.40	27.60	45.94	173.84	245.02
1	41.40	13.80	17.95	116.27	166.87
2	41.40	27.60	41.85	180.48	253.70
3	41.40	41.40	72.95	199.50	297.64
4	41.40	55.20	110.65	217.82	314.56
5	41.40	68.90	149.82	222.71	326.36
6	27.60	13.80	24.09	111.24	164.18
7	27.60	27.60	45.48	165.80	233.36
8	27.60	41.40	74.72	198.28	279.69
9	27.60	55.20	109.14	209.33	307.50
10	27.60	68.90	147.91	217.86	317.68
11	13.80	13.80	23.60	110.00	170.25
12	13.80	27.60	44.02	167.24	247.16
13	13.80	41.40	74.86	185.70	275.87
14	13.80	55.20	109.83	196.62	299.88
15	13.80	68.90	148.75	205.51	321.12

Table 4.27 The Average of Resilient Modulus (M_R) Test Results for Untreated and Treated Specimens Collected from Southeast Parkway

Sequence Number	Confining Pressure (kPa)	Maximum Stress (kPa)	Untreated (MPa)	Lime Treated (MPa)	Combined Lime and Cement Treated (MPa)
0	41.40	27.60	47.13	156.66	260.61
1	41.40	13.80	29.40	88.54	187.67
2	41.40	27.60	45.67	148.76	252.11
3	41.40	41.40	71.58	215.97	293.56
4	41.40	55.20	101.48	265.13	310.26
5	41.40	68.90	134.55	291.61	329.30
6	27.60	13.80	29.64	99.45	162.03
7	27.60	27.60	46.87	148.45	231.07
8	27.60	41.40	72.50	227.88	282.94
9	27.60	55.20	100.43	263.12	307.73
10	27.60	68.90	131.99	294.42	318.22
11	13.80	13.80	29.05	99.71	160.09
12	13.80	27.60	46.55	157.99	232.93
13	13.80	41.40	72.14	215.62	263.69
14	13.80	55.20	101.16	262.01	289.87
15	13.80	68.90	134.27	292.85	297.59

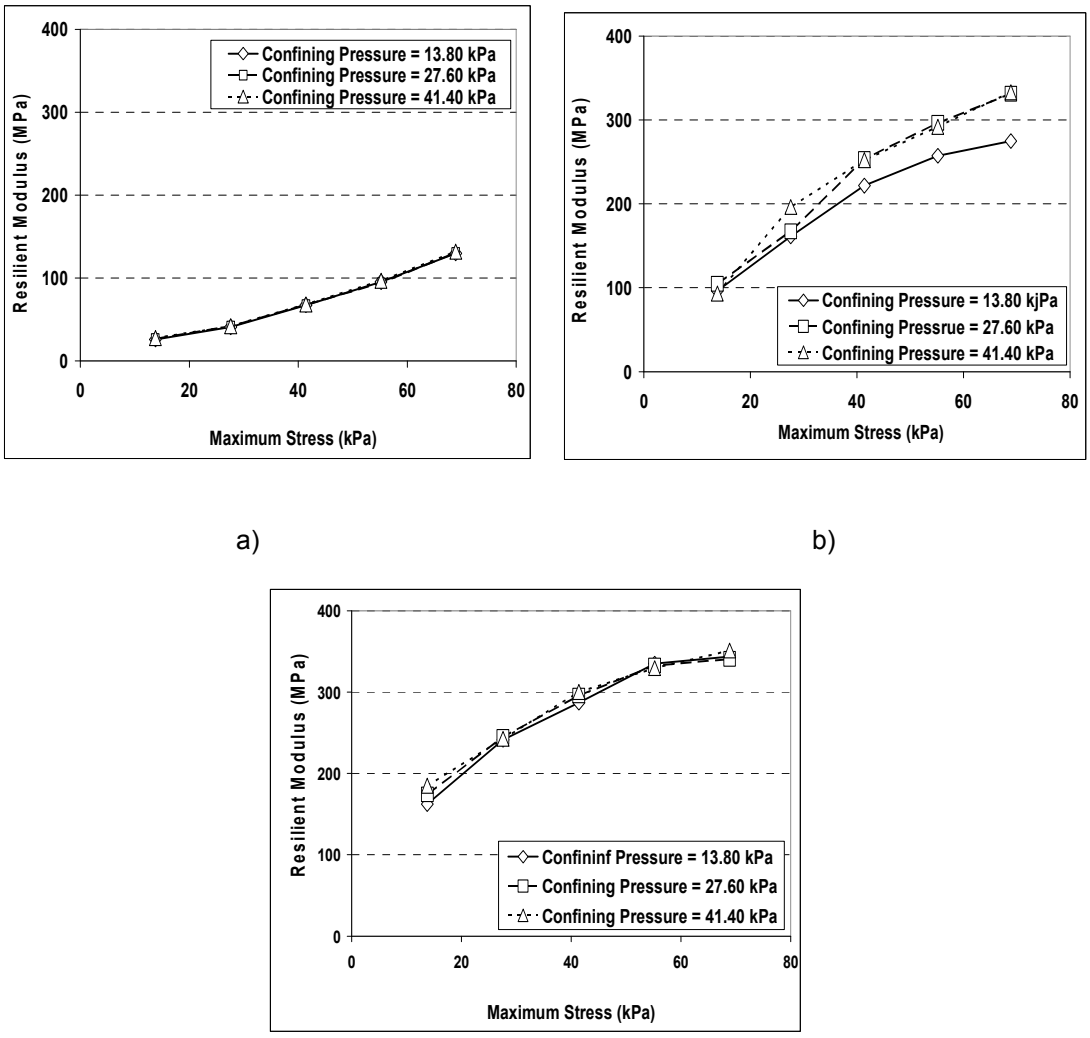

Figure 4.26 Variation of Resilient Modulus with Deviatoric Stresses at Different Confining Pressure at International Parkway for: a) Untreated, (b) Lime treated and (c) Lime Cement treated specimens.

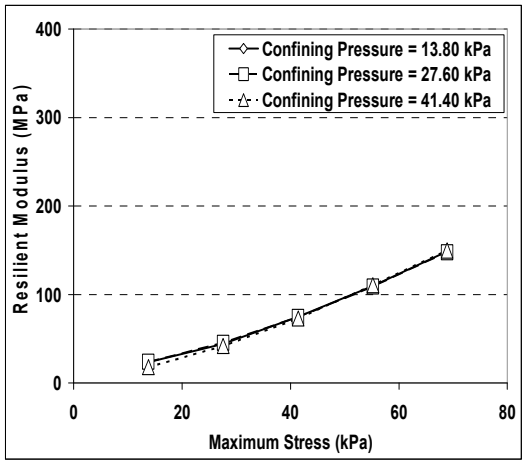

a)

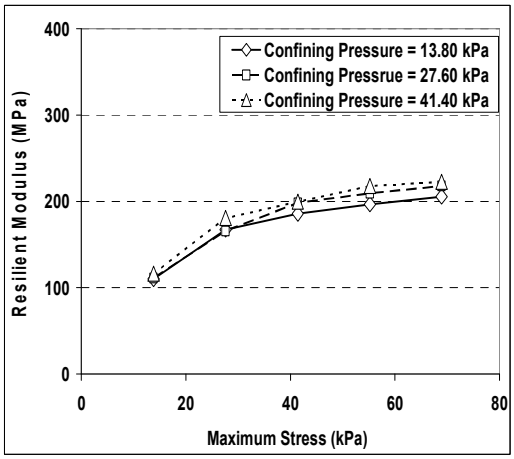

b)

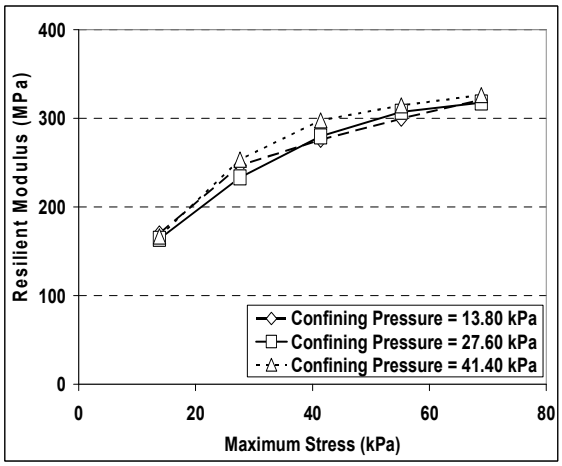

c)

Figure 4.27 Variation of Resilient Modulus with Deviatoric Stresses at Different Confining Pressure at Southmoor Drive for: a) Untreated, (b) Lime treated and (c) Lime Cement treated specimens.

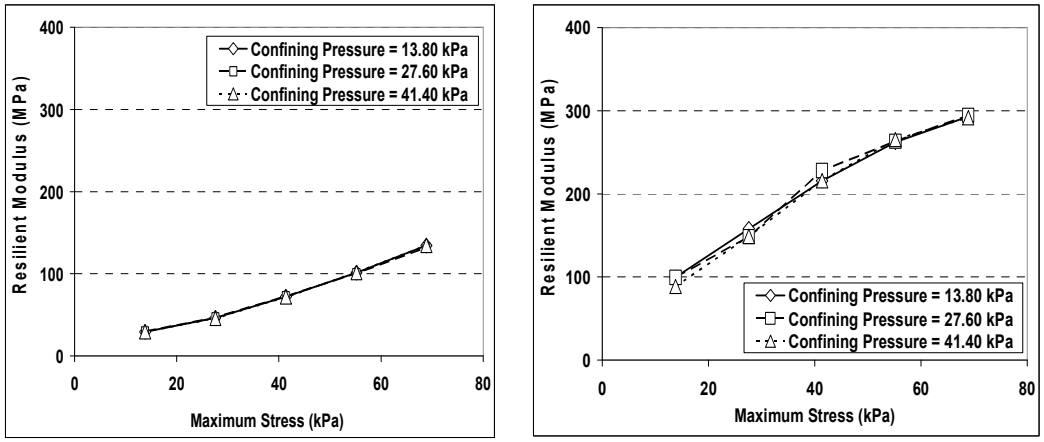

a) b)

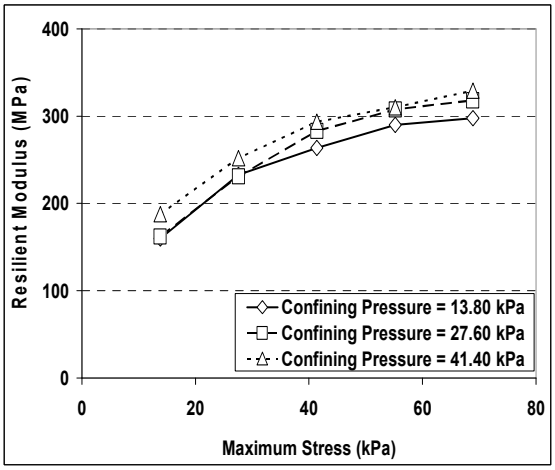

c)

Figure 4.28 Variation of Resilient Modulus with Deviatoric Stresses at Different Confining Pressure at Southeast Parkway for: a) Untreated, (b) Lime treated and (c) Lime Cement treated specimens

The resilient modulus (M_R) test results for the untreated and treated soils specimen taken from International Parkway, Southmoor and Southeast Parkway are also presented in Figure 4.26, Figure 4.27 and Figure 4.28, respectively. It can be seen from these figures that combined lime and cement treated soils have yielded the highest resilient modulus enhancements when compared to lime treated and control soils at the same confining pressure and corresponding deviator stress. This is expected as combined lime and cement treatment results in a stronger and stiffer material than the relatively medium to soft nature of untreated soil specimens.

From the graphs, it can be observed that the increase in confinement does not significantly affect the M_R value of untreated specimens due to its high plasticity nature of the clays. On the other hand, the influence of increasing confinement is more evident for lime and lime cement treated specimens as the specimens tend to behave as granular materials which have lower plasticity after treatments. It also can be seen that the M_R values of the treated specimens increase with increasing confining pressure. The increase in M_R value is attributed to the fact that applying higher confinement to the treated specimens tends to compress the specimens to be denser and stronger specimens. Hence, results in greater stiffness and higher M_R value. Figure 4.29 shows the comparison of resilient modulus at maximum deviatoric stresses of 68.90 kPa with variety of confining pressure for all locations.

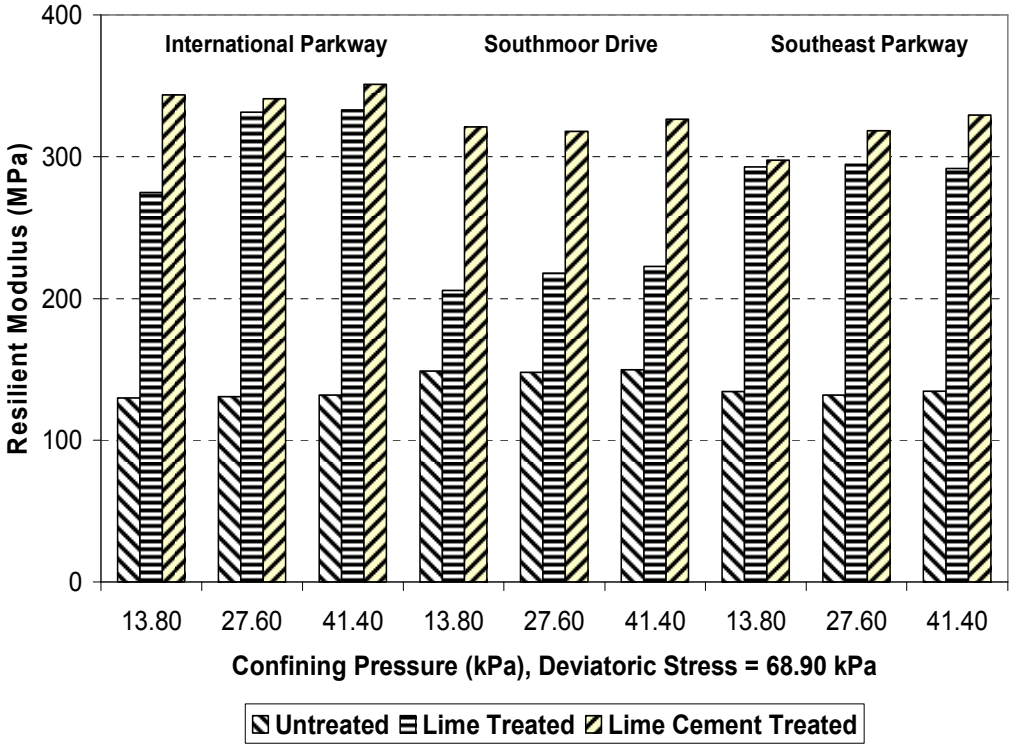

Figure 4.29 Comparison of Resilient Modulus at Maximum Deviatoric Stresses of 68.90 kPa with variety of confining pressure for all locations.

4.4 Summary and Conclusions

This chapter provides a comprehensive analysis and summary of the results taken from several laboratory tests including basic soils properties, chemical and mineralogical characteristics and strength properties of the soils. This chapter also summarizes the chemical and mineralogical characteristics of the stabilized soils.

From the experimental program of the effect of four stabilizers on sulfate-rich Harwood road soil, the following conclusions have been made: free swell potential of the soils was decreased due to the decrease in plasticity property of the soils after chemical treatments. Among all stabilizers, lime and fiber treated specimen exhibited the highest swell potential. This was due to the addition of fibers induces the open fabric and decreases the unit weight of the treated specimen. The shrinkage strain values were also significantly decreased by the

stabilizers. All four stabilization methods displayed similar low shrinkage strains which were due to the reduced plasticity property of the soils after treatment. There is no major leaching recorded after the pavement has been in services for 26 months. The pH range for all the stabilized subgrade soils has remained practically same in the range of between 11.3 and 13.6. As the pH for all the stabilized soils are above 10, it can be concluded that all stabilizers are still present and It also leads to a concern that ettringite formation may still occur since alumina disassociation from clay minerals typically occurs at high pH conditions. Hence, these soils may experience heaving in the future. The UCS results show that sulfate resistant Type V cement, Class F Fly ash and GGBFS has yielded a noticeable strength enhancement to the treated specimens. The strength increase in the stabilized soil specimens were attributed to the cementitious reactions from the stabilization process. Moreover, the sulfate resistant cement yielded the highest enhancement in M_R and lime with polypropylene fibers yielded the lowest enhancement in M_R. From the overall performance, Type V Cement and Type V Cement with Fly ash stabilizers performed the best on sulfate-rich soils followed by GGBFS and lime with polypropylene fibers.

From the experimental program of the effect of combined lime and cement treatment on three non-sulfate soils, the following conclusions have been made: Combined lime modification and cement stabilization enhanced the strength, and reduced swell and shrinkage strain behaviors of treated subgrades. Swell and shrinkage behaviors are also enhanced in the way that treated specimens show less water absorbing capacity. The volume change of zero magnitude is also observed in both swell and shrinkage test. The volume change of zero magnitude is also observed in both swell and shrinkage test. The compressive strength of untreated soil specimens is considerably enhanced (more than ten times) after both treatments. The combined lime and cement treatment has resulted in slightly higher compressive strength than the isolated lime treatment. Strength enhancements overall are attributed to pozzalonic compounds formed due to chemical reactions between stabilizers and soil in the presence of

moisture. The Resilient tests show that combined lime and cement treated soils have the highest Resilient Modulus enhancements compared to lime treated soils and natural soils. The resilient value of subgrade soils increase with increasing deviator stress. For the same deviator stress, combined lime and cement treated soils have the higher resilient values and untreated soils show lower resilient values. This is due to the soft nature of untreated specimens which can produce high elastic strains.

Overall, both chemical treatments attempted for both sulfate and non-sulfate soil types resulted in considerable enhancements of their engineering properties. Laboratory results and their enhancements are used as one of the factors in the evaluation of the chemical stabilization methods for these soil types.

CHAPTER 5

FIELD STUDIES

5.1 Introduction

This chapter provides detailed descriptions of the field studies including pavement instrumentation, elevation surveys, Dynamic Cone Penetrometer tests (DCP) and visual field inspection studies. These field studies' results are used to assess the performance of stabilized subgrade soils in the field conditions.

Since the main objective of the present research project is to select the appropriate stabilization methods for sulfate-rich and non-sulfate soils in Arlington, Texas. Stabilizers that showed promising results in the laboratory were used in the field. The performance monitoring of stabilized soils in the field, where they were exposed to various temperatures, humidity and external disturbances, was addressed here. The field study programs for both sulfate-rich and non-sulfate soils are shown in Figure 5.1 and Figure 5.2, respectively.

Field monitoring was also conducted through instrumentation studies to monitor the performance of pavements built over the stabilized sulfate rich subgrade soils. Site investigation with an array of sensors and appropriate data acquisition in pavement instrumentation provides valuable data that are utilized to assess the performance of pavement layers in real field conditions. This chapter presents the details of the site conditions pavement sections built on both soil types.

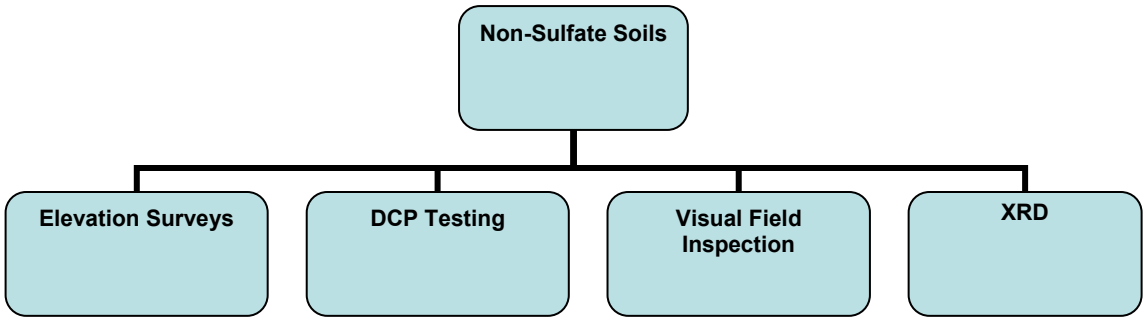

Figure 5.1 Details of the Field Study Programs for Sulfate-Rich Soils

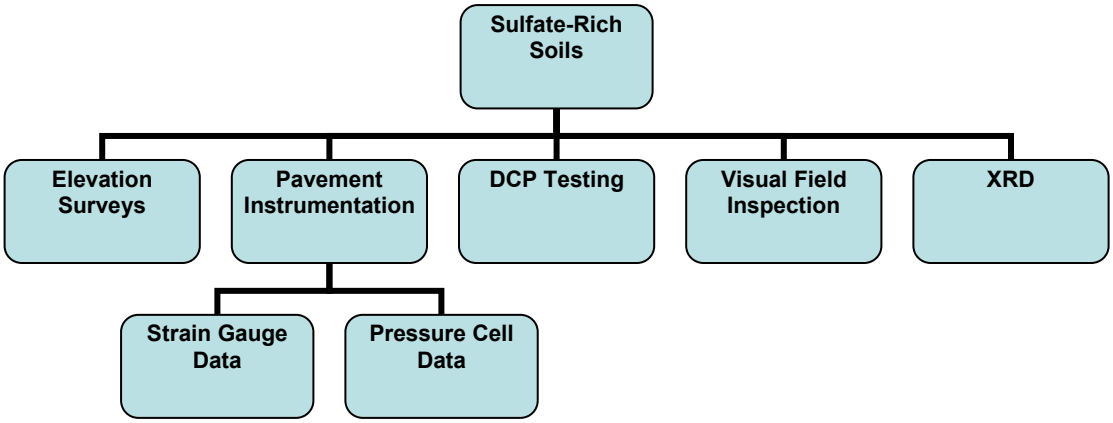

Figure5.2 Details of the Field Study Programs for Non-Sulfate Soils.

5.2 Field Sections and Studies for Sulfate-rich Soils

The city of Arlington was located in north Texas and was a large suburban city in the DFW metroplex. This area has an arid climate and the local geology consists of montmorillonite clay minerals. Textural and compositional differences in this parent material have led to significantly high plastic soils in this region. The montmorillonite mineral has a gibbsite structure and it tends to absorb water that consequently results in swelling or shrinking with moisture

fluctuations. Soils at this area comprised of sulfate-rich expansive soils and prone to sulfate heave when they were stabilized with calcium-based stabilizers such as cement and lime.

5.2.1 Site Information

The field studies for sulfate-rich soils were conducted at Harwood Road. This road is a sublet from Collins Street, located at Southeast Arlington, Texas. Soils at this site are expansive in nature, rich in sulfates and prone to sulfate heave when stabilized with calcium based stabilizers. The map of Harwood Road is shown in Figure 5.3. Figure 5.4 shows a schematic of Harwood Road and the vegetation along the pavement section is moderate with no large trees.

Figure 5.3 Map of Harwood Road, Arlington.

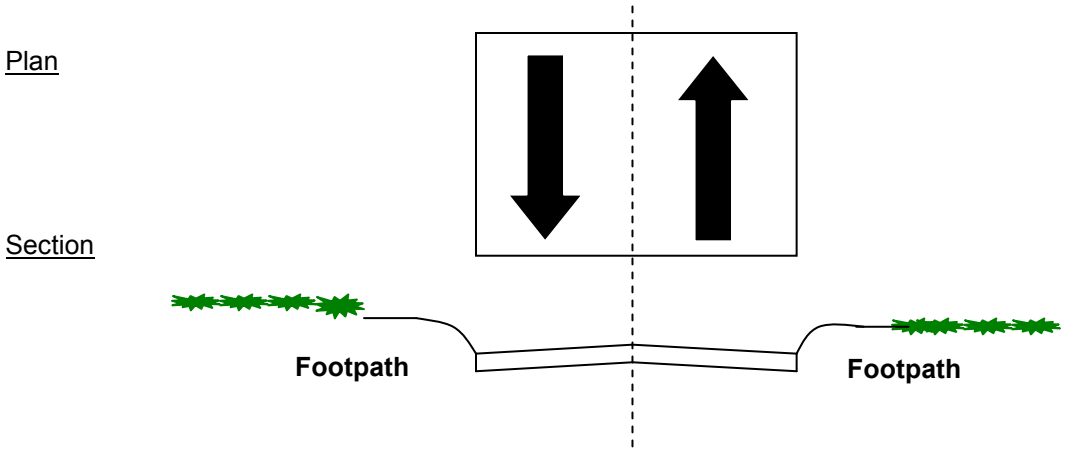

Figure 5.4 Site Schematic – Harwood Road

5.2.2 Field Monitoring

The field studies conducted here included elevation surveys, pavement instrumentations, DCP tests, and field visual inspections for distress identification.

5.2.2.1 Pavement Instrumentation

The growing demands of a better performance pavement have been a challenge to pavement engineers. During the past three decades, attempts were made to enhance the performance of pavements by pavement structure analysis, which involved a measurement of stresses and strains at critical sections inside a pavement system, and then compared them to the calculated strain levels at critical sections in the pavement structure for determining failure strains (Battiato et al., 1977). This analysis can be done via pavement instrumentation.

Pavement instrumentation is an approach used to monitor the behavior of roads. It is used to identify the critical sections in the pavement, select and calibrate sensors, and identify the possible errors in the pavement structure. The pavement instrumentation has been recognized as an important tool for quantitative measurement of pavement performances and

responses under different environmental and loading conditions. The environmental factors include temperature, freeze-thaw cycles, and moisture content changes due to seasonal changes. The load factors include magnitude, type and distribution of traffic loads.

The variables measured by the pavement instrumentation are traffic induced stresses, strains and deflections of pavements. Additionally, pavement instrumentation also provides the assessments of each stabilizer in terms of the ability to control pavement distress such as heave-related movements, rutting and pavement cracking. In-situ measurements of these parameters provide the data required to analyze the performance of pavements.

5.2.2.2 Instrumentation Design

The total cost of the instrumentations depends mainly on the engineering parameters which are expected to be assessed in the field. Hence, a selection of appropriate engineering parameters used to evaluate the performance of stabilizers plays a vital role in instrumentation design. Commonly, the instrumentation is used to assess the engineering parameters such as strains and deflections. The measurement of these parameters in the field allows the assessment of stabilizers, mechanisms of heave behavior and load-carrying potentials of underlying treated subgrades.

Soils of southeast Arlington have high sulfate content, low strength, and high swell and shrinkage potential. These soils are highly susceptible to pavement distress such as rutting and vertical strains. Therefore, in order to evaluate the strains of treated subgrade under traffic loads, strain-measurement devices are included in the field studies program.

A subgrade layer underneath pavements is exposed to various amounts of dynamic loads from traffic. These dynamic loads are transferred to the stabilized subgrades. Therefore, it is required to measure the pressure or load transferred from the surface courses to the subgrades. Consequently, pressure cells are included in the instrumentation program to measure the subgrade pressure under traffic loads. The primary function of the pressure cells is to measure the subgrade pressure under traffic loads (Sargand et al., 1997; Metcalf, 1998). The

main objective of pavement stabilization is to transmit the traffic loads to the underlying subgrade with considerable amounts absorbed by surface and stabilized layers. The pressure cells were hence installed in the subgrade layer to monitor the pressure levels, and also provide the dynamic vehicular induced stresses in the base and subgrade layers. The data obtained from strain gauges and pressure cells were used to address the effectiveness of stabilizers and load-carrying potentials of the underlying soils.

5.2.2.3 Sensors

In this research project, various types of strain measurement devices are considered including surface-mounted mechanical strain gauges, extensometer, and embedment type and vibrating wire. Based on their accuracy, embedment type gauges are most suitable. To address the low survivability criterion of strain gauges as mentioned and documented by Glaser (2001), two strain gauges were installed for each pavement section, so that one would act as a back-up in case one of the gauge failed.

In the current instrumentation program, swell strain changes in the soil were expected to be gradual and would require long period of time. Hence, portable data acquisition module was found to be suitable for stain monitoring purposes. A mobile data acquisition module was considered and used due to its portability, high precision (can detect even 1 micro strain change) and its affordable cost (Mohan, 2002). In addition to the above mentioned sensors, a laptop computer was required for reading the data from DAQ module. The catalog of the data acquisition module provided the configuration for the computer (Pillappa, 2005). Table 5.1 lists the sensors installed at five sections of the test site.

Table 5.1 Details of Instrumentation (Mohan, 2002)

Instrument Type	Name	Manufacturer	Quantity
Strain Gauge	EGP-5-350	Micro-Measurements	40
Pressure cells	Geokon 3500-2-200	Geokon	10
Data Acquisition	Wavebook WBK16	IOtech	1

Five pavement sections, each of 300 ft long, were built on subgrades stabilized with four novel stabilizers and one control (lime) stabilization method. Since the soils at every section are similar, same instrumentation are installed for all sections. All sections have an 8-inch-thick stabilized subgrade and 6-inch-thick concrete pavement. The pavement is designed to serve a low-volume traffic condition. Different stabilization methods and their corresponding dosage proportions are presented in Table 5.2. Construction of test sections were started on September 20, 2004 and completed on November 5, 2004. More details of the construction of the test sections can be found in Pillappa (2005).

Table 5.2 Stabilizer Proportions

Soil Designation	Percentage by dry weight
Type V Cement	8
Class F Fly ash and Type V Cement	15 and 5
Lime and Polypropylene fibers	8 and 0.15
GGBFS	20

After completed the construction of individually treated sections, the pressure cells, strain gauges and data boxes were immediately installed. Figure 5.5 shows the typical plan view and cross-section details of treated and instrumented sections.

The key objective of instrumentation studies is to monitor the most critical section to measure maximum strains under traffic loads. The pavement critical sections were underneath

the wheel path (Mohan, 2002). Therefore, strain gauge was placed in a vertical direction while pressure cells were in horizontal direction. Figure 5.6 shows a schematic diagram of the placement of sensors in the test section. Figure 5.7 and Figure 5.8 shows the placement of strain gauges and pressure cells respectively. The wires from the ends of the sensors were cased within a high density polyethylene pipe to ensure that the load from the vehicles would not disrupt their continuity. The wires were then led into the galvanized steel boxes via the conduit pipes. Then, the ends were soldered to the DB9 pins.

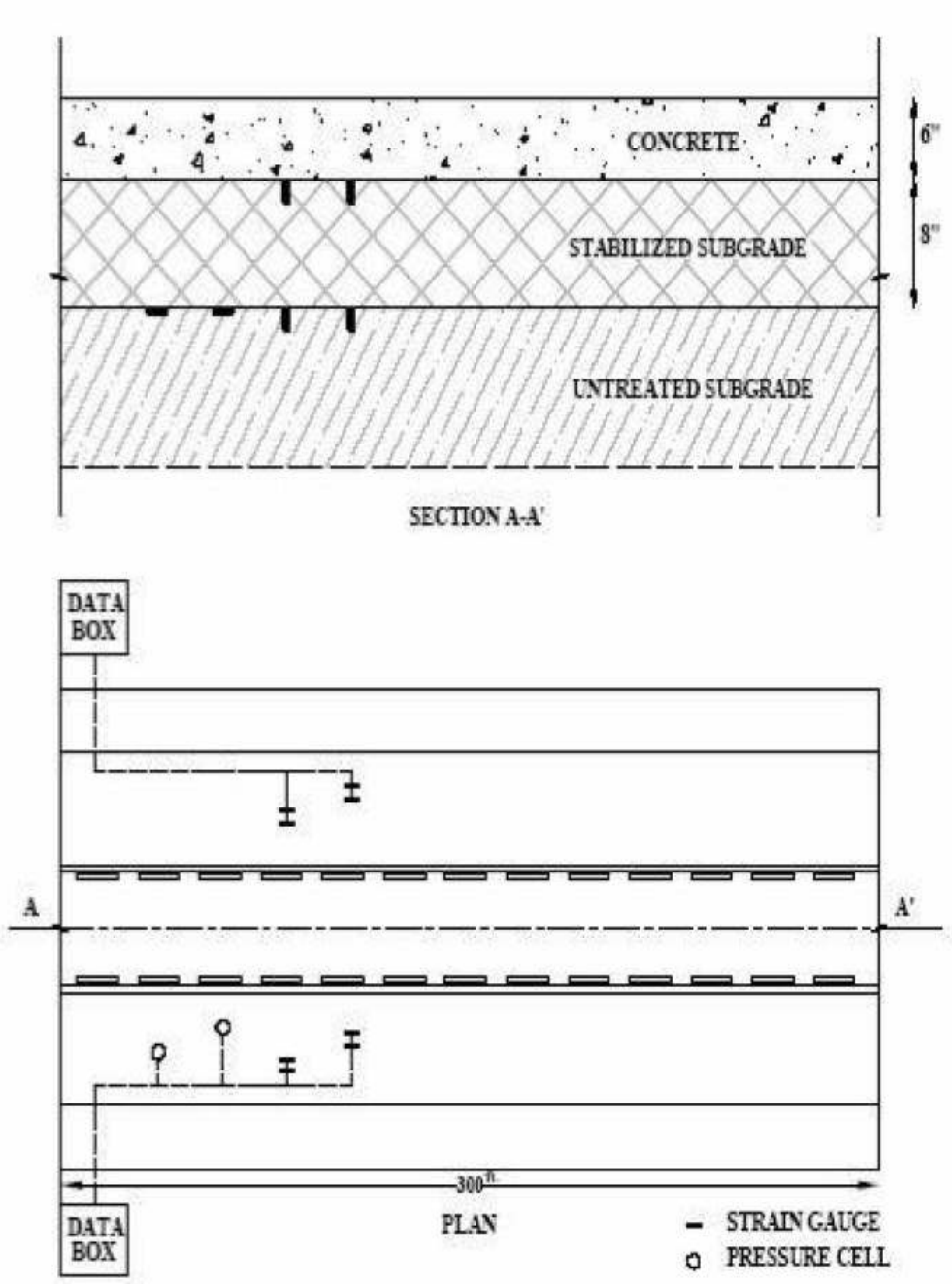

Figure 5.5 Typically Stabilized Pavement Test Section.

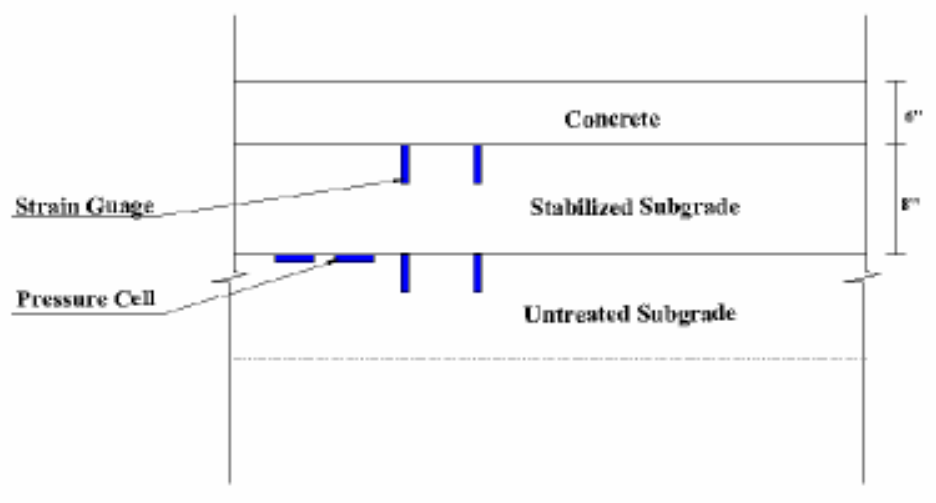

Figure 5.6 Placement of Sensors.

Figure 5.7 Placement of Strain Gauges (Pillappa, 2005).

Figure 5.8 Placements of Pressure Cells (Pillappa, 2005).

The locations of monitoring stations were designed and selected depending on the distance between the gauges, the length of the sensor cables, and the length of each individually treated section. Minimizing the distance between the sensors and the data logger will minimize noise in the readings. Also, it is convenient to group many sensors together for data collection. Based on these considerations the sensors were grouped and positioned as shown in Figure 5.9.

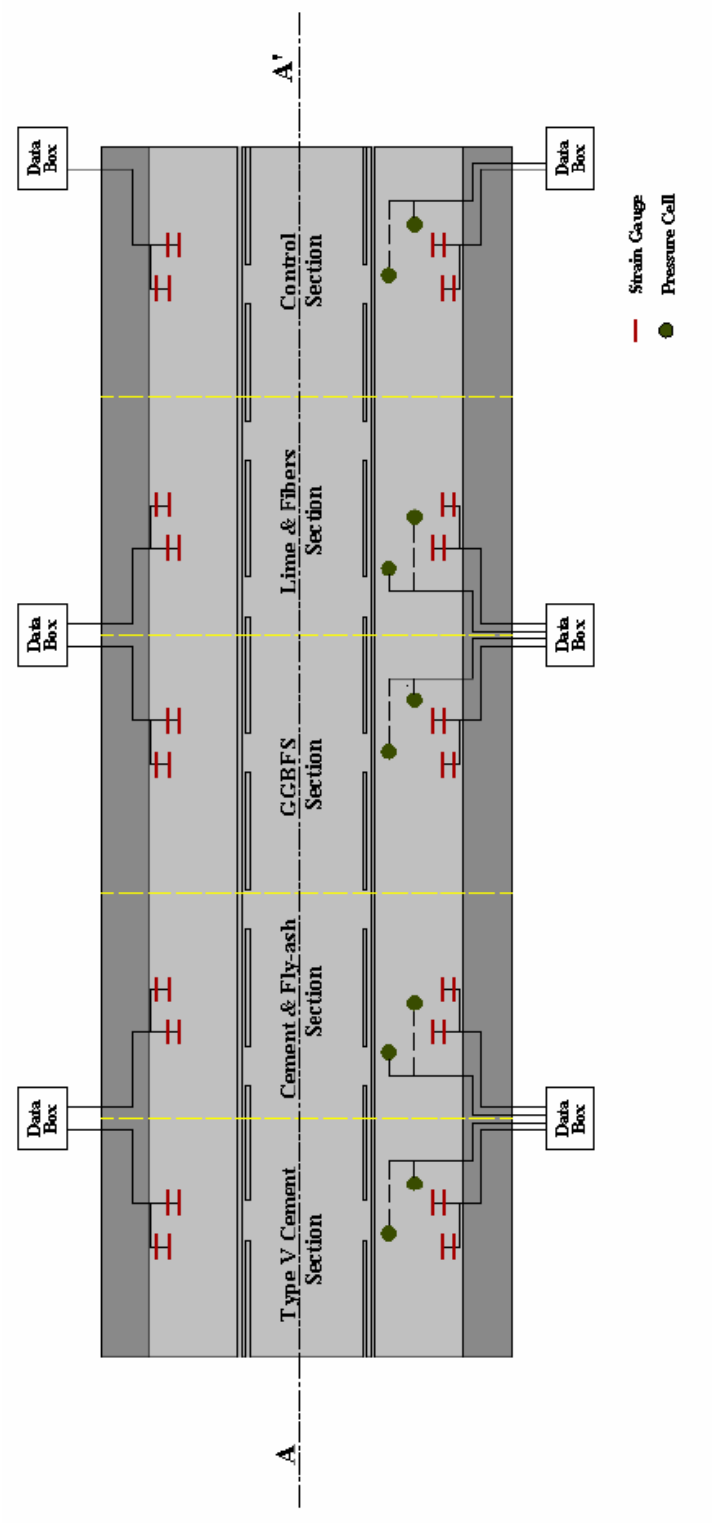

Figure 5.9 Placement of Sensors Plan View.

The DAQ module comprising of wavebook and WBK-16 were integrated and then connected to the laptop through parallel port and interfacing cables. Software to access the acquisition modules were installed on the computer. The selected strain gauge measures strain based on the Wheatstone bridge imbalance principles explained in the previous chapter. EGP-5-350 (strain gauge) was a quarter-bridge type strain gage and hence it was required to use bridge calibration resistors to complete the circuit (Mohan, 2002). The pressure cells were full-bridge strain gage type sensors. The WBK-16 module provided CN-115 headers (a small resistor holder) to include the bridge calibration resistors (Mohan, 2002). Shunt calibration method was used in order to compensate the resistance increase of the strain gages (Mohan, 2002).

The pavement section was opened to traffic in early February 2005 (Pillappa, 2005). Data collection was initiated during the month of January 2005 and continued till April 2007. The data was collected on a weekly basis. In case of sudden climatic changes like an occurrence of heavy rainfall, data was collected continuously within twenty-four hours of precipitation. A mid-size passenger car with a gross weight of approximately 3,000 pounds was used for data collection. The loading on the sensors was performed using different methodologies. In the first method, the data from both strain gauges and pressure cells were collected with no direct dynamic load applied to the sensors. In the second method, the passenger car was paced on the sensors and the sensor data was collected. The third method of loading on the sensors was to drive the car back and forth over the sensors and simultaneously collect the data from strain gauges and pressure cells. These three methods were implemented for all the stabilized sections.

The sensor readings contained a significant amount of noise from the data acquisition. In order to minimize these noises, the collected data was first imported into MATLAB®. A five point running average algorithm was then implemented to reduce the noise. A single iteration of running average did not give significant reduction in the noise due to high sampling rate, and

hence a total of sixty iterations were implemented for strain gauges and thirty iterations were used for pressure cells. The peaks corresponding to the vehicular activity on both the travel lanes were taken into consideration. In case of loading condition, combination of data collected from the sensors which were both directly below the wheel path and in between the wheel loads were considered to analyze strains and pressures. Furthermore, the difference of the readings (one with the loading and one without loading) was used in order to evaluate strains and pressures for each treated section.

5.2.2.4 Elevation Surveys

Elevation surveys were performed using a 'total station setup' in order to evaluate the heave and other types of soil related movements including erosions of stabilizer from the treated soils. This monitoring data of the past twenty-six months is used in the present analysis. Eight points were chosen in each section, four along each lane. Figure 5.10 shows the plan view of the elevation survey points and the reference total station point. The points are evenly spaced at sixty-foot intervals. The nearest permanent non-heaving structure was chosen as a benchmark or reference point.

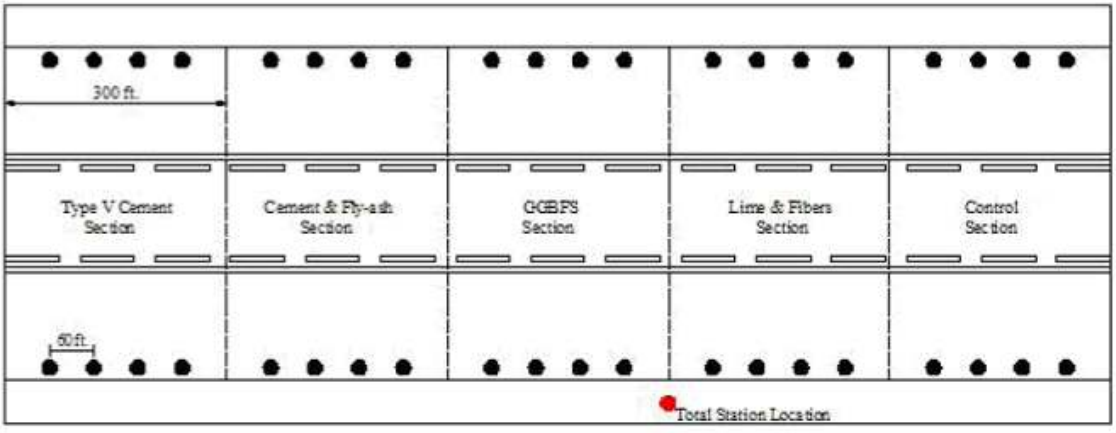

Figure 5.10 Plan Views of Elevation Survey Points.

Another field monitoring task was based on the use of the Dynamic Cone Penetrometer or DCP testing and indirectly evaluating the in-situ strength and moduli properties of the treated subsoils. DCP tests were carried out on all of the five treated sections in the field.

5.2.2.5 DCP Device

One of the important information needed in the field stabilization is to identify the time at which stabilized subgrades achieved sufficient strength. Dynamic Cone Penetrometer (DCP) is an in situ device that has been used extensively in the past decade to evaluate indirect strengths of compacted subsoils in the field. The DCP device is simple to operate, inexpensive, and provides repeatable results and rapid property assessments (Enayatpour et al. 2006). Once strength of the underlying subsoils is achieved, then the construction of subsequent layers can be resumed.

The DCP is composed of upper and lower shafts. These shafts are attached to each other near to a mid-point of the distance between a driving anvil and a cone. Figure 5.12 shows the various components of (DCP) equipment. A handle is located at the top and it is held vertically during the test. A 15-lb steel hammer is fitted against the upper shaft. This hammer is raised and dropped manually from a height of 20 in. onto the driving anvil. The impacted force is then exerted to penetrate the cone into the soil. The lower shaft is marked in 5 mm increments.

It is very important to hold the DCP shaft upright to avoid the development of friction at the sides of the shaft, which can disturb the transfer of energy from shaft to cone. During penetrations of the cone, a reading with respect to the number of blows used to drive the cone into the soil is then taken from this lower shaft. A 45 degree apex angle of cone tip is fitted at the bottom of the lower shaft. A termination of the DCP test is defined when a penetration of this cone tip is less than 3 mm for 10 consecutive drops, which that the test has to be stopped otherwise the cone tip will be damaged as noted by Jones and Holtz (1973).

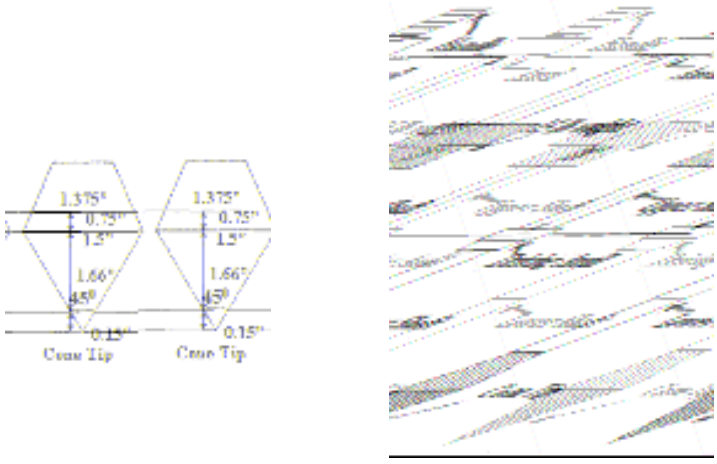

a) b)

Figure 5.11 Component of DCP device a) Tip of the cone b) Body of DCP.

The DCP shown in Figure 5.11 utilizes a 15-lb steel mass falling from a height of 20 in. to strike the anvil in order to drive a 1.5-in diameter hardened cone tip. The kinetic energy from the dropping hammer is transferred through the lower shaft to the cone to drive the tip into the soil. To maintain the consistency of the energy imparted to the cone, the pullout anvil is fixed in place to ensure the height drop is always 20 in. Resistance of the soil can be defined as the work done to stop the cone and it can be calculated as follows:

$$\mathbf{R_s} = \frac{\mathbf{W_s}}{\mathbf{P_s}}$$

R_s is the soil resistance; W_s is the work done to stop the cone; and P_s is the distance traveled by the penetrometer through the soil. The energy produced due to each hammer drop can be calculated using kinetic energy relation. Soil resistance (R_s) for this hammer is 3.39

kN/cm i.e. each cm of penetration of the cone through the soil will experience a force of 3.39 kN. The DCP test results are expressed in terms of dynamic penetration index or DPI of soil. The DPI is the amount of cone penetration due to one drop of the hammer and hence the unit used for expressing DPI is cm per blow or inches per blow. Figure 5.12 presents the schematic showing parameters to calculate DPI.

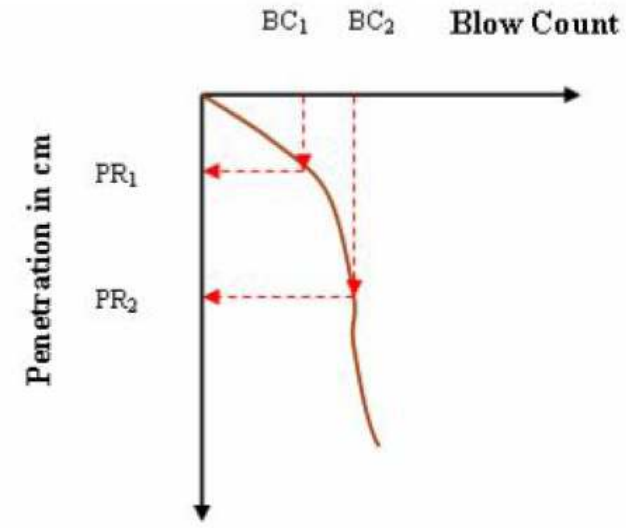

Figure 5.12 Parameters to Calculate DPI

Results acquired from DCP test are expressed in terms of dynamic penetration index or DPI of soil. DPI is defined as the amount of cone penetration due to one drop of the hammer (Jones, 1991). The DPI is a proportion of penetration reading (cm) to a blow count. Therefore, the unit of DPI is cm per one blow or inches per one blow. A general expression of DPI is:

$$\mathbf{DPI} = \frac{\mathbf{PR}_2 - \mathbf{PR}_1}{\mathbf{BC}_2 - \mathbf{BC}_1}$$

PR is a penetration reading (cm) and BC is the blow count. (PR_2- PR_1) is the different between two consecutive penetration readings at different depths or a difference between

readings at either ends of a certain layer and (BC_2-BC_1) is the difference between two consecutive blow counts or those corresponding to the ends of a certain layer.

Researchers at The University of Texas at Arlington have been attempting to utilize the DCP test to evaluate the efficiency of the stabilizers. In this research project, the DCP test was used to indirect assessment of the strength of the stabilized soils by comparing the DPI values of treated layers. This research also provided an opportunity to utilize a DCP device to measure the DCP parameters in the field at various curing periods and then correlate the measured DCP values with the UCS parameters measured from the laboratory tests on the field specimens.

In order for the correlations to be developed, several DCP tests were conducted on both sulfate-rich and non-sulfate soils stabilized with different chemical additives. For example, sulfate-rich soils were treated with four novel stabilizers including Sulfate Resistant Type V cement, Class F fly ash with Type V cement, Ground Granulated Blast Furnace Slag (GGBFS) and Lime with Polypropylene Fibers whereas non-sulfate soils were treated with a combined chemical additive comprising of lime and cement mixture The results acquired from the DCP tests were summarized along with their prediction abilities in Chapter 6.

5.3 Field Sections and Studies for Non-Sulfate Soils

The field sections for non-sulfate soils were located at three different street locations in the City of Arlington, including International Parkway, Southmoor Drive and Southeast Parkway. The soils at these sites are natural expansive soils consist of montmorillonite clay minerals with low sulfates. The soils are known to be highly expansive soils which demonstrated high plasticity behavior in the laboratory. Clay mineralogy and water absorbing ability are responsible for swelling and shrinking when these soils are subjected to moisture fluctuations.

The presence of sulfates is not a concern at these sites since soils from these sites contain only low to moderate amount of sulfate (not more than 2,000 ppm). Hence, at this site, a modified stabilization method termed here as “Combined lime and cement stabilization” was selected and used to stabilize the natural soils. Both old and distressed pavement layers at all

three locations were replaced with a new concrete pavement layer laid over the combined stabilized subgrade soil section.

5.3.1 Site Information

5.3.1.1 International Parkway

International Parkway is located at East Division Street near Texas 360. This area is near a commercial complex and both sides of the road section are covered with vegetations. Prior to the pavement reconstruction, the old asphalt layer was subjected to severe longitudinal and transverse cracks, and vertical movements due to the expansion of the old non-stabilized subgrade. The City of Arlington decided to reconstruct the whole pavement structure by paving a new concrete layer over a combined lime and cement stabilized subgrade. Map of International Parkway is shown in Figure 5.13 and the site schematic is shown in Figure 5.14.

Figure 5.13 Map of International Parkway

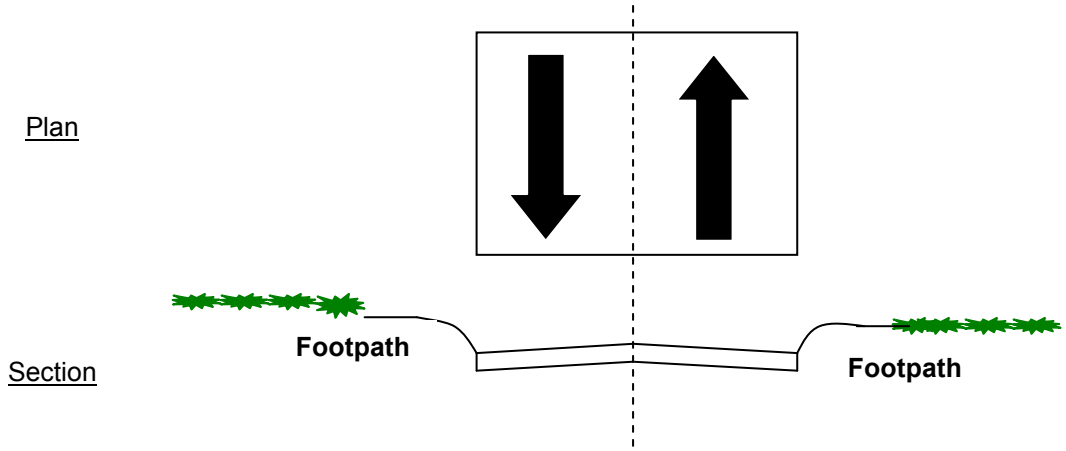

Figure 5.14 Site Schematic – International Parkway

5.3.1.2 Southmoor Drive

Southmoor Drive is located near South Collins Street in south Arlington area and both sides of the road are also covered with grass and vegetations. Map of Southmoor Drive is shown in Figure 5.15 and the site schematic is shown in Figure 5.16. As the road located in the middle of residential area, the traffic is considered to be low volume types with majority of the vehicles serviced by this pavement are cars. The whole pavement structure was reconstructed by paving a new concrete layer over a combined lime and cement stabilized subgrade section. Prior to the pavement reconstruction, this road was constructed by asphalt concrete over a non-stabilized subgrade. The road was subjected to severe longitudinal and transverse cracking, and vertical movements due to the expansion of subgrade soils. The pavement ride quality was much improved after the reconstruction.

Figure 5.15 Map of Southmoor Drive

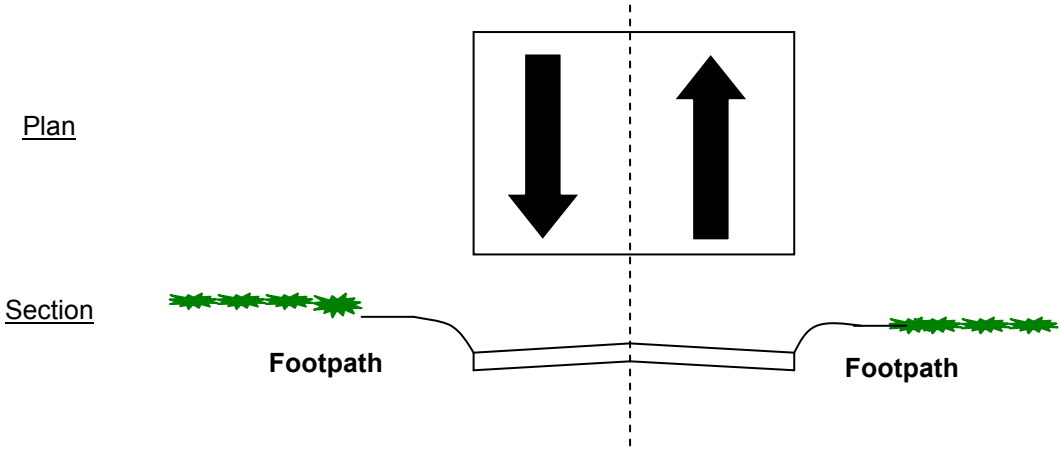

Figure 5.16 Site Schematic – Southmoor Drive

5.3.1.3 Southeast Parkway

Southeast Parkway is located at the end of South Collins Street in a residential area. Prior to the pavement reconstruction, this street was constructed by asphalt concrete pavement over a non-stabilized subgrade. Severe longitudinal and transverse cracks and vertical movements were observed at the first visit. The city of Arlington decided to reconstruct the

whole pavement structure by replacing the old warn asphalt concrete layer with a new concrete layer laid over a stabilized subgrade. Map of Southeast Parkway is shown in Figure 5.17 and the site schematic is shown in Figure 5.18.

Figure 5.17 The Schematic of Southeast Parkway

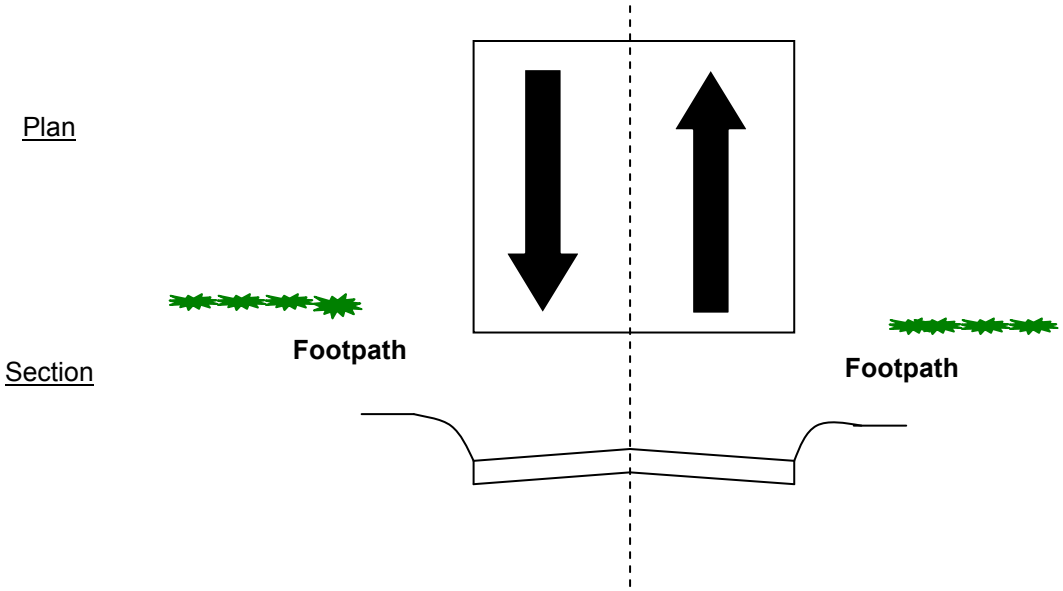

Figure 5.18 Site Schematic – Southeast Parkway.

5.3.2 Field Specifications

The combined lime-cement treatment specifications used in the field are as follows, for lime modification:

1. A 100% of all material should pass through a 2-in (50.8 mm) sieve after initial mixing pulverization in order to allow uniform mixing of cement stabilization in the next phase. A minimum mellowing period of 48 hours should be allowed after mixing and pulverization of lime.
2. The average in situ moisture content of stabilized soil from both streets is 29%. Water content in lime treated soil should be maintained at least 2% above the optimum moisture content

For cement stabilization:

1. Cement is mixed with pulverized soil as thoroughly as possible The water content of cement treated soil is to be maintained at a minimum of 2% above the optimum moisture content of the soil
2. Pulverization of lime treated subgrade should be such that 100 % pass a 1-1/2-in. (38.1 mm) sieve and a minimum of 60% should pass a No.4 sieve (4.75mm)
3. A curing period of 7 days should be allowed for the treated subgrade to gain their full strength after final compaction
4. The water content is kept at least 4% above optimum moisture content throughout the curing

5.3.3 Field Construction Steps

In a pavement construction job, the primary requirement of a subbase is to secure a completed course of treated material containing a uniform blend of lime and cement, free from loose or segregated areas, of uniform density and moisture content, well bound for its full depth and with a smooth surface suitable for placing subsequent courses. As in this project combined

lime and cement stabilization was employed, construction sequence consisted of initial lime modification followed by cement stabilization.

The sequences consist of initial lime modification, followed by cement stabilization. Prior to the modification, the subgrade is prepared in accordance with the specification. The proper amount of lime is then spread over the soil by the mechanical spreader. Pulverization and mixing are used to combine lime and soil thoroughly in an appropriate depth (Little, 1987). The construction sequences are as follow:

1. The construction sequences start with an excavation down to the subgrade soils for a depth of 9 in
2. The lime stabilizer was placed on the subgrade. This treatment method is known as “mix-in-place stabilization”. Stabilizer is spread before pulverization and mixing of the soil and stabilizer
3. The equal amounts of lime and cement are used at an amount of 42 lb per square yard (15.93 kg per square meter) each and to a depth of 9 in. (22.86 cm) below the ground surface. The content of lime and cement used is approximately 6% separately (Sherwood. 1993). Lime modification is relatively simple compared to cement stabilization because lime has much lower bulk density than cement. Hence, it is possible to achieve a more uniform distribution
4. Cement binder is either in the form of slurry or in the form of a powder. Lime treated subgrade and cement binder in dry form are thoroughly mixed with a pulvimixer
5. After mixing, the cement, lime and soil mixture is compacted with a sheep foot roller to a density not less than 95% of maximum dry density as determined by ASTM D698 moisture/density relationships

   Figure 5.19 shows the sequence of combined lime and cement treatment of subgrade.

(a) (b)

(c) (d)

Figure 5.19 (a) Lime Slurry Placement, (b) Re-scarification, (c) Final Mixing of Soil with Lime and Cement, (d) Final Compaction

5.3.4 QC/QA Issues

During the construction process, quality control or QC checks need to be made in order to ensure that the stabilization follows all the requirements of the specification. In situ gradation was performed to check for the specifications i.e. whether the treated subgrade materials passed through a 2-in (50.8 mm) sieve. Compaction densities measured with a nuclear gauge were also within the targeted moisture contents and dry unit weights. Quality assessment or QA studies were performed by collecting Shelby tube soil specimens from the stabilized subgrade section and then subject them to unconfined compressive strength, swell and linear shrinkage tests. The results of these tests are presented and discussed in Chapter 6.

5.3.5 Field Testing Programs

5.3.5.1 Elevation Surveys

Elevation surveys were performed on a monthly basis at all three locations including International Parkway, Southmoor Drive and Southeast Parkway. The surveys were conducted by using a total station device to monitor heave related movements in the field. The monitoring started right after the pavement was laid and the road was cleaned by the contractor and continued until September, 2008.

At International Parkway, the elevation survey was started in March, 2006 and continued on monthly basis over 30 months. Ten observation points were located at both sides of the road, five along each direction. The distance between each observation point was approximately 150 ft. Figure 5.20 shows the plan view of the elevation survey points at International Parkway. The total station located at one side of the road and the benchmark was located at a non-moving structure.

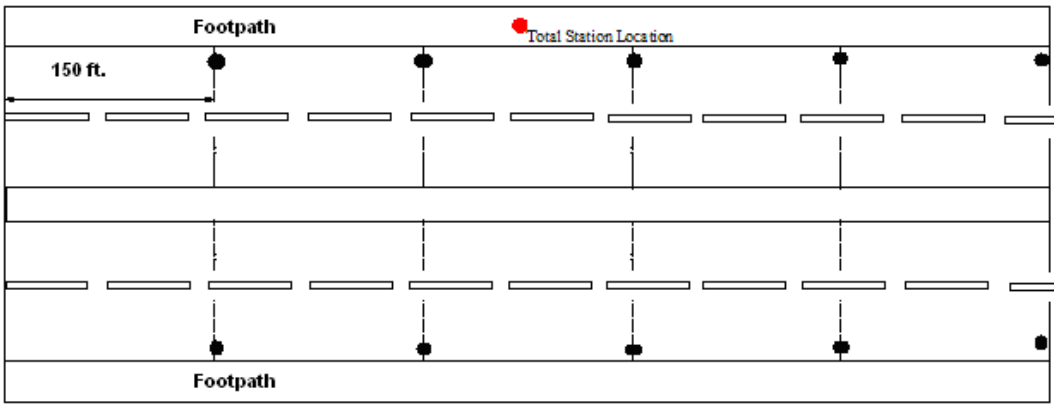

Figure 5.20 Plan Views of Elevation Survey Points at International Parkway

At Southmoor Drive, the elevation survey was also started in March 2006 and continued on monthly basis over 30 months. Both sides of the road have no footpath and they are covered with trees and vegetations which make locating of total station point difficult. This problem was overcome by putting a small wooden wedge on the ground and marked it as a total station

point. Ten observation points were located at both sides of the road, five along each direction. The distance between each observation point was approximately 300 ft. Figure 5.21 shows the plan view of the elevation survey points and the total station located at one side of the road. The benchmark was located at a non-moving nearby structure.

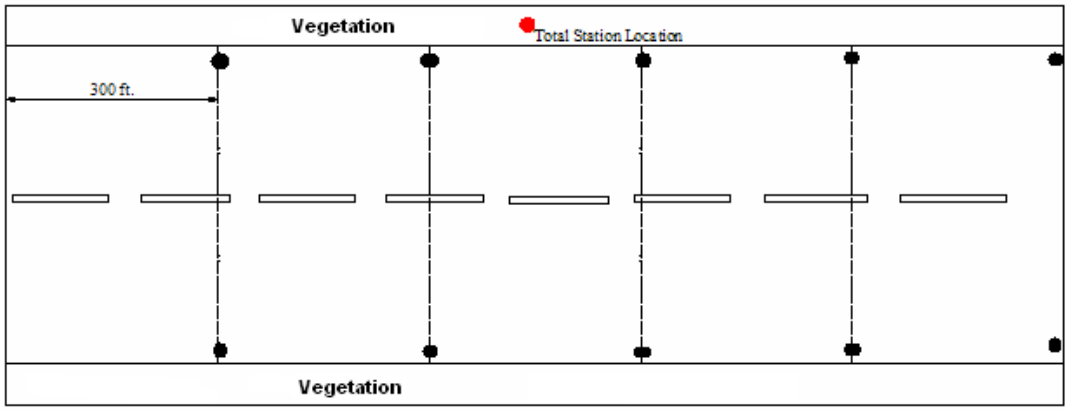

Figure 5.21 Plan Views of Elevation Survey Points at Southmoor

Southeast Parkway was divided into 2 parts, west bound and east bound because the road construction started on west bound and continued on east bound. After the constructions of both sides of the road have finished and the road was cleaned, the elevation survey was then started in November 2007 and continued over 10 months. Twenty observation points were located at both sides of the road, ten along each bound. The distance between each observation point was approximately 300 ft. Figure 5.22 and Figure 5.23 shows the plan view of the elevation survey points on west bound and east bound of Southeast Parkway, respectively.

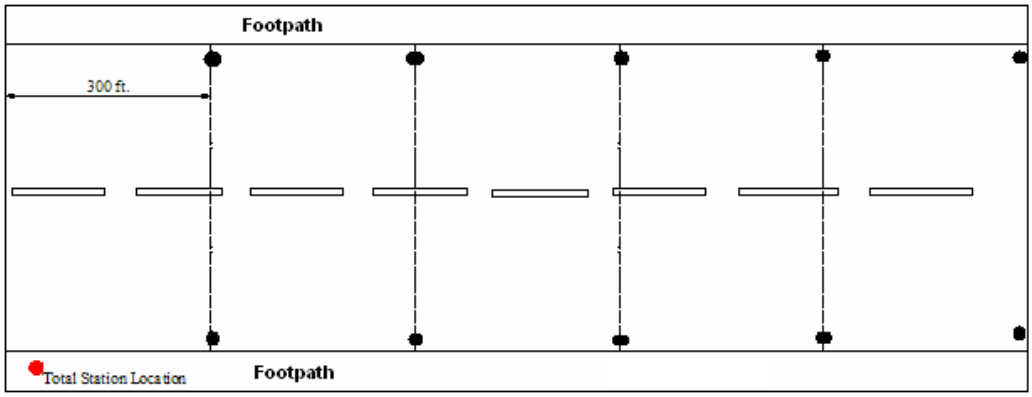

Figure 5.22 Plan Views of Elevation Survey Points at Southeast Parkway – West Bound

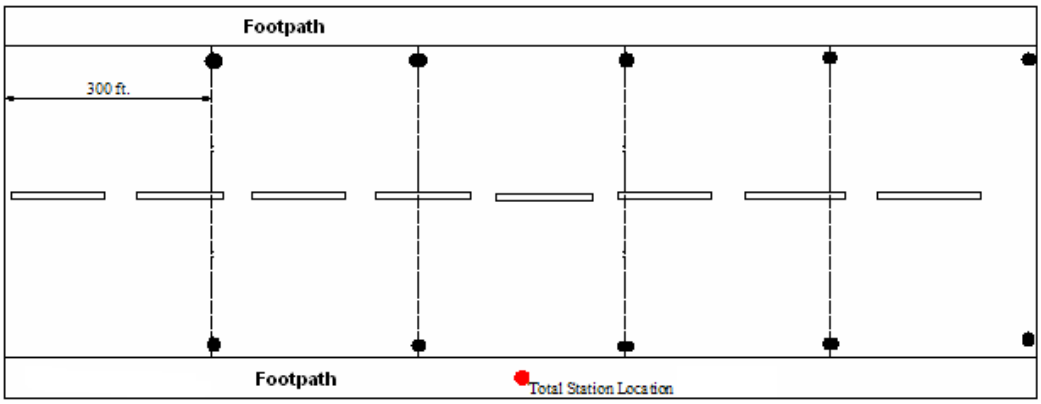

Figure 5.23 Plan Views of Elevation Survey Points at Southeast Parkway – East Bound

5.4 Summary

This chapter provides complete descriptions of field studies conducted to assess the performance of stabilizers. Descriptions of instrumentation design, installation of sensors, data collection procedures, elevation survey and DCP test were also discussed. For sulfate soils, the test site is located at Harwood Road, Southeast Arlington. For non-sulfate soils, the test sites are located at three different locations including International Parkway, Southmoor and Southeast Parkway. The field monitoring was conducted on a monthly basis. Results of the field

monitoring are analyzed to evaluate the performance of the different stabilizers and are discussed in Chapter 6.

CHAPTER 6

ANALYSIS OF FIELD RESULTS

6.1 Introduction

The main objective of this research project was to design and select appropriate stabilization methods for stabilizing expansive subgrade soils in Southeast Arlington, Texas. Field monitoring and documentation of their performance are considered important to validate the effectiveness of stabilizers. The success of accomplishing the present research objective depends on addressing the long-term performance of soil stabilization in real field conditions where they are exposed to variations in temperature, humidity, rainfall and various external disturbances. Field monitoring is generally associated with instrumentation studies to monitor the performance of pavements built on stabilized subsoils.

This chapter presents a comprehensive summary of the results acquired from field monitoring including field instrumentations, elevation surveys and DCP tests of untreated and treated test sections. The field monitoring results are presented in two sections. The first section presents the results of field monitoring for untreated and treated 'sulfate-rich' soils conducted at Harwood Road. Then, the second part covers the field monitoring results of 'non-sulfate' soils conducted at three test sites, including International Parkway, Southmoor Drive and Southeast Parkway. This chapter also presents the DCP test results, which were performed to indirectly analyze strength properties of the treated subgrade soils at different time periods after stabilization. Also, cost benefit analysis using life cycle cost analysis method was performed on stabilizers considered for both soil types.

Both field (this Chapter) and laboratory test results (Chapter 4) are used to develop design guidelines for selecting stabilizers for sulfate-rich soils and non-sulfates soils in Arlington, Texas. Following sections discuss these results in detail.

6.2 Field Instrumentation, Data Collection and Analysis for Sulfate-rich Soils

For sulfate soils, four stabilization methods were evaluated by comparing their results with those of lime stabilization method (termed as a control method). The main objective was to stabilize sulfate soils without any heaving and pavement cracking problems. As noted earlier, the following four stabilization methods were considered for field evaluations:

- Sulfate Resistant Type V Cement
- Class F Fly ash with Type V Cement
- Ground Granulated Blast Furnace Slag
- Lime with Polypropylene Fibers

A total of five test sections were constructed using all 4 selected stabilizers and one control, i.e. lime treated subgrade section along the Harwood road in Southeast Arlington. These treated sections were extensively instrumented with strain gauges and pressure cells to monitor the performance of these test sections under traffic loading conditions. Details of construction of test sections were already presented in Chapter 5.

The instrumentation data monitoring was initiated in the month of January 2005 and was continued until March 2008. Data from these sensors were collected once a week. In the case of sudden climatic changes like an occurrence of heavy rainfall, data was collected within twenty-four hours as this data is valuable to provide any initiation of heaving or cracking of the pavement sections as well as any ponding problems at the test sites. For the completeness of data, monthly average precipitations were also included in an analysis part in order to compare with pavement elevation changes. The data was acquired from National Environmental Satellite, Data and Information Service (NESDIS) homepage (http://www.ncdc.noaa.gov/oa/climate/stationlocator.html).

A mid-size passenger car with a gross weight of approximately 3,000 lb was used for loading the test sections, and the sensor data was collected during this loading phase. In order to ensure that the tire contact area with the pavement was equal throughout the data collection period, the tire pressure was kept at a standard pressure of 32 psi.

Data from each sensor was acquired over a ten-minute monitoring period. The raw data was obtained in ASCII format, which was then converted to engineering data with Excel software. This raw data typically contain noise or peaks and valleys of voltage fluctuations due to external disturbances. To segregate the useful data from the noise, raw data was subjected to filtering using MATLAB (Version 7.0.4) and the filtered data was segregated section-wise and normalized using Excel program. After filtering the data, their averages were calculated. Both strain and pressure differences were calculated by subtracting the averaged data acquired with and without car on the sensors. The filtered and edited data was then compared against each of the test sections.

This section presents a summary of field instrumentation data and analysis of the collected data for sulfate-rich soils. The instrumentation and elevation survey data was acquired for a period of 39 months (more than 3 years) and this data has been analyzed in this chapter.

Analysis of test results is presented in three different sections. The first section covers the instrumentation data collected from both strain gauges and pressure cells installed in the test sections. The second section presents the results of elevation surveys carried out to monitor the settlement/heave related movements of the treated sections. The third section discusses the DCP tests, which were performed to analyze the strength properties of the treated subgrades at different curing time periods.

6.2.1 Strain Gauge Data

Figure 6.1 through Figure 6.5 present the accumulated vertical compressive strains collected from strain gauge embedded from the top of stabilized and subgrade sections. All test sections including type V cement, type V cement – fly ash, GGBFS, and lime-fiber treated

sections were monitored for the time period starting from February 2005 to March 2008. All these results are presented in a bar chart format. The data collected in February 2005 from early construction to conditions close to March, 2008 were reported here.

Figures 6.6 and 6.7 present comparisons of vertical strains collected from all test sections at different periods of data collection. Figure 6.8 presents the comparison of strains observed from all treated test sections in line graphs, which shows an increase in vertical strains in all treated subgrades under field monitoring over the entire period of data collection. The increase in strain is expected as this strain represents the plastic strains, which continue to accumulate with the loading cycles.

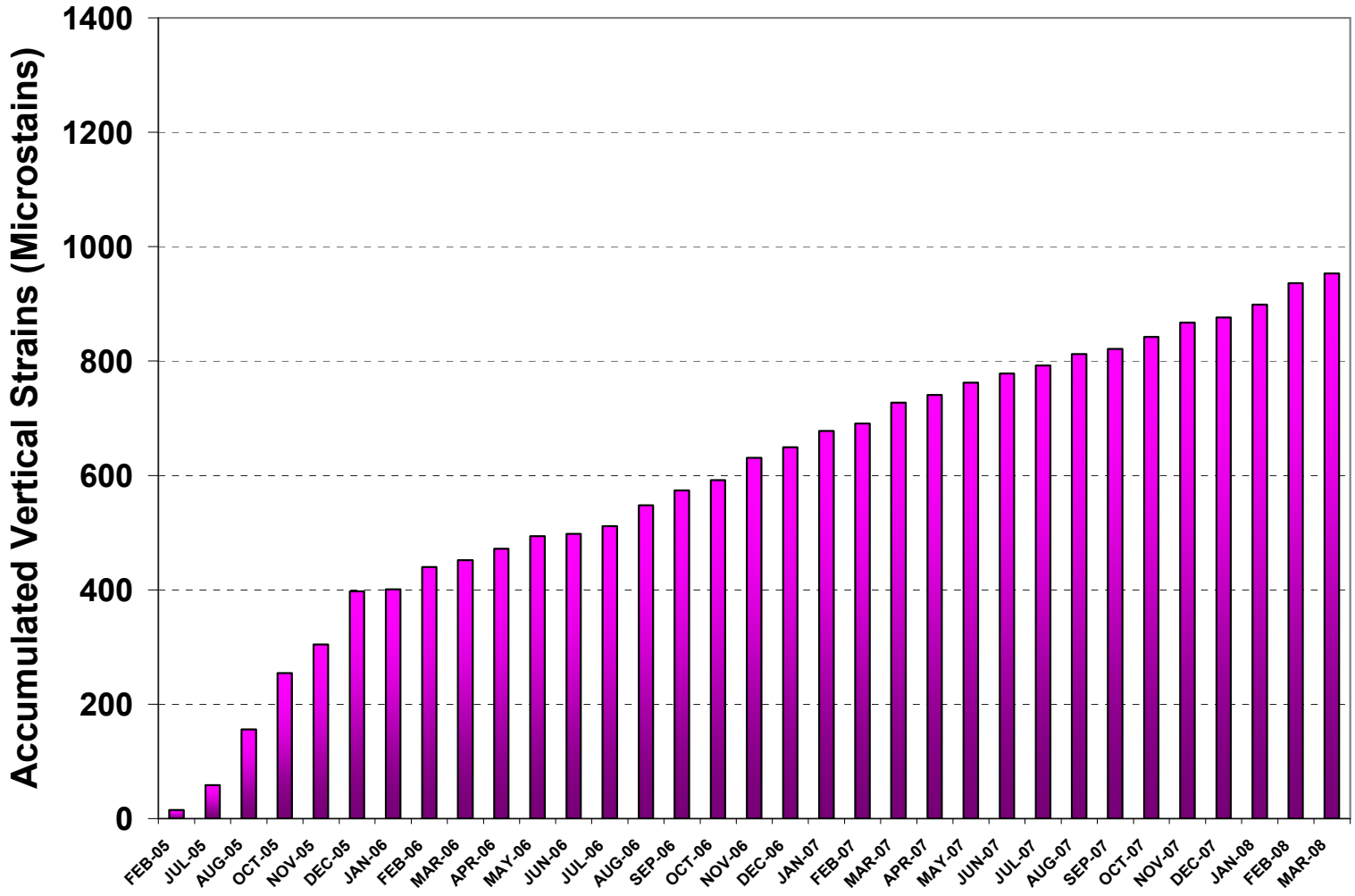

Figure 6.1 Vertical Compressive Strains at Type V Cement Section.

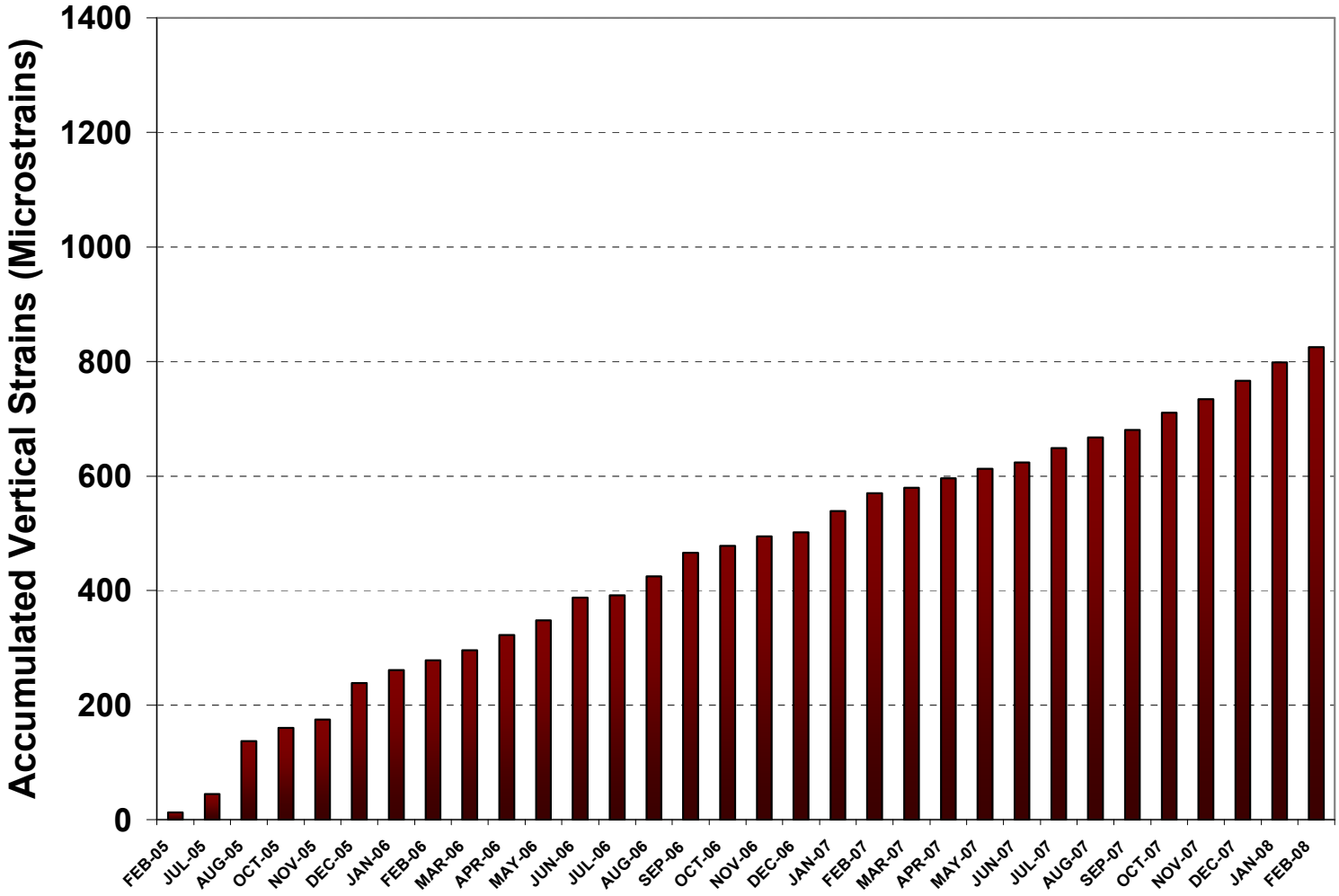

Figure 6.2 Vertical Compressive Strains at Cement with Fly ash Section.

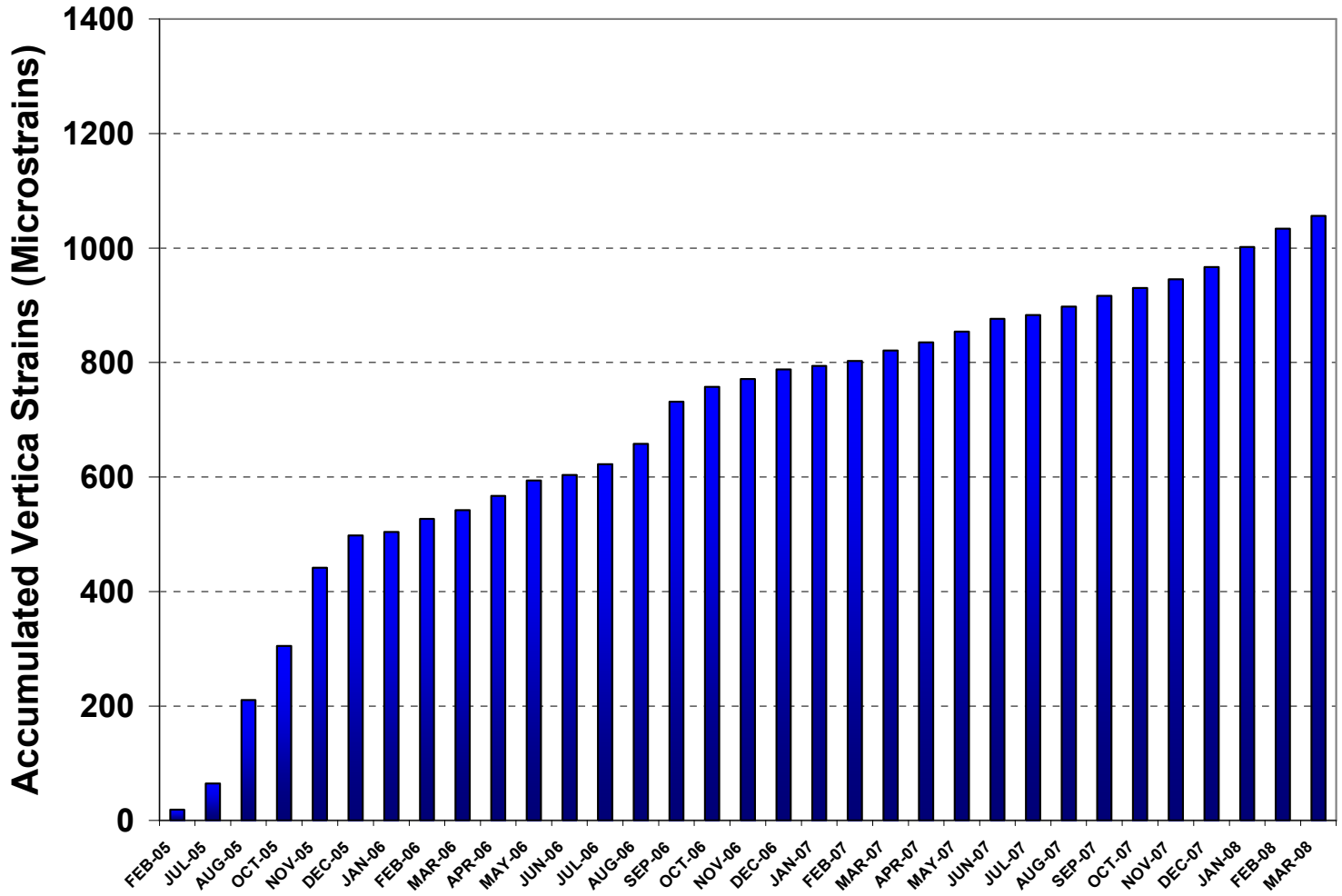

Figure 6.3 Vertical Compressive Strains at GGBFS Section.

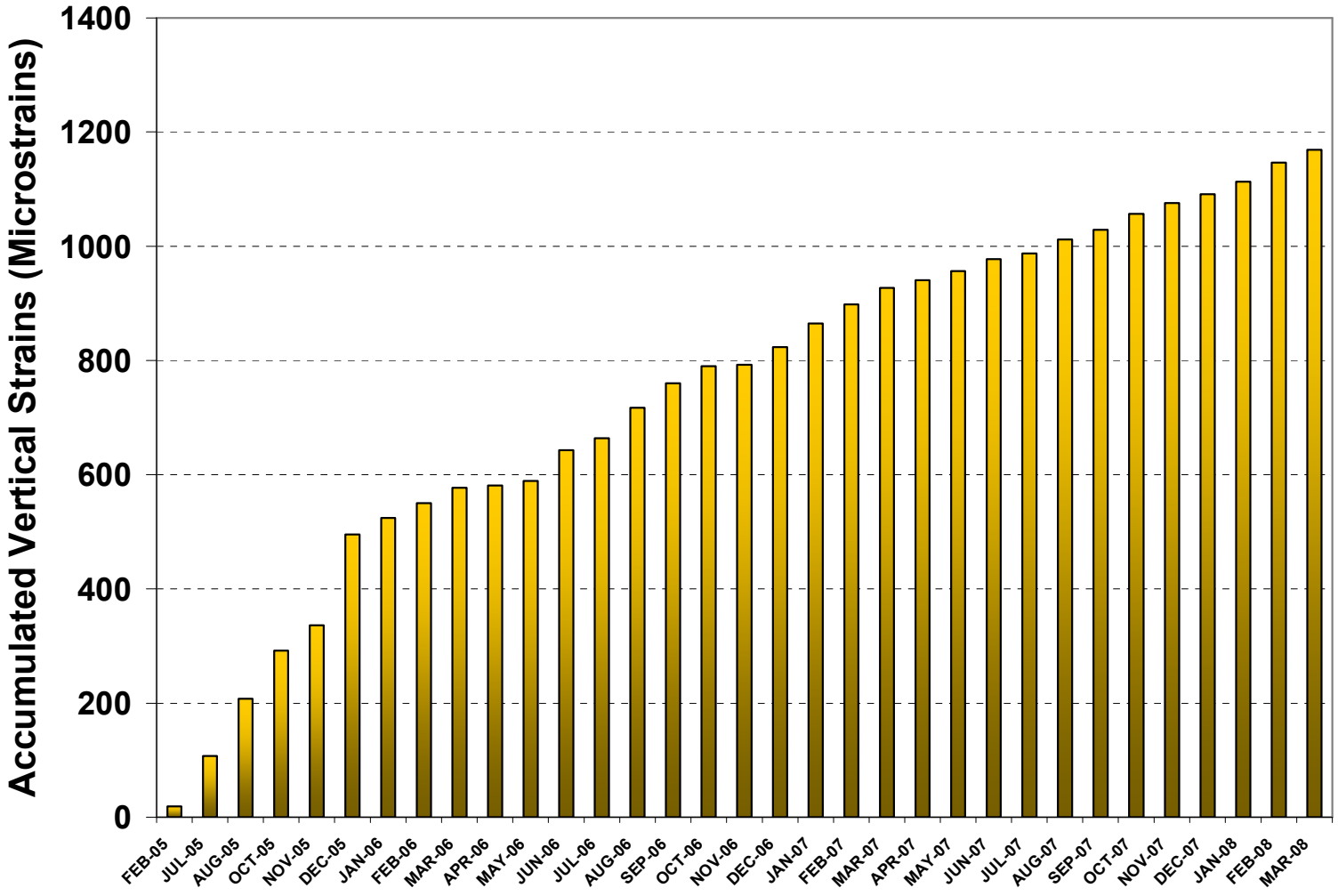

Figure 6.4 Vertical Compressive Strains at Lime with Fibers Section.

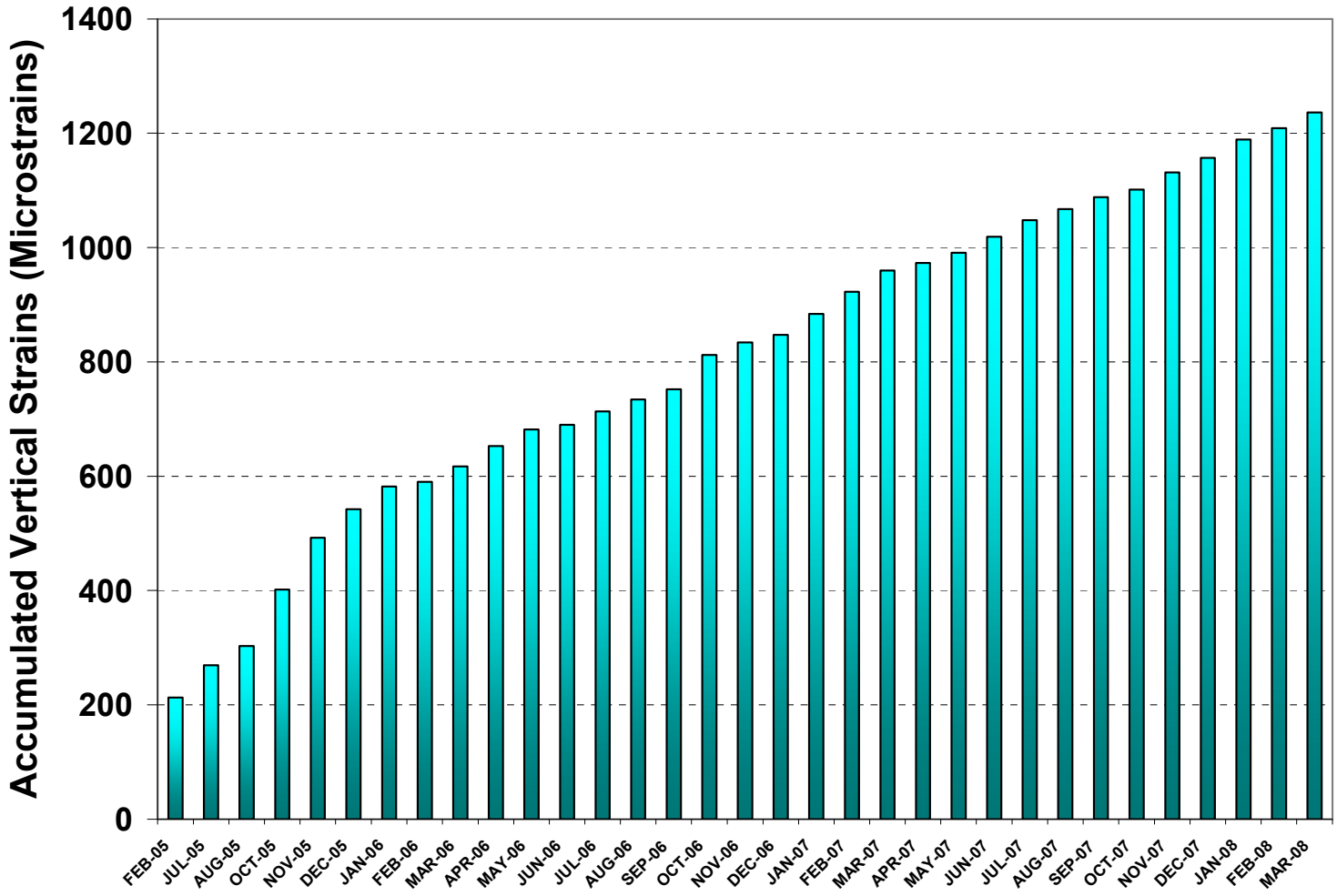

Figure 6.5 Vertical Compressive Strains at Lime (Control) Section.

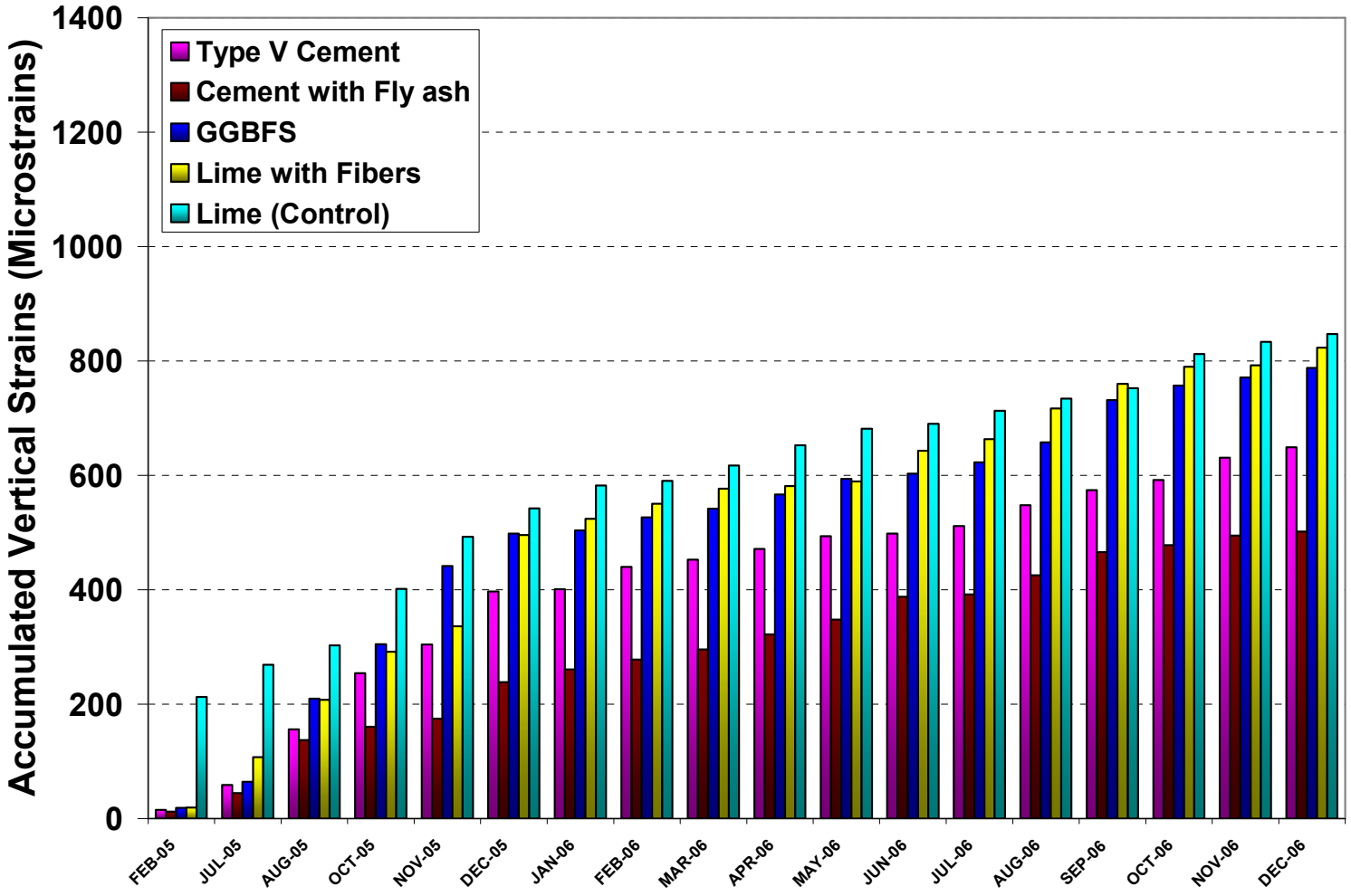

Figure 6.6 Comparisons of Strains at Different Periods of Data Collection.

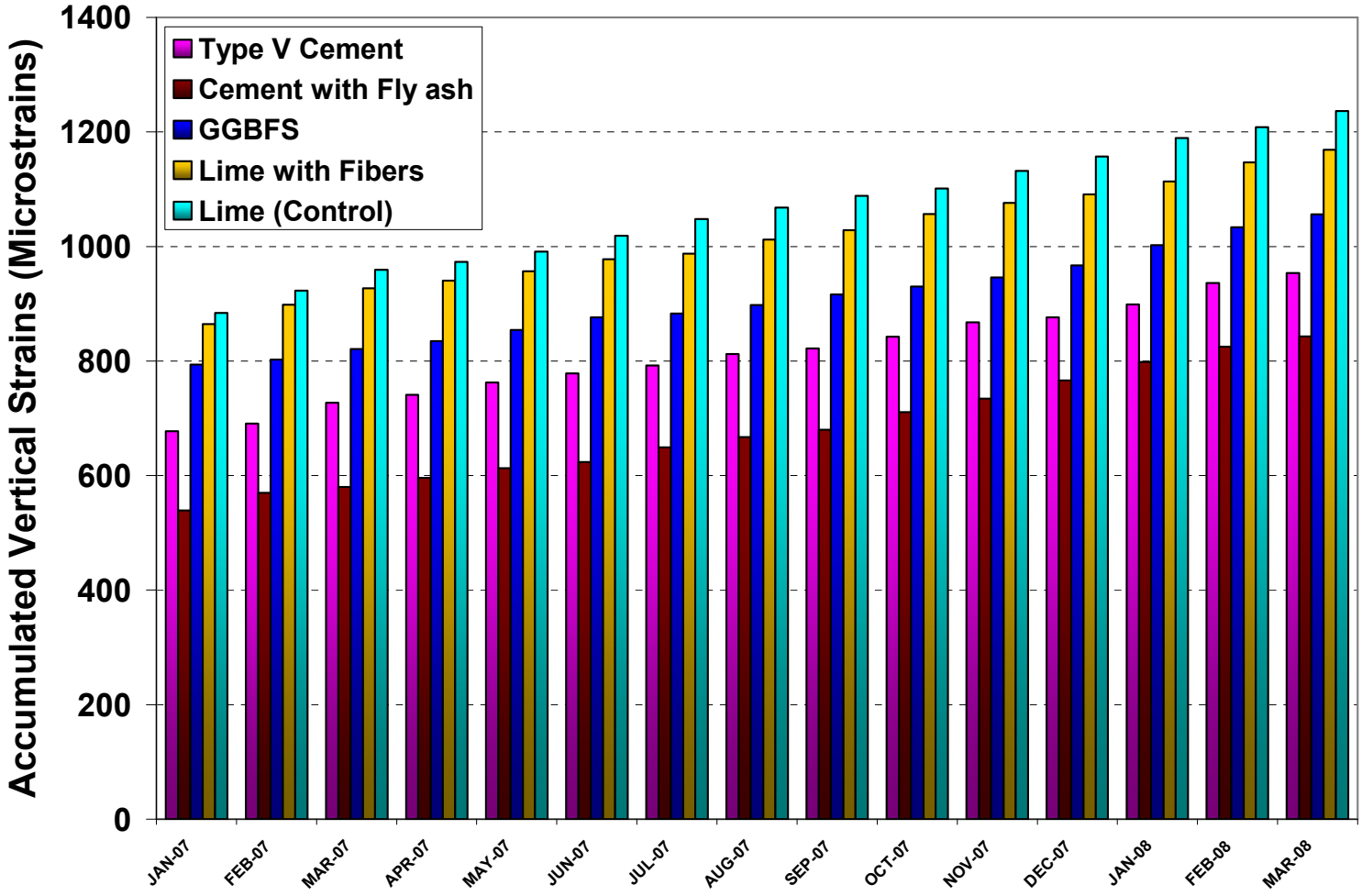

Figure 6.7 Comparisons of Strains at Different Periods of Data Collection (Continue).

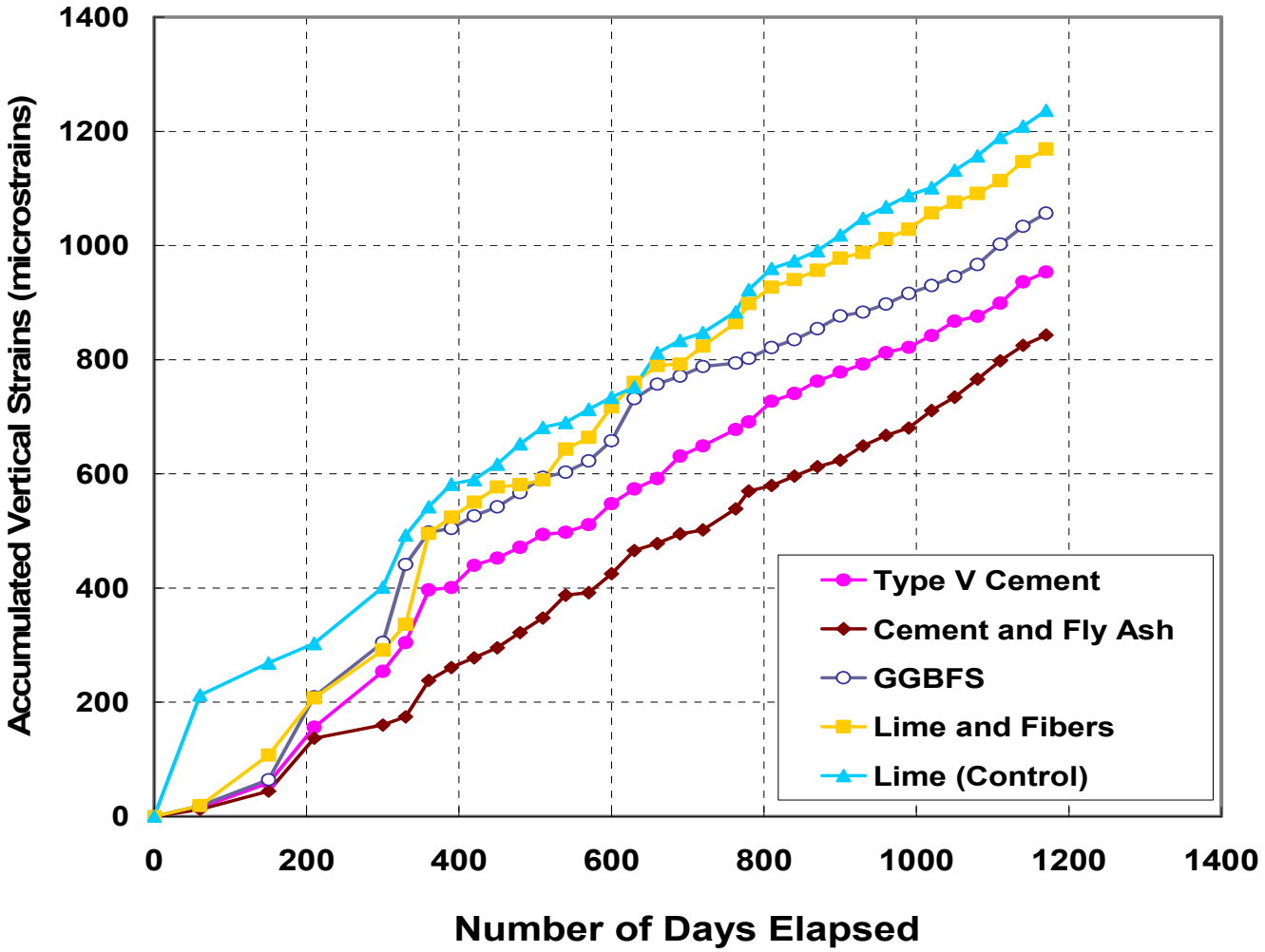

Figure 6.8 Comparison of Vertical Strains in different test sections for the Entire Period of Data Collection.

From all figures illustrated above, it can be seen that the lime/fiber section and lime treated control section experienced slightly larger accumulated vertical strains under vehicular loads. Considerable increase in compressive strain was also observed in the GGBFS treated subgrade section. Overall, in comparison, both Type V cement and Type V cement combined with fly ash treated sections demonstrated the lowest strains indicating that the stiffer material was being formed with the stabilizer treatments. These results also indicate that the pavements built on cement stabilized subgrades did experience low permanent strains. Overall, the accumulated microstrains on all test sections are around 1200 microstrains, which is considered small and not approaching the results that could compromise the integrity of the overlain concrete pavement. Nevertheless, these comparison results suggest that cement treated sections experienced lower vertical strains those of lime and lime - fiber treated sections.

6.2.2 Pressure Cell Data

The same procedure was followed to determine pressures measured by pressure cells under traffic wheel loading. However, in the case of GGBFS section, the data could not be acquired as the connecting cables were severed during the construction of pavement section and they could not be repaired as the cables were buried underneath the pavement.

Figures 6.9 to 6.12 show the pressure cell data obtained from all test sections from February 2005 to March 2008. Figures 6.13 and 6.14 present comparison of pressures collected from all test sections from different monitoring periods.

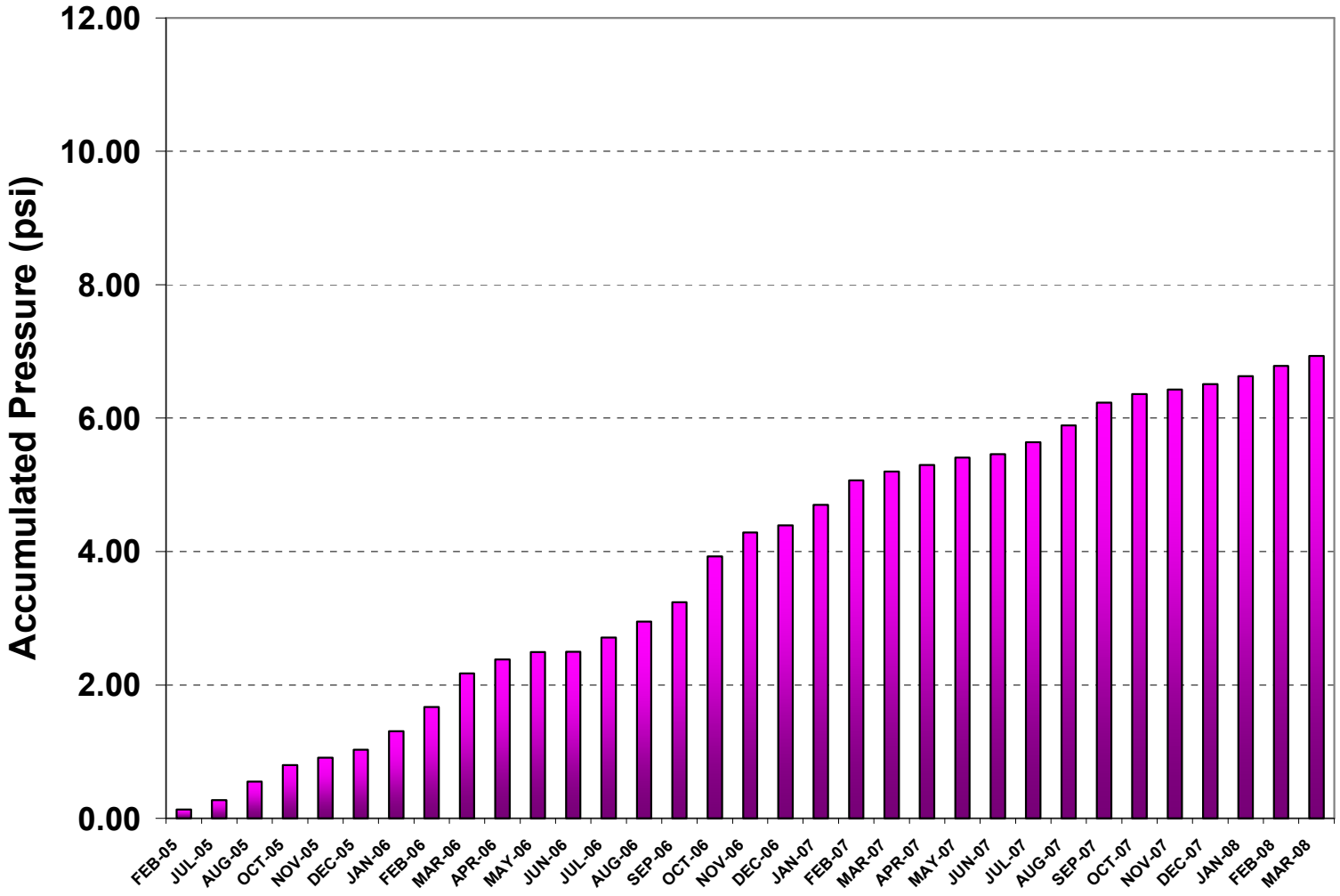

Figure 6.9 Pressures at Type V Cement Section.

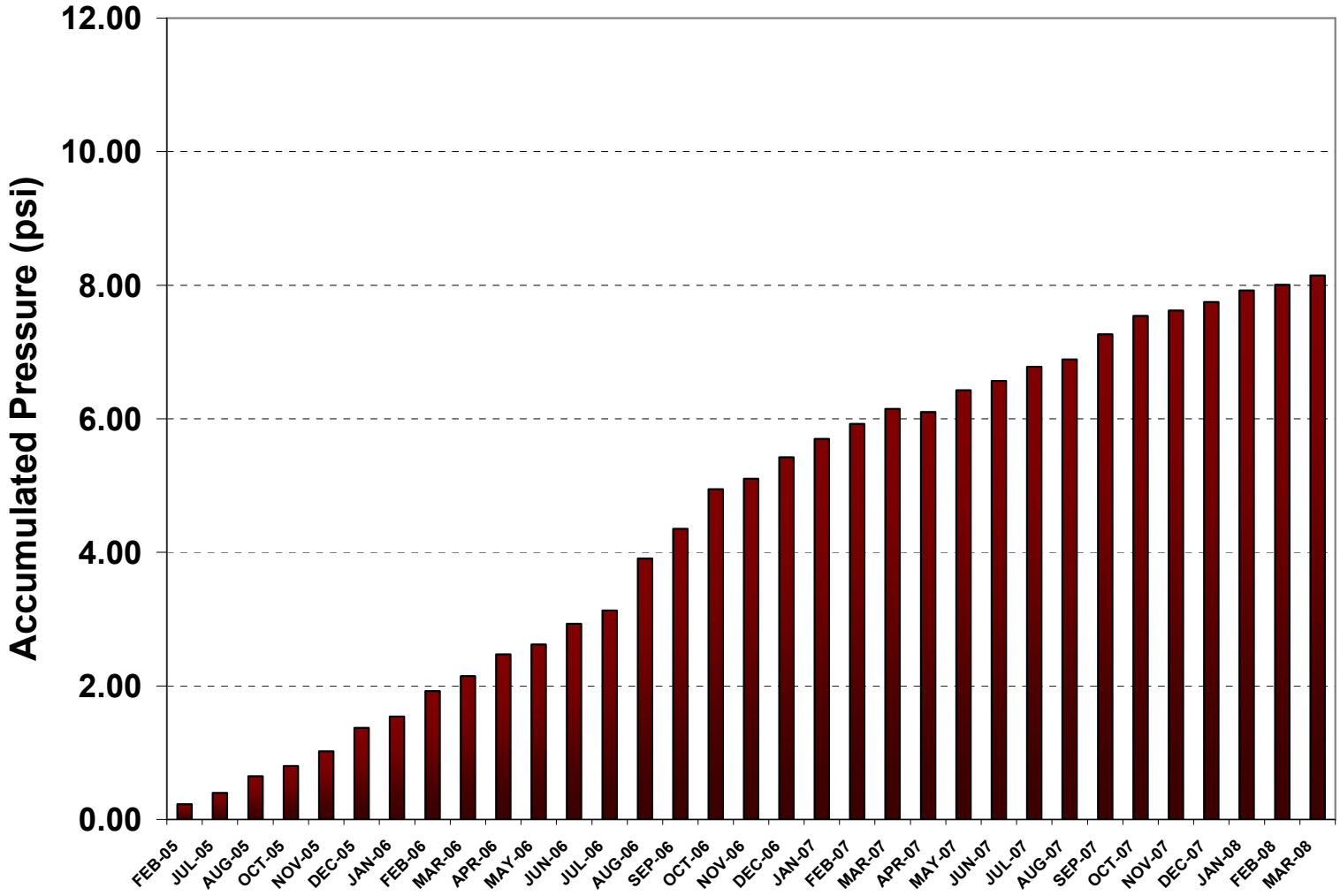

Figure 6.10 Pressures at Cement with Fly ash Section.

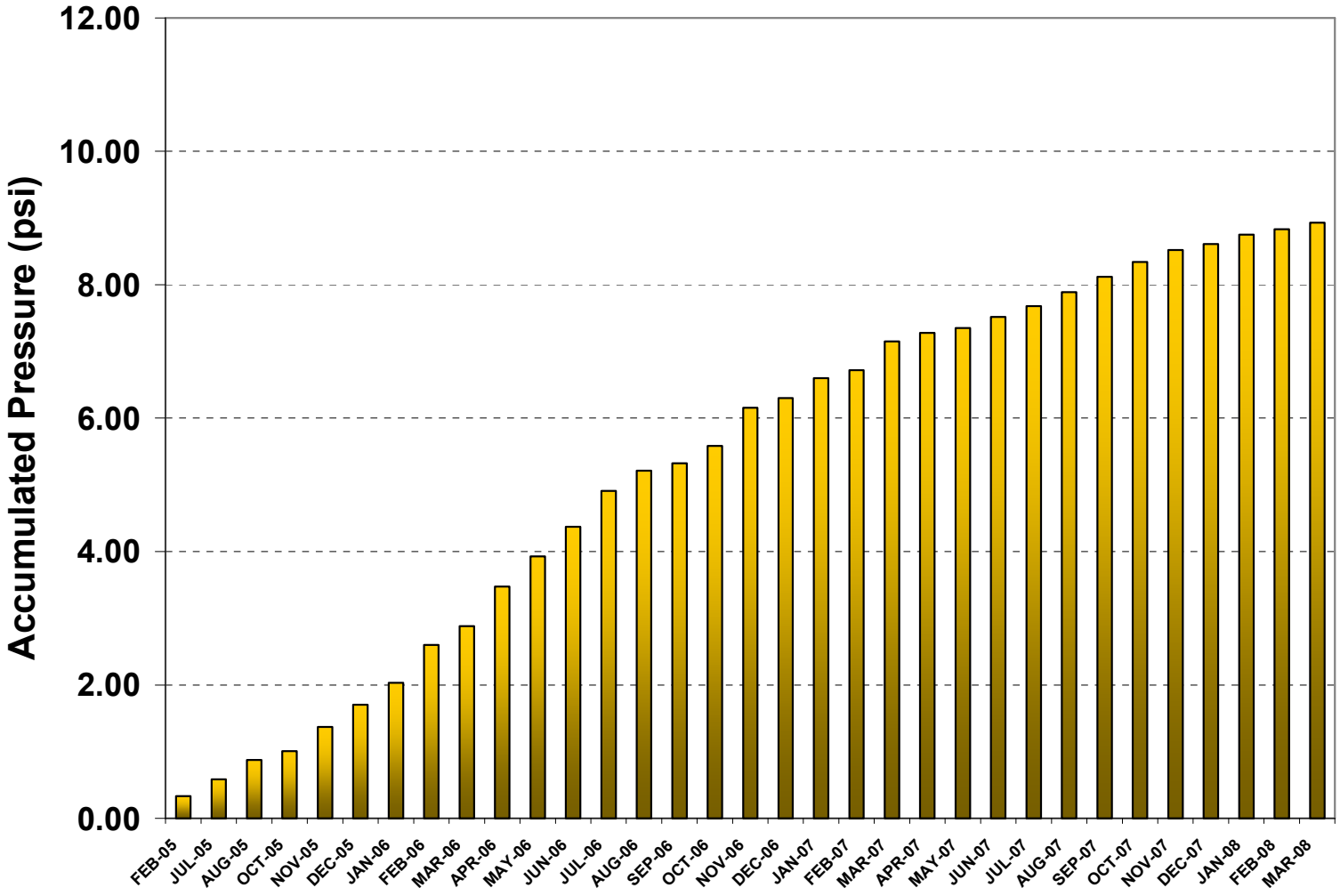

Figure 6.11 Pressures at Lime with Fibers Section.

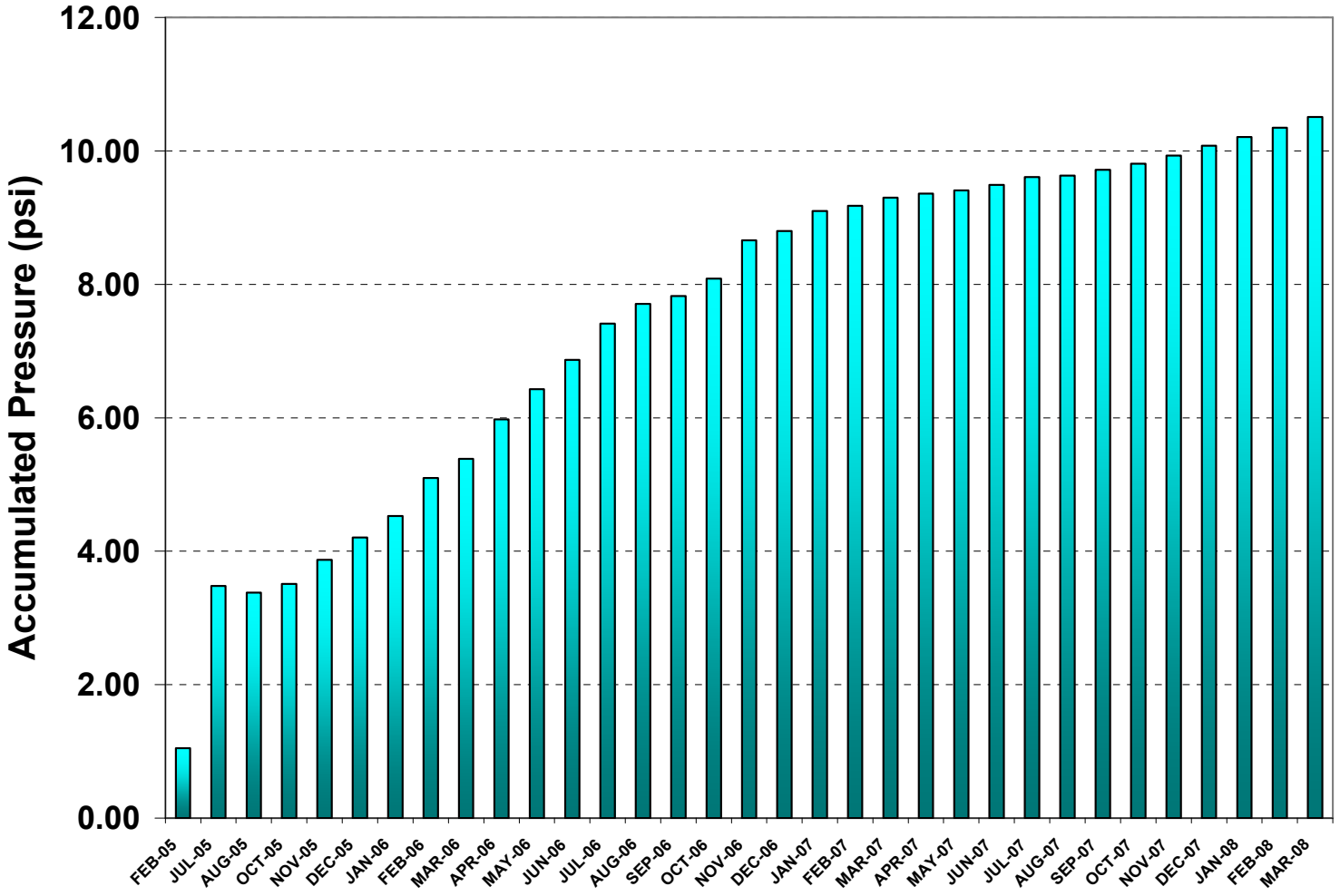

Figure 6.12 Pressures at Lime (Control) Section.

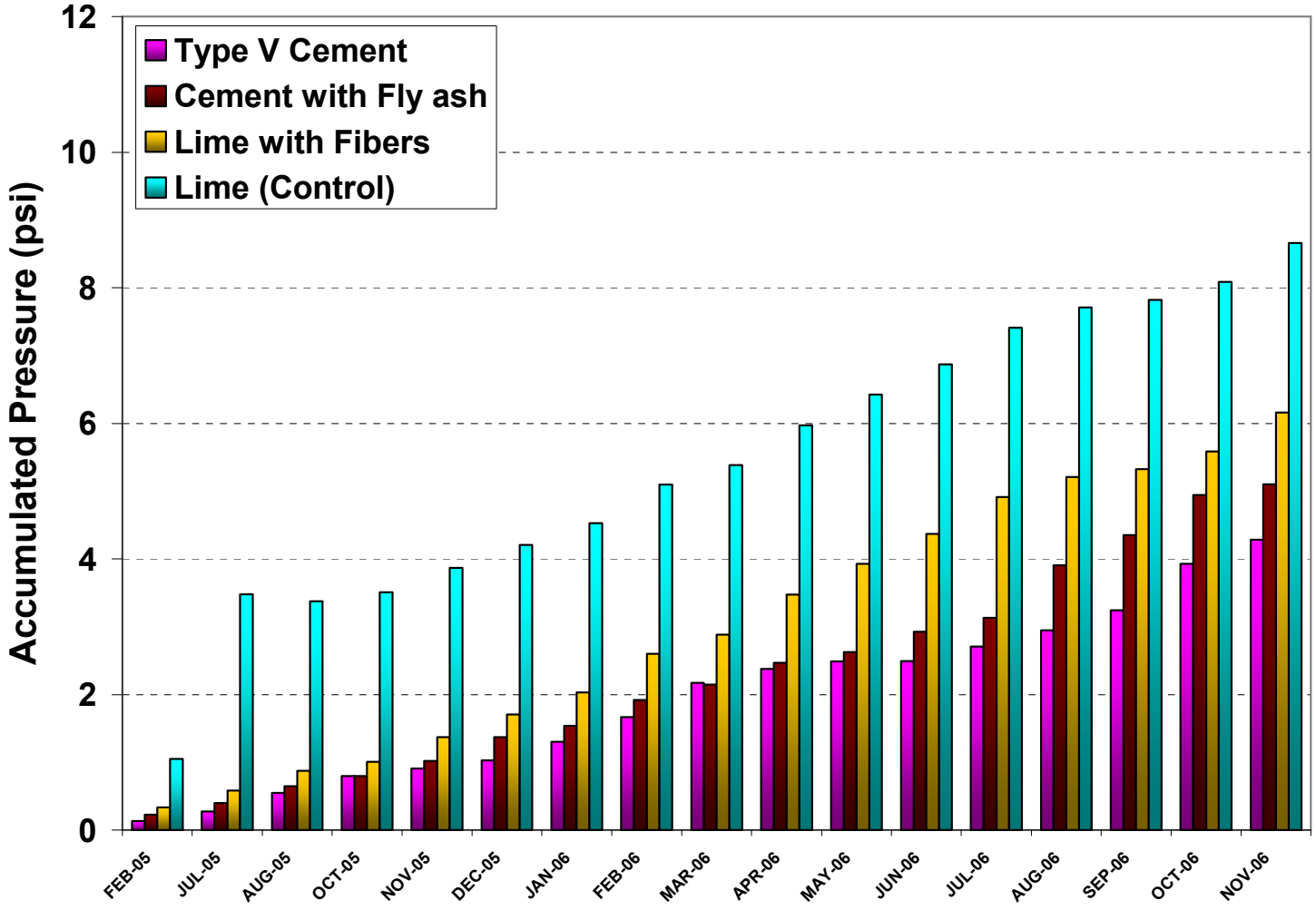

Figure 6.13 Comparisons of Pressures at Different Time Periods of Data Collection.

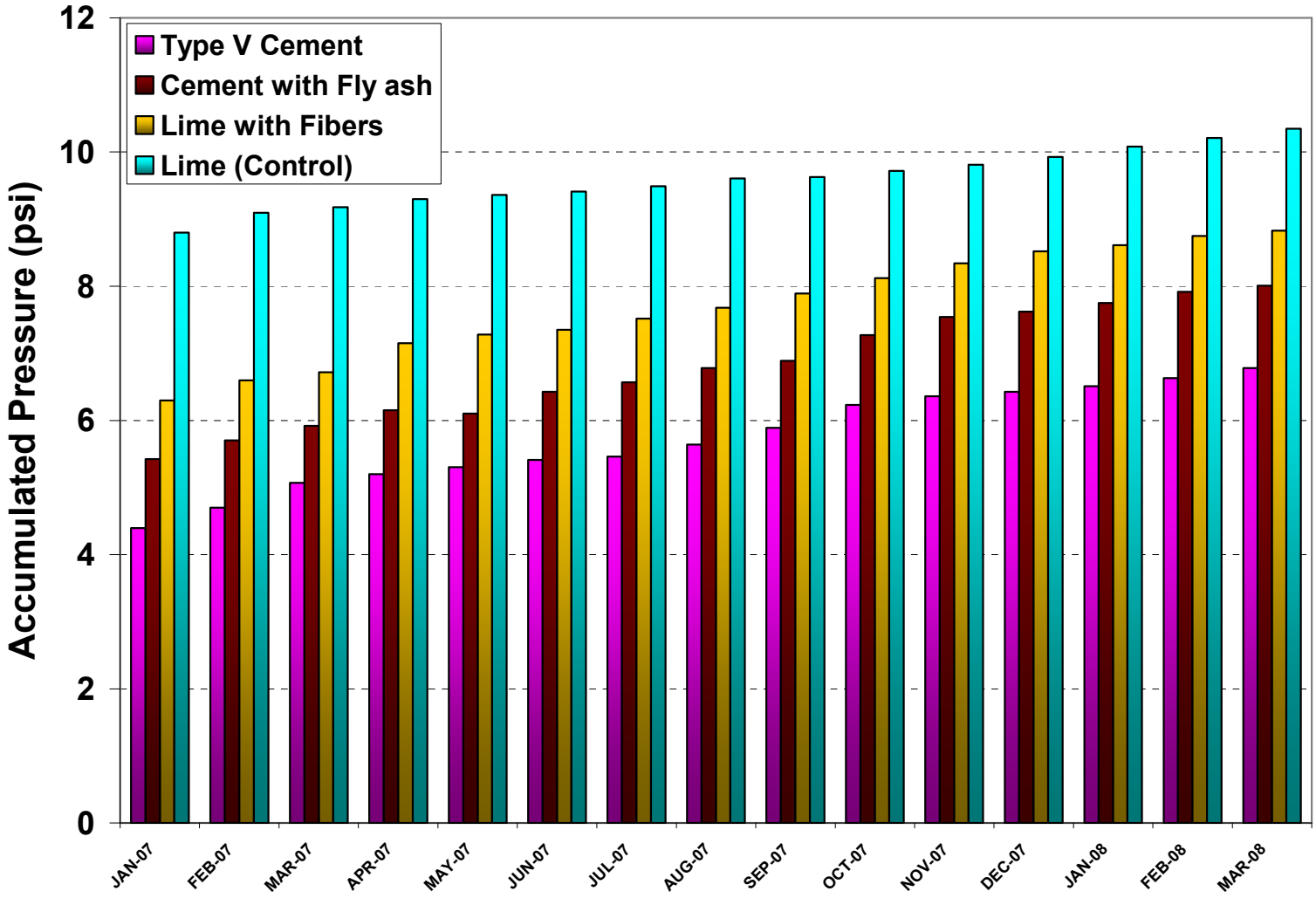

Figure 6.14 Comparisons of Pressures at Different Time Periods of Data Collection.

It should be noted that the pressures measured at the bottom of the treated section during traffic loading is a combination of pressures coming from all four wheel loads and a moderate static overburden pressure coming from the pavement system. Figure 6.15 presents a comparison of an increase in pressure observed in different test sections over the entire period of data collection.

The initial readings taken at the site showed very small pressure values. However, these values were increased with elapsed time period. The increase in pressures could be attributed to micro-cracking in the treated subgrade sections. However, these pressures are constant over the last year and they did not show any increase indicating that the pressure transfer was stabilized.

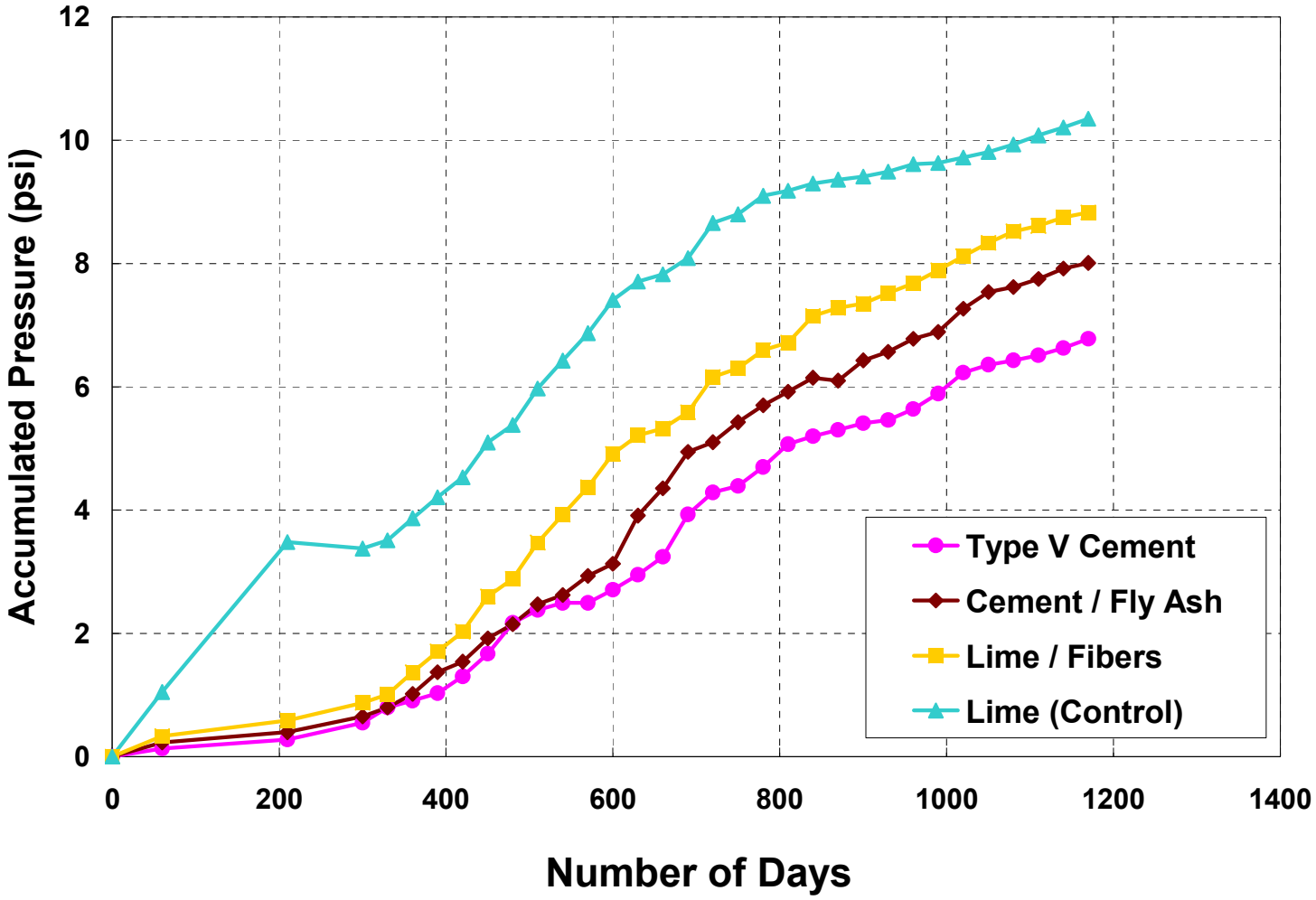

Figure 6.15 Comparison of Pressures in different test sections for the Entire Period of Data Collection.

Overall, from the results presented above, the cement treated section (Type V) has demonstrated good performance with low pressure readings, which is followed by the cement with fly ash treated section. Lime-fiber treated section demonstrated moderate performance and Lime treated (control) section has experienced the high pressure readings indicating the treated section is not absorbing overlying traffic loads. This implies the tire load induced pressure distribution or tire pressure transfer to the subgrade soils is high which may lead to more deformation and low performance. Overall, Type V cement treated section and Type V cement and fly ash treated sections are expected to undergo low rutting under present loading conditions due to low pressure transferring to subsoils.

6.2.3 Analysis of Elevation Survey Data

Elevation surveys were performed over a period of thirty nine (39) months in order to monitor the settlement/heave related movements of the stabilized pavement sections. Figure 6.16 shows the elevation survey results monitored along with monthly average precipitations as a part of this research.

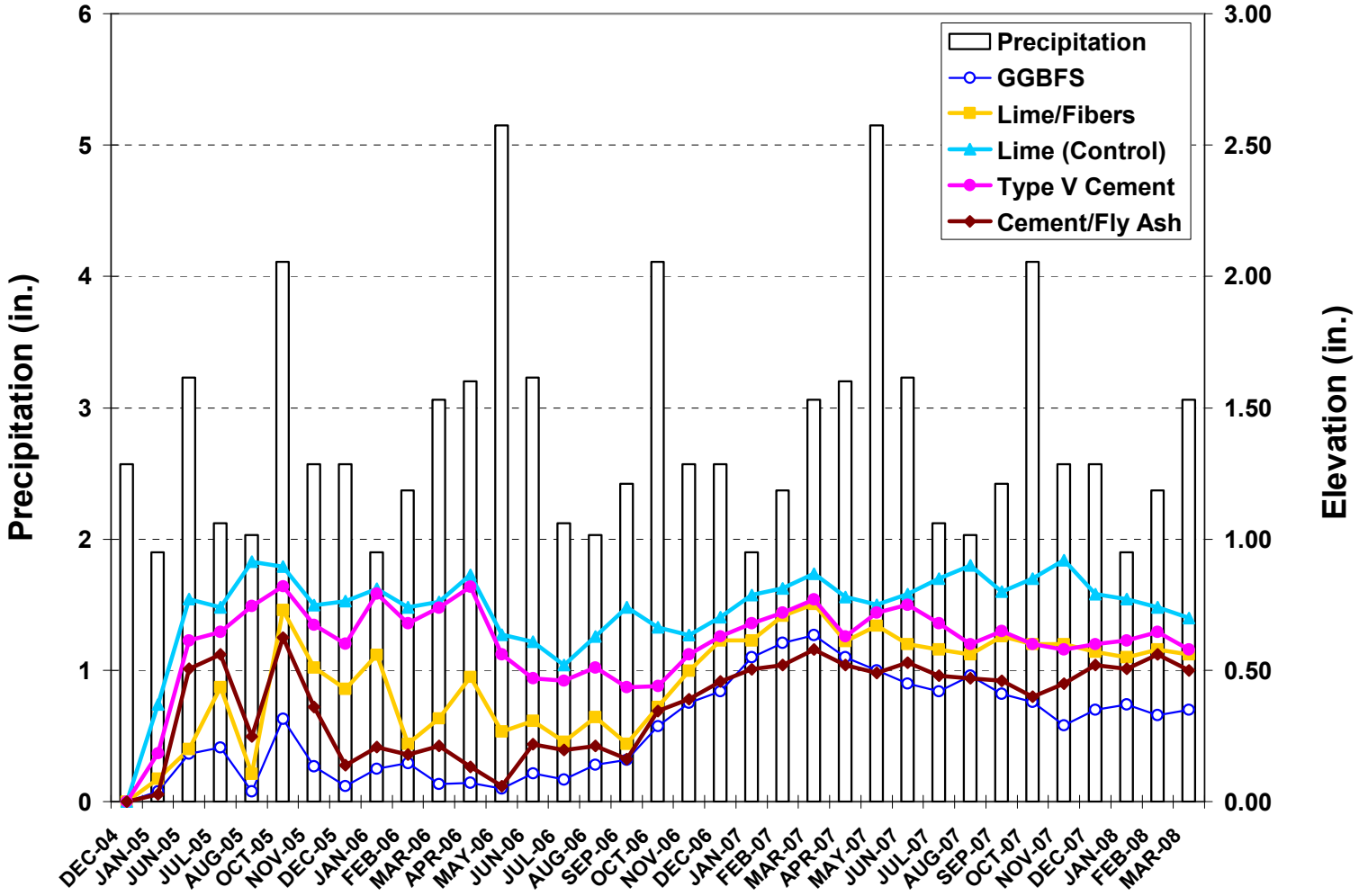

Figure 6.16 Plots of Pavement Elevation Changes and Monthly Rainfall Data (www.ncdc.noaa.gov) at Harwood Road for 39 Months.

By considering the monthly average precipitation profile shown Figure 6.16, moisture fluctuations were observed. The maximum monthly average precipitation was recorded in the month of May (late spring) and the minimum monthly average precipitation was recorded in the month of August (summer). The maximum and minimum precipitation values from the monitoring period of December 2004 to March 2008 are varying from 2 to 5 in.

It is noticeable that, in the early monitoring period (from December 2004 to October 2005), precipitation variations were more than 2 in. (Figure 6.16) which is considered to be high. This moisture content fluctuation could cause exposed expansive subgrade soils to undergo swell and volume change movement in a short period of time. Consequently, high differential elevation had been observed in the lime treated (control) section. Therefore, from the elevation surveys and precipitation profiles results, it can be mentioned that the fluctuations in the elevation surveys can be attributed to the seasonal precipitation variations that test sections experienced during the monitoring period.

It is clear from the Figure 6.16 that all test sections have shown a trend of moderate surface heaving. For example, lime (control) section experienced the highest heave related movements among all test sections. However, the volume change movements in this section diminished with time when compared to its initial high heaving pattern. The next highest heaving was observed in the cement treated section, followed by lime - fiber treated section. On the other hand, both GGBFS and Type V cement - fly ash treated soil sections demonstrated good performance with low heave related movements. Fluctuations in the elevation surveys can be attributed to the seasonal related soil movements that these sections experienced during the monitoring period.

6.2.4 DCP Test Results for Treated Sections

Dynamic cone penetration or DCP tests were conducted after 28 days of curing period, 26 and 37 months after the pavement construction and all these results are presented in this section. Figure 6.17 depicts the DCP apparatus used adjacent to the pavements.

Figure 6.17 Penetrations of DCP Apparatus into the Pavement Courses.

Figures 6.18, 6.19 and 6.20 show the DCP test results for the test conducted after 28 days, 26 months and 37 months of curing period, respectively. DCP test results are expressed in terms of Dynamic Penetration Index (DPI) of soil, which is the amount of cone penetration due to one drop of the hammer. The DPI is expressed in cm/blow. The DPI values were taken between 10 cm and 15 cm of penetration at the slopes of DCP data between those two depths. Hence, in the present research, the PR_1 and PR_2 depths are 10 and 15 cm respectively. Table 6.1 summarizes the DPI values determined from the DCP tests conducted after 28 days, 26 months and 37 months of pavement construction.

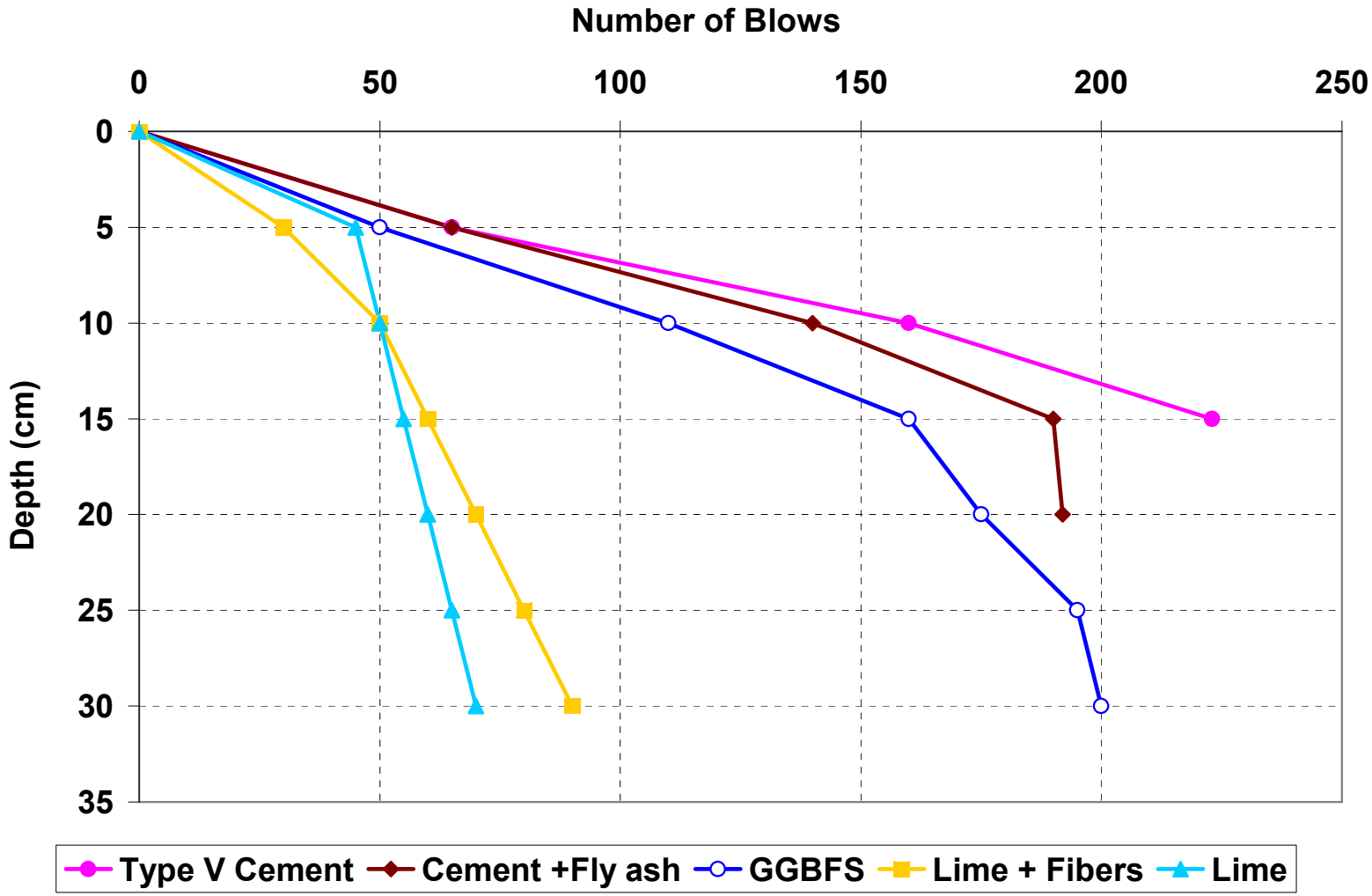

Figure 6.18 DCP Results after 28 days of curing (Enayatpour, 2005).

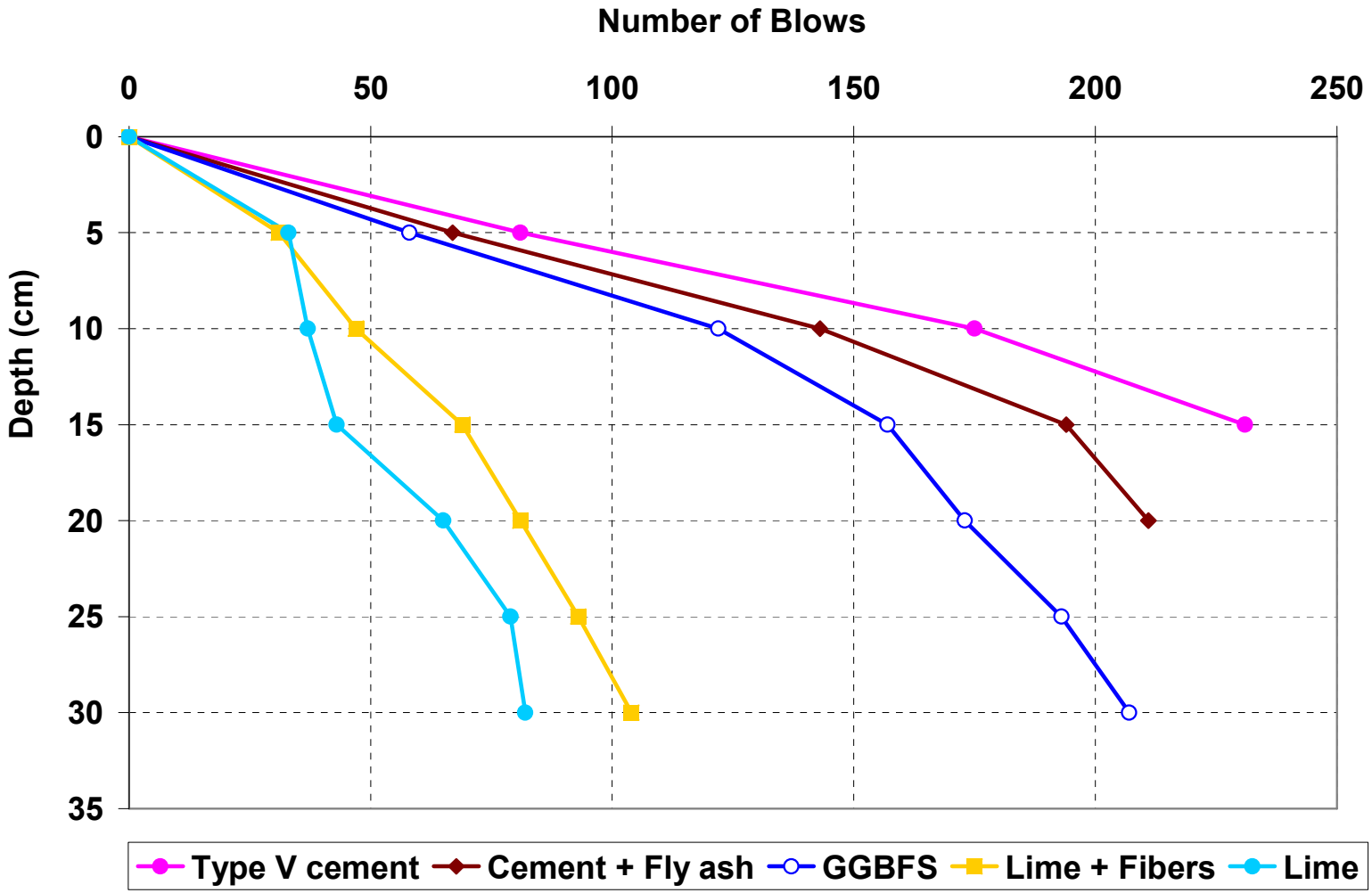

Figure 6.19 DCP Results after 26 months of Pavement Construction.

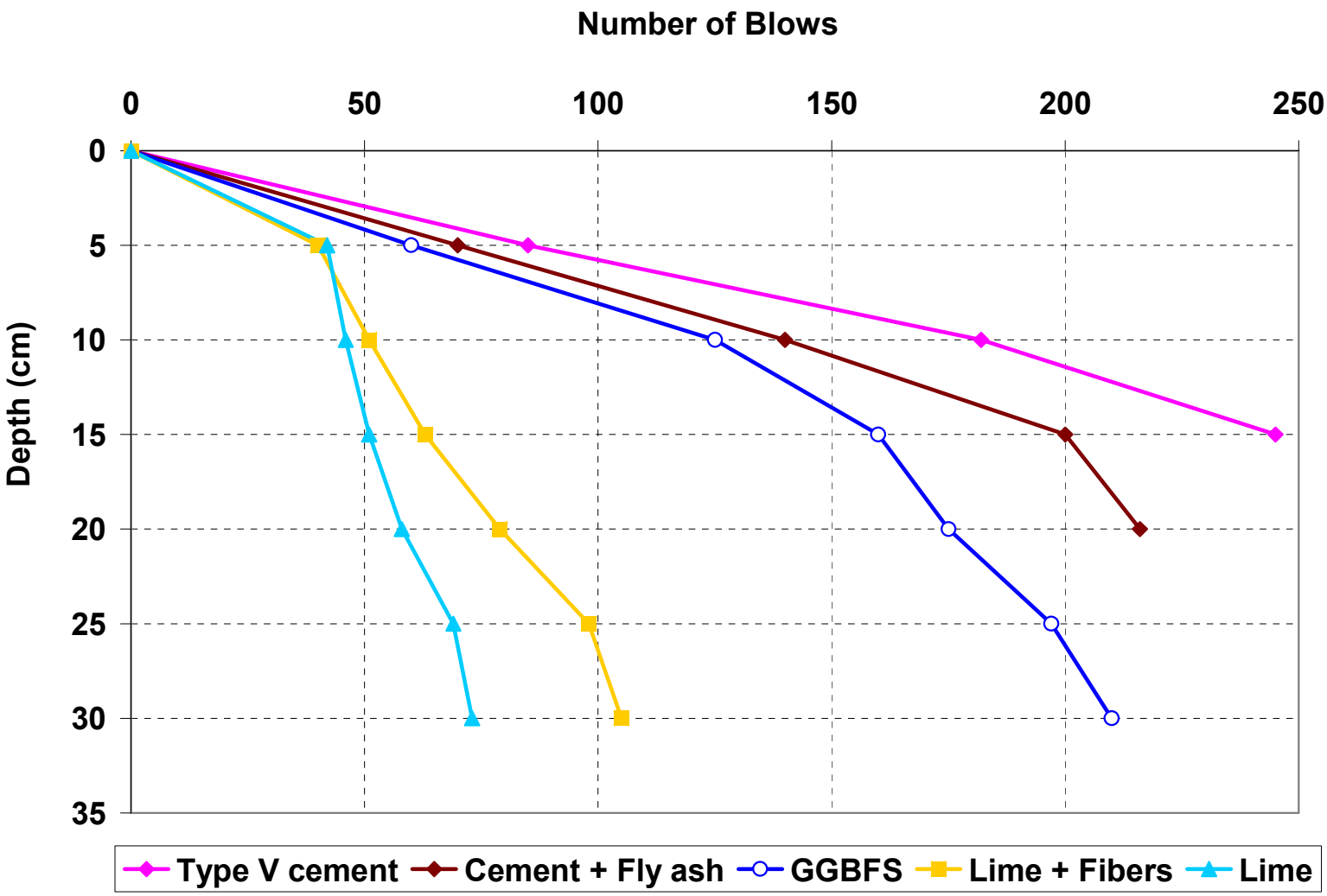

Figure 6.20 DCP Results after 37 months of Pavement Construction.

Table 6.1 Summary of DPI Values obtained after 28 days 26 months and 37 months of construction

Stabilizer	DPI (cm/blow)		
	After 28 days curing	After 26 months	After 37 months
Type V Cement	0.063	0.066	0.079
Cement and Fly Ash	0.080	0.078	0.083
GGBFS	0.090	0.101	0.143
Lime and Fibers	0.330	0.263	0.417
Lime	1.000	1.110	1.000

Figures 6.18, 6.19 and 6.20 present the slopes at which the DCP penetration decreases beyond the 15 cm depth, which is an indicative of the 15 cm stabilized base section beyond which the number of blows required to advance the cone penetrometer decreased. DCP tests had to be stopped in certain tests due to difficulties in advancing the cone through stiff treated base layer.

Figure 6.18 representing results after 28 days of curing, the number of blows for 15 cm of penetration for treated layers with cement, cement with fly ash, GGBFS, lime-fibers and lime (control) sections are 223, 190, 110, 50 and 50 respectively. Figure 6.20 shows the same trend even after 37 months of pavement construction. The results in Figures 6.18, 6.19 and 6.20 have shown the same trend as the strength enhancement is rapid in the first two weeks of curing and thereafter they become similar. The results indicate that the cement treatment, cement with fly ash and GGBFS treatments exhibited higher strength gains when compared to lime - fibers and lime (control) treatment sections. It is to be noted that there is no considerable deterioration seen in the DCP values in any of the treated layers over the last three years, which indicates that the stabilization effectiveness still remained intact and same. No leaching and durability problems were evident in the present stabilizer treated sections.

After the completion of each field elevation survey and rainfall events, visual surveys of test sections were typically performed. The intent of these visual surveys is to identify any heave bumps or heave related cracking in the pavement test sections. A recent visual survey results conducted in March 2008 are presented here. Photos of the pavement surface were taken during the visual monitoring and these photos were taken on all pavement sections built on Type V Cement, Cement and Fly Ash, GGBFS and, Lime and Fiber stabilized subgrades. These photos are presented in Figures 6.21 to 6.24, respectively.

All photos indicate that there is no major pavement distress both in the forms of longitudinal and transverse cracks observed in these pavement sections. This demonstrates that, from the present field performance assessments, the present stabilized subgrade sections provided uniform and stable support for concrete pavements.

Figure 6.21 Condition of pavement at section 1 (Type V Cement stabilized) after 39 months.

Figure 6.22 Condition of pavement at section 2 (Cement and Fly ash stabilized) after 39 months.

Figure 6.23 Condition of pavement at section 3 (GGBFS stabilized) after 39 months.

Figure 6.24 Condition of Pavement at Section 4
(Lime and Fiber stabilized Subgrade) After 39 Months.

Photos taken from the present lime stabilized subgrade section (Control) are shown in Figures 6.25 to 6.27. Figure 6.27 presents a water ponding problem with accumulated rainfall water from the previous week's rainfall. Figures 6.26 and 6.27 also show pavement cracking in various directions and settlements of the pavement section. This indicates that the pavement section built on the control section have experienced certain distresses, though not in substantial terms that induces major repairs or rehabilitation during the current monitoring period.

Figure 6.25 Water accumulation on pavement at control (lime treated) section.

Figure 6.26 Longitudinal and Transverse cracks observed at control section.

Figure 6.27 Settlement at control section.

6.3 Field Monitoring and Analysis for Non-sulfate Soils

The field sections for non-sulfate soils were located on three street locations in different regions of the City of Arlington, Arlington, Texas. These streets included International Parkway, Southmoor Drive and Southeast Parkway. Soils at these sites are natural expansive soils which demonstrated high plasticity behavior. Typical practice on the city roads is to use a lime treated subgrade as a base material to support the pavements. Due to the need to increase the design life of the pavements, a modified stabilization method termed here as "Combined lime and cement stabilization" was selected and used to stabilize the natural soils. Both old and distressed pavement layers at all three locations were replaced with a new concrete pavement layer laid over the combined stabilized subgrade soil section.

Field monitoring of these three sites included elevation surveys, DCP tests and visual inspections. Monitoring was conducted at regular time intervals, by performing visits to these three test sites to assess the performance of pavements built over the stabilized subgrade soils. The monitoring was initiated in the month of March 2006 for International Parkway and Southmoor Drive, and from November 2007 for Southeast Parkway. The monitoring was then continued until October 2008. The field monitoring information with visual inspection data has provided valuable data that could be utilized to assess the performance of pavement layers in real field conditions. This section presents the results of the field monitoring along with their analysis for pavement sections built on cement-lime treated subgrades.

In the case of sudden climatic changes such as heavy rainfall, field data was also collected within twenty-four hours. This data is valuable to provide any initiation of heaving or cracking of the pavement sections as well as any ponding problems at the test sites.

For the completeness of data, monthly average precipitations were also included in this section, which are used to compare with pavement elevation changes that transpired from the moisture movements into subsoils. The rainfall data was acquired from National Environmental Satellite, Data and Information Service (NESDIS) homepage (http://www.ncdc.noaa.gov/oa/climate/stationlocator.html).

Field monitoring results for each site are presented in the form of plotting of monthly average precipitation against pavement elevation changes at monitoring time periods. Moreover, those data are correlated with any occurrences of pavement cracks at the site. Details of elevation survey results, photographs of pavement conditions and visual inspection results were also presented. It should be noted that no field instrumentation was used due to expenses involved with the instrumentation and also the data obtained from earlier instrumentation was not highly beneficial in the present evaluations. One reason for this is that the new sections do not undergo any considerable deformation in the early periods after construction, and hence one would not see any appreciable differences in the field data. If the field sections are subjected to accelerated loading conditions or those near failure, the instrumentation will provide data that will be more valuable than the data collected on in service pavements immediately after construction.

6.3.1 International Parkway

Prior to the pavement reconstruction, the old asphalt layer was subjected to severe longitudinal and transverse cracks, and vertical movements due to the expansion of the old non-stabilized subgrade. This road was reconstructed in March 2006. The subgrade layer was stabilized with combined lime and cement treatment. The old asphalt layer was replaced with a new concrete layer laid over the stabilized subgrade soils. The pavement condition was improved considerably after the reconstruction.

The new concrete pavement sections built at International Parkway were subjected to elevation surveys periodically. These surveys were started from March 2006 and were continued over 30 months until September 2008. The surveys were conducted on the pavements using total station equipment. Results of the elevation surveys are shown in Figure 6.28. The results are presented along with monthly average precipitation.

By considering the monthly average precipitation profile in Figure 6.28, moisture fluctuations were observed at the site. The maximum monthly average precipitation is in the month of May (late spring) and the minimum monthly average precipitation is in the month of

August (summer). The maximum and minimum precipitation values from the monitoring period of March 2006 to September 2008 are varying from 2 to 5 in.

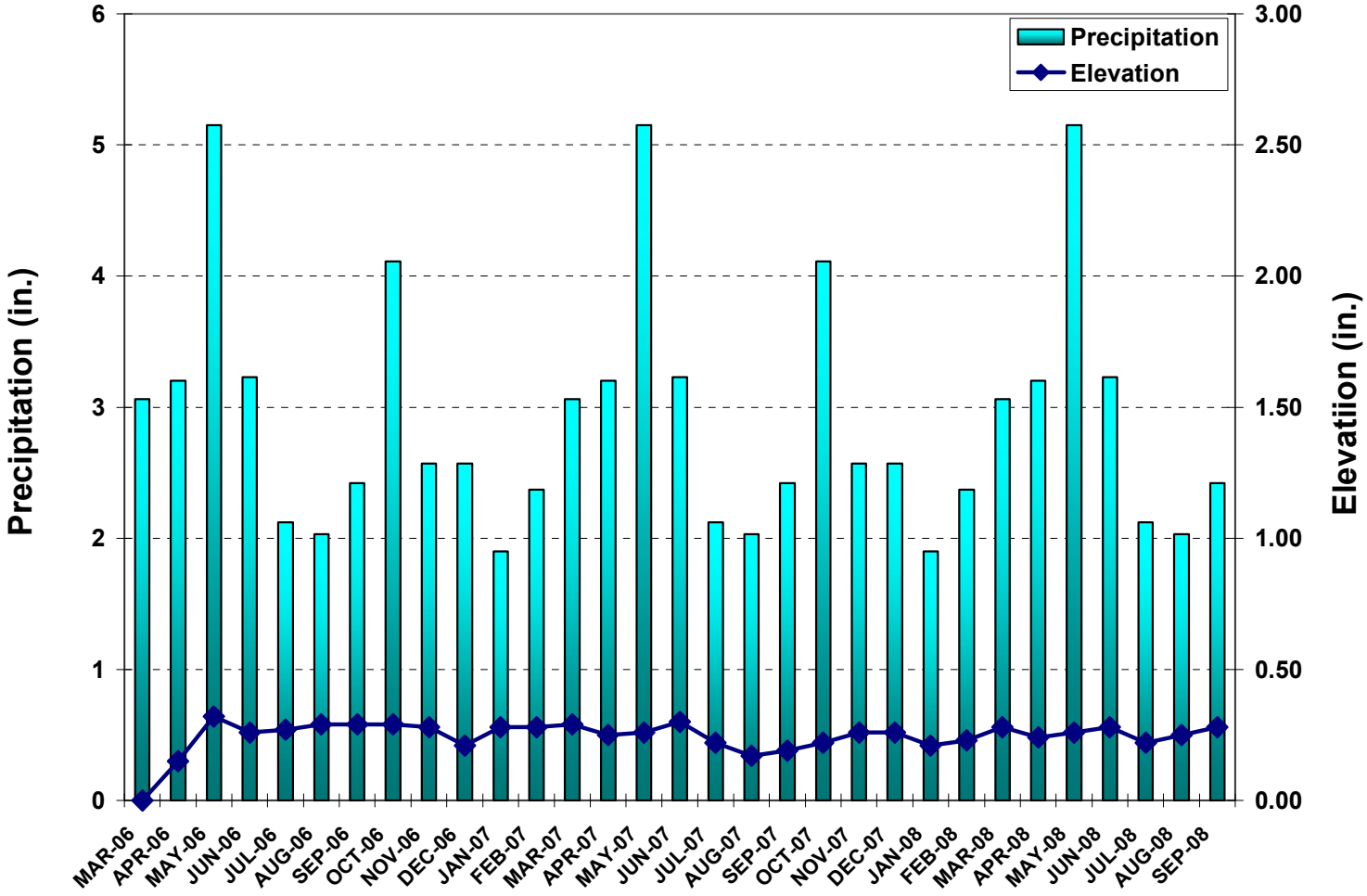

Figure 6.28 Plots of Pavement Elevation Changes and Monthly Rainfall Data (www.ncdc.noaa.gov) at International Parkway for 30 Months.

It is noticeable that, in the early monitoring period (from March 2006 to May 2006), precipitation variations were more than 2 in. (Figure 6.28) which is considered to be high moisture content changes that could cause expansive subgrade soils to undergo swell and volume change movement in a short period of time. Accordingly, a differential elevation of 0.35 in. had been observed. However, this heave is considered to be low (< 0.5 in.) and it can be noted, from the elevation profile observed in a later monitoring period from May 2006 to September 2008, that the volume change movements in the test section diminished when compared to its initial high heaving pattern. From the Figure 6.28, it can be observed that heaving is attributed to the seasonal precipitation variations that the test sections experienced during the monitoring period.

Figures 6.29 shows the DCP test results for the tests conducted in March 2006 (after 7 days curing), March 2007 (12 months after the construction) and September 2008 (30 months after the construction). The DPI values were taken at a slope between 10 cm and 15 cm of DCP data between those two depths. Table 6.2 summarizes the DPI values determined from the DCP tests conducted at International Parkway.

Table 6.2 Summary of DPI Values obtained From International Parkway after 7 days 12 months and 30 months of construction.

Curing Period	**DPI (cm/blow)**
After 7 days	0.182
After 12 months	0.127
After 30 months	0.127

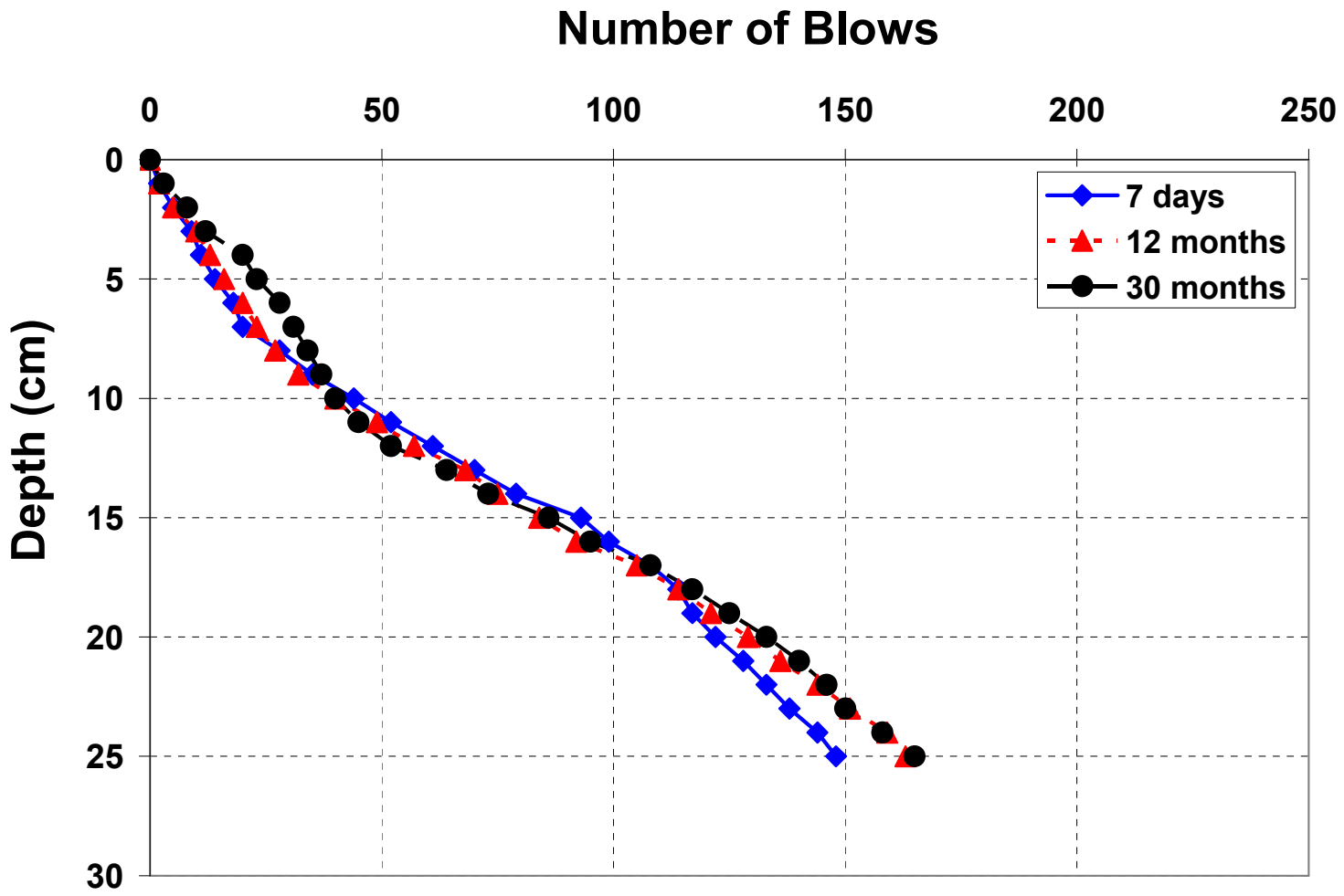

Figure 6.29 DCP Results for International Parkway at 7days, 12 months, and 30 months.

It can be observed from Figure 6.29 that there is no considerable deterioration seen in DCP values in the treated layers over the last 30 months, which indicates that the stabilization still remain effective. These three tests were conducted along the test section at random locations and the near closeness of the DCP data at different depths indicates a uniform treatment of lime-cement additives with the native local soil.

Visual inspections of test sections were included in a field monitoring program. The visual inspections were conducted on a monthly basis. The intent of these inspections is to identify any heave related distresses in pavement test sections. Photographs of recent visual inspection conducted on September 2008 were presented in Figures 6.30 to 6.33. It can be noted from Figure 6.33 that there are some small hairline cracks observed in this test section. This might be due to heavy traffic loadings from Lorries as this section is located at near commercial area. However, all photos indicate that there is no major pavement distress both in the forms of longitudinal or transverse cracks observed in this test section. This demonstrates that, from the present field performance assessments, the present stabilized subgrade sections provided uniform support for concrete pavements.

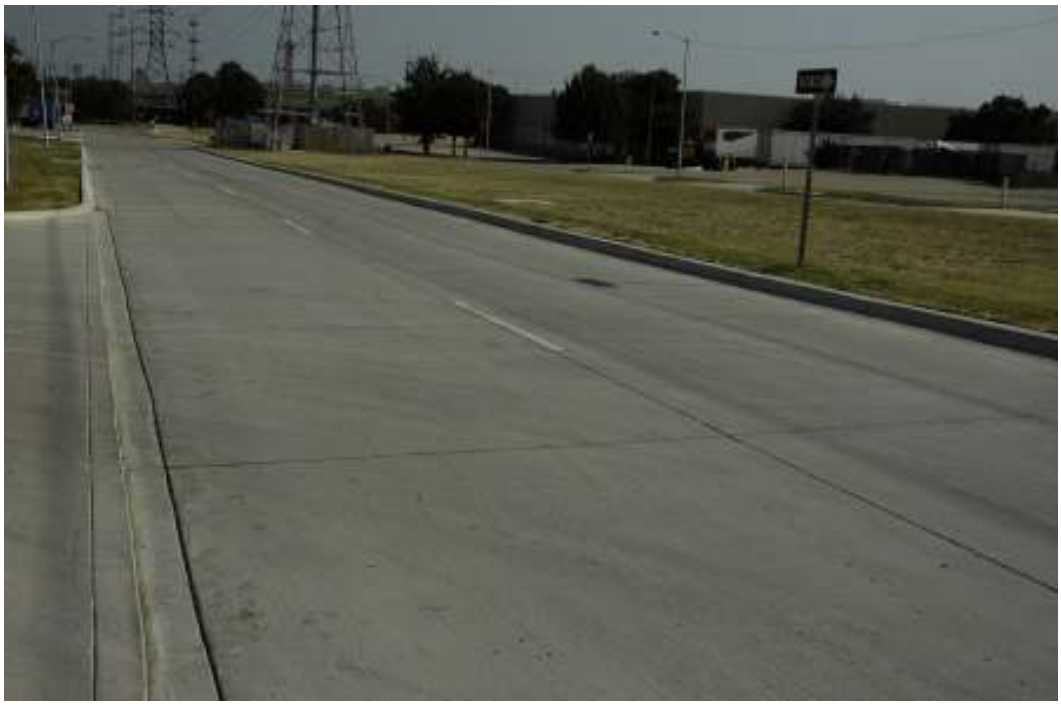

Figure 6.30 Current Condition of Pavement at International Parkway (30 Months after Reconstruction).

Figure 6.31 Current Condition of Pavement at International Parkway (Continue).

Figure 6.32 Heavy Traffic Load at International Parkway.

Figure 6.33 Hair Line Crack Observed at International Parkway.

6.3.2 Southmoor Drive

Southmoor Drive was reconstructed in March 2006. The reconstruction was carried out by paving a new concrete layer over a combined lime and cement stabilized subgrade section. Prior to the pavement reconstruction, this road was constructed with an asphalt concrete over a non-stabilized subgrade. The road was subjected to severe longitudinal and transverse cracking, and vertical movements due to the expansion of subgrade soils. The pavement ride quality was noticeably improved after the reconstruction.

Field monitoring was carried out on a monthly basis. The field monitoring includes elevation surveys and visual inspections. The monitoring was started from March 2006 and was continued over 30 months until September 2008. Results of the elevation surveys are shown in Figure 6.34 along with monthly average precipitation in order to demonstrate pavement elevation changes due to moisture fluctuations.

The monthly average precipitation of Southmoor Drive is the same as International Parkway as this road is also located at Arlington area. From figure 6.34, the maximum monthly average precipitation is observed in the month of May (late spring) and the minimum monthly average precipitation is in the month of August (summer). The maximum and minimum precipitation values from the monitoring period of March 2006 to September 2008 are varying from 2-5 in.

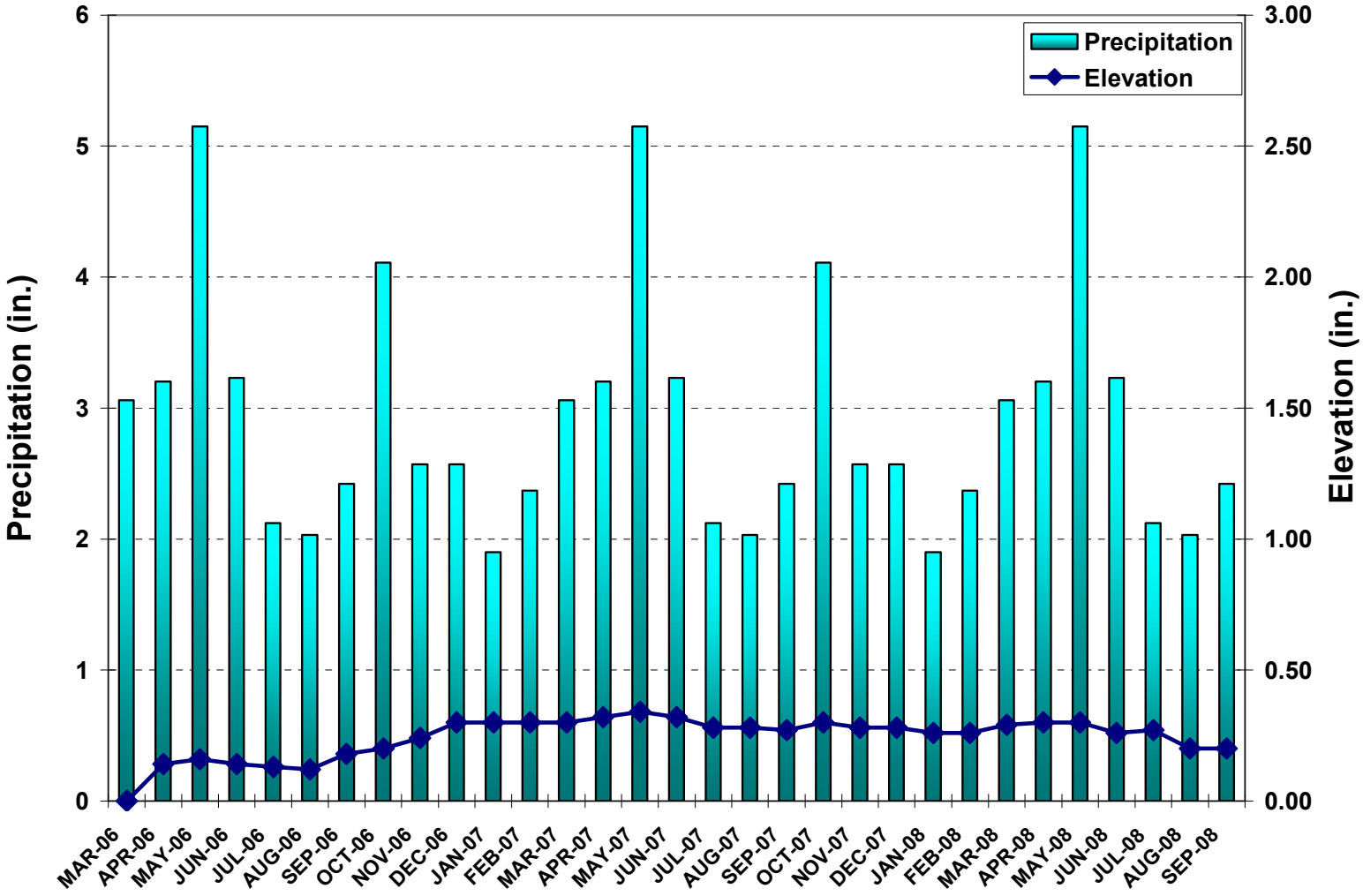

Figure 6.34 Plots of Pavement Elevation Changes and Monthly Rainfall Data (www.ncdc.noaa.gov) at Southmoor Drive for 30 Months.

From figure 6.34, differential elevations of about 0.20 in. had been observed in the early monitoring periods and about a maximum of 0.35 in. was observed in the later periods. However, these heaves are considered low (< 0.5 in.) and it can be noted, from the elevation profile observed in a later monitoring period (from December 2006 to September 2008), that the heaves in the test section diminished when compared to its initial high heaving pattern. Figure 6.34 also shows the same trend as Figure 6.28 (International Parkway) that elevation fluctuations are attributed to the seasonal precipitation variations that the test sections experienced during the monitoring period.

Figures 6.35 shows the DCP test results for the tests conducted in March 2006 (after 7 days curing), March 2007 (12 months after the construction) and September 2008 (30 months after the construction). The DPI values were taken between 10 cm and 15 cm of penetration at the slopes of DCP data between those two depths. Table 6.3 summarizes the DPI values determined from the DCP tests conducted at Southmoor Drive.

Table 6.3 Summary of DPI Values obtained From Southmoor Drive after 7 days 12 months and 30 months of construction

Curing Period	**DPI (cm/blow)**
After 7 days	0.089
After 12 months	0.107
After 30 months	0.129

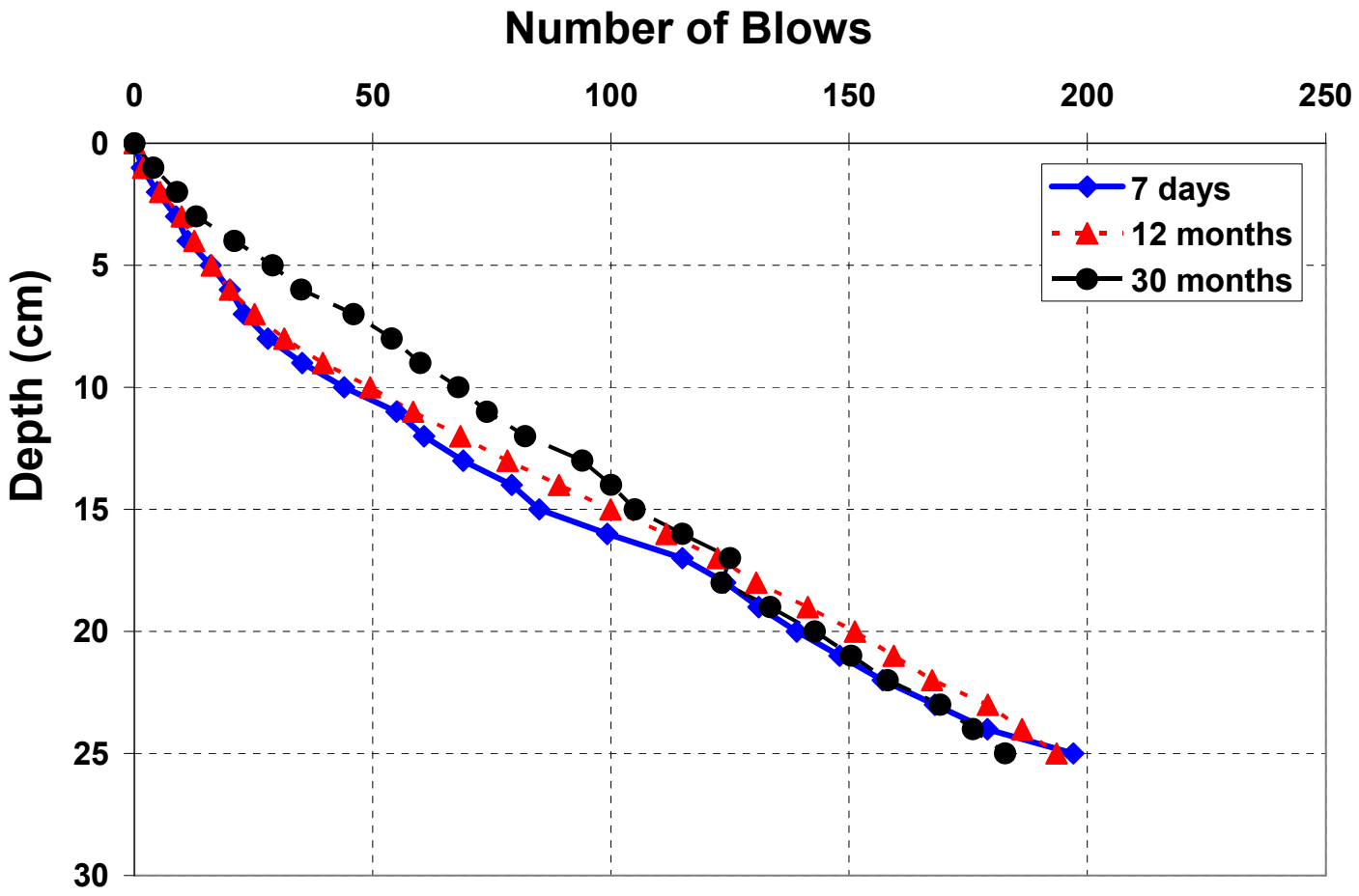

Figure 6.35 DCP Results for Southmoor Drive at 7days, 12 months, and 30 months.

It can be observed from Figure 6.35 that there is no considerable deterioration seen in DCP values in any of the treated layers over the last 30 months, which indicates that the stabilization still remain effective.

At Southmoor Drive, the visual inspections were conducted on the monthly basis. Photographs of recent visual inspection conducted on September 2008 were presented in Figures 6.36 to 6.39. It can be noted from Figure 6.38 and Figure 6.39 that there are some small hairline cracks observed on the paved area and at near the manhole of Southmoor Drive. However, no major rutting, ponding or other forms of permanent deformation as well as swell and shrink related surface movements were observed.

Figure 6.36 to Figure 6.39 also indicate that there is no major pavement distress both in the forms of longitudinal or transverse cracks observed in this test section. Therefore, it can be said that the present stabilized subgrade sections provided uniform support for concrete pavements. However, the monitoring time period is not long enough to make comprehensive assessments.

Figure 6.36 Current Condition of Southmoor Drive.

Figure 6.37 Current Condition of Southmoor Drive (Continue).

Figure 6.38 A Hairline Crack Observed on the Paved Area of Southmoor Drive.

Figure 6.39 A Hairline Crack Observed at Near The Manhole, Southmoor Drive.

6.3.3 Southeast Parkway

Southeast Parkway was reconstructed in November 2007. The subgrade layer was stabilized with combined lime and cement treatment. The old asphalt layer was replaced with a new concrete layer laid over the stabilized subgrade soils. Prior to the pavement reconstruction, this street was constructed by asphalt concrete pavement over a non-stabilized subgrade. Severe longitudinal and transverse cracks and vertical movements were observed at the first visit. The condition of the pavement after the reconstruction was observed to be noticeably improved.

From figure 6.40, heaving is observed in a magnitude of about 0.10 - 0.30 in. had been observed through out monitoring periods. However, these heaves are considered low (< 0.5 in.). It can be noted, from the elevation profile observed in a later monitoring period (from May 2008 to September 2008), that the heaves in the later monitoring period diminished when compared to its initial high heaving pattern. From the plots, it can be observed that fluctuations in the elevation are attributed to the seasonal precipitation variations that the test sections experienced during the monitoring period.

Figures 6.41 shows the DCP test results for the tests conducted in November 2007 (after 7 days curing) and September 2008 (10 months after the construction). The DPI values were taken between 10 cm and 15 cm of penetration as the slopes of DCP data between those two depths. Table 6.4 summarizes the DPI values determined from the DCP tests conducted at Southeast Parkway.

Table 6.4 Summary of DPI Values obtained From Southeast Parkway after 7 days and 10 months of construction

Curing Period	DPI (cm/blow)
After 7 days	0.116
After 10 months	0.112
After 30 months	n/a

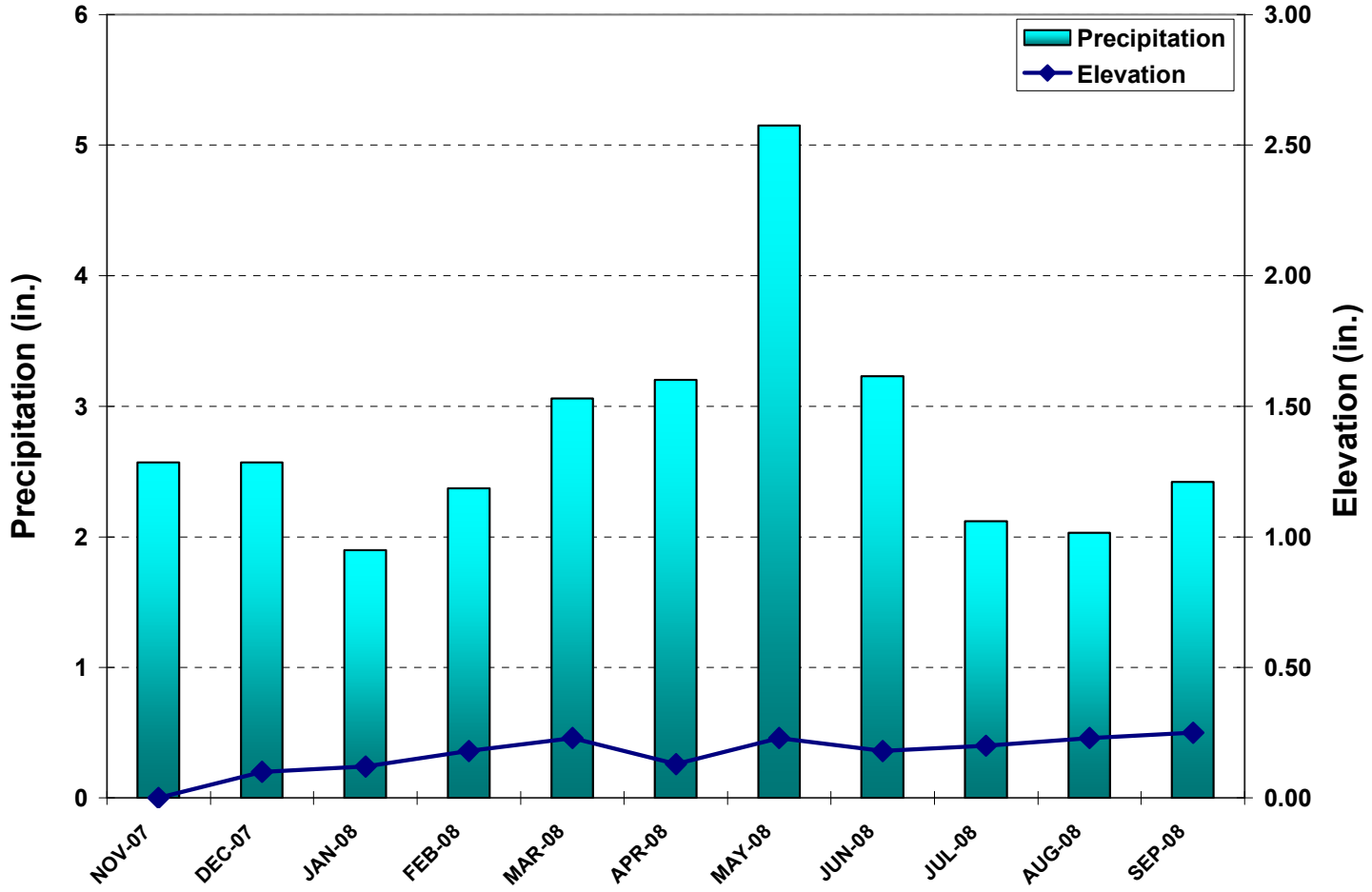

Figure 6.40 Plots of Pavement Elevation Changes and Monthly Rainfall Data (www.ncdc.noaa.gov) at Southeast Parkway for 10 Months.

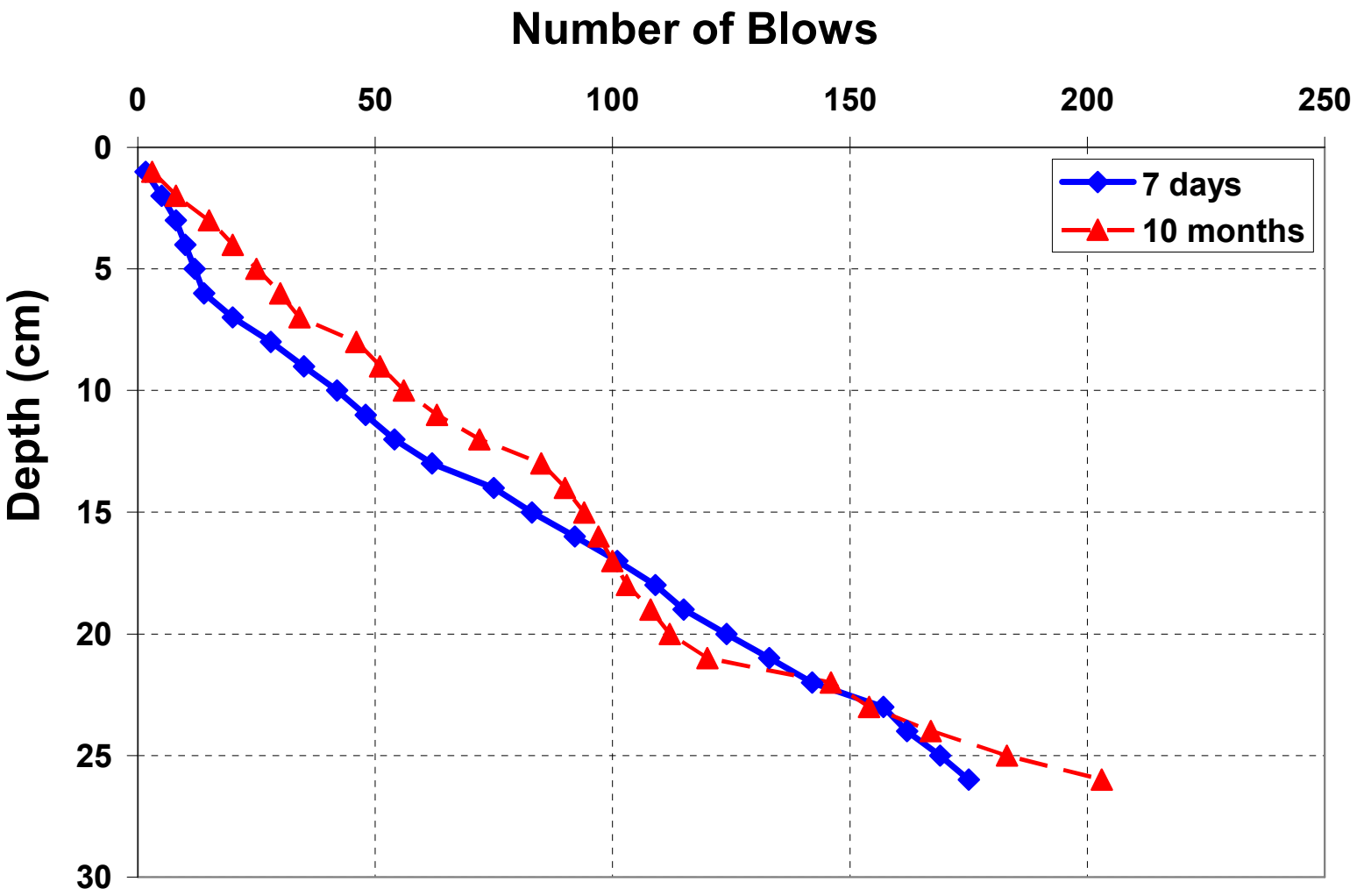

Figure 6.41 DCP Results for Southeast Parkway at 7days and 10 months after the construction.

It can be observed from Figure 6.41 that there is no considerable deterioration seen in DCP values in any of the treated layers over the last 10 months, which indicates that the stabilization still remain effective.

At Southeast Parkway, visual inspections were also included in field monitoring programs. The visual inspections were conducted on a monthly basis. Photographs of recent visual inspection conducted on September 2008 are presented in Figures 6.42 to 6.45. It can be seen from the figures that no major rutting, ponding or other forms of permanent deformation as well as swell and shrink related surface movements were observed on Southeast Parkway over the last ten months of its operation.

Figure 6.42 Current Condition of Southmoor Drive.

Figure 6.43 Current Condition of Southmoor Drive (Continue).

Figure 6.44 Current Condition of Southmoor Drive (Continue).

Figure 6.45 Current Condition of Southmoor Drive (Continue).

Figure 6.42 through Figure 6.45 also indicated that there is no major pavement distress both in the forms of longitudinal or transverse cracks observed in this test section. Therefore, it can be said that the combined treatments used in the field treatment appear to provide stable and uniform support to the pavement infrastructure.

Table 6.5 Summary of DPI Values obtained after 28 days 26 months and 37 months of construction

Stabilizer	DPI (cm/blow)		
	After 28 days curing	After 26 months	After 37 months
Type V Cement	0.063	0.066	0.079
Cement and Fly Ash	0.080	0.078	0.083
GGBFS	0.090	0.101	0.143
Lime and Fibers	0.330	0.263	0.417
Lime	1.000	1.110	1.000

Table 6.6 Summary of DPI Values obtained From Three Test Sites at Different Periods after the Construction

Locations	DPI (cm/blow)		
	After 7 days curing	After 12 months	After 30 months
International Parkway	0.182	0.127	0.127
Southmoor Drive	0.089	0.107	0.129
Southeast Parkway	0.116	0.112*	n/a

* After a curing period of 10 month

Table 6.7 UCS versus DPI for Sulfate Soils (after 7days)

Stabilizers	UCS psi (kPa)	DPI (cm/blow)
Type V Cement (8%)	50.90 (351.00)	0.263
Type V Cement (5%) and Class F Flyash (15%)	225.80 (1557.00)	0.063
GGBFS (20%)	154.00 (1067.00)	0.080
Lime (8%) and Polypropylene fibers (0.15%)	108.80 (750.00)	0.090

Table 6.8 UCS versus DPI for Sulfate Soils (after 7days)

Specimens	UCS psi (kPa)	DPI (cm/blow)
International Parkway	250.90 (1729.89)	0.182
Southmoor Drive	256.93 (1834.03)	0.089
Southeast Parkway	499.24 (3442.14)	0.116

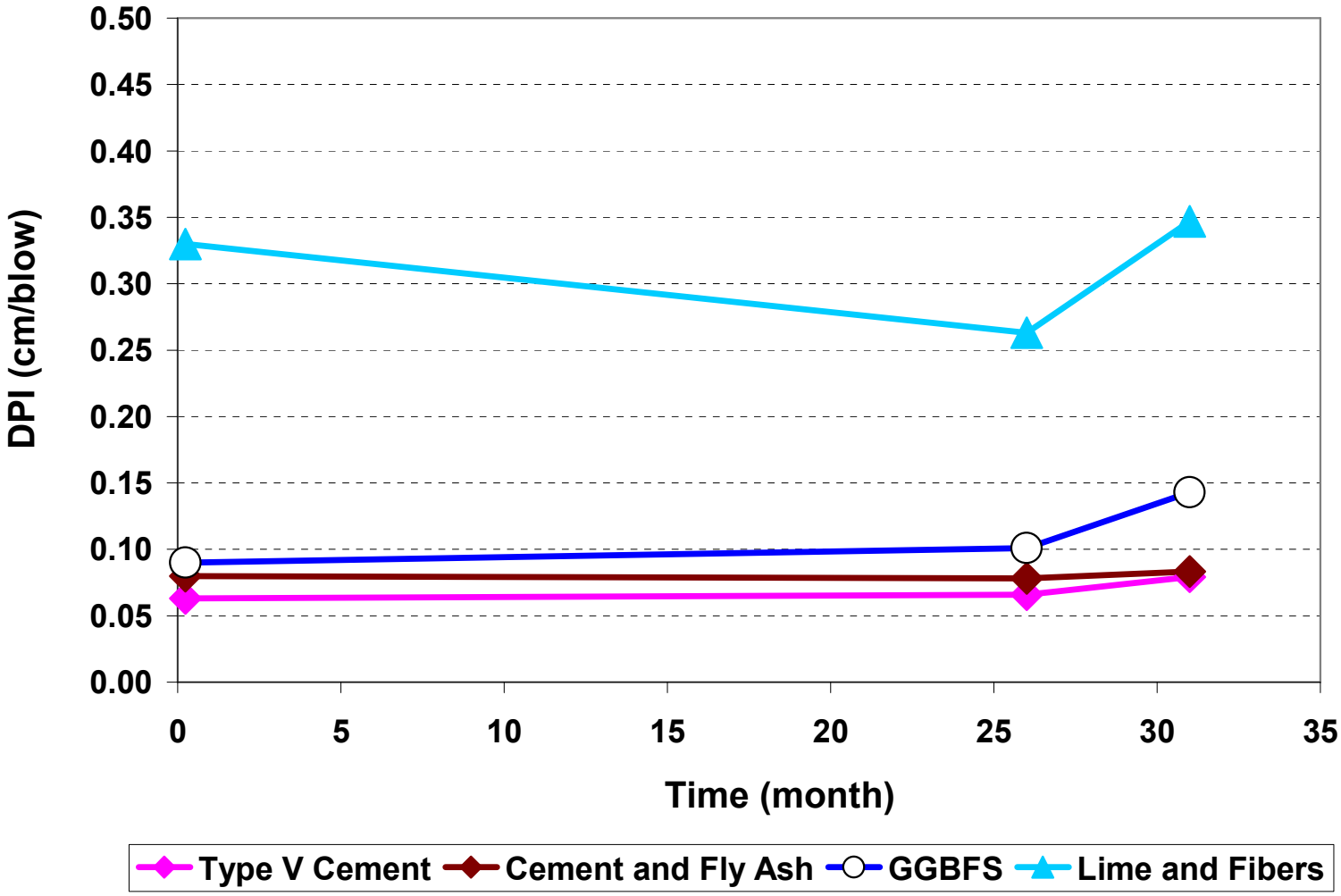

Figure 6.46 DPI versus Time on Sulfate Soil Specimens from Harwood Road.

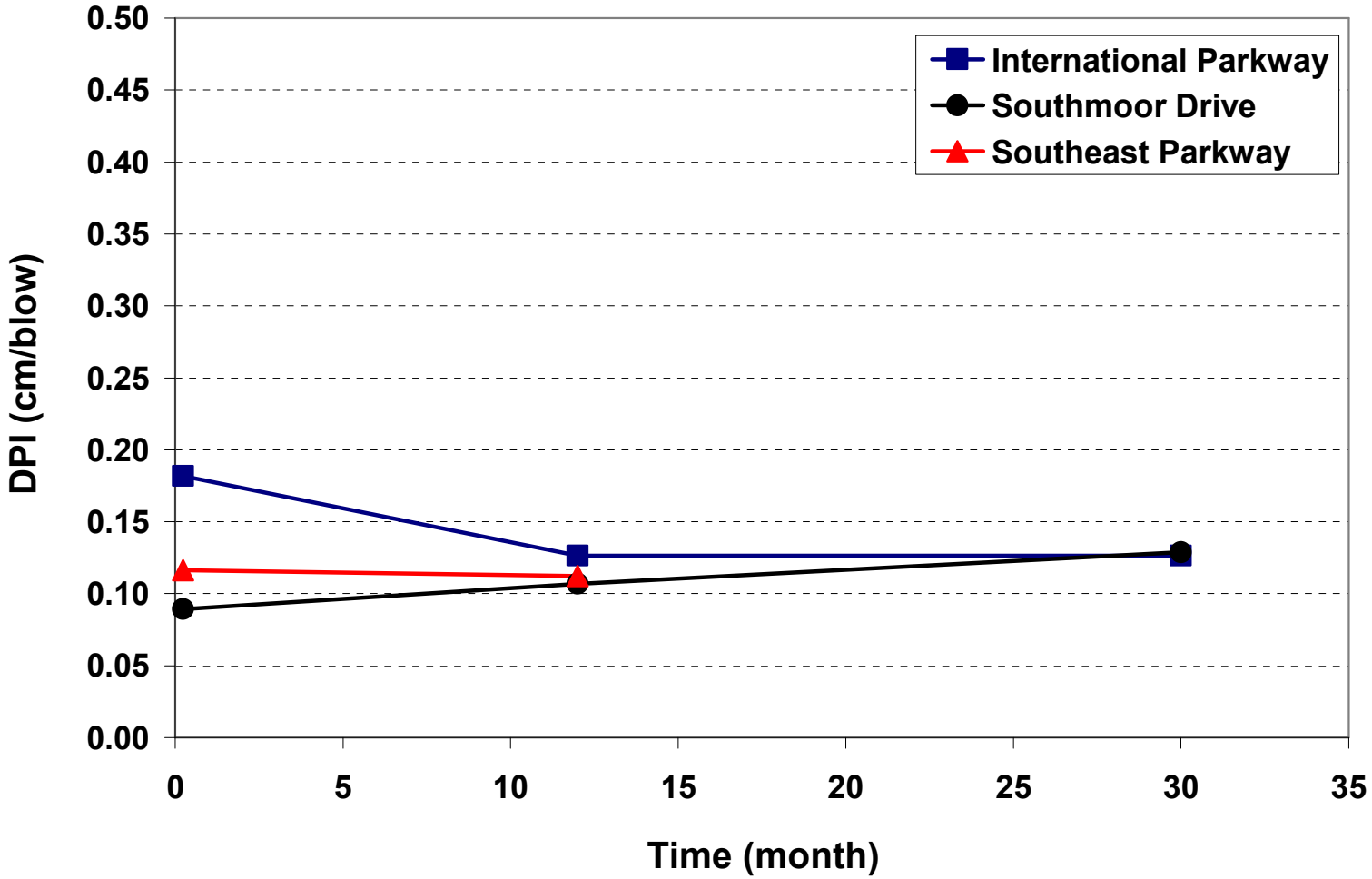

Figure 6.47 DPI versus Time on Non-sulfate Soil Specimens from 3 Test Sites.

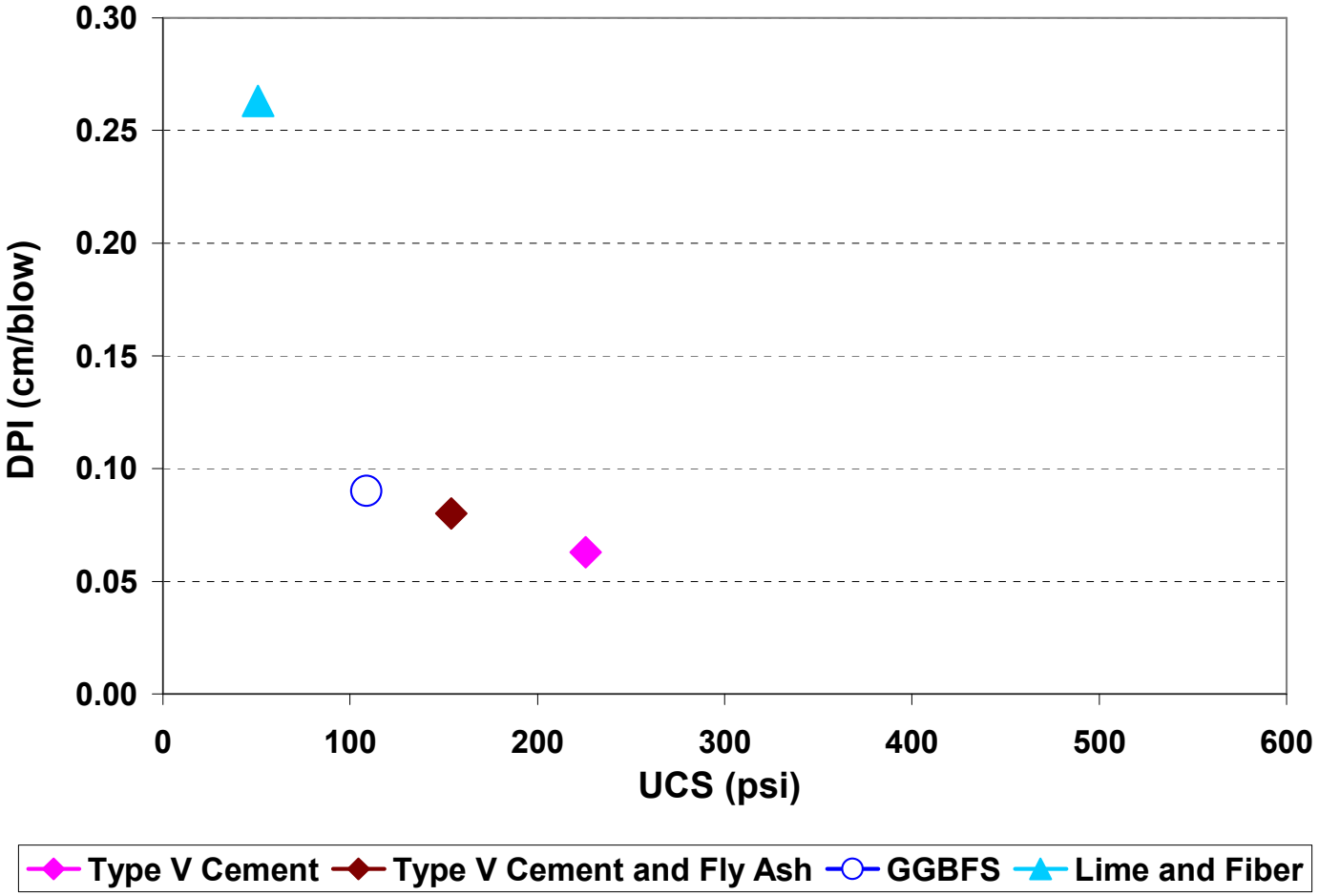

Figure 6.48 DPI versus UCS on Sulfate Soil Specimens from Harwood Road.

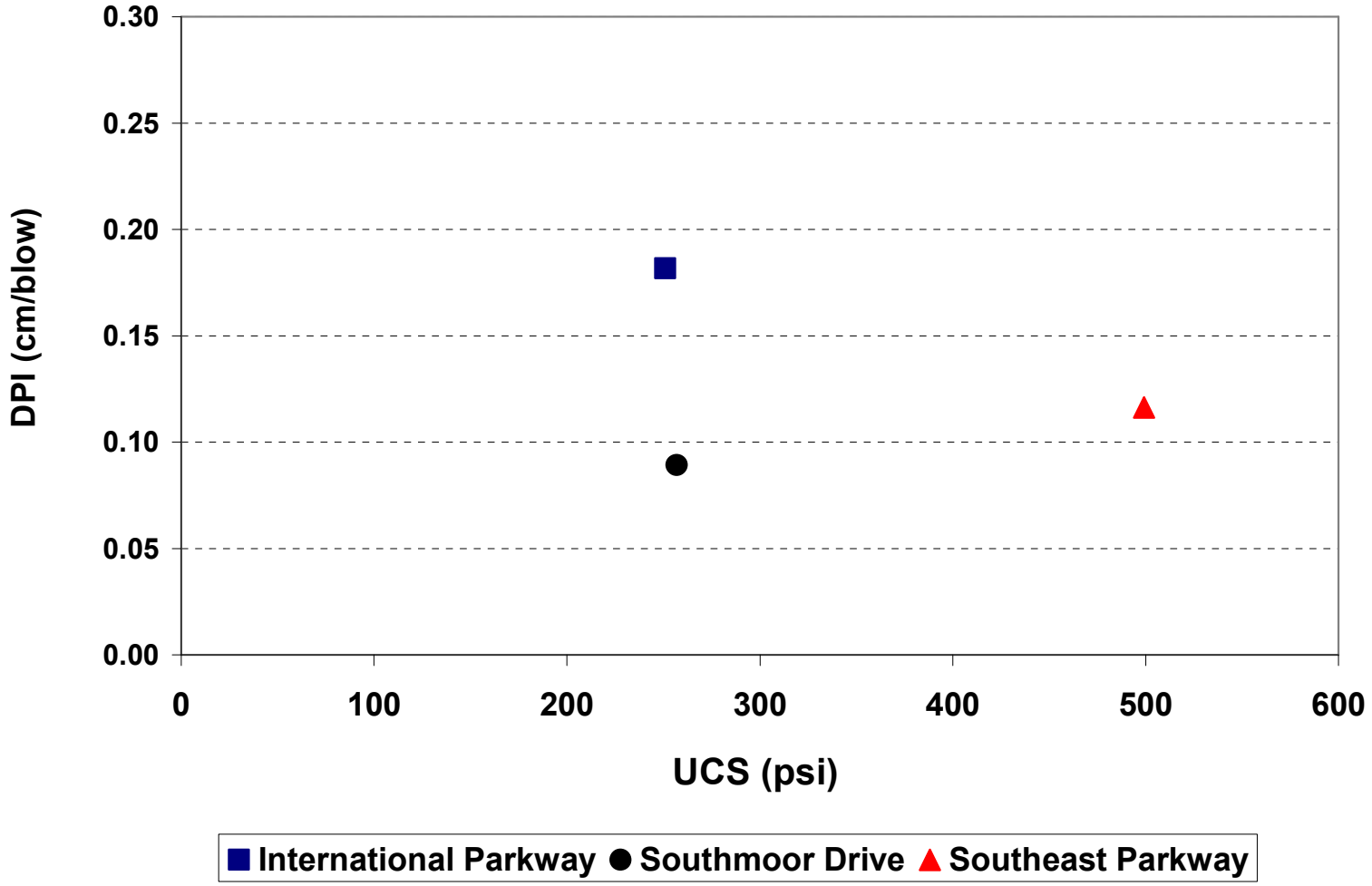

Figure 6.49 DPI versus UCS on Non-sulfate Soil Specimens from 3 Test Sites.

Summaries of DPI value for sulfate and non-sulfate soils at different curing time after the construction are shown in Table 6.5 and Table 6.6. Figure 6.46 and 6.47 present the DPI value versus time on both sulfate soils and non-sulfate soils specimens. It can be observed from the figure that the DPI values for every stabilization method are consistent after the first tests (at 7 days after the construction) in spring. The DPI values are ranging from 0.06 to 0.20. Except for lime with polypropylene fibers, the DPI values are in the magnitude of 0.26 to 0.35 which are considered higher. This is due to the fact that lime stabilization does not provide substantial strength improvement to the soils. Overall, the DPI values for every treatment method, except for lime with fibers, are considered consistent even at after 30 months period. This means that the strength improvement ability of the stabilizers still remain effective after long operational period. The acceptable value for DPI is in the range of 0.06 to 0.20.

The UCS strength and corresponding DPI numbers for sulfate soils and non-sulfate soils are shown in Table 6.7 and Table 6.8 respectively. The UCS results are also plotted against DPI value in Figure 6.48 and Figure 6.49, respectively. For sulfate soils, it can be observed from Figure 6.7 that GGBFS, Type V Cement with Fly Ash and Type V Cement demonstrated higher UCS properties (more than 108.80 psi, 750.00 kPa) compared to Lime with Fibers (50.90 psi ,351.00 kPa) The higher strength properties were attributed to the cementitious reactions from the stabilization process. For non-sulfate soils, combined lime and cement stabilizations provide high UCS properties in the magnitude of more than 250 psi (1723.69 kPa). Overall, it can be concluded that GGBFS, Type V Cement with Fly Ash, Type V Cement and combined lime and cement have yielded a noticeable strength enhancement to the treated specimens with the magnitude of more than 100 psi (689.47 kPa).

The next section describes a life cycle cost analysis of various stabilization methods used for both sulfate and non-sulfate soils.

6.4 Life Cycle Cost Analysis (LCCA)

Life Cycle Cost Analysis (LCCA) is an engineering economic analysis tool which is useful in terms of comparing the relative merits of competing project implementation alternatives. By considering all of the costs of agency and user-incurred cost during the service life of an asset, this analytical process helps transportation officials to select the lowest cost option. Life-cycle cost analysis requires several cost components including, the initial costs such as construction costs and material costs, annual maintenance costs, the designed rehabilitation costs (i.e., resurfacing at the tenth and twentieth years of a pavement with a design life of 35 years), and the user costs. All these costs in the life cycle cost process can be divided into two major categories: construction costs and user costs.

Construction costs are estimated from historical bids provided by the City of Arlington. These documents include production rates, labor and equipment costs, and material costs. A scanned copy of these bids can be seen in Figure 6.50 and Figure 6.51 for Harwood Road and for International Parkway, Southmoor Drive and Southeast Parkway, respectively. All these documents were used to estimate the unit price. The historical bid approach derives the unit price by the weighted average of bids submitted by contractors prior to the period of construction.

				CONTRACT AWARDED TO Jackson Construction	
ITEM No.	BID QUANTITY	ITEM DESCRIRTION	MEA	UNIT PRICE	TOTAL COST
		PAVING & DRAINAGE IMPROVEMENTS			
106	103000	Stabilization with Lime	SY	$ 2.00	$206,000.00
107	2340	Lime for Stabilization	TN	$ 102.00	$238,680.00
108	104,350	Add Moisture to Subgrade	SY	$ 0.15	$ 15,652.50
109	1333	Subgr Stabilization 11-32D (poly fibers)	SY	$ 5.00	$ 6,665.00
110	2,615.35	Polypropylene Fibers	LB	$ 2.00	$ 5,230.70
111	1,333	Subgrade Stabilization (cement) 11-32E	SY	$ 5.00	$ 6,665.00
112	57	Cement for stabilization	TN	$ 140.00	$ 7,932.40
113	1,333	Subgr Stabilization 11-32F (ground granulated slag)	SY	$ 6.00	$ 7,998.00
114	87.18	Ground granulated blast fumace slag for stabilization	TN	$ 153.00	$ 13,338.54
115	1333	Subgr Stabilization 11-32G (fly ash)	SY	$ 6.00	$ 7,998.00
116	65.38	Fly Ash for stabilization	TN	$ 34.00	$ 2,222.92
					$518,383.06

Figure 6.50 Scanned copy of the bid for Sulfate Rich Harwood Road: Stabilizers and Their Costs.

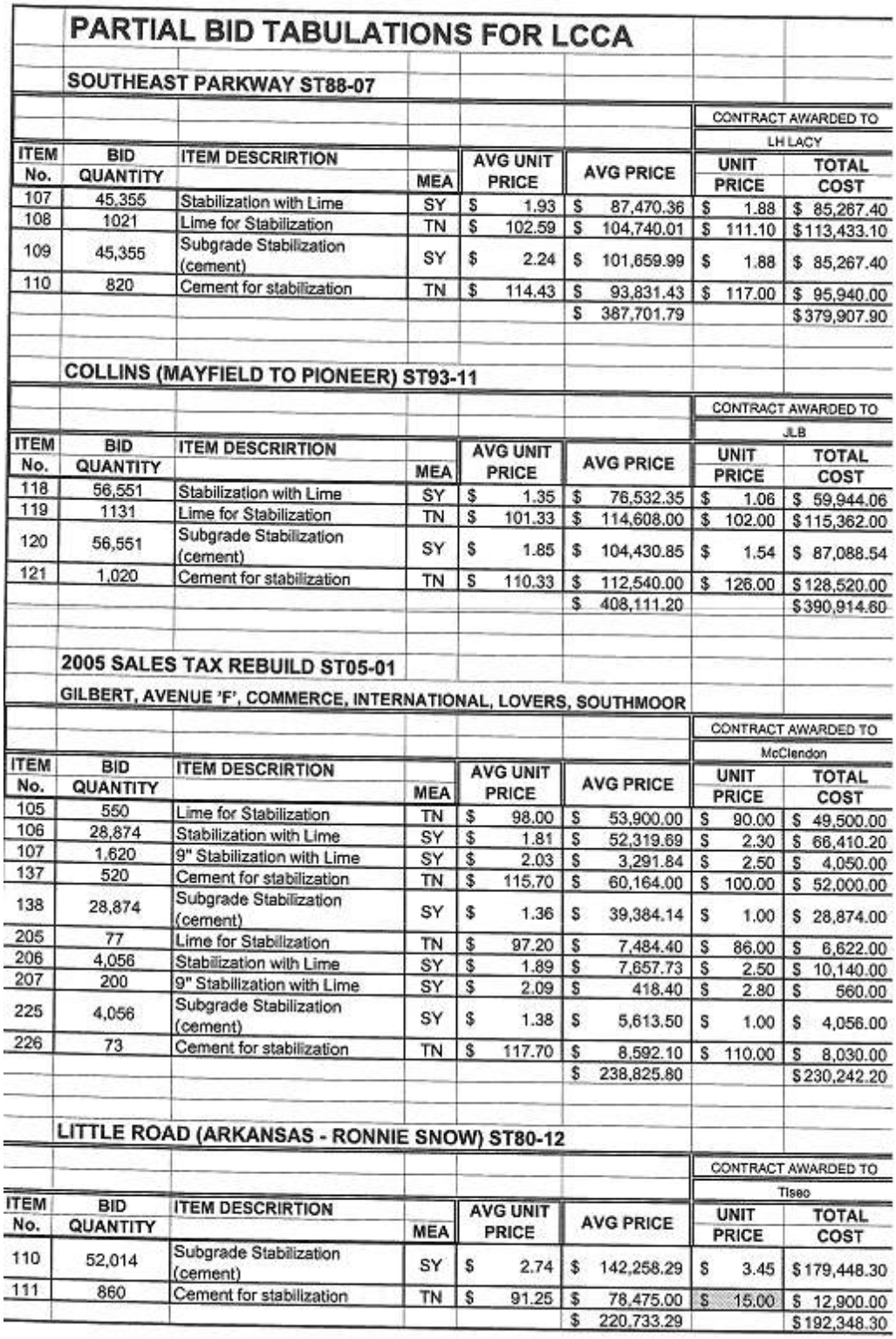

PARTIAL BID TABULATIONS FOR LCCA

SOUTHEAST PARKWAY ST88-07

CONTRACT AWARDED TO: LH LACY

ITEM No.	BID QUANTITY	ITEM DESCRIRTION	MEA	AVG UNIT PRICE	AVG PRICE	UNIT PRICE	TOTAL COST
107	45,355	Stabilization with Lime	SY	$ 1.93	$ 87,470.36	$ 1.88	$ 85,267.40
108	1021	Lime for Stabilization	TN	$ 102.59	$ 104,740.01	$ 111.10	$ 113,433.10
109	45,355	Subgrade Stabilization (cement)	SY	$ 2.24	$ 101,659.99	$ 1.88	$ 85,267.40
110	820	Cement for stabilization	TN	$ 114.43	$ 93,831.43	$ 117.00	$ 95,940.00
					$ 387,701.79		$ 379,907.90

COLLINS (MAYFIELD TO PIONEER) ST93-11

CONTRACT AWARDED TO: JLB

ITEM No.	BID QUANTITY	ITEM DESCRIRTION	MEA	AVG UNIT PRICE	AVG PRICE	UNIT PRICE	TOTAL COST
118	56,551	Stabilization with Lime	SY	$ 1.35	$ 76,532.35	$ 1.06	$ 59,944.06
119	1131	Lime for Stabilization	TN	$ 101.33	$ 114,608.00	$ 102.00	$ 115,362.00
120	56,551	Subgrade Stabilization (cement)	SY	$ 1.85	$ 104,430.85	$ 1.54	$ 87,088.54
121	1,020	Cement for stabilization	TN	$ 110.33	$ 112,540.00	$ 126.00	$ 128,520.00
					$ 408,111.20		$ 390,914.60

2005 SALES TAX REBUILD ST05-01

GILBERT, AVENUE 'F', COMMERCE, INTERNATIONAL, LOVERS, SOUTHMOOR

CONTRACT AWARDED TO: McClendon

ITEM No.	BID QUANTITY	ITEM DESCRIRTION	MEA	AVG UNIT PRICE	AVG PRICE	UNIT PRICE	TOTAL COST
105	550	Lime for Stabilization	TN	$ 98.00	$ 53,900.00	$ 90.00	$ 49,500.00
106	28,874	Stabilization with Lime	SY	$ 1.81	$ 52,319.69	$ 2.30	$ 66,410.20
107	1,620	9" Stabilization with Lime	SY	$ 2.03	$ 3,291.84	$ 2.50	$ 4,050.00
137	520	Cement for stabilization	TN	$ 115.70	$ 60,164.00	$ 100.00	$ 52,000.00
138	28,874	Subgrade Stabilization (cement)	SY	$ 1.36	$ 39,384.14	$ 1.00	$ 28,874.00
205	77	Lime for Stabilization	TN	$ 97.20	$ 7,484.40	$ 86.00	$ 6,622.00
206	4,056	Stabilization with Lime	SY	$ 1.89	$ 7,657.73	$ 2.50	$ 10,140.00
207	200	9" Stabilization with Lime	SY	$ 2.09	$ 418.40	$ 2.80	$ 560.00
225	4,056	Subgrade Stabilization (cement)	SY	$ 1.38	$ 5,613.50	$ 1.00	$ 4,056.00
226	73	Cement for stabilization	TN	$ 117.70	$ 8,592.10	$ 110.00	$ 8,030.00
					$ 238,825.80		$ 230,242.20

LITTLE ROAD (ARKANSAS - RONNIE SNOW) ST80-12

CONTRACT AWARDED TO: Tiseo

ITEM No.	BID QUANTITY	ITEM DESCRIRTION	MEA	AVG UNIT PRICE	AVG PRICE	UNIT PRICE	TOTAL COST
110	52,014	Subgrade Stabilization (cement)	SY	$ 2.74	$ 142,258.29	$ 3.45	$ 179,448.30
111	860	Cement for stabilization	TN	$ 91.25	$ 78,475.00	$ 15.00	$ 12,900.00
					$ 220,733.29		$ 192,348.30

Figure 6.51 Scanned copy of the bid for Non-Sulfate International Parkway, Southmoor Drive and Southeast Parkway Subgrades: Cost Details of Stabilizers.

The user costs are directly caused and attributable to the presence of a work zone and the construction activities undertaken by the transportation agency. However, many life cycle cost analysis approaches do not include any consideration for user costs, since historically these costs have been difficult to measure and valuate (William et al. 1999). Furthermore, this project is on the local road which has low traffic volume, hence the user costs are not taken into consideration.

6.4.1 The LCCA Process

The objective of LCCA studies is to compare competing four stabilizers. The LCCA data is input into a decision matrix that was outlined in the 1993 version of the AASHTO Guide for Design of Pavement Structures for a 35-year analysis period (as recommended by FHWA). The LCCA summary report that details the ranking for each alternative based on the following factors:

- Initial construction costs
- Maintenance costs
- Agency cost
- Value of remaining service life beyond the analysis period
- Design life
- Production rate

All these details for the present research are either available or collected from the City furnished information. This data was input into LCCA customized costing spreadsheet to calculate the total initial cost of each alternative. The base values for the cost data from the City of Arlington are loaded into the spreadsheet.

The next step is to establish the preservation and rehabilitation activity timing for each alternative. City of Arlington currently uses a 10-year activity cycle for Portland Cement Concrete (PCC) pavement sections. The life cycle costs associated with preservation and rehabilitation activities and the differential costs incurred by roadway users as they traverse these work zones are calculated. This project implements the present and annualized value of these costs using a discount rate of four percent.

Finally, the LCCA results is input into the custom decision matrix spreadsheet, which assigns weights to each alternative based on its ability to meet the criteria listed above. The project development framework is shown in Figure 6.52.

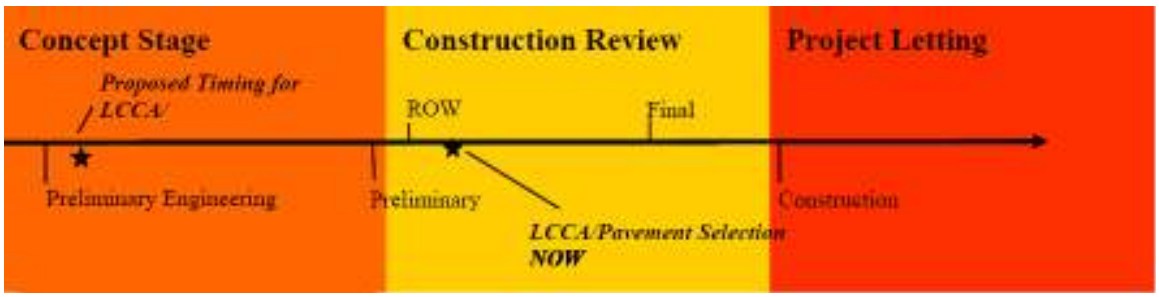

Figure 6.52 Project development frameworks (William et al. 1999).

The life cycle cost analysis for this project was conducted by programming the Microsoft Excel software. This software allows the user to perform a detailed analysis, provided that all the required inputs are available and provided that the user can properly utilize them in the analysis. The software also allows users define the extent of the entire project over which the particular type of maintenance or rehabilitation will be performed.

6.4.2 Pavement Performance Prediction

In the life cycle cost framework, the evaluation of pavement performance is a crucial step. The ability to predict the remaining life or the distress levels of a pavement section provides the useful information for making a plan ahead for maintenance and rehabilitation activities, budget for future expenditures and make decisions based on the timing of rehabilitation activities. With sufficient time to plan, city agencies can minimize their costs as well as minimize the impact of their construction activities on the road users and others affected by a construction.

The effects of maintenance and rehabilitation on the life cycle cost of a highway pavement project can be significant (William et al. 1999). As a low volume road, the effect of work zones on user costs is neglected. The cost of major rehabilitation is the only cost added to life cycle cost analysis (William et al. 1999).

In general, two approaches have been identified for pavement rehabilitation. Those two approaches are termed as 'Proactive' and 'Reactive' maintenance approaches. The basic difference between proactive and reactive maintenance approaches is that when taking a proactive approach to maintenance, the agency performs repairs on potential problem areas before they become greater problems. For reactive approach, an agency will wait until problems become severe before acting to remedy the distress situation. In general, the proactive approach is more cost effective and can preserve pavement performance (William et al. 1999).

Pavement section maintenance is usually undertaken either annually, for minor levels of distresses, or less often when distress levels are higher but ride quality has not dropped to critical levels (William et al. 1999). Minor maintenance activities repair distresses as they occur, and sometimes prolong the life of the pavement, depending on the extent of the repair that is performed. When the distresses exceed the preset limits, maintenance activities are triggered. When one maintenance activity triggers a work zone, the framework simulates the repair of all existing distresses. At this time, the extent of each distress is calculated, and the time required to perform each individual distress repair is determined.

The itemized cost for the construction at Harwood Road is presented in Table 6.9. The life cycle cost analysis for all test sections, including Type V Cement, Cement with Fly ash, GGBFS, Lime with Fibers and Lime (Control) sections, were performed with the available data and assumptions. Table 6.10 and 6.11 present the calculations for material and labor costs. The results are shown in Table 6.12.

Based on the 'net present value' (NPV) calculations, the long-term costs of cement treatment, cement with fly ash treatment and lime treatment sections were close to each other and they have indicated best performance as far as LCCA studies. GGBFS treatment was expensive primarily due to the costs of the material and transportation costs incurred during the construction phase.

Maintenance costs presented in Table 6.12 are only the estimated value as the distress levels at the test sections have not deteriorated to levels that require major maintenance work.

Therefore, these cost details may change in the future which may affect the present LCCA cost calculations.

Table 6.9 Itemized Costs for the Construction at Harwood Road

Descriptions	Magnitude	Units
Construction		
Analysis period	35	years
Concrete Pavement (8"), (Materials + Labors)	$50.41	sqyd
Lime (Materials)	$102.00	TN
Fibers (Materials)	$3.00	lb
Type V Cement (Materials)	$140.00	TN
Class F Fly ash (Materials)	$34.00	TN
GGBFS (Materials)	$153.00	TN
Lime Stabilization (Labors)	$1.00	sqyd
Lime with Fibers (Labors)	$1.20	sqyd
Cement Stabilization (Labors)	$1.00	sqyd
Type V Cement with Fly ash (Labors)	$1.20	sqyd
GGBFS (Labors)	$1.00	sqyd
Routine Maintenance		
Seal @ 5 yrs	$3	sqyd
Resurfacing 2" @10yrs	$10	sqyd
Resurfacing 2" @20yrs	$10	sqyd
Discount Rate (i)	4*	percent

*Discount rates used in LCCA typically range from 3 to 5 percent, representing the prevailing rate of interest on borrowed funds, less inflation. The discount rate of 4% is currently used in Texas

Table 6.10 Calculation for Material Costs for the Construction at Harwood Road

Materials	**% Material by weight**	**Application Rate**		**Area of Application (SY) (Entire roadway (13.33 yd width) will Be Stabilized using these methods)**		**Total Material**	**Unit**	**Unit Cost**		**Cost per section**	**Total cost of material for stabilization**
Polypropylene Fibers	0.15	0.981	LBS/SY	6665	SY	6,538.37	LBS.	$3.00	Bag	$13,076.73	**$30,861.08**
Lime	8.00	52.32	LBS/SY	6665	SY	174.36	TN	$102.00	TN	$17,784.35	
Sulfate Resistant Cement	8.00	52.32	LBS/SY	6665	SY	174.36	TN	$140.00	TN	$24,409.90	**$24,409.90**
GGBFS	20.00	130.8	LBS/SY	6665	SY	435.89	TN	$153.00	TN	$66,691.32	**$66,691.32**
Class F Fly Ash	15.00	98.1	LBS/SY	6665	SY	326.92	TN	$34.00	TN	$11,115.22	
Sulfate Resistant Cement	5.00	32.7	LBS/SY	6665	SY	108.97	TN	$153.00	TN	$16,672.83	**$27,788.05**
											$149,750.35

Table 6.11 Calculation for Labor Cost for the Construction at Harwood Road

Material	Estimated Application Costs (8" Depth)		Application Area		Application Cost
Combined Lime and Polypropylene Fibers	1.20	SY	6665	SY	$7,998.00
Sulfate Resistant Cement	1.00	SY	6665	SY	$6,665.00
GGBFS	1.00	SY	6665	SY	$6,665.00
Combined Class F Fly Ash and Sulfate Resistant Cement	1.20	SY	6665	SY	$7,998.00

Table 6.12 Life Cycle Cost for Construction of Test Sections on Harwood Road

Project Description					
Alternative	**Lime (Control)**	**Type V Cement**	**Type V Cement with Fly ash**	**Lime with Fiber**	**GGBFS**
Application Areas (SY)	6665	6665	6665	6665	6665
Amount of Stabilizers (TN)	174.36	174.36	108.97 (cement) 326.92 (fly ash)	174.36 (lime) 2.965 (fibers)	435.89
Surface Course	8 in.	8 in.	8 in.	8 in.	8 in.
Stabilized Subgrade	8 in.	8 in.	8 in.	8 in.	8 in.
Routine Maintenance					
Seal @ 5 yrs, ($/SY)	3	n/a	n/a	3	n/a
Seal @ 10 yrs, ($/SY)	3	n/a	n/a	n/a	n/a
Resurfacing 2" @10yrs, ($/SY)	10	n/a	n/a	10	n/a
Resurfacing 2" @20yrs, ($/SY)	10	10	10	10	10

Table 6.12 - *Continued*

Construction Cost					
Concrete Pavement (8 in.), ($)	335,983	335,983	335,983	335,983	335,983
Stabilization (Material), $	17,784	24,410	27,788	30,861	66,693
Stabilization (Labor), ($)	6,665	6,665	7,998	7,998	6,665
Total Construction Cost, ($)	360,432	367,058	371,769	374,842	409,340
Maintenance Cost					
Maintenance Cost, ($)	173,290	66,650	66,650	153,295	66,650
Total Cost					
Net Present Value (NPV) @ i =4%	475,484	383,948	388,659	413,689	426,230
width of street (YD)	13.33	13.33	13.33	13.33	13.33
Length of Section (YD)	500	500	500	500	500
Cost per Mile, ($)	**1,423,299**	**1,351,496**	**1,368,079**	**1,456,185**	**1,500,331**

Note: Net Present Value is calculated by: $$\mathbf{NPV = InitialCost + \sum_{k=1}^{N} FutureCost\left[\frac{1}{(1+i)^n}\right]}$$

Where NPV = Net Present Value, Future Cost = Rehabilitation Cost + Maintenance Cost, i = discount rate (%), n = number of year

The LCCA for International Parkway, Southmoor Drive and Southeast parkway were conducted in the same fashion. The analysis period was taken at 35 years based on the recommendations from the 1993 AASHTO Guide. The construction and material costs were taken from the bid costs provided by the Public Works Department, City of Arlington. The maintenance costs were estimated based on the performance of the pavements monitored for the periods of 30 months for International Parkway and Southmoor Drive and 10 months for Southeast Parkway. The Itemized costs for the construction at the three test sites are presented in Table 6.13. The life cycle cost analysis for the test sites were performed with the available data and assumptions made. The calculated results for LCCA are shown in Table 6.10.

Based on the net present value (NPV) calculations, the NPV of combined lime and cement stabilized subgrade sections were close to each other and they have indicated the lowered long-term costs compared to non-stabilized subgrade as seen in the LCCA studies. Although, the costs of stabilization were added up to the initial construction cost in the treated sections, the long-term costs are lowered as a results of lowered maintenance activities required due to bettered performance of the pavements.

Maintenance costs presented in Table 6.14 are only the estimated value based on current condition of pavements observed from the field monitoring in September 2008. Although, there are some minor cracks observed at International Parkway and Southmoor Drive, the distress levels at the test sites are not significant and the major maintenance works are not required. Therefore, these maintenance costs may change in the future and may reflect the actual LCCA cost calculations.

Table 6.13 Itemized Costs for the Constructions at International Parkway, Southmoor Drive and Southeast Parkway

Descriptions	Magnitude	Units
Construction		
Analysis period	35	years
Concrete Pavement (8")	$50.41	sqyd
Lime (Materials)	$102.59	TN
Cement Stabilization (Materials)	$114.43	TN
Lime Stabilization (Labors)	$1.93	sqyd
Cement Stabilization (Labors)	$2.24	sqyd
Routine Maintenance		
Seal @ 5 yrs	$3	sqyd
Resurfacing 2" @10yrs	$10	sqyd
Resurfacing 2" @20yrs	$10	sqyd
Discount Rate (i)	4*	percent

*Discount rates used in LCCA typically range from 3 to 5 percent, representing the prevailing rate of interest on borrowed funds, less inflation. The discount rate of 4% is currently used in Texas

Table 6.14 LCCA for the Stabilized Sections Compared to Non-stabilized Sections

Project Description					
Location	**Untreated**	**International**	**Southmoor**	**Southeast Parkway**	**Lime stabilization**
Application Areas (SY)	28,874	28,874	28,874	45,355	28,874
Amount of Lime (TN)	0	550	550	1,021	755
Amount of Cement (TN)	0	520	520	820	0
Surface (in.)	8	8	8	8	8
Stabilized Subgrade (in.)	8	8	8	8	8
Routine Maintenance					
Seal @ 5 yrs ($/SY)	3	3	n/a	n/a	3
Seal @ 10 yrs ($/SY)	3	3	3	3	3
Resurfacing 2" @10yrs ($/SY)	10	n/a	n/a	n/a	n/a
Resurfacing 2" @20yrs ($/SY)	10	10	10	10	10
Construction Cost					
CONC PVMT (JOINTED-CPCD)(8") ($)	1,455,538	1,455,538	1,455,538	2,286,346	1,455,538
Stabilization (Material), ($)	0	115,928	115,928	198,577	77,492
Stabilization (Labor), ($)	0	2,226	2,226	3,807	1,458
Total Construction Cost, ($)	1,455,538	1,573,693	1,573,693	2,488,730	1,534,489
Maintenance Cost					
Cost ($)	750,724	461,984	375,362	589,615	461,984
Total Cost					
Net Present Value (NPV) @ i=4%	1,962,700.58	1,885,792.58	1,827,273.86	2,887,052.64	1,846,588.40
width of street (YD)	13.33	13.33	13.33	13.33	13.33
Length of Street (YD)	2,166.09	2,166.09	2,166.09	3,402.48	2,166.09
Cost per Mile ($)	**1,594,740.10**	**1,532,250.55**	**1,484,702.73**	**1,493,386.94**	**1,500,396.25**

6.5 Summary

This chapter provides a comprehensive summary of field data analyses, which includes field instrumentation results, elevation surveys, DCP test results, and visual observations collected from routine field monitoring programs for both sulfate-rich soils and non-sulfate soils. Also, a comprehensive life cycle cost analysis data based on the present field data including available maintenance records is given.

For sulfate-rich soils, Type V Cement with Fly ash proved to be the most effective treatment by increased strength and reduced swell and shrinkage potentials. The second most effective treatment was Type V Cement which was followed by GGBFS treatment. Compared to the earlier treatments, Lime-Fiber and Lime (control) treatment methods exhibited moderate and poor performances in enhancing the soil properties, respectively.

From results of elevation surveys, all test sections have shown a trend of moderate surface heaving. Lime (control) section experienced the highest heave related movements among all test sections. However, the volume change movements in lime section diminished with time when compared to its initial high heaving pattern. The next highest heaving was observed in the cement treated section, followed by lime - fiber treated section. On the other hand, both GGBFS and Type V cement - fly ash treated soil sections demonstrated good performance with low heave related movements. Fluctuations in the elevation surveys can be attributed to the seasonal related soil movements that these sections experienced during the monitoring period.

The results of DCP tests indicate that the strength enhancement is rapid in the first two weeks of curing and then they become similar later on. The results indicate that the cement treatment, cement with fly ash and GGBFS treatments exhibited higher strength gains when compared to lime - fibers and lime (control) sections. There is no considerable deterioration seen in DCP values in any of the treated layers over the last three years, which indicates that the stabilization effectiveness still remain same.

Photos taken from the present lime stabilized subgrade section (control) presents a water ponding problem with accumulated water from rainfall. Moreover, cracking and settlements of the pavement are also presented in this section. This indicates that the pavement section built on control section has experienced some distresses, though not in substantial terms that induces major repairs during the current monitoring period.

Based on the LCCA studies, the long-term costs of cement treatment, cement with fly ash treatment and lime treatment sections were close to each other and they have indicated best performance as far as LCCA studies. GGBFS treatment was expensive primarily due to the costs of the material and transportation costs incurred during the construction phase.

Overall, based on the results of field monitoring provided above, Type V Cement with Fly Ash, and Type V Cement have performed well in all aspects. GGBFS and lime-fiber sections provided adequate performance whereas the lime (control) section has demonstrated the poorest performance in the field.

For non-sulfate soils, heaves were observed in the early monitoring period at all 3 test sites. These heaves were attributed to high moisture content changes which cause expansive subgrade soils to undergo swell and volume change movements in a short period of time. However, these heaves are not significant and the volume change movements in the later monitoring periods diminished when compared to their initial high heaving pattern. The plots of monthly average precipitations against the observed elevations show that the heaves are attributed to the seasonal precipitation variations that the test sections experienced during a particular monitoring period.

From the results of DCP tests, the DPI values for lime cement treated soils were lower than the DPI values for untreated soils. This indicates that treated soils have higher strength properties than untreated soils. Moreover, there is no considerable deterioration seen in DCP values in any of the treated layers through out the monitoring period which indicates that the stabilization still remain effective.

Visual inspections of the test sections were conducted in a recent field monitoring program. There are some small hairline cracks presented at International Parkway and Southmoor Drive. However, all photos indicate that there is no major pavement distress both in the forms of longitudinal or transverse cracks or permanent deformation as well as swell and shrink related surface movements observed in this test section. This demonstrates that, from the present field performance assessments, the present stabilized subgrade sections provided uniform support for concrete pavements.

From the LCCA studies, the NPV of combined lime and cement stabilized subgrade sites were close to each other and they have indicated lowered long-term costs compared to non-stabilized subgrade. Although, the stabilization costs were added up to the initial construction cost in the treated sections, these costs are compensated by the cheaper maintenance costs due to bettered performance of pavements.

CHAPTER 7

NUMERICAL MODELING OF PAVEMENT SYSTEMS UNDER TRAFFIC LOADING

Numerical methods including finite differences and finite element methods (FEM) can be utilized to model pavement systems by accounting for the effects of traffic wheel loads on pavements. These simulations are often more realistic than theoretical solutions (Kuo and Huang 2006). The analysis in this chapter is based on simulation of rigid pavement slab as an infinite slab, along with other idealized assumptions. Due to the required computation running time period, a three dimensional (3-D) finite element analysis was not considered in this research (Hammons 1998; Kim and Hjelmstad 2000). Several applications in the areas of pavement engineering have successfully modeled pavement systems by idealizing them with an axi-symmetric two-dimensional ABAQUS® model. Same type of model was used utilizing a static wheel loading as the external loading on the pavement system.

One of the objectives of this numerical study is to investigate the vertical pressure and strains exerted from the top layer (concrete pavement) to the bottom layer, i.e. stabilized subgrade layer during loading conditions. Comparisons with pressure results are in close agreement with the field measurements, though strains are not in total agreement as measured strains represent permanent strains whereas the model results represent total compression strains under traffic loads. Overall, an understanding of the vertical pressures and strains of the pavement layers was helpful in the final evaluation of the performance of stabilized layers with respect to traffic loads. The results obtained from the FEM modeling are presented in this Chapter.

7.1 FEM Modeling Details

In the ABAQUS®, there is no built-in model that can be used to simulate the pavement system under traffic loads. An indirect method was hence used to investigate the effects of stabilized subgrade on the performance of the pavement system. The pavement parameters or variables used in this research are thickness and strength or moduli of the top concrete layer, base course or treated subgrade layer and the moduli of natural subgrade soil. All parameters were acquired from laboratory results that were already presented in Chapter 4. Table 7.1 summarizes the variables that were studied in this research study. Details of the model simulation are presented in the following.

In this research, the simulation of rigid pavements is based on the assumptions that the pavement has an infinite length and the load is static. Therefore, this study did not consider or simulate both longitudinal and transverse joints present in the pavement system. The two-dimensional axi-symmetric finite element model was used to analyze different pavement test sections consisting of various types of concrete layer, base layer and a subgrade layer. These layers are typical for low volume roads which experience less than 2000 vehicles per day (AASHTO, 1993).

The pavement model is composed of a concrete layer of 8 in. thickness, and a base course layer of 8 in. thickness. Different types of base layers considered and these were Type V Cement, Cement with Fly ash, Lime with Fibers, Lime and Cement, GGBFS and Lime (control) treated subgrades. Table 7.2 presents the notations used for the four pavement sections that were analyzed in this study.

Table 7.1 Variables that were used in this research study

Element layers	Material Types	Element Types	Thickness (in.)
Top Layer	Concrete	PCC	8
Middle Layer	Stabilized Subgrade	Six stabilizers	8
Bottom Layer	Natural Subgrade	Expansive soils	120

From the FEM studies, both vertical compressive strain and pressure on the stabilized subgrade or base layer is determined under 18 kip single axle load over a tire contact area of 6 in. Comparisons were made between different pavement sections and subgrade modulus to evaluate the effects of stabilized subgrade layer and other pavement characteristics on the performance of the pavement structure under different treated layers. Resilient modulus data was used as an elastic modulus parameter for material input in the model.

In this study, the FEM model is composed of a mesh section that is 120 in. (10 ft.) in radius and 120 in. (10 ft.) in depth. The 8-noded bi-quadratic was utilized. The depth of the test section was selected such that the maximum induced vertical stress in the subgrade has become minimal (< 1% of the applied tire pressure). The radius was also selected based on a similar criterion in which the vertical and horizontal strains induced due to loading became insignificant in all the layers.

7.1.1 Boundary Conditions and Loading

The axi-symmetric elements were utilized in this finite element study. Basically, the rotation is not allowed at all nodes. Therefore, only two degrees of freedom have to be considered in defining the boundary conditions. The boundary conditions applied to the model are horizontal (x-direction) restraint along the left and the right boundaries and a vertical (y-direction) restraint at the bottom boundary. Hence, except for the top boundary, all the remaining three boundaries were restrained against deformation. Figure 7.1 presents the boundary conditions in the developed model with the wheel loading applied on top of the concrete layer.

The traffic load applied to the pavement system is composed of an idealized vehicle load of 18-kips single axle wheel with a total load on each wheel of 9 kips. Therefore, the calculated wheel contact pressure is 80 psi and this was applied over a circular area of 6 in. in radius. This static load was then applied to the model in the finite element analyses. Dynamic analysis using load versus time relationship was not implemented due to computational time needed.

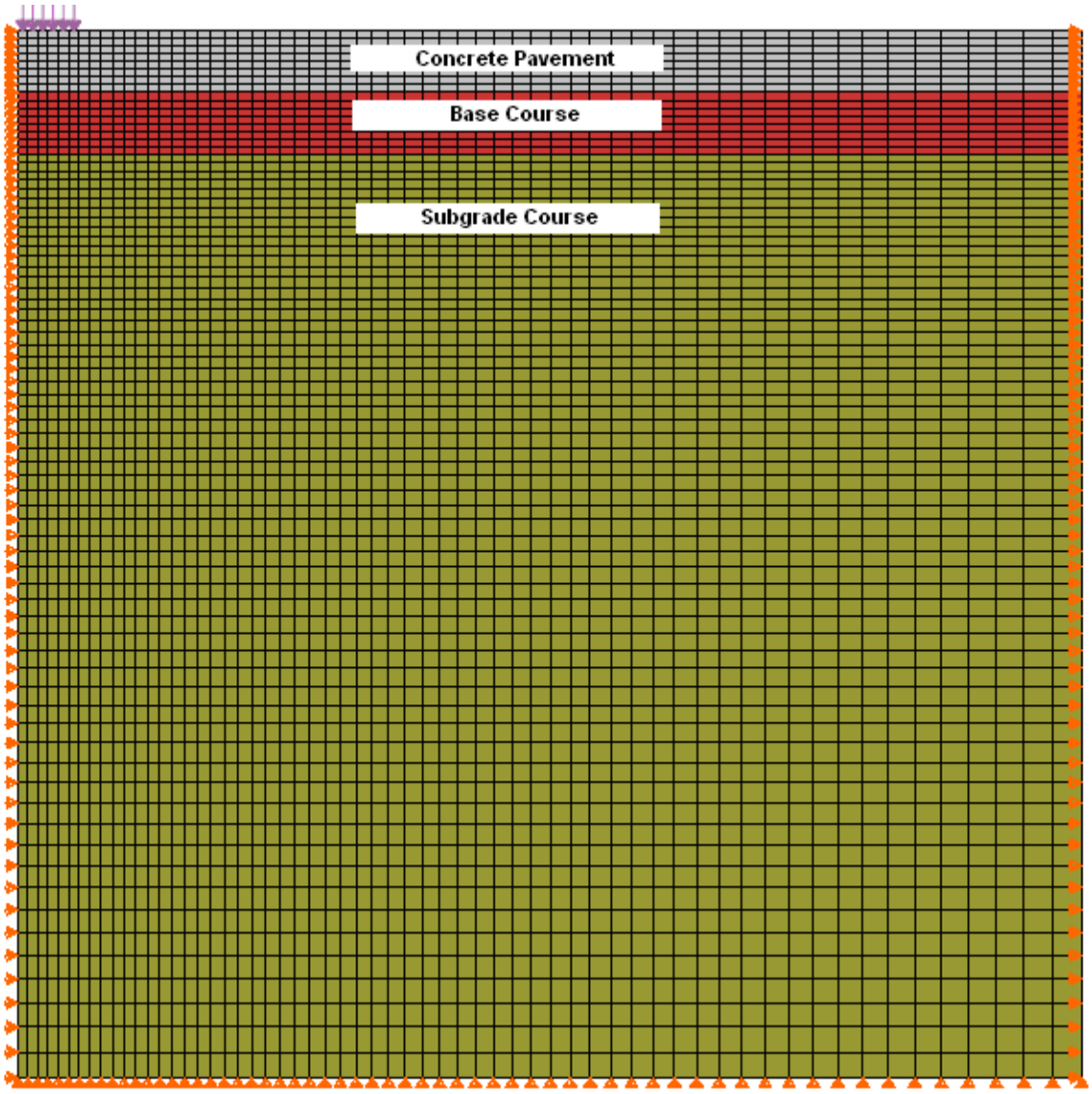

7.1 Boundary Conditions in FEM Model with Static Wheel Loading Applied on Top of Concrete Layer.

7.1.2 Material models

The elastic moduli of materials, including one concrete pavement section, six base course sections and one subgrade section, are presented in Table 7.2. These moduli were input in the model for the analyses. The modulus of elasticity (E) of concrete pavement was taken from the AASHTO 1993 design guideline. The moduli for base (stabilized subgrade) and subgrade were taken from the present experimental results presented in Chapter 4.

For sulfate soils modeling simulations, the elastic moduli were taken from five test sections at Harwood Road in Arlington. These are five different base materials including Type V Cement, Cement with Fly ash, GGBFS, Lime with Fibers and Lime (control).

For non-sulfate soils, the elastic modulus was taken as an average from the results acquired in the laboratory for all three test sites. These are two different base materials which are lime treated and combined lime and cement treated soils.

Table 7.2 Elastic and Plastic Properties of the Materials Used in the Analyses

Soil	**Resilient Modulus, MPa (psi)**			**Poisson's Ratio, μ**
Surface Course				
Portland Cement Concrete	30,000 (4,351,130)			0.3
Base Course (stabilized subgrade)				
	Dry of Optimum	**Optimum Moisture Content**	**Wet of Optimum**	
Lime (control)	133(19,304)	80(11,646)	35(5,192)	0.35
Type V Cement	268(39,000)	762(110,620)	198(928,717)	0.35
Cement with Fly ash	169(24,511)	389(56,535)	186(26,977)	0.35
GGBFS	151(21,929)	351(51,024)	195(28,282)	0.35
Lime with Fibers	187(27,223)	80(11,603)	53(7,788)	0.35
Lime and Cement	170(24,656)	320(46,400)	150(21,000)	0.35
Subgrade				
Natural Soils	70(10,150)	120(17,400)	50(7,250)	0.35

7.2 Results

The FEM model was used to simulate and investigate the behavior of the pavement systems stabilized with chemical stabilizations under traffic loads and compare them with the control or lime-stabilized system. The pavement layers which are used in these studies are including concrete layer, base (stabilized subgrade) layer and natural subgrade layer.

The two-dimensional axi-symmetric finite element model was used to analyze the pavement system under the traffic loads. For sulfate soils, five different stabilized subgrade layers were put in the model as a base layer for the analyses. For non-sulfate soils, two different stabilized subgrade layers were used. The vehicle load is introduced at the top (concrete) layer of the pavement system. The pressure and compressive strain responses were determined on the base layer and were compared with those obtained on lime treated section (Figures 7.2 to 7.6). Comparisons were made to evaluate the effects of stabilized subgrade course and other pavement characteristics on the long-term performance of the pavement structure.

7.3 Analysis of Test Results

7.3.1 FEM Model Results on Sulfate Soils

Figure 7.2 to Figure 7.6 present the pressures observed from FEM model with five different stabilized base courses. The pressures observed from the model are plotted with the corresponding depth along with the average values monitored from the field during the first year of monitoring period for comparisons. It can be observed from the plots that the highest pressure is measured at the top (concrete) layer and the pressure decreases significantly at lower layers, which are attributed to stiffness variations. The pressure at the concrete layer (from 0 to 8 in.) is higher than the same at the base (from 8 to 16 in.) and subgrade layers (at 16 in.). This is due to the fact that the concrete layer absorbs more pressures from loading than the sub-layers. The concrete layer then transfer the load to the base layer and the subgrade layer, respectively.

For sulfate soils, there are five different base materials, including Type V Cement, Cement with Fly ash, GGBFS, Lime with Fibers and Lime (Control). The resilient moduli are used as the elastic moduli of the base course's properties as the treated soils exhibit small plastic

strains at low traffic loads. Hence, for practical purposes, both elastic modulus and resilient modulus are close to each other. These moduli are given in Table 7.2 in the previous section. The moduli input to the model were taken from the laboratory tests on the soils at different moisture conditions, including at dry of optimum, at optimum moisture content and at wet of optimum, to simulate the behavior of the pavement system under various climate conditions including wetting and drying cycles and the results are plotted in Figure 7.2 to 7.6.

It can be observed from the figures that the effect of climate condition to the pavement is minimal, as there are only slight differences in pressure observed from the base and subgrade layers of the pavement. The comparison between the pressure observed from the FEM model and the pressure from the field monitoring are also compared in Figure 7.2 to 7.6. From Figure 7.7, it can be noted that, for the new stabilized sections, the field values are slightly lower than the observed values from the model. On the other hand, for the control section, the field value is higher than the model's value. This means that the new stabilized sections have been performing well. Nevertheless, the monitored pressure responses are close to predicted pressures from FEM Models. In the monitoring, the pressures increased with the monitoring period and this increase was attributed to decrease in the performance of treated layer due to increased repeated loading from the traffic. This decrease could be due to loading induced damage to the stabilized material and potential leaching in the soil from moisture variations due to seasonal changes.

Figures 7.8 and 7.9 present comparisons of pressures observed from all FEM models at five different test sections. From the figures, it can be seen that the pressures observed from the subgrade of type V Cement section are lower than subgrades of other treated base layer sections including control section. This demonstrated that a slightly higher pressure absorbing ability of the type V cement treated soil than other treated layers.

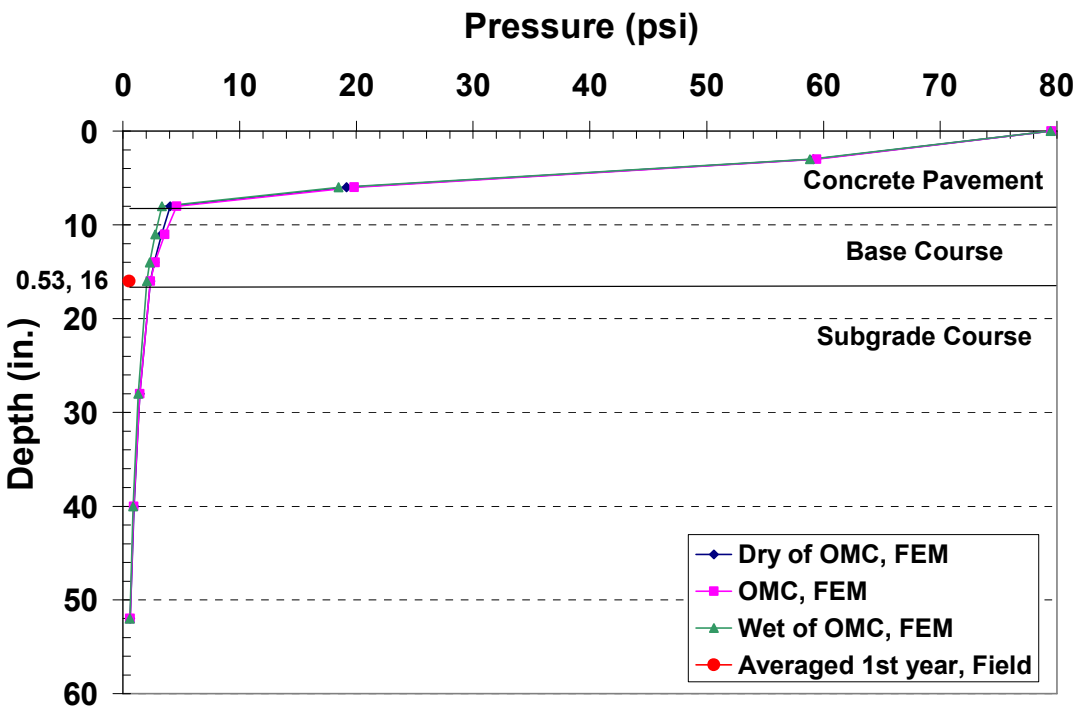

Figure 7.2 Pressure Observed from Type V Cement Section in the FEM Model.

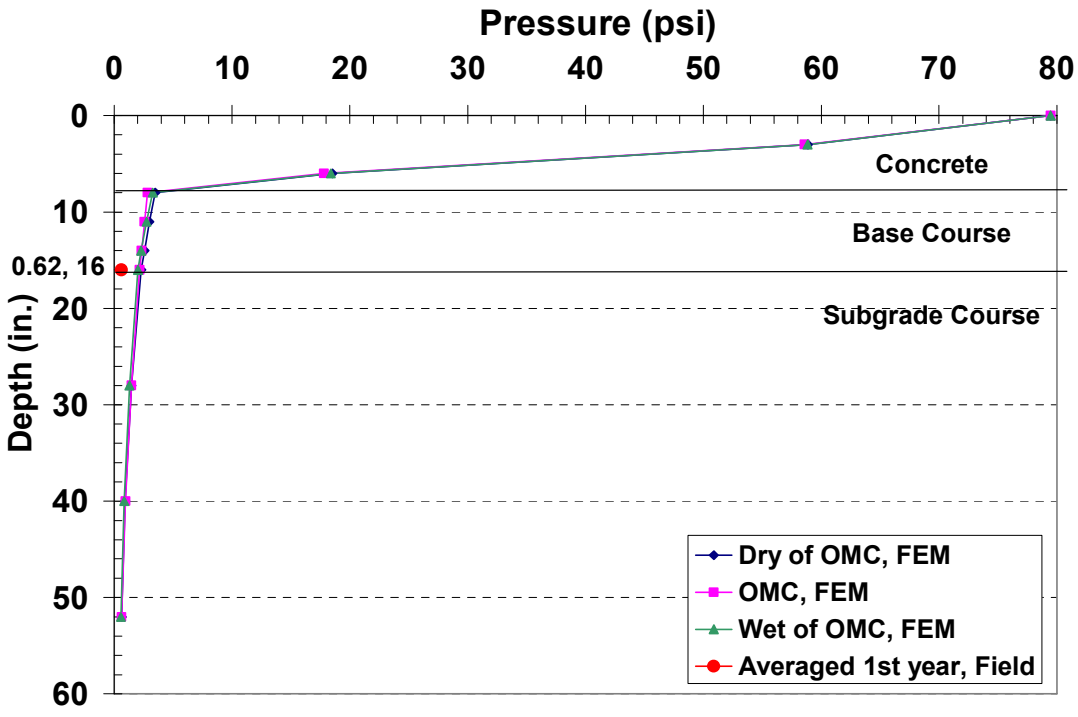

Figure 7.3 Pressure Observed from Cement with Fly ash Section in the FEM Model.

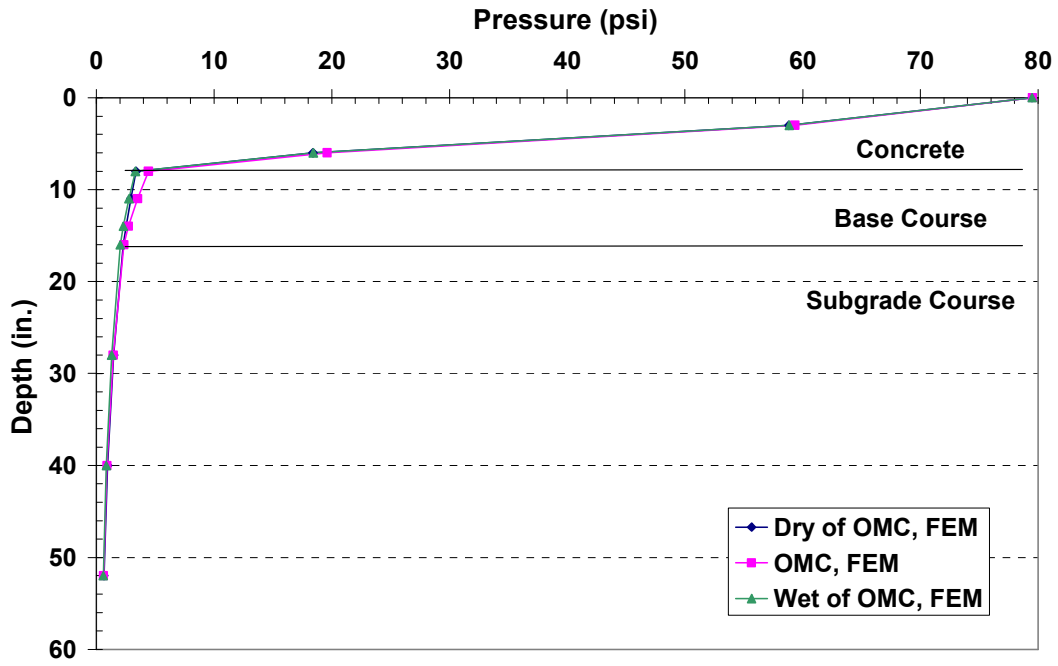

Figure 7.4 Pressure Observed from GGBFS Section in the FEM Model.

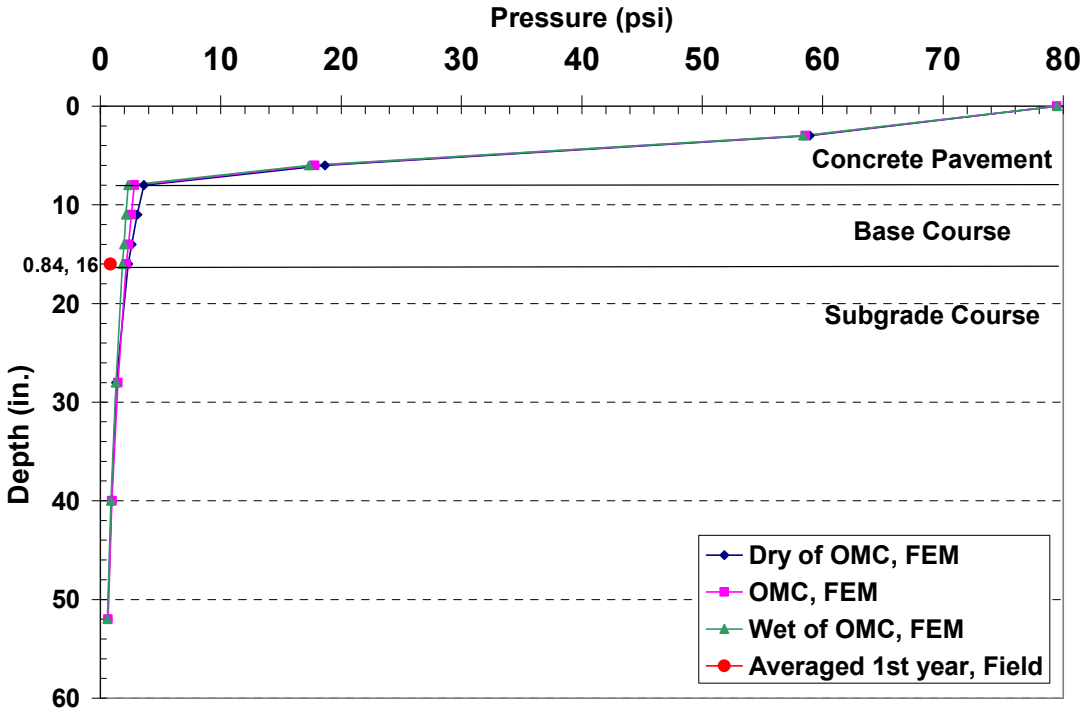

Figure 7.5 Pressure Observed from Lime with Fibers Section in the FEM Model.

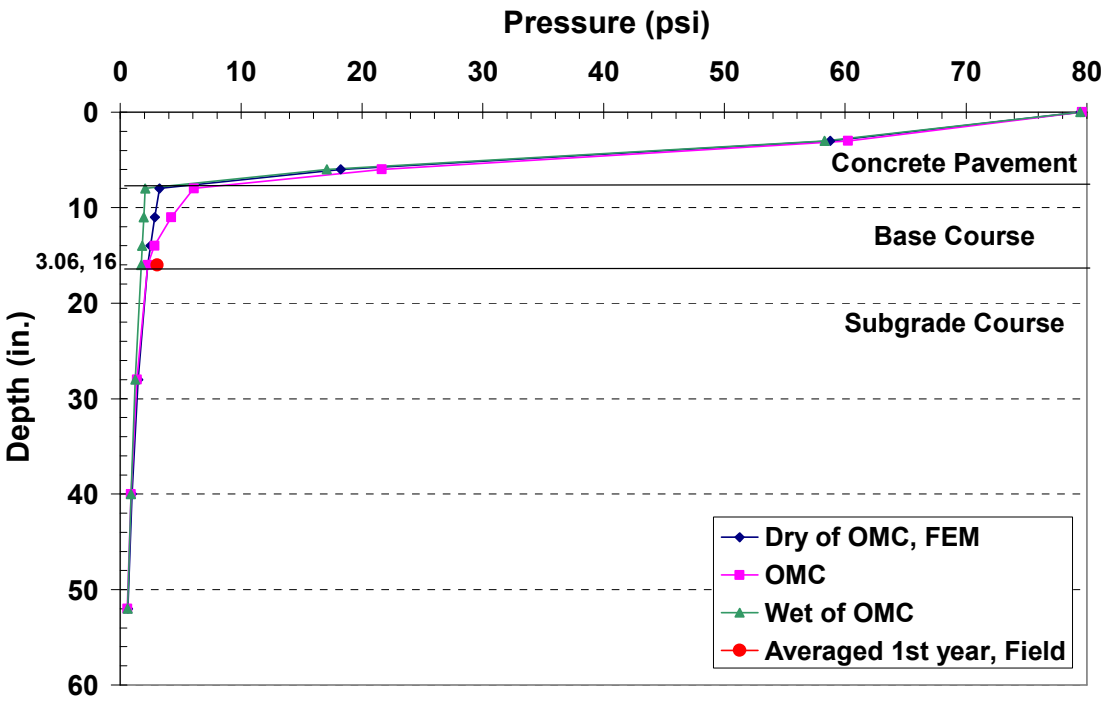

Figure 7.6 Pressure Observed from Lime (Control) Section in the FEM Model.

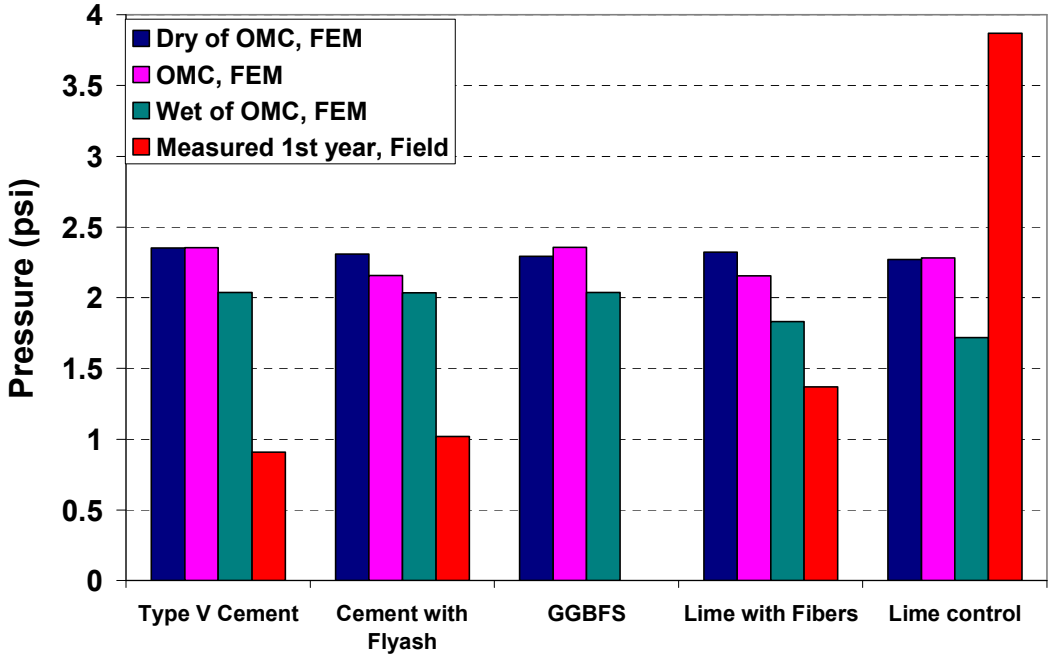

Figure 7.7 Comparison of Pressures Observed from the FEM Model and from the Field.

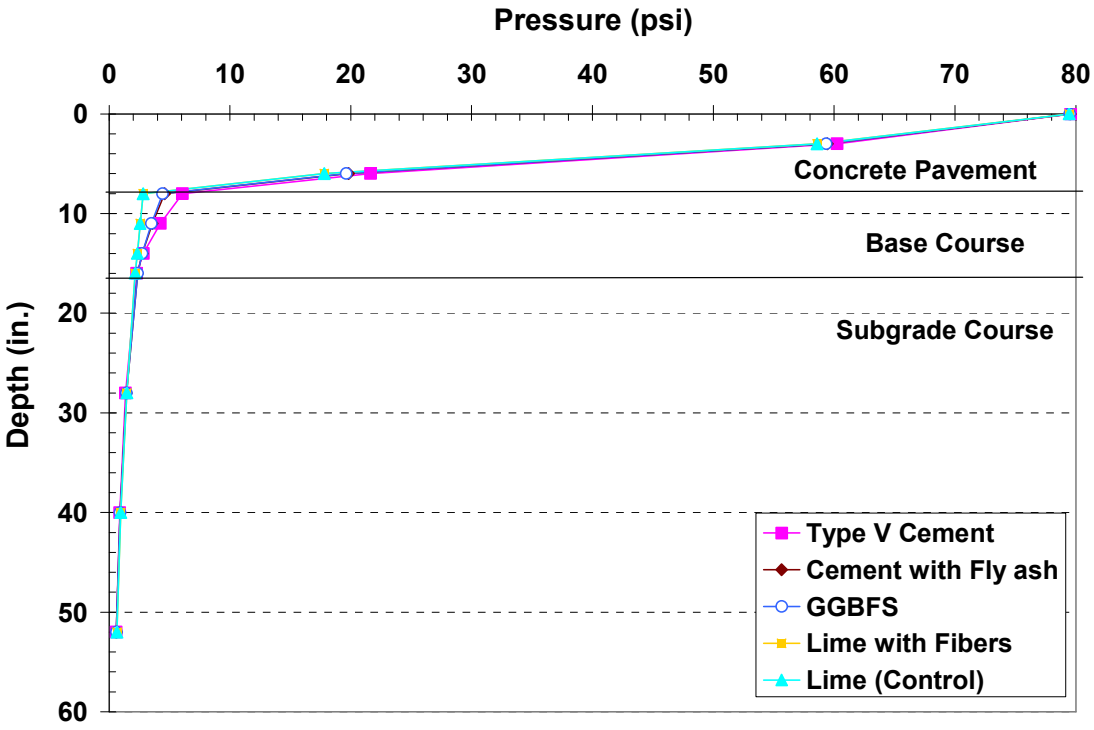

Figure 7.8 Comparisons of Pressure Observed from FEM for Sulfate Soils.

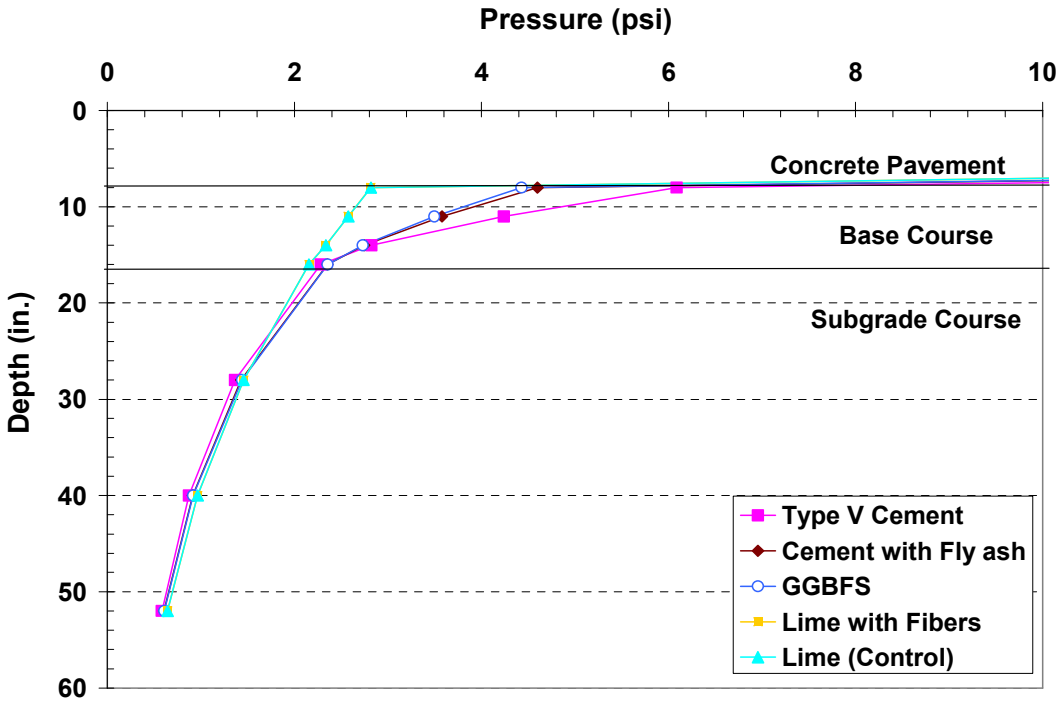

Figure 7.9 Comparisons of Pressures Determined from FEM Models for Sulfate Soils.

Figure 7.10 to 7.19 present the pressure and displacement contours for the pavement section in the FEM model with five different base materials. The pavement system is composed of three layers including 8 in. concrete pavement, 8 in. base course and 120 in. subgrade course. It can be observed from the figures that the observed pressure decreases as the depth increases from top layer to the sub-layer. The maximum concentration of the pressures is at the point where the static load is applied (Figure 7.9). The pressure then spread all over the top concrete layer and exerted to the base course and subgrade course, respectively. On the other hand, the deflection increases as the depth increases. The maximum deflection is measured at the bottom of the pavement system where the depth is maximized as shown in Figure 7.10.

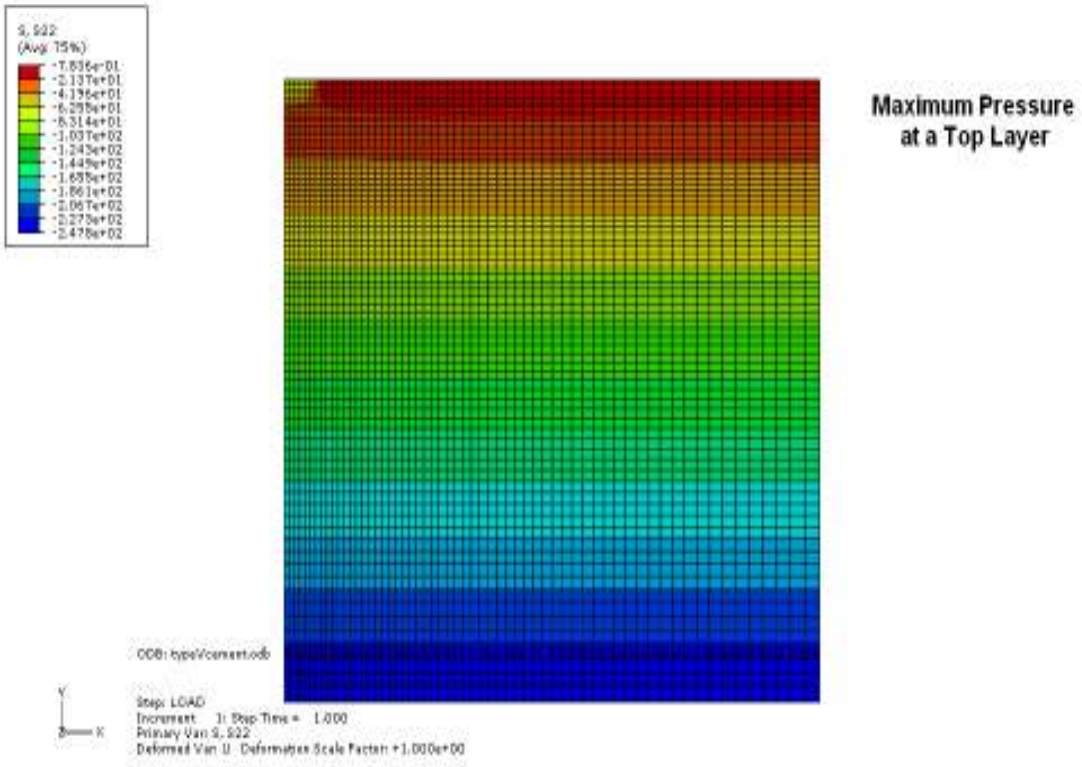

Figure 7.10 Pressure contours showing the pavement response for Type V Cement section.

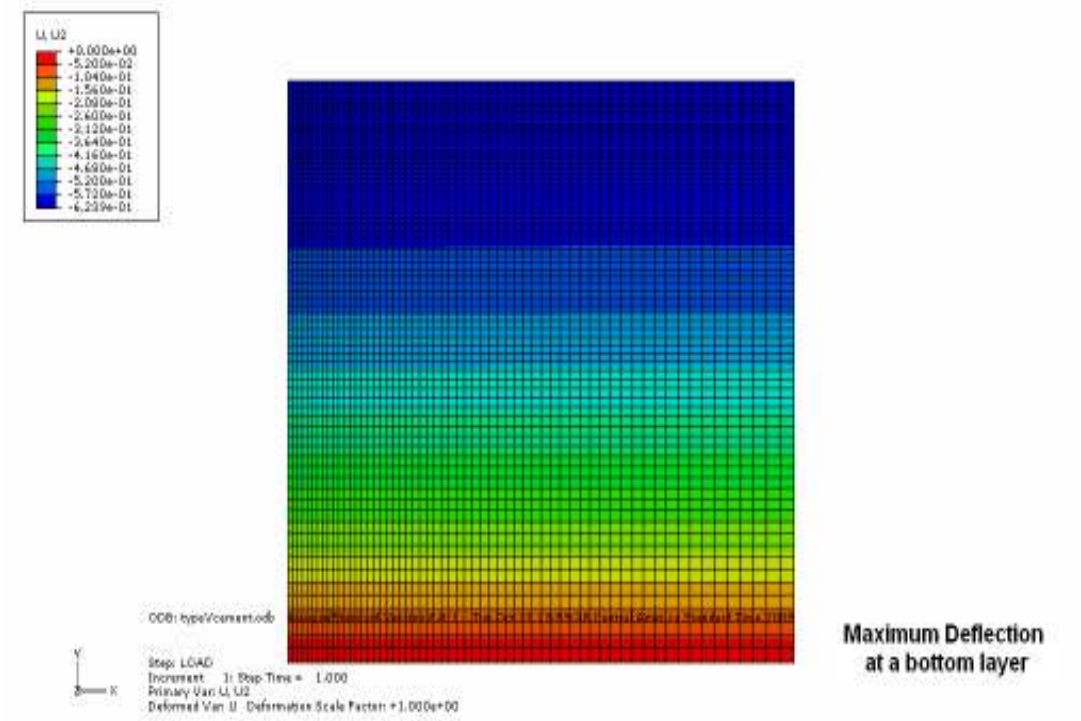

Figure 7.11 Deflection contours showing the pavement response for Type V Cement section.

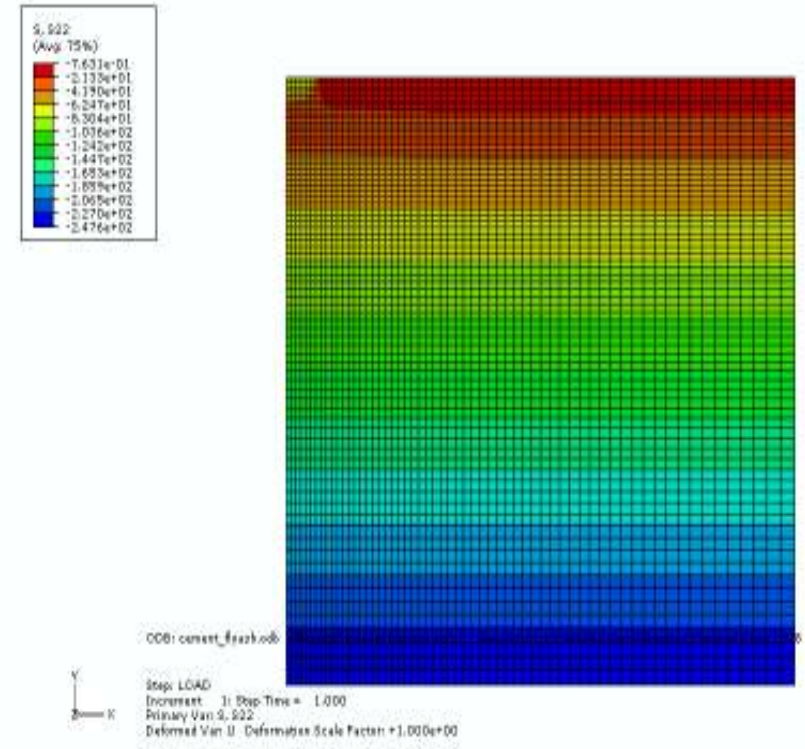

Figure 7.12 Pressure contours showing the pavement response for Cement with Fly ash Section.

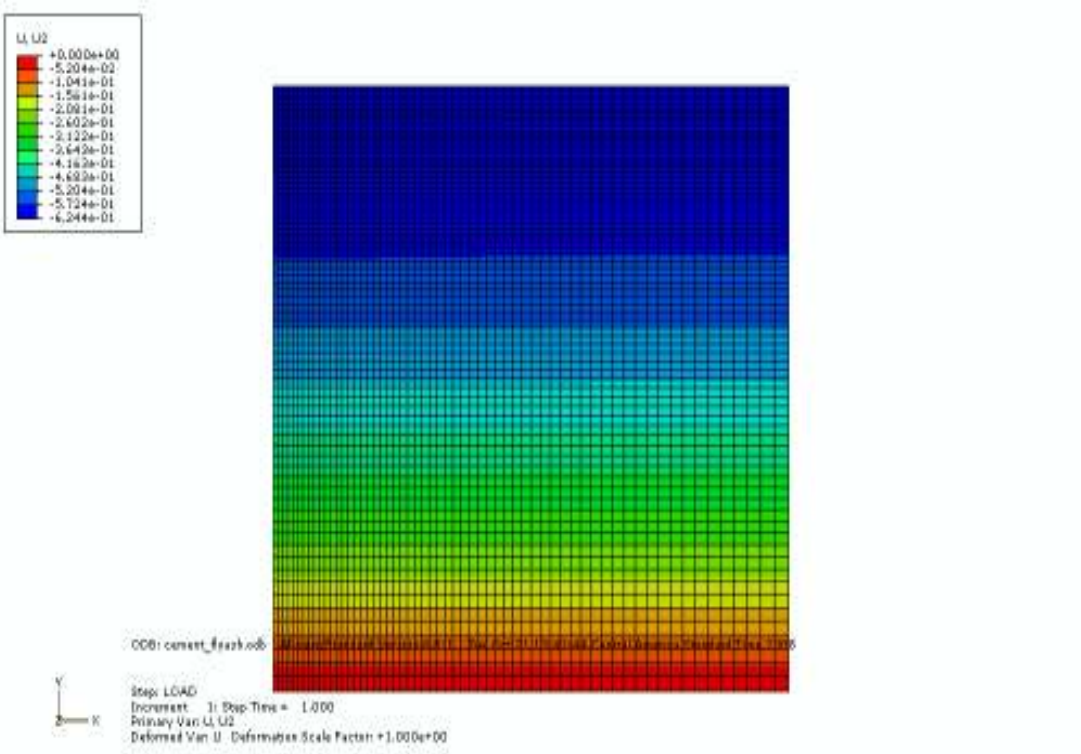

Figure 7.13 Deflection contours showing the pavement response for Cement with Fly ash section.

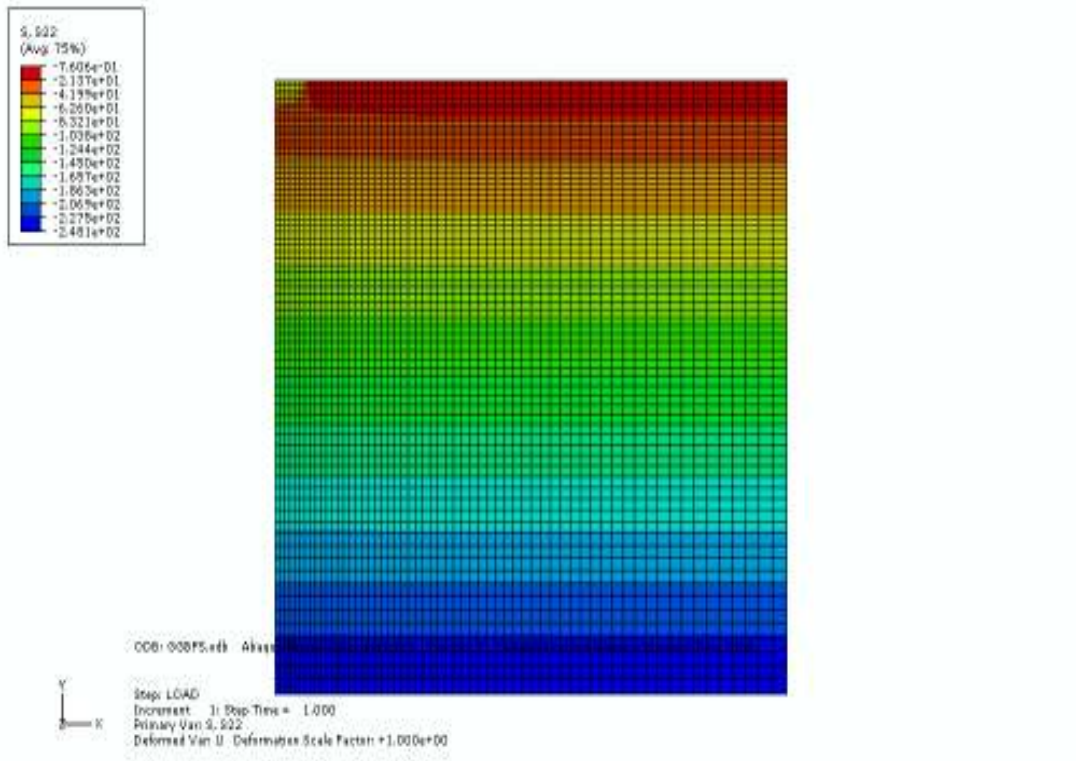

Figure 7.14 Pressure contours showing the pavement response for GGBFS Section.

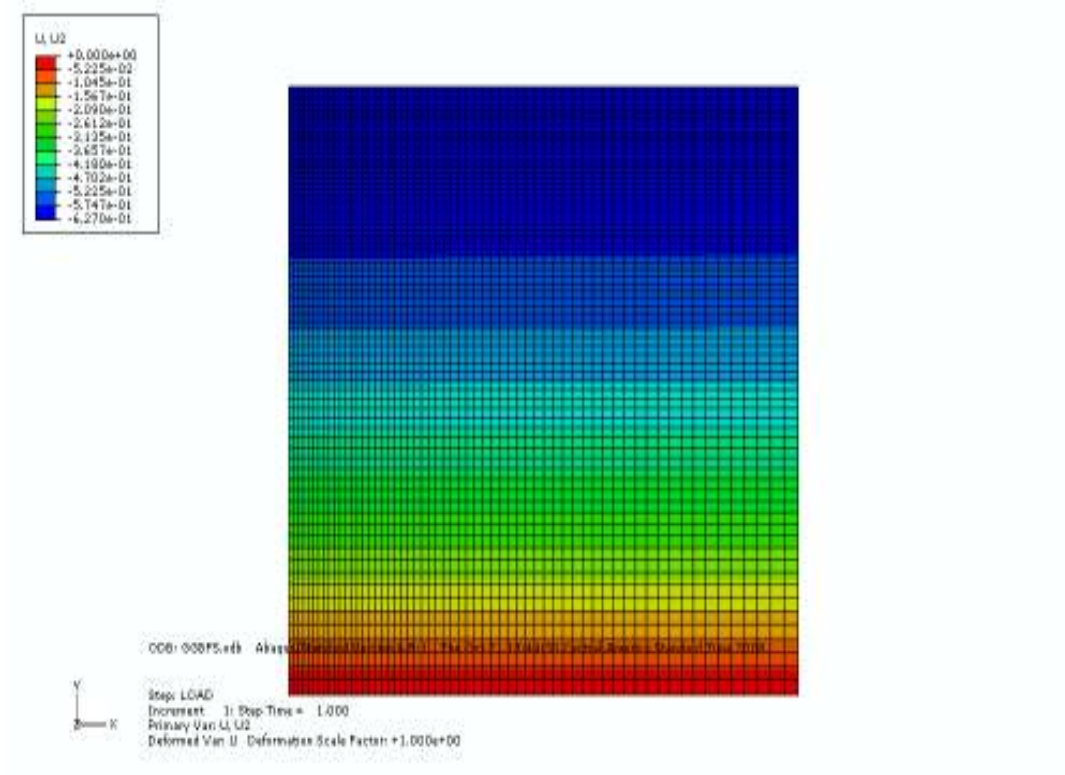

Figure 7.15 Deflection contours showing the pavement response for GGBFS Section.

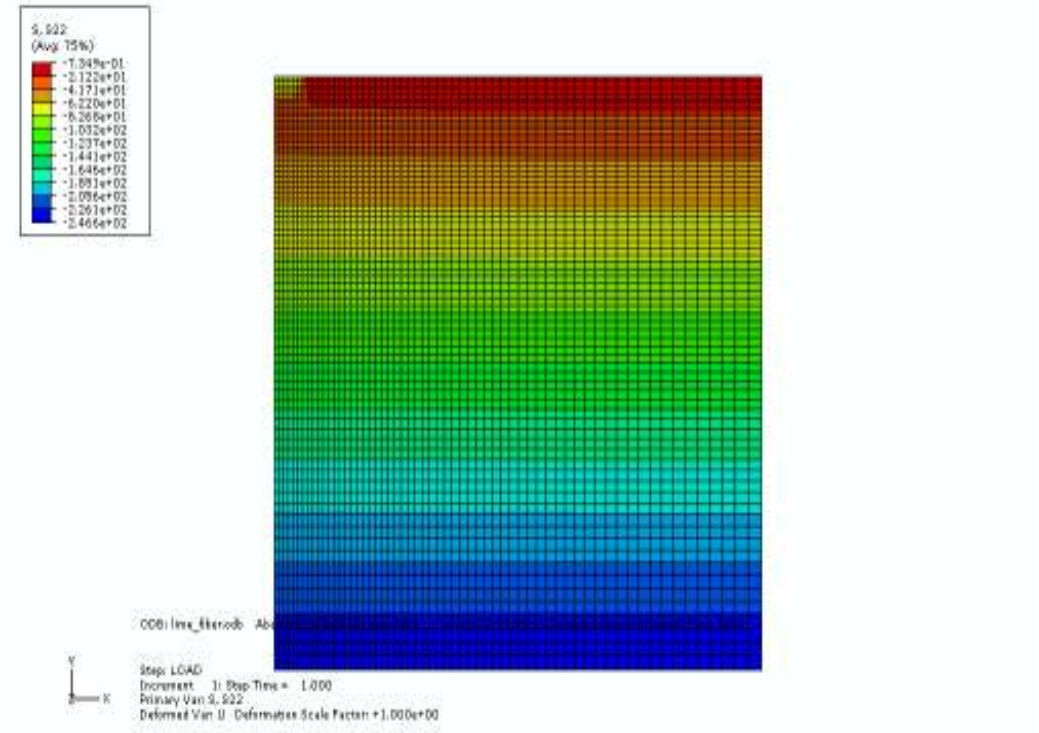

Figure 7.16 Pressure contours showing the pavement response for Lime with Fibers Section.

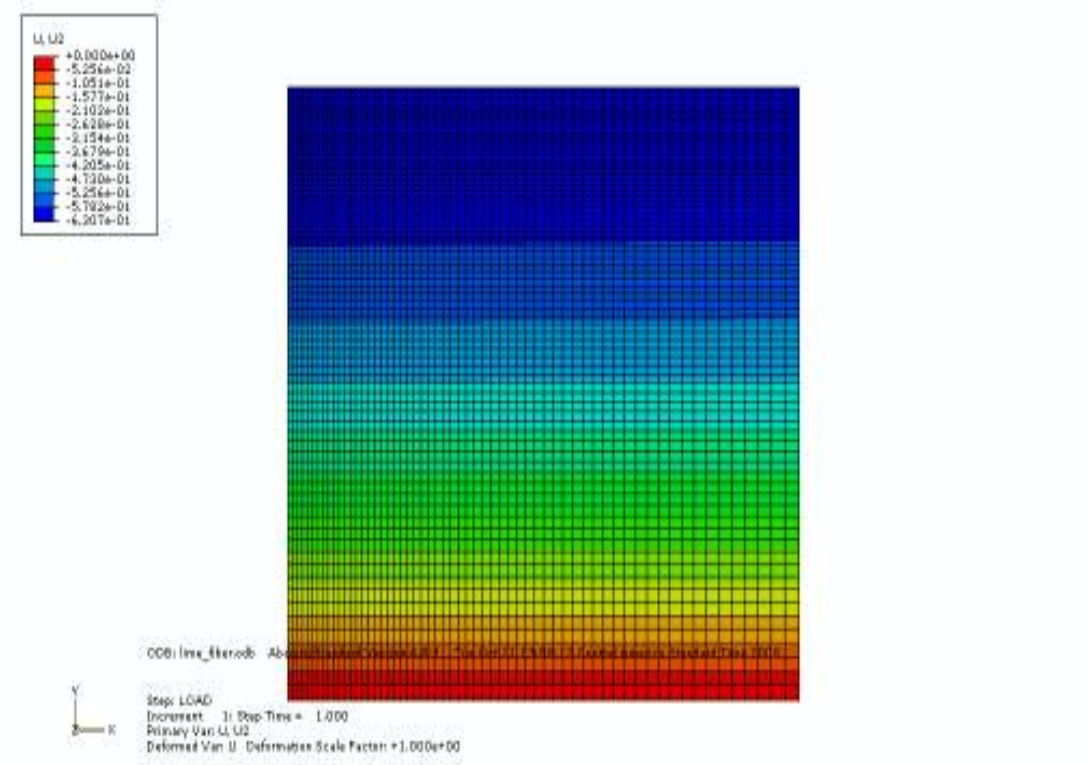

Figure 7.17 Deflection contours showing the pavement response for Lime with Fibers Section.

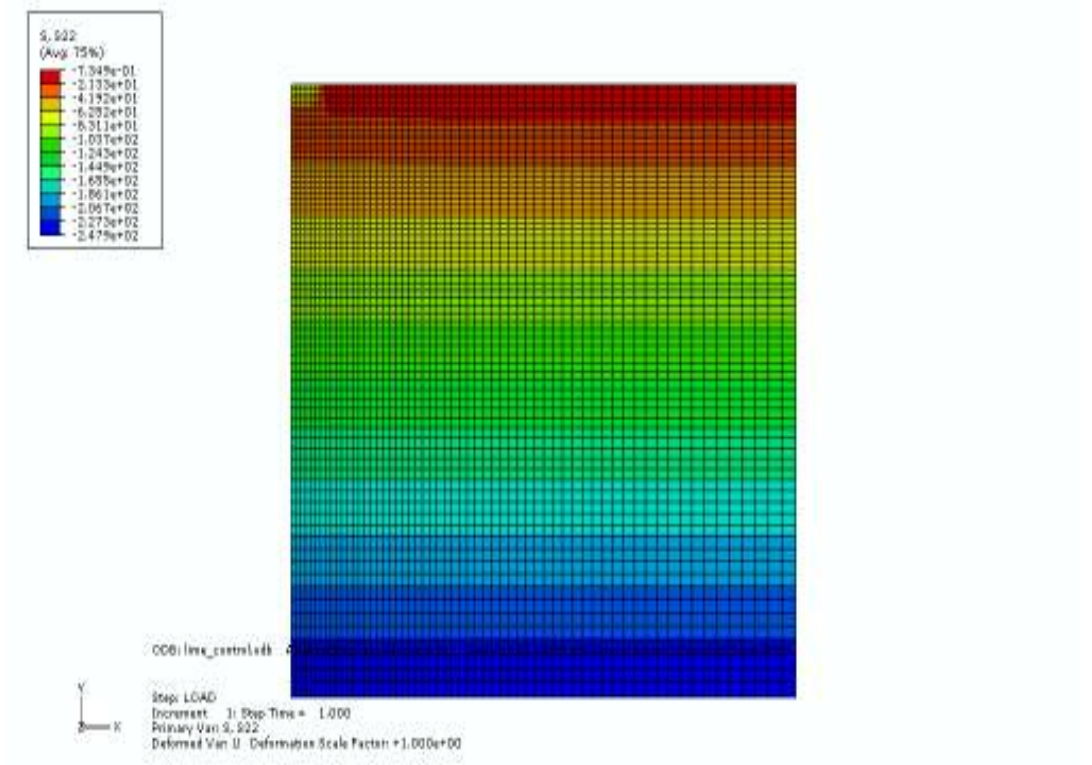

Figure 7.18 Pressure contours showing the pavement response for Lime (Control) Section.

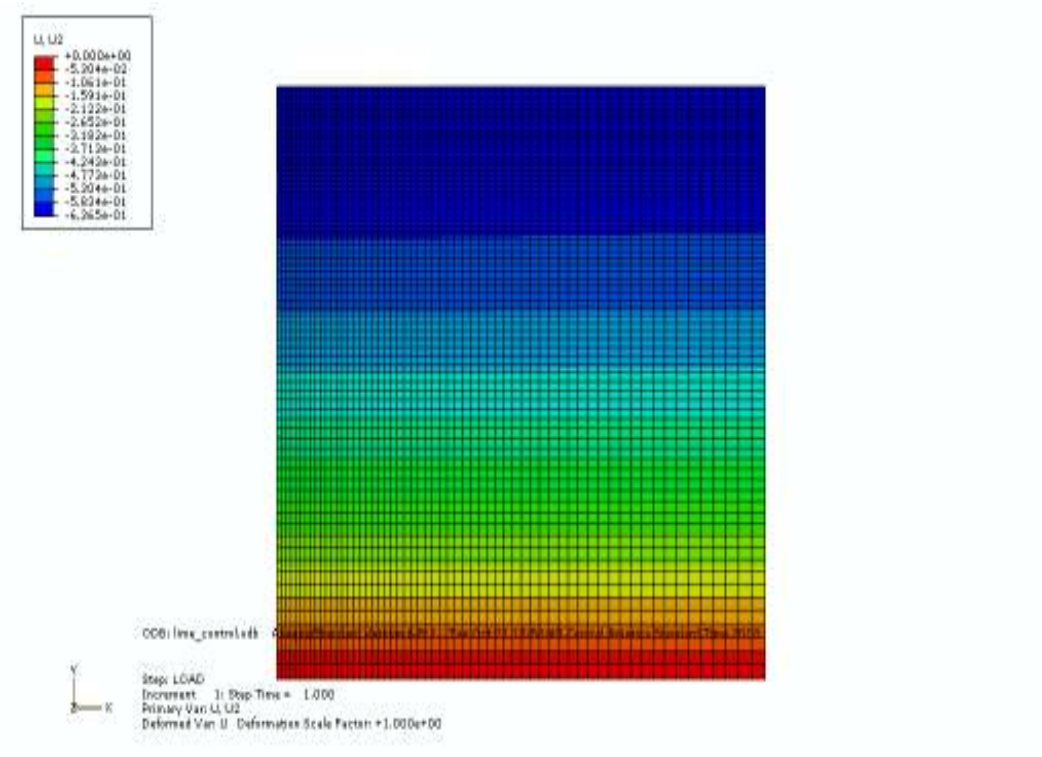

Figure 7.19 Deflection contours showing the pavement response for Lime (Control) Section.

Figure 7.20 and 7.21 present the deflections and vertical compressive strains observed from the FEM model along with the field values for sulfate soils. From the figures, Type V Cement section demonstrated the lowest deflections and strains observed from the FEM model. Class F Fly ash and GGBFS sections have yielded a moderate amount of deflections in the model. The deflections observed from these layers are lower than those of lime with fibers and lime sections. Though these differences under modeling of static load of immediate construction scenario are small, their trends reconfirm with the field monitored data, which showed that the deflections increase with elapsed time period. In conclusion, from the FEM models, Type V Cement section performed the best performance on sulfate-rich soils followed by Type V Cement with Fly ash stabilizers, GGBFS and lime with polypropylene fibers.

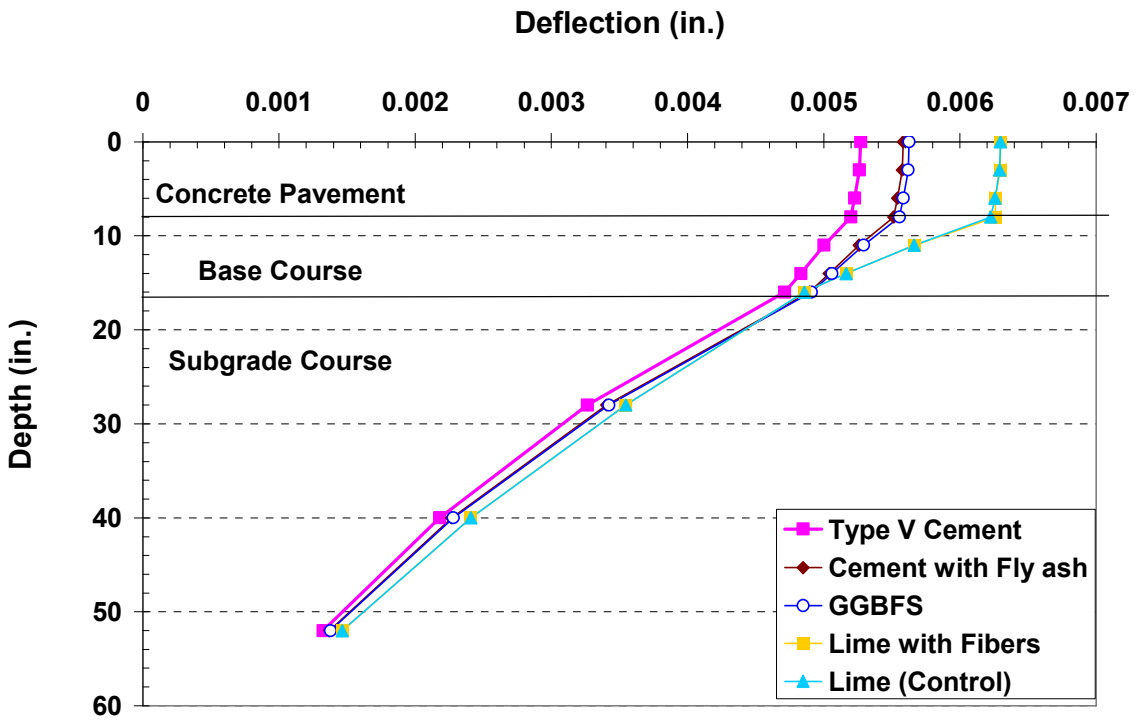

Figure 7.20 Comparison of Deflection observed from FEM Model for Sulfate Soils.

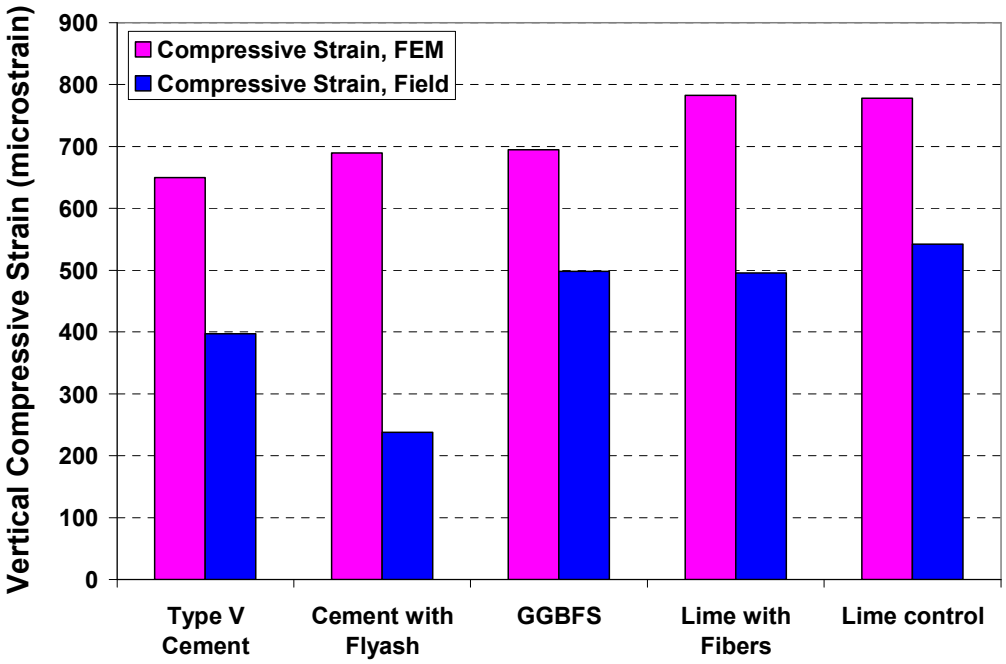

Figure 7.21 Comparison between Vertical Compressive Strains Observed from the Model and from the Field Monitoring.

7.3.2 FEM Models for Non-Sulfate Soils

Figure 7.22 present comparisons of pressures observed from FEM model for non-sulfate soils with two different stabilized base courses including lime stabilized and lime cement stabilized base course. The pressures observed from the model are plotted with the corresponding depth for both stabilization methods for comparison. It can be observed from the plots that pressures observed from the subgrade of lime cement section are lower than those of a control or lime section. The lime-cement section has demonstrated the highest strength improvement as the pressures exerted from base layer to the subgrade layer is lower than that of the lime section.

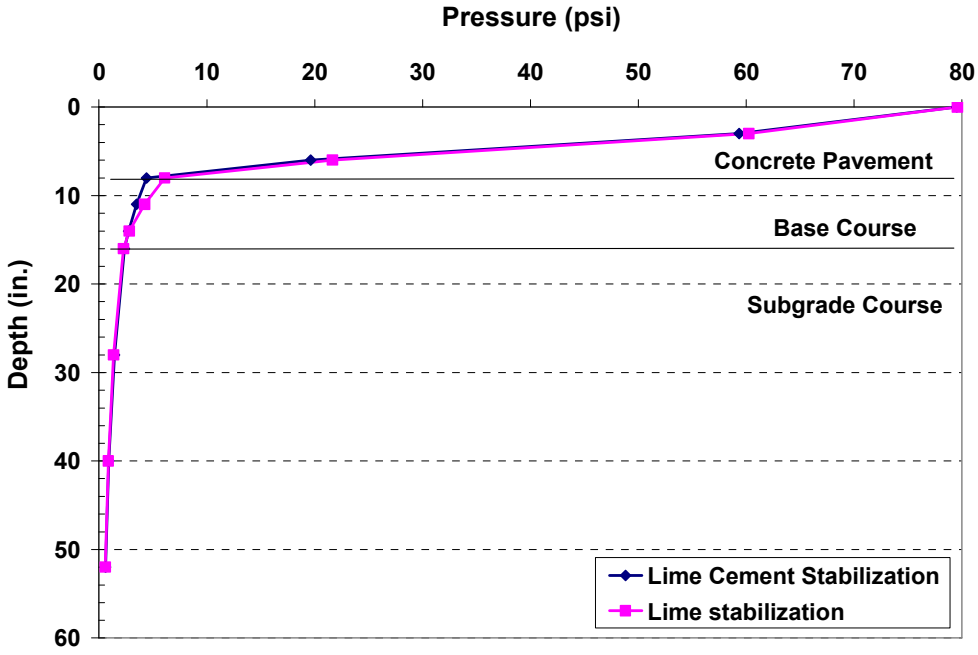

Figure 7.22 Comparisons of Pressure Observed from FEM for Non-Sulfate Soils.

Figures 7.22 to 7.25 show the pressure and displacement contours for the pavement section in the FEM model with two different base materials.

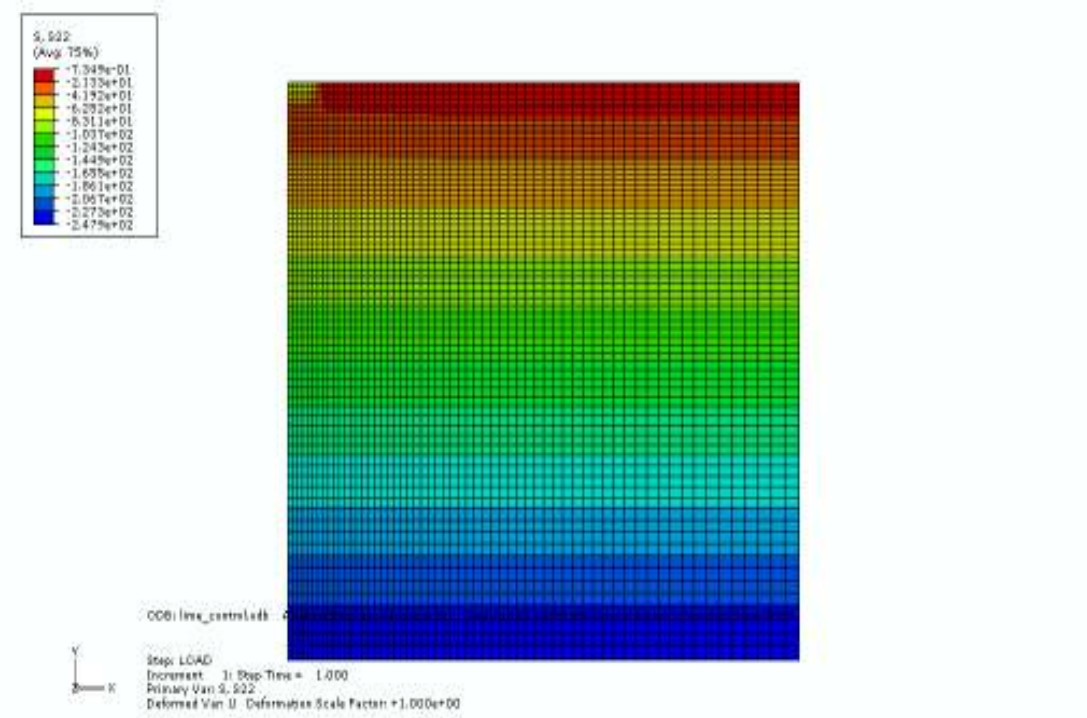

Figure 7.23 Pressure contours showing the pavement response for Lime stabilized Section.

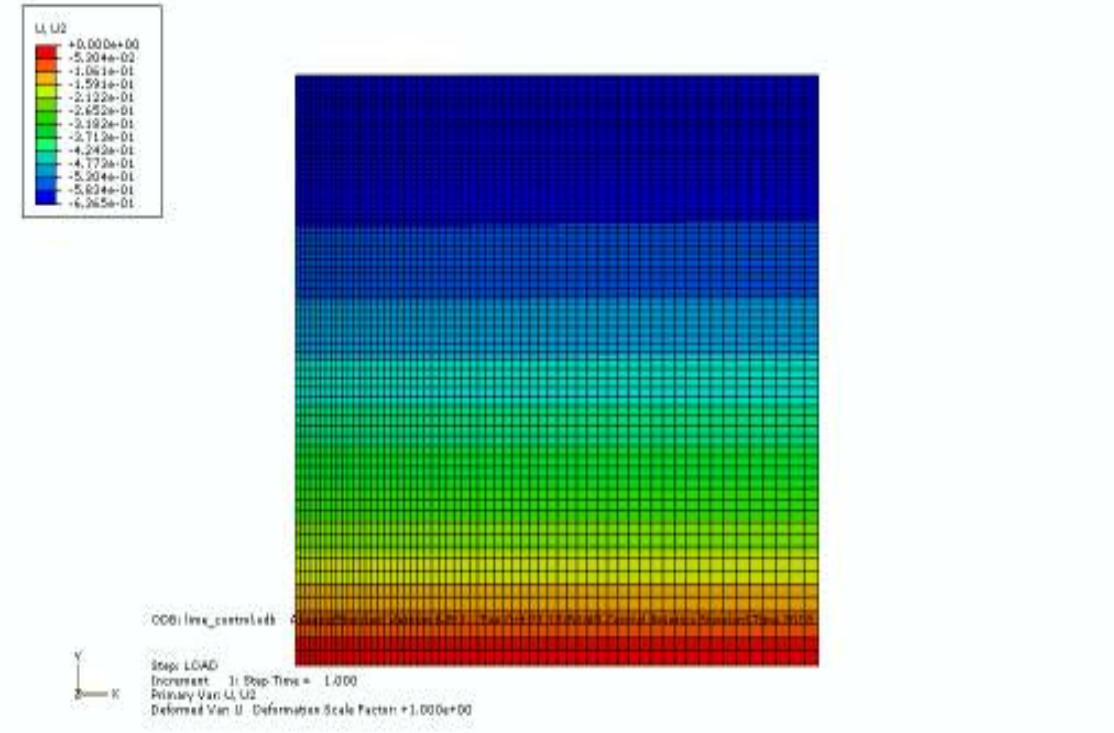

Figure 7.24 Deflection contours showing the pavement response for Lime stabilized Section.

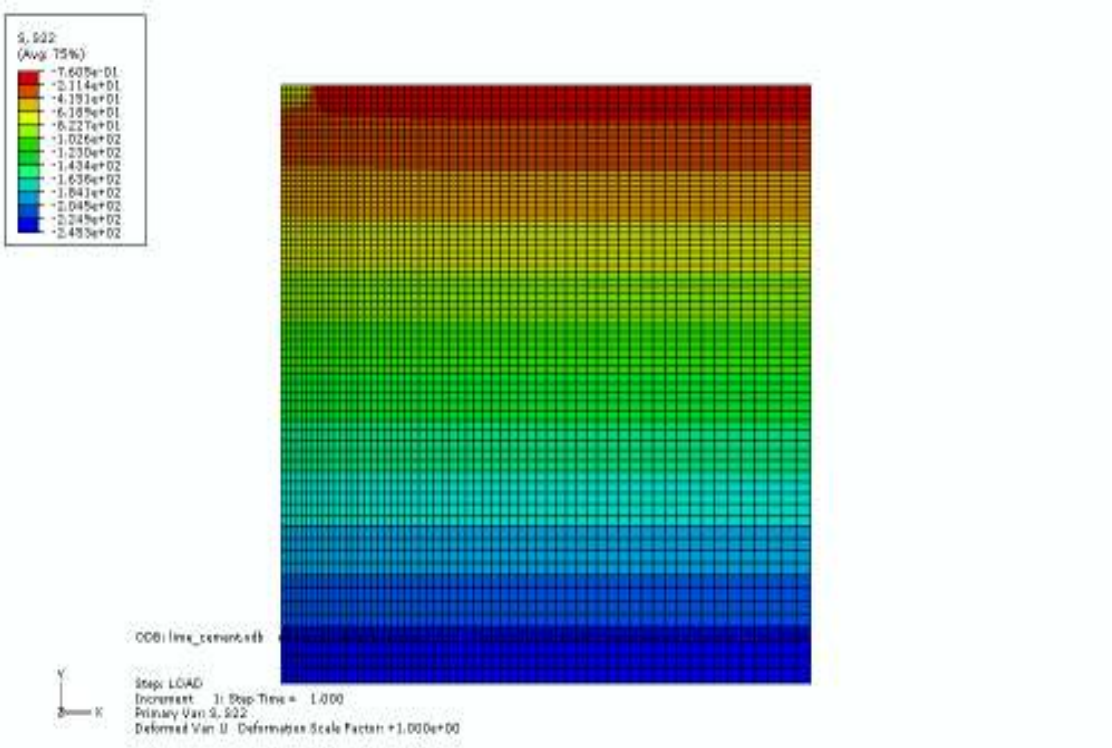

Figure 7.25 Pressure contours showing the pavement response for Lime Cement stabilized Section.

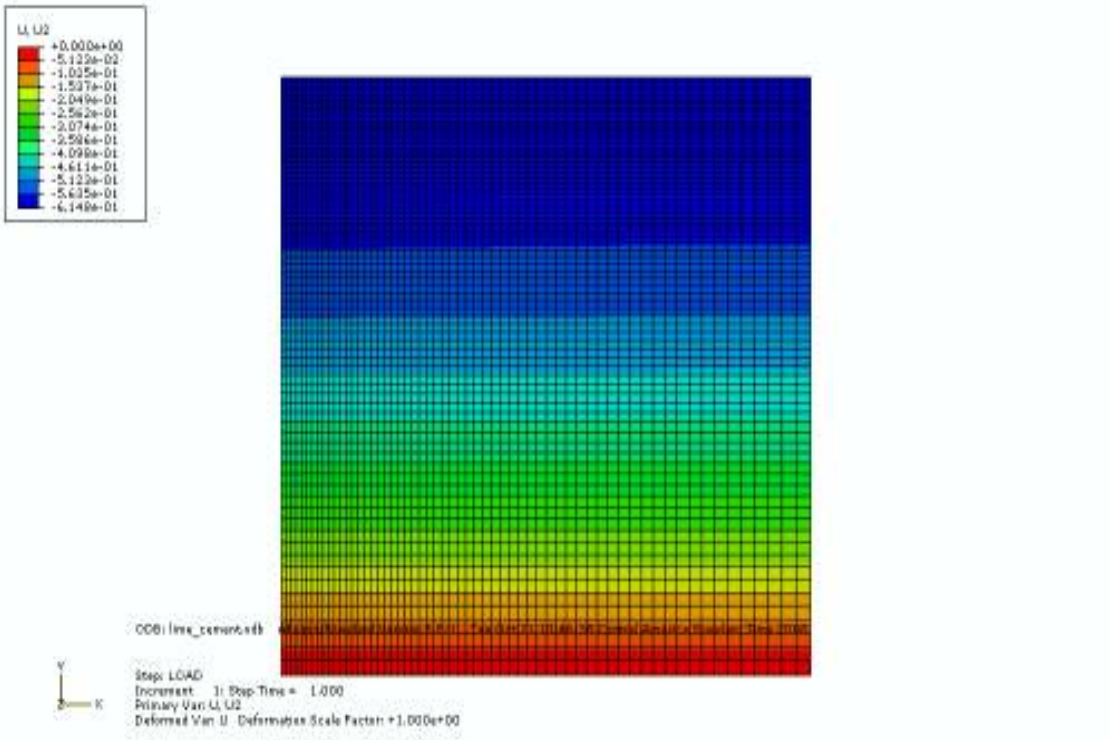

Figure 7.26 Deflection contours showing the pavement response for Lime Cement stabilized Section.

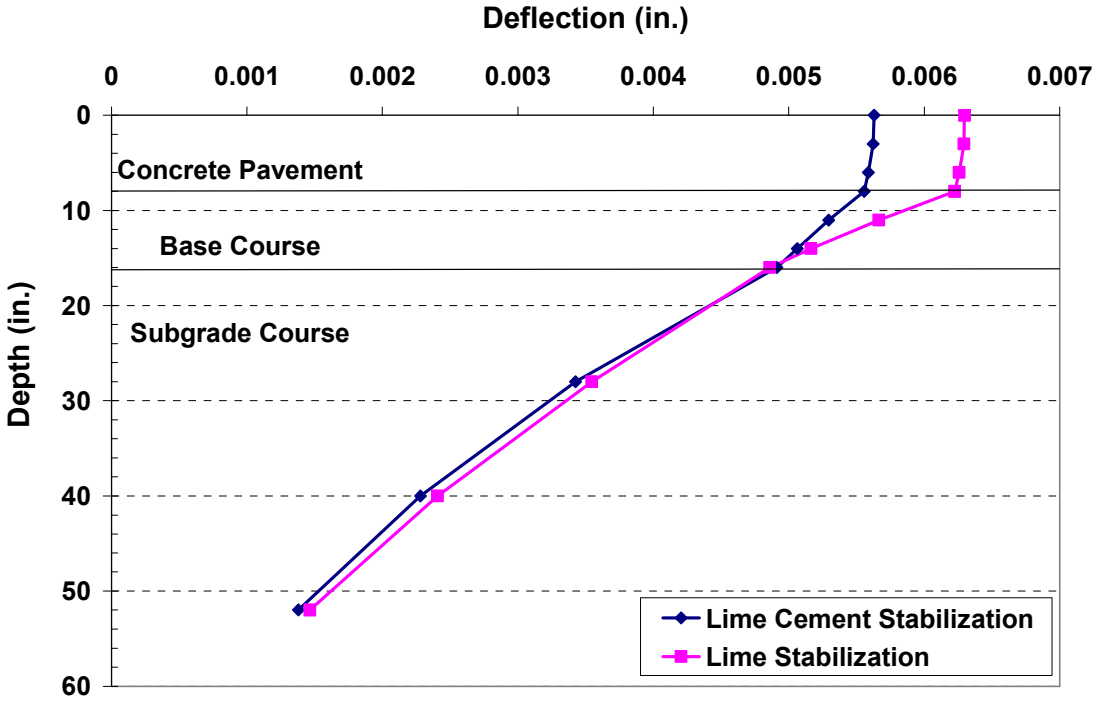

Figure 7.27 Comparisons of Deflection Observed from FEM for Non-Sulfate Soils.

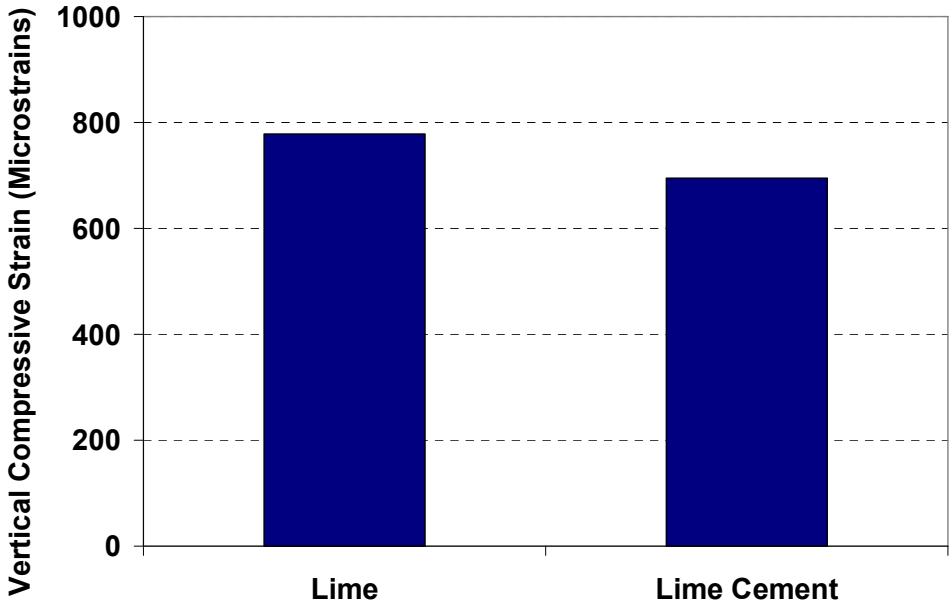

Figure 7.28 Comparisons of Strain Observed from FEM for Non-Sulfate Soils.

Figures 7.27 and 7.28 present the deflections and vertical compressive strains observed from the FEM models for non-sulfate soils. From the figures, lime-cement section demonstrated the lowest deflections and strains. The deflections observed from the pavement layers at lime-cement section are lower than the deflections at the lime sections, indicating the better performance of using lime-cement treated base layer in the place of lime treated layer. In conclusion, for non-sulfate soils, lime cement stabilization has yielded the best performance based on the FEM analysis.

Based on field and laboratory studies, Table 7.3 and 7.4 presents the summary of performance of stabilizers for sulfate and non-sulfate soils, respectively. These rankings are based on the trends noted in the analysis of test results covered in the previous chapters. For sulfate soils, based on the summary provided in the following table, Type V Cement with Fly Ash, and Type V Cement have performed well in all aspects of monitoring include chemical studies, sulfate heave assessments, cost analyses and visual observations. Both GGBFS and lime-fiber treated sections provided adequate performance whereas the lime (control) section has demonstrated relatively poor performance.

Table 7.3 Summary of Qualitative Performance of Stabilizers for Sulfate Soils

Assessment Type	Type V Cement	Cement and Fly ash	GGBFS	Lime and Fibers	Lime (Control)
Laboratory Studies	H (1)	H (2)	H (3)	M	L
Instrumentation Studies	H (1)	H (2)	M	M	M
DCP Studies	H (1)	H (2)	M	L	L
Elevation Studies	M	H (2)	H (1)	M	L
Mineralogical Studies	M	M	M	L	L
Current Pavement Conditions	H (2)	H (1)	H (3)	M	L
LCCA Studies	H (1)	H (2)	M	M	L
FEM Model	H (2)	H (1)	M	M	L
FINAL ASSESSMET	**1**	**2**	**3**	**4**	**5**

Note- H= High Performance; M = Medium Performance; L= Low Performance;
1, 2, 3 = Ranks among the stabilizers based on best performance

Table 7.4 Summary of Qualitative Performance of Stabilizers for Non-sulfate Soils

Assessment Type	Lime Stabilization	Combined Lime Cement
Laboratory Studies	n/a	n/a
DCP Studies	L	H
Elevation Studies	L	H
Mineralogical Studies	L	H
Current Pavement Conditions	L	H
LCCA Studies	M	H
FEM Model	M	H
FINAL ASSESSMENTS	-	Recommended

Note- H= High Performance; M = Medium Performance; L= Low Performance

7.4 Summary

This chapter presents the finite element analyses by using commercially available ABAQUS® software. The analysis model is based on infinite slab and other idealized assumptions. The two-dimensional axi-symmetric finite element model was used to analyze different pavement test sections consisting of a concrete layer, a base layer and a subgrade layer. Comparisons of pressures and deflections were made between different pavement sections to evaluate the effects of stabilized subgrade layer and other pavement characteristics on the performance of the pavement structure.

For sulfate soils, Type V Cement section demonstrated the lowest deflections and strains observed from the FEM model. Class F Fly ash and GGBFS sections have yielded a moderate amount of deflections in the model. The deflections observed from these layers are lower than from lime with fibers and lime sections. Pressure absorbed by the cement layer is higher than the other treated soils. In conclusion, from the FEM model analyses, Type V Cement performed the best among other treatments on sulfate-rich soils.

For non-sulfate soils, Lime cement stabilization has demonstrated the highest strength improvement to the pavement system as the pressure exerted from base layer to the subgrade of this section is lower than the same under lime section. Lime cement section also demonstrated the lower deflections and strains compared to lime section. The deflections observed from pavement layers are lower than lime sections. In conclusion, for non-sulfate soils, lime cement stabilization has yielded the best performance base on the FEM analyses.

CHAPTER 8

SUMMARY OF FINDINGS AND FUTURE RESEARCH DIRECTIONS

This final chapter provides a comprehensive summary of field and laboratory data analyses, which includes results from field instrumentation, elevation surveys, DCP tests, laboratory studies, mineralogical studies and visual inspections for assessing various treatment methods, and life cycle cost analyses (LCCA) performed on both stabilized sulfate and non-sulfate soils. The assessments are used to develop design guidelines on the selection and constriction of stabilizer treated subgrades for supporting pavements in sulfate rich and non-sulfate soil environments.

For sulfate soils, the treatments performed with novel stabilization methods including Type V cement, Type V cement with Fly ash, GGBFS, and lime with fibers, were compared against a control section treated with lime. For non-sulfate soils, comparisons were made between combined lime cement stabilization and the traditional or control lime stabilization method. The assessment program included both field monitoring and laboratory studies in which the stabilized pavement sections were monitored and evaluated based on which ideal stabilization methods provided the best performance for the present soil conditions.

8.1 Summary of Findings

From the laboratory test results presented earlier in Chapter 4, all stabilizers have proven to enhance liquid limits, plasticity index properties, unconfined compressive strength, swelling and shrinkage potentials of the natural subgrades.

For sulfate soils, Type V Cement with Fly ash proved to be the most effective treatment based on the enhanced strength and minimized swell and shrinkage potential properties. The second most effective treatment was Type V Cement which was followed by the GGBFS

treatment. Among other treatments, Lime-Fiber and Lime treatment methods exhibited moderate and poor improvements in enhancing soil properties, respectively.

For non-sulfate soils, combined lime and cement stabilization method yield significant improvements to the soils in all aspects, including basic soil properties, mineral and chemical characteristic and strength enhancement. The field monitoring results also demonstrated that both lime and cement stabilization methods considerably enhanced the performance of the pavement structures after the stabilization. Therefore, it can be concluded that combined lime and cement treatment provided the most effective enhancements to the non-sulfate soils compared to the traditional lime stabilization.

From the laboratory studies and field monitoring data presented in Chapters 3 to 7, the following major conclusions have been made:

Sulfate Soils:

1. From the strain gauge readings, all sulfate soil test sections underwent compression related strains under the ongoing traffic condition. From the total strains observed, lime control section experienced the most significant amounts of axial compression strain which was followed by Lime- Fibers, GGBFS and Type V Cement sections. Type V Cement with Fly Ash section demonstrated the lowest amount of the strain under the same traffic condition.
2. Based on the pressure cell results, the amount of pressure transferred to subgrade soils increased with the repetition of traffic loads transferred to the pavement during its service life. These increases were due to permanent strain experienced in the treated subgrade soils. Lowest pressure transferred was in Type V cement and Type V cement with fly ash treated sections indicating that these sections underwent low compression due to low amount of pressures transmitted to these layers. Lime-fiber sections exhibited moderate pressures under traffic loading whereas lime treated section have experienced the highest pressure readings. This concludes that the Type V Cement and Type V Cement

with Fly Ash treated sections have low potential to undergo permanent distresses during their service life.

3. From the elevation survey results observed at the test site for sulfate soils, control (lime treated) section yielded the highest swell and shrink movements during seasonal changes. The next high movements were observed at Type V Cement, Lime – Fiber and Type V Cement - Fly Ash stabilized sections. GGBFS treated section performed the best with the lowest heave related movements. According to high swell and shrink movements observed from the elevation survey results, it is noted that both longitudinal and transverse pavement cracks, settlement and water ponding problems were detected in the control section.
4. From the DCP test results for sulfate soils, the Type V Cement treatment, Type V Cement with Fly Ash treated sections exhibited higher strength gain, which is followed by GGBFS treated section.
5. Lime with Fibers and Lime (control) sections demonstrated lower strength gain compared to other treated sections. From the measured DPI values, it can be observed that there is no considerable deterioration in strength in any of the treated layers due to climatic changes, leaching of stabilizers and varying traffic volume in the last three years after the stabilization.
6. X-ray diffraction (XRD) analysis for sulfate soils showed traces of ettringite in all the treated sections. The presence of ettringite is clearly evident in Lime-Fiber section and lime (control) sections due to larger number of matches with the basal spacing of ettringite. Other sections also showed the trace of ettringite formation which implies that sulfate heave is still possible in the present test sections. Lime (control), Lime-Fiber and Type V Cement treated sections experienced higher heave related movements and some part of it could be attributed to the formation of ettringite and its hydration.
7. For sulfate soils, the EDAX results demonstrated that all treated soils have all the chemical components necessary, i.e. calcium, alumina, and sulfates to produce sulfate

heaving mineral, ettringite. As a result, ettringite formation was observed in the present treated soils. However, the heaving observed in Type V Cement, Type V Cement with Fly Ash and GGBFS treated sections appeared to be small. Ettringite induced heaving may have resulted in certain amount of overall heaving which is still at lower levels and could not cause cracking to pavements.

8. For sulfate soils, Type V Cement section demonstrated the lowest deflections and strains observed from the FEM model. Class F Fly ash and GGBFS sections have yielded a moderate amount of deflections in the model. The deflections observed from these layers are lower than from lime with fibers and lime sections. Pressure absorbed by the cement layer is higher than the other treated soils. In conclusion, from the FEM model analyses, Type V Cement performed the best among other treatments on sulfate-rich soils.
9. From visual photos taken at the test sections, all sections except lime treated sections have not experienced any ponding and cracking problems. On the lime treated sections, both ponding and longitudinal cracking were noted.
10. From LCCA studies, Type V cement treatment resulted in a field treatment that has an Net Present Value or NPV of 383k whereas all other methods have NPV values ranging from 388 to 475. For this analysis, the maintenance information is based on the field monitoring and visual distress patterns found at the test sections. Overall, both cement and GGBFS treatments resulted in pavements with low distress problems and hence yielded low NPVs.

Non-Sulfate Soils:

11. The combined lime cement treatment yielded the best enhancement to pavement performance. Although, heaves were observed in the early monitoring period at all 3 test sites, these heaves are not significant and the volume change movements in the later monitoring periods diminished when compared to their initial high heaving pattern. These heaves were attributed to high moisture content changes which cause expansive subgrade soils to undergo swell and volume change movements in a short period of time.

The plots of monthly average precipitations against the observed elevations show that the heaves are attributed to the seasonal precipitation variations that the test sections experienced during a particular monitoring period.

12. The results of DCP tests demonstrated that the DPI values for lime cement treated soils were lower compared to the DPI values for untreated soils. This indicates that lime cement treatment provided higher strength enhancements to the soils. Moreover, there is no considerable deterioration seen in DCP values in any of the lime cement treated layers through out the monitoring period which indicates that the stabilization still remain effective.
13. For non-sulfate soils, the XRD results on non-sulfate soil specimens collected from lime cement treated test sites demonstrated that the stabilized soils are subjected to pozzolanic reaction where the strongest on XRD traces is founded in the development of C_4AH_{13} and C-S-H gel. The structure of the stabilized soils is common to all soils subjected to the addition of hydrated lime as an alkaline activator. The XRD results also show that there is no evident of ettringite formation as in the observation period of thirty months. This is due to the fact that soils from these locations contain low sulfate amount which is less than 2,000 ppm.
14. For non-sulfate soils, Lime cement stabilization has demonstrated the highest strength improvement to the pavement system as the pressure exerted from base layer to the subgrade of this section is lower than the same under lime section. Lime cement section also demonstrated the lower deflections and strains compared to lime section. The deflections observed from pavement layers are lower than lime sections. In conclusion, for non-sulfate soils, lime cement stabilization has yielded the best performance base on the FEM analyses.
15. From LCCA studies, combined lime-cement treatment yielded a lower NPV than a hypothetical lime treated control section. Again, maintenance costs for combined method

are lower due to lesser amounts of distress problems detected during the current monitoring period.

For sulfate soils, Type V Cement with Class F Fly Ash stabilized section has demonstrated consistent performance with low compressive strains, low pressures at the bottom of the treated subgrade, higher strength properties from DCP tests and lower heaves related movements. Overall, based on the long term field studies and laboratory tests as well as LCCA studies, it can be mentioned that the 'Type V Cement with Fly Ash' and 'Type V Cement' are recommended for stabilization of sulfate rich subgrades in Southeast Arlington. GGBFS yielded effective stabilization of sulfate soils, however from the cost perspective, it was not highly recommended. Though enhancements are not as high as the cement and GGBFS treated sections, both 'lime with fiber' and 'lime (control)' sections performed adequately in the field with some heave related concerns. Continuous monitoring and periodic assessments will provide long-term effectiveness of these treatments in the field.

For non-sulfate soils, combined lime and cement stabilization demonstrated the ability to enhance the strength, and reduce swell and shrinkage strain behaviors of treated subgrades. The volume change of zero magnitude is observed in both swell and shrinkage test. The compressive strength of untreated soil specimens is considerably enhanced (more than ten times) after both treatments. The combined lime and cement treatment has resulted in slightly higher compressive strength than the isolated lime treatment. Strength enhancements overall are attributed to pozzalonic compounds formed due to chemical reactions between stabilizers and soil in the presence of moisture. The Resilient tests show that combined lime cement treated soils have the highest resilient modulus enhancements compared to lime treated soils and natural soils. Overall, based on the long term field studies and laboratory tests and LCCA studies, it can be concluded that the 'Combined lime and cement stabilization' is recommended for stabilization of non-sulfate subgrade soils Arlington area.

8.2 Future Recommendations

1. Field studies and laboratory studies at various different environmental site conditions with different kind of soils are recommended for further validation of the finding and development of database for better pavement design guidelines.

2. Investigations on other factors which are potentially related to the expansion behavior of the soils are recommended. Other factors are including percentage of minerals contained in the soils are considered important to understand the expansion behavior of the soils.

3. A development of the numerical modeling of pavements built over expansive subgrade soils subjected to dynamic traffic loading is also recommended for a better simulation of the pavement system under real traffic conditions and also estimation of rutting or permanent strains under repetitive loading.

APPENDIX A

FIELD PHOTOS: SULFATE SOILS

Figure A1 Current Condition of Harwood Road (Cement Treated Section).

Figure A2 Current Condition of Harwood Road (Cement with Fly ash Treated Section).

Figure A3 Current Condition of Harwood Road (GGBFS Treated Section).

Figure A4 Current Condition of Harwood Road (Lime with Fibers Treated Section).

APPENDIX B

FIELD PHOTOS: NON-SULFATE SOILS

Figure B1 Current Condition of International Parkway.

Figure B2 Current Condition of Southmoor Drive.

Figure B3 Current Condition of Southeast Parkway.

REFERENCES

1. AASHTO (1993). “Guide for Design of Pavement Structures,” *American Association of State Highway and Transportation Offices*, Washington, D.C.
2. Al-Qadi, I. L. and Bhutta, S. A. (1999). “In Situ Measurements of Secondary Road Flexible Pavement Response to Vehicular Loading,” *Transportation Research Record No.1652, Transportation Research Board*, Washington, DC, pp. 206-216.
3. Al-Rawas, A.A., Hago, A.W. and Al-Sarmi, H. (2005). “Effect of lime, Cement and Sarooj (Artificial Pozzolan) on the Swelling Potential of an Expansive Soil from Oman.” *Building and Environment 40,* pp.681–687.
4. ASTM (1995). “Annual Book of ASTM Standards, Section 4, Construction, Vol. 4.08 Soil and Rock; Dimension Stone; Geosynthetics,” *American Society of Testing and Materials*, Philadelphia, Pennsylvania.
5. Austin, R.A. and Gilchrist, A.J.T. (1996). “Enhanced Performance of Asphalt Pavements Using Geocomposites.” *Geotextiles and Geomembranes*, pp.175-186.
6. Basma, A.A., Tuncer, E.R. (1991). “Effect of Lime on Volume Change and Compressibility of Expansive Clays.” *Transportation Research Board, TRR No. 1296*, Washington DC. pp. 54-61.
7. Balasubramaniam, A.S. (1991). “Mechanically Stabilized Earth (MSE) and other Ground Improvement Techniques for Infrastructure Constructions on Soft and Subsiding Ground.” *Geotech Aspects Embankments Excavations Buried Structures*, pp.461-482.

8. Bergado, D.T., Sampaco, C.L., Alfaro, M.C., Shivashankar, R. and Balasubramaniam, A.S. (1991). “Mechanically stabilized earth (MSE) and other ground improvement techniques for infrastructure constructions on soft and subsiding ground,” *Geotech Aspects Embankments Excavations Buried Structures*, pp.461-482.
9. Broms, B. B., Anttikoski, U. (1984). “Soil stabilization.” *Proceedings of the European Conference on Soil Mechanics and Foundation Engineering*, pp. 1289-1315
10. Browning, G. (1999). “Evaluation of Soil Moisture Barrier.” *FHWA/MS-DOT-RD-99-21 and 23; Final Report.*
11. Broms, B., Boman, P., (1979). “Lime Columns: A New Foundation Method.” *Journal of the Geotechnical Engineering Division, ASCE*, pp. 539-555.
12. Bugge, W. A. & Bartelsmeyer, R. R. (1961). “Soil Stabilization with Portland Cement.” *Highway Research Board, 292, National Research Council*, Washington, D.C., pp. 1-15.
13. Chavva, P. K., (2002). “Evaluation of Strength, Swell and Shrinkage Characteristics of Chemically Treated Soil from North Texas,” *Masters Thesis, The University of Texas at Arlington,* Texas, pp. 70.
14. Chavva P.K., S.K. Vanapally, A.J. Puppala and L.Hoyos (2005), “Evaluation of Strength, Resilient Moduli, Swell, and Shrinkage Characteristics of Four Chemically Treated Sulfate Soils from North Texas”, *GSP 136, ASCE Special Publication, Geofrontiers*, Austin, 2005.
15. Chen, F. H. (1983). “Foundation on Expansive Soils,” *Elsevier Scientific Publishing Co.,* New York, USA.
16. Chen, F. H. (1988). “Foundations on Expansive Soils,” *Developments in geotechnical engineering, Vol.12*, pp.12.
17. Clesceri, Greenberg and Trussell (1989). “17th Edition of Standard Methods for the Examination of Water and Wastewater.”

18. Dally, W., Riley, F., Kenneth, G., and McConnell. (1994). “Instrumentation for engineering measurements,” John Wiley and sons Inc.
19. Das, B. M. (1998). “Principles of Geotechnical Engineering,” PWS Publishing Company.
20. Davidson, D. T., Sheeler, J. B., & Delbridge, N. G., Jr, (1958). “Reactivity of four types of fly ash with lime,” *Highway Research Board, Vol. 193, National Research Council,* pp. 24-31. Washington, D.C.
21. Day, R.L., (1992). “The Effect of Secondary Ettringite Formation on Durability of Concrete: A Literature Analysis,” *PCA Research and Development Bulletin RD108T*, pp. 1-115.
22. Day, R. W., (2001), “Soil Testing Manual: Procedures, Classification Data, and Sampling Practices.” *McGraw-Hill*, New York.
23. Dermatas, D.(1995). “Ettringite-induced Swelling in Soils: State-of-the-art.” *Applied Mechanics Rev*, Vol. 48, pp. 659-673.
24. Diamond, S. & Kinter, E. B. (1965). “Mechanisms of Soil-lime Stabilization: and Interpretive Review,” *Highway Research Record, 92, Transportation Research Board*, Washington, D.C., pp. 83-96.
25. Enayatpour, S., (2005), “Field Investigation for Comprehensive Assessments of Four Selected Stabilization Methods for Soft Subgrade Soils,” *Master Thesis, The University of Texas at Arlington, Texas*, pp. 45.
26. Evans, R. P.; McManus, K. J. (1999). “Construction of Vertical Moisture Barriers To Reduce Expansive Soil Subgrade Movement.” *Transportation Research Record 1652, 7th International Conference on Low-Volume Roads*, pp.108-112.
27. Ferguson, G. (1993). “Use of Self-Cementing Fly Ashes as a Soil Stabilization Agent,” *Geotechnical Special Publication, Vol. 36*, pp. 1-3.
28. Gillot, J. E., (1987). “Clay Mineralogy in Engineering Geology,” *Industry and Agriculture. Applied Clay Science*, Vol. 2, pp.187-308.

29. Giroud, J.P. and Han, J. (2004a). “Design Method for Geogrid-Reinforced Unpaved Roads. I. Development of Design Method.” *Journal of Geotechnical and Geoenvironmental Engineering*, pp. 775-786.
30. Giroud, J.P. and Han, J. (2004b). “Design Method for Geogrid-Reinforced Unpaved Roads. II. Calibration and Applications.” *Journal of Geotechnical and Geoenvironmental Engineering*, pp. 787-797.
31. Glaser, D., (2001). “Advanced MEMS Sensors for Civil Engineering Applications. Exploring the Uses of Auto Adaptive Media in Geotechnical Earthquake Engineering,” *Workshop Opinion Papers*.
32. Glenn, G. R. & Handy, R. L. (1963). “Lime-Clay Mineral Reaction Products,” *Highway Research Record, 29, Transportation Research Board,* pp. 70-82. Washington, D.C.
33. Hammons, M. I., (1998). “Advanced Pavement Design: Finite Element Modeling for Rigid Pavement Joints.” *Rep. No. II*: *Model Development, DOT/FAA/AR-97-7*, Federal Aviation Administration, U.S. Dept. of Transportation.
34. Hawkins, A. B. (1998). “Engineering Significance of Ground Sulfates.” *Geotechnical Site Characterization*, pp. 685-692.
35. Hausmann, M. R. (1990). “Engineering Principles of Ground Modification,” *McGraw Hill*, New York.
36. Hicks, R.G. (2002). “Alaska Soil Stabilization Design Guide.” *FHWA-AK-RD-01-6B.*
37. Hopkins, T.C., Sun, L. and Slepak, M. (2005). “Bearing Capacity Analysis and Design of Highway Base Materials Reinforced with Geofabrics.” University of Kentucky Transportation Center, College of Engineering, *Research Report KTC-05-21/SPR 238-02-1F*.
38. Holtz, W. G., Gibbs, H. J. (1956). “Engineering Properties of Expansive Clays.” *Trans. ASCE, 121*, pp. 641-663.

39. Hufenus R., Rueegger, R., Banjac, R., Mayor, P., Springman, S.M. and Brönnimann, R. (2006). “Full-Scale Field Tests on Geosynthetic Reinforced Unpaved Roads on Soft Subgrade.” *Geotextiles and Geomembranes, Vol. 24* , pp.21-37.
40. Hunter, D. (1988). “Lime-Induced Heave in Sulfate-Bearing Clay Soils,” *Journal of Geotechnical Engineering*, ASCE, Vol. 114, pp. 150-167.
41. Jayatilaka, R., Gay, D.A., Lytton, R.L.,and Wray, W.K. (1993). “Effectiveness of Controlling Pavement Roughness Due To Expansive Clays with Vertical Moisture Barriers.” *Texas Transportation Institute Research Report 1165-2F*.
42. Jones, D. E., Holtz, W. G. (1973) “Expansive Soils - the Hidden Disaster,” Civil Engineering, *ASCE*, Vol. 43, pp.49.
43. Kezdi, A. (1979). “Stabilized Earth Roads,” *Developments in Geotechnical Engineering*, Vol. 19, Elsevier Scientific Publication, Col, Amsterdam.
44. Kota, B. V. S. (1996). “Sulfate Bearing Soils: Problems with Calcium Based Stabilizers.” *Transportation Research Record*, *National Research Council, Vol. 1546*, pp. 62-69, Washington, D.C.
45. Kuo, C.Huang, C., (2006). “Three-Dimensional Pavement Analysis with Nonlinear Subgrade Materials.” *Journal of Materials in Civil Engineering*, v 18, n 4, August, 2006, pp. 537-544.
46. Lee, F., Huang, Chen, G.W., & Wang, S.C. (2004), “Geosynthetics Applications for Heavy Load Railway Mitigation,” pp. 572-579.
47. Littlle, N.D., (1987). “Fundamentals of the Stabilization of Soil with Lime.” *National Lime Association Bulletin, Vol.* 332, pp. 20.
48. Little, D.N., E.H. Males, J.R. Prusinski and B.Stewart, (1998). “Cementious stabilization.” *Transportation Research Board, Millenium Paper.*
49. McManus, K.L. and Nataraj, M. and Philips G.M. (1993). “Long Term Evaluation and Identification of the Proper Testing Program for ASTM Class C Fly Ash Stabilized Soils,” Louisiana Transportation Research Center.

50. Metcalf, J. B. (1998). “Accelerated Pavement Testing, a Brief Review Directed Towards Asphalt Interests.” *Journal of the Association of Asphalt Paving Technologists*, Vol. 67, pp. 553-572.
51. Metcalf, L. (1996). “Application of Full-Scale Accelerated Pavement Testing.” *NCHRP Synthesis 235, Transportation Research Board*, *National Research Council*, Washington, DC.
52. Metcalf, L., Romanschi J. B., and Rasoulian S. A. (1999). “Development of the Louisiana ALF Program, the First Experiment.” *Transportation Research Record, No. 1655, Transportation Research Board*, Washington DC, pp. 219-226.
53. Metha, P.K. and Wang, S. (1982). “Expansion of Ettringite by Water Absorption,” *Cement and Concrete Research,* Vol. 12, pp.121-122.
54. Mitchell, J. K.(1986). “Practical Problems from Surprising Soil Behavior.” *Journal of Geotechnical Engineering Division, ASCE, Vol. 112, No. 3*, pp. 259-289.
55. Mitchell, J. K., and Dermatas, D. (1990). “Clay Soil Heave Caused By Lime-Sulfate Reactions.” *ASTM Special Publication 1135,* pp. 41-64.
56. Mitchell J. K. and Dermatas D.(1992). “Clay Soil Heave Caused by Lime-Sulfate Reactions.” *Innovations in Uses for Lime, ASTM STP 1135, American Society for Testing and Materials (ASTM*), Philadelphia, PA, pp. 41-64.
57. Mitchell, J. K., (1993). “Fundamentals of Soil Behavior,” New York: John Wiley and Sons.
58. Mohan, V. (2002). “Laboratory Investigations to Calibrate Instrumentation System for Expansive Soils.” *Masters Thesis, The University of Texas at Arlington*, Arlington, Texas.
59. Montmorillonite Image: Montmorillonite.svg.
60. Mowafy, Y.M. and Bauer, G.E. (1985a). “Prediction of Swelling Pressure and Factors Affecting the Swell Behavior of an Expansive Soil.” *Transportation Research Record 1032*. pp. 23-33.

61. Nassar, M.W. (2001). “Utilization of Instrument Response of SuperPave™ Mixes at the Virginia Smart Road to Calibrate Laboratory Developed Fatigue Equations.” *Masters Thesis, Virginia Polytechnic Institute and State University*, Virginia, 218 pages.
62. National Environmental Satellite Data and Information Service (NESDIS), http://ncdc.noaa.gov/oa/climate/stationlocator.html.
63. Nelson, D. J. and Miller, J. D. (1992). “Expansive Soils: Problems and Practice in Foundation and Pavement Engineering,” John Wiley and Sons.
64. Nicholson, P. G. and Kashyap, V. (1993). “Fly Ash Stabilization of Tropical Hawaiian soils.” *ASCE Geotechnical Special Publication, Vol. 36*, pp. 15-19.
65. Olorunsogo, F. T., Wainwright, P. J. (1998). “Effect of GGBFS Particle-Size Distribution on Mortar Compressive Strength.” *Journal of Materials in Civil Engineering, Vol. 10,* pp. 180-187.
66. Ozyildirim, H. C. (1990). “Admixtures and Ground Slag for Concrete.” *Transportation Research Board 365, National Research Council*, Washington, D.C., pp. 33-43.
67. Pengelly, A. and Addison, M. (2001). “In-Situ Modificaiton of Active Clays for Shallow Foundation Remediation.” *Expansive Clay Soils and Vegetative Influences*, pp.192-214.
68. Perrin, L. (1992). “Expansion of Lime-treated Clays Containing Sulfates.” *ASCE Expansive Soils Research Council*, New York, Vol. 1, pp. 409-414.
69. Petry, T. (1994). “Studies of Factors Causing and Influencing Localized Heave of Lime-Treated Clay Soils (Sulfate-Induced Heave),” *Technical Report for U.S. Army Corps of Engineers, Waterways Experiment Station*, Vicksburg, MS.
70. Petry, T. M., and Little, D. N. (1992). “Update on Sulfate-Induced Heave in Treated Clays: Problematic Sulfate Levels.” *Transportation Research Record, 1362, TRB, National Research Council*, Washington, DC, pp. 51.
71. Picornell, M. and Lytton, R.L. (1986). “Behavior and Design of Vertical Moisture Barriers.” *Transportation Research Record, 1137*, pp.71-81.

72. Pillappa, Gautham. (2005). “Field and Experimental Studies to Assess the Performance of Stabilized Expansive Clay.” *MS Thesis, The University of Texas at Arlington*, Arlington, Texas, 132 pages.
73. Prusinski J.R. and S.Battacharja (1999), “Effectiveness of Portland cement and lime in stabilizing clay soils.” *Transportation Research Record*, Vol 1, 1652, pp. 215-217.
74. Puppala, A.J., Mohammad, N.L., Allen, A. (1996). “Permenant Deformation Characterization of Subgrade Soils from RLT Test.” Vol. 11, Issue 4, pp. 274-282.
75. Puppala, A.J., Hanchanloet, S., Jadeja, M., Burkart, B. (1999). “Sulfate Induced Heave Distress: A Case Study. Proceedings,” *Transportation Research Board Annual Meeting*, Washington D.C, USA.
76. Puppala, A.J., and Musenda, C. (2000). “Effects of Fiber Reinforcement on Strength and Volume Change Behavior of Expansive Soils.” *Transportation research board 79thAnnual Meeting, paper No. 00-0716*, Washington, D.C.
77. Puppala, Anand J., Viyanant, C., Kruzic, A. P., Perrin, L. (2002). “Evaluation of a Modified Soluble Sulfate Determination Method for Fine-Grained Cohesive Soils.” *Geotechnical Testing Journal*, v 25, n 1, March, 2002, pp. 85-94.
78. Puppala, A.J., Wattanasantichatoen E., Intharasombat L., Hoyos L.R.(2003). “Studies to Understand Soil Compositional and Environmental Variables Effects on Sulfate Heave Problems,” 12 th Panamerican Conference on Soil Mechanics and Geotechnical Engineering.
79. Puppala, A.J., Wattanasanticharoen, E. and Punthutaecha, K. (2003). “Experimental Evaluations of Stabilization Methods for Sulphate-rich Expansive Soils.” *Ground Improvement Vol. 7, No. 1*, 2003. pp. 25-35.
80. Puppala, A.J., Griffin, J.A., Hoyos, L.R. and Chomtid, S. (2004a). “Studies on Sulfate-Resistant Cement Stabilization Methods to Address Sulfate-Induced Soil Heave.” *Journal of Geotechnical and Geoenvironmental Engineering,* 130, pp. 391-402.

81. Puppala, A.J., Intharasombat, N., Vempati, R. (2005). "Experimental Studies on Ettringite Induced Heaving in Soils." *ASCE Journal of Geotechnical and Geoenvironmental Engineering, Vol. 31, No. 3*, pp. 325-337.

82. Puppala, A.J., Griffin, J.A., Hayes, L.R., Chomtid, S. (2005). "Discussion on Studies on Sulfate Resistant Cement Stabilization Methods to Address Sulfate Induced Heave Problems. Discussion," *ASCE, Journal of Geotechnical and Geo-environmental Engineering.*

83. Ramakrishna, A. M., (2002). "Evaluation of Resilient Moduli Characteristics of Chemically Treated Soil from North Texas," *Masters Thesis, The University of Texas at Arlington, Texas*, pp. 96.

84. Rollings, R. S. (1999). "Sulfate Attack on Cement-Stabilized Sand." *Journal of Geotechnical and Geoenvironmental Engineering*, pp. 364-372.

85. Rollings Jr., R.S., Burkes, J.P., and Rollings, M.P. (1999). "Sulfate Attack on Cement Stabilized Sand." *Journal of Geotechnical and Geoenvironmental Engineering*, *vol. 125 No.5,* pp. 364-372.

86. Rogers, C.D.F., Glenginning, S., Roff, T.E.J. (1997). "Lime Modification of Clay Soils for Construction Expediency." *Proc. Instn. Engrs., Geotech. Engng., Vol. 125*, pp. 249.

87. Rufino, D., Roesler, J. (2006). "Effect of Slab-Base Interaction on Measured Concrete Pavement Responses", *ASCE*.

88. Sargand, S. M., Green, R. and Khoury, I. (1997). "Instrumentation Ohio Test Pavement." *Transportation Research Record, No. 1596, Transportation Research Board*, Washington, DC, pp. 23-30.

89. Schoute, E. J. (1999). "Chemical Stabilization of Soft Clay," *Ms. Thesis*, Memoirs of the Center of Engineering Geology in the Netherlands, Vol.188, pp. 15-39.

90. Sci-Tech Dictionary: Montmorillonite, http://www.answers.com/topic/montmorillonite.

91. Sherwood, P.T. (1962). "Effect of Sulfates on Cement and Lime Treated Soils." *Highway Research Board, Bulletin 353*, pp. 98-107.

92. Sherwood P.T (1993). “Soil Stabilization with Cement and Lime.” *Transport Research Laboratory*, Department of Transport, London, 1993.
93. Sherwood, P. T. (1995). “Soil stabilization with cement and lime,” HMSO Publication Center, pp. 14-55.
94. Sparrevik, P. (1996). “Development of New Platform Foundation Concept through Instrumentation,” Norwegian Geotechnical Institute.
95. Stavridakis, E.L., 2003. “Assessment of Anisotropic Behavior of Swelling Soils on Ground and Construction Work.” *Geotechnical Engineering Division, Department of Civil Engineering, Aristotle University of Thessaloniki*, Greece.
96. Steinberg, M.L. (1992). “Vertical Moisture Barrier Update.” *Transportation Research Record 1362*. pp.111-117.
97. Talero, R. (2002). “Kinetochemical and Morphological Differentiation of Ettringite by the Le Chatelier-Anstett Test,” *Cement and Concrete Research 32*, pp. 707-717.
98. The Mineral Montmorillonite: http://mineral.galleries.com.
99. Turner and Hill. (1999). “Instrumentation for Engineers and Scientists.” *Oxford Science publication*.
100. Tutumluer, E. and Kwon, J. (2005). “Evaluation of Geosynthetics use for Pavement Subgrade Restraint and Working Platform Construction.” *Proc. of 13th Annual Great Lakes Geotechnical/Geoenvironmental Conference on Geotechnical Applications for Transportation Infrastructure*, May 13, 2005.
101. Usmen, M. A. & Bowders, J. J., Jr. (1990). “Stabilization Characteristics of Class F Fly Ash.” *Transportation Research Record, 1288, transportation research Board*, Washington, D.C., pp. 59-60.
102. Wang, L. (2002). “Cementitious Stabilization of Soils in the Presence of Sulfate,” *Ph.D. Thesis*, Louisiana State University.

103. Wang, L., Tian, P., & Yao, Y. (1998). “Application of Ground Granulated Blast Furnace Slag in High Performance Concrete in China,” *International Workshop on Sustainable Development and Concrete Technology*. China Building Academy, PRC.

104. Wattanasanticharoen, E. (2000). “Investigate to Evaluate the Performance of Four Selected Stabilizations on Soft Subgrade Soils of Southeast Arlington,” *Masters Thesis, The University of Texas at Arlington*, Texas, pp. 128.

105. Wikipedia: The Free Encyclopedia, http://en. Wikipedia.org.

106. William, J.W., Steve, W., Rob, H. (1999). “Life Cycle Cost Analysis of Portland Cement Concrete Pavements.” *Research Report. The University of Texas at Austin*, Texas.

107. Vasudev, D., (2007), “Performance Studies on Rigid Pavement Sections Built on Stabilized Sulfate Soils,” *Master Thesis*, The University of Texas at Arlington, Texas, pp. 99-105.

108. Viyanant, C. (2000). “Laboratory Evaluation of Sulfate Heaving Mechanisms in Artificial Kaolinite Soil.” *M.S. Thesis, The university of Texas at Arlington*, Arlington, Texas, 2000.

BIOGRAPHICAL INFORMATION

Chakkrit Sirivitmaitrie was born in Bangkok, Thailand. He graduated from Thammasat University, Bangkok, Thailand, with a Bachelor's Degree in Civil Engineering in 2000. He also graduated from The University of Nottingham, Nottingham, UK with a Bachelor's Degree in Civil Engineering in 2002. He joined in Master's Program in Infrastructure at the University of Nottingham, UK, and graduated in 2004. He then joined in doctoral program in the Department of Civil Engineering at the University of Texas at Arlington (UTA), Arlington, Texas in 2006 with Geotechnical Engineering as the major area of research. Subsequently, he worked as a Research Assistant with Prof. A.J. Puppala for 3 years. He performed research in chemical stabilization of expansive soils under the guidance of Prof. A.J. Puppala and successfully defended his dissertation in November 2008. During the course of his study, he worked in various research areas related to ground improvement of expansive soils.